Missing energy signals at the LHC

Uli Haisch
MPI München

IFT Seminar Madrid, 18 February 2019

Mono-jet searches

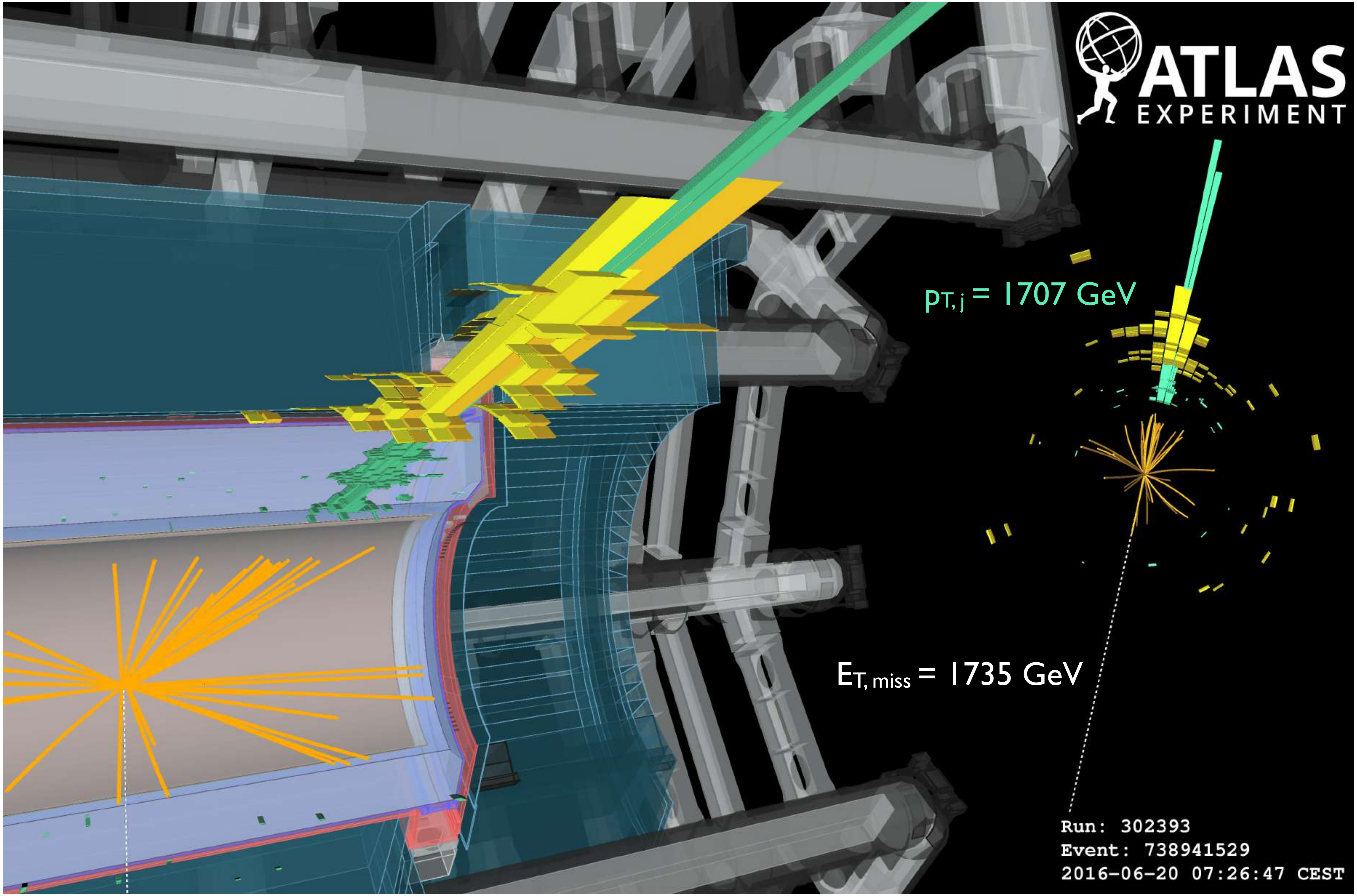

Mono-jet: signal vs. background

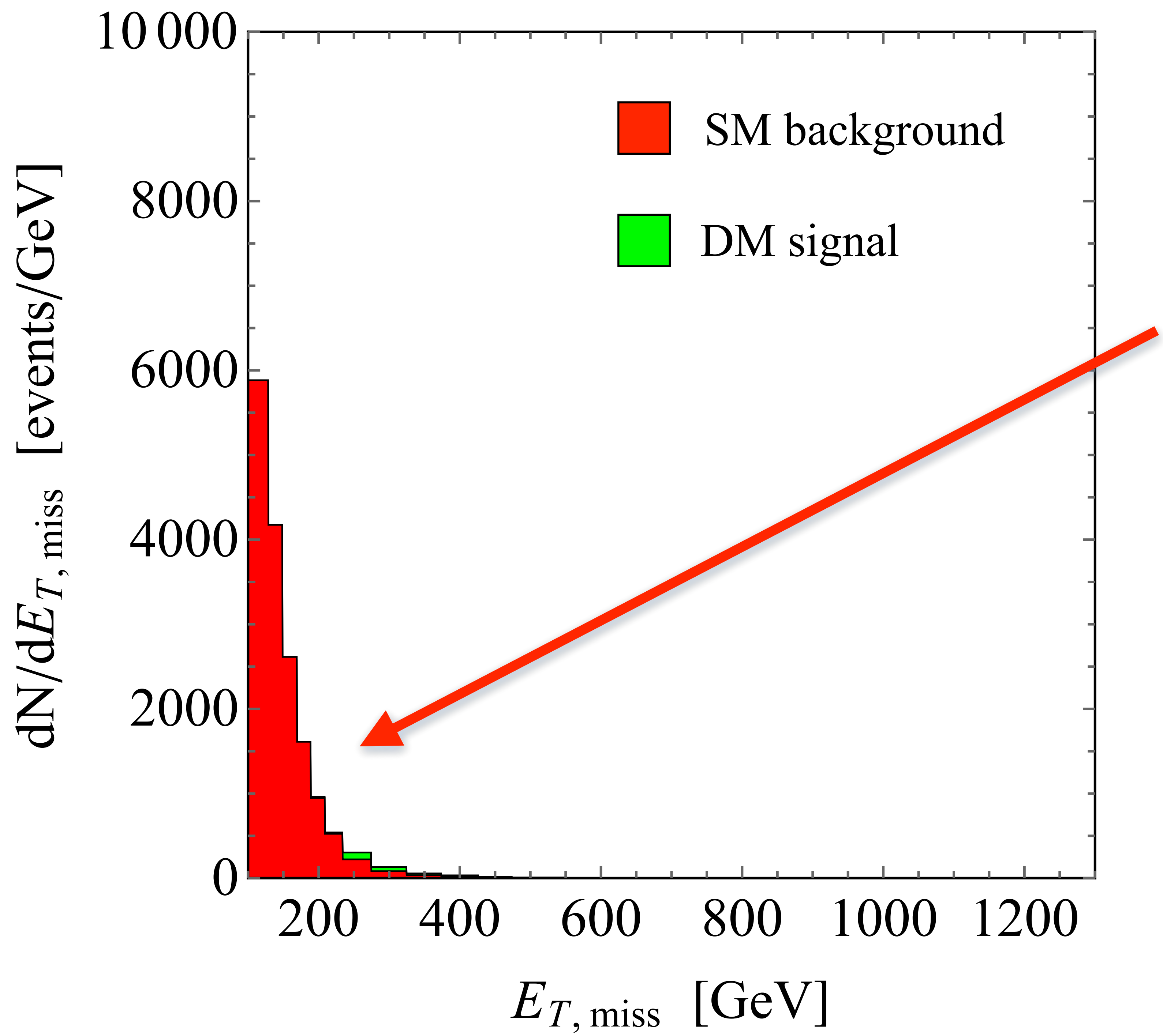

huge Standard Model (SM) background from Z+jet production with Z decaying to neutrinos

Mono-jet: signal vs. background

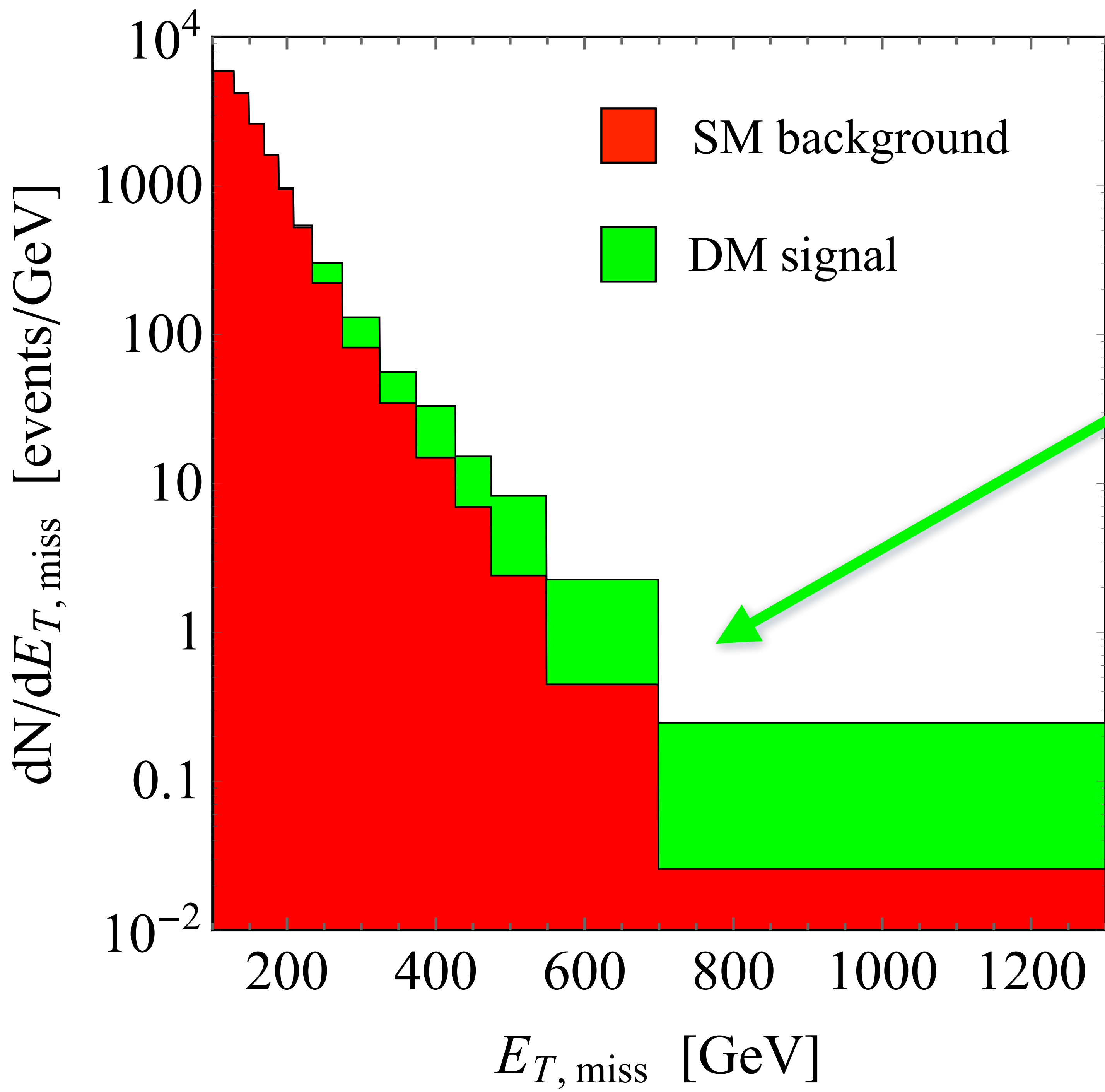

presence of dark matter (DM) manifests itself in small enhancement in tail of missing transverse energy ($E_{T,\,\mathrm{miss}}$) distribution

$E_{T,miss}$ signals: challenges

Exploiting full physics potential of DM searches at HL-LHC requires precise control of backgrounds in signal region. In case of mono-jet searches for example, following problems have to be tackled:

(i) Take accurate data in control regions dominated by $Z(l^+l^-)$+jet, $W(l\nu)$+jet & γ+jet production & extrapolate to $Z(\nu\bar{\nu})$+jet background by means of precise theoretical predictions

(ii) Understand $E_{T,\,miss}$ measurement performance accurately in very high pile-up environment of HL-LHC

Similar issues arise in many other $E_{T,miss}$ channels

Mono-jet: statistical precision

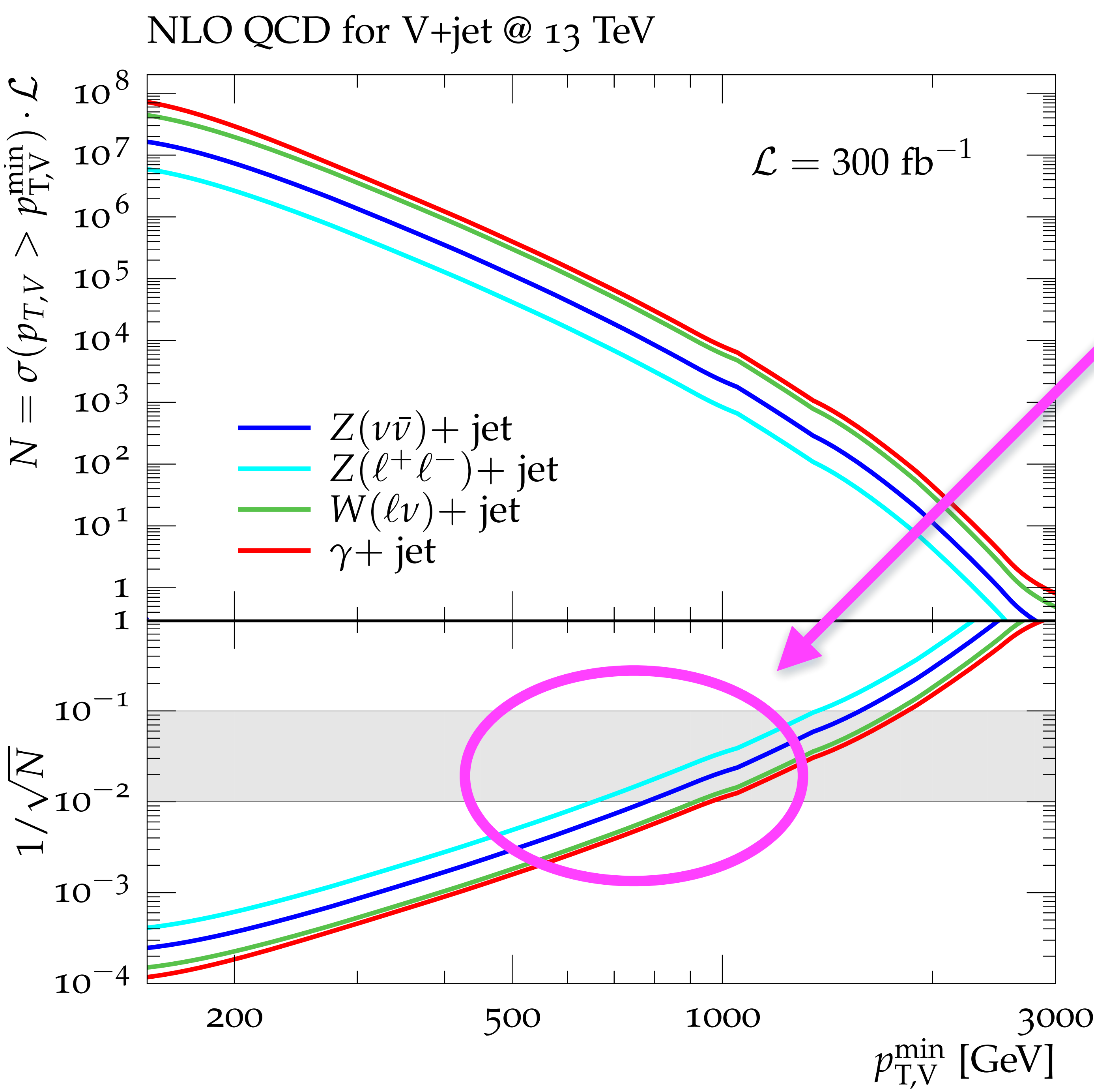

for $p_{T,V} \in [0.5, 1]$ TeV statistical uncertainty on background of O(1%) already at LHC Run-3

To exploit full LHC potential, need to control systematic uncertainties at % level as well

[Lindert et al., 1705.04664]

Mono-jet: recent theory progress

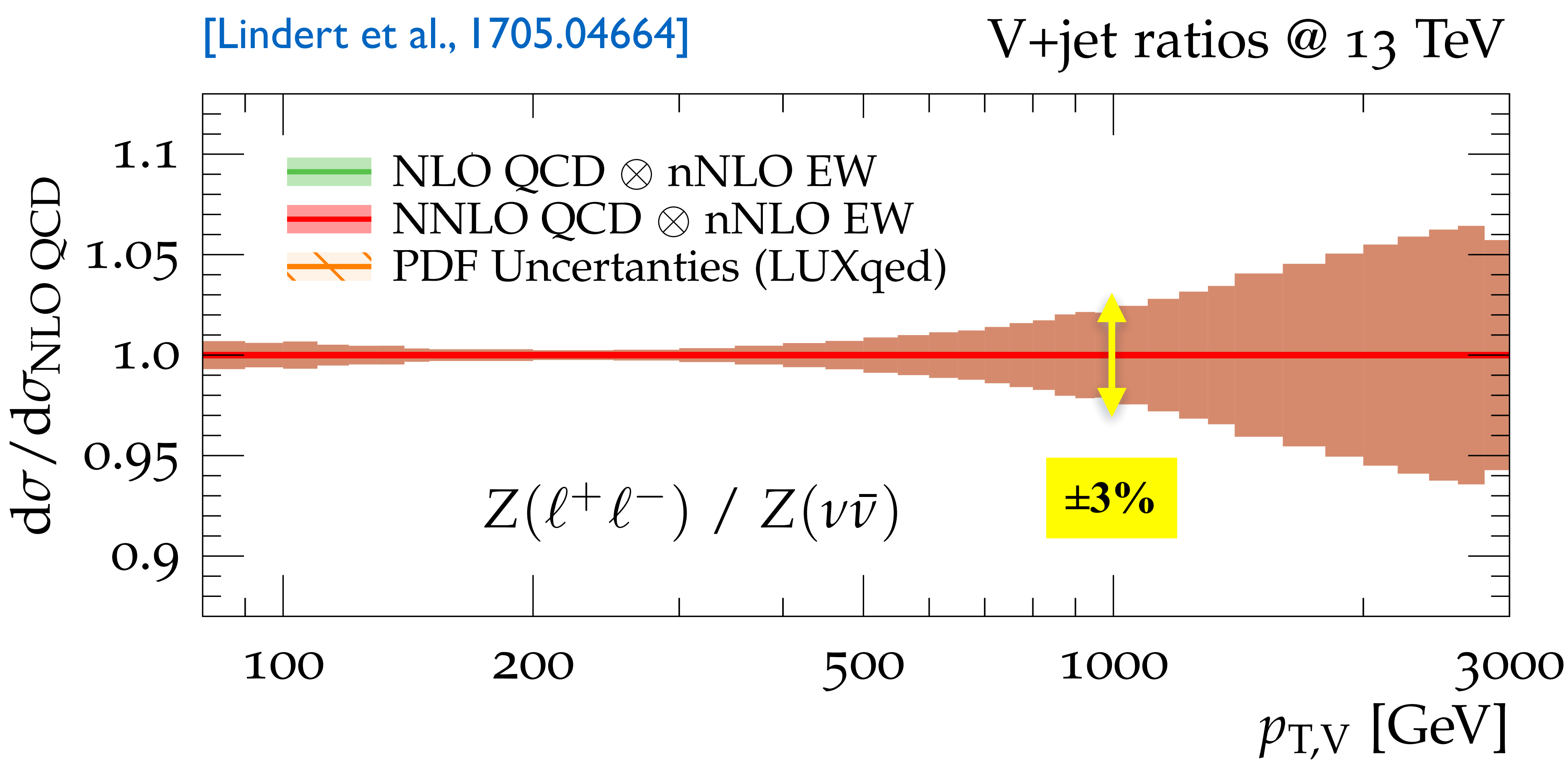

At NNLO QCD + nNLO EW, uncertainties are O(few %) for transverse momenta of $p_{T,V}$ < 1 TeV. Results already used in latest ATLAS & CMS searches & allow to set unprecedented limits on mono-jet production

[N.B. would be nice to have state-of-the-art results also for other V+jets observables, e.g. jet-jet angular correlations]

Mono-jet: HL-LHC prospects

[ATL-PHYS-PUB-2018-043]

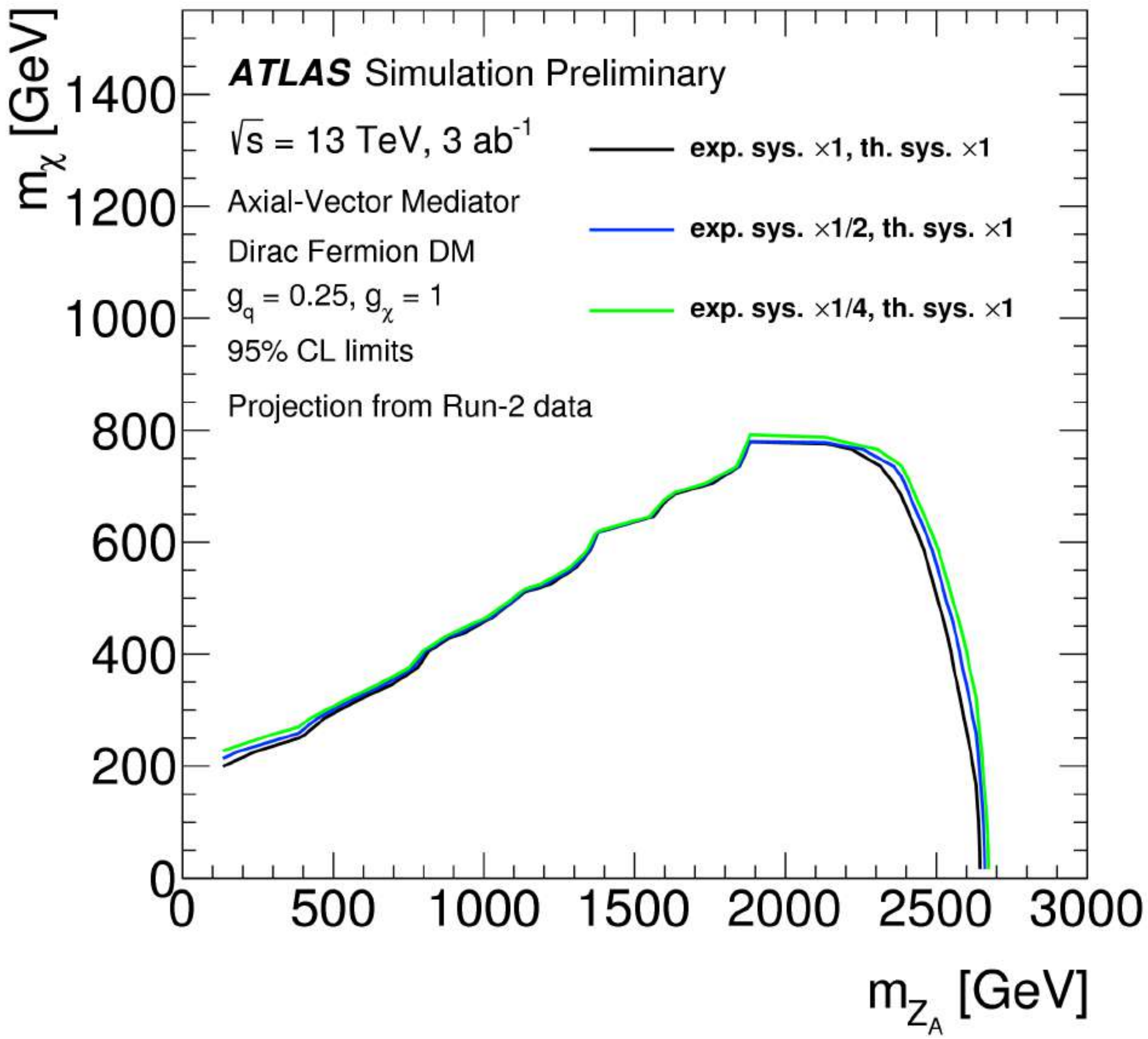

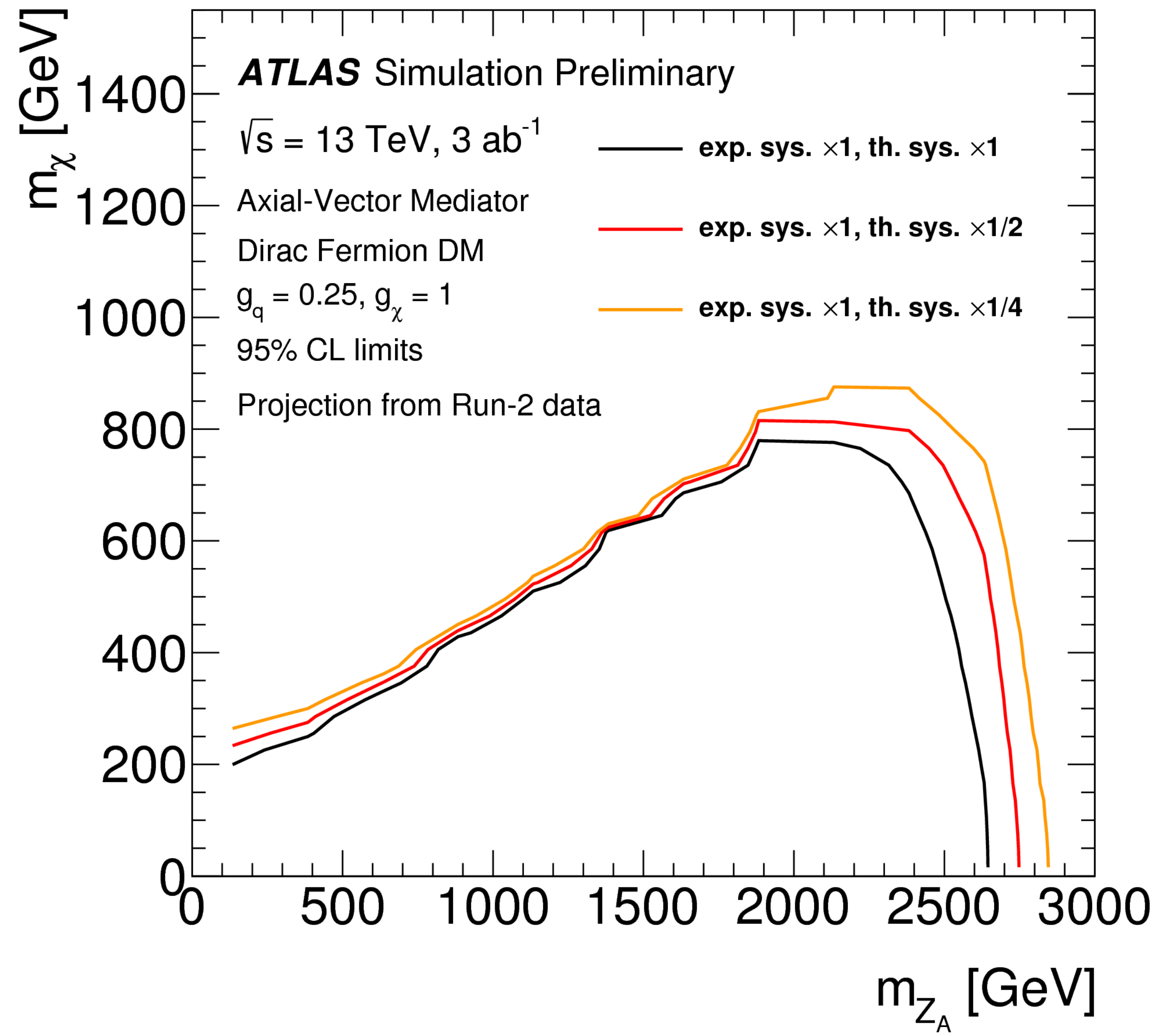

Assumed theoretical systematics seems to have more pronounced impact on future LHC reach than assumed experimental systematics

Evolution of LHC DM models

Effective field theory (EFT)	Simplified models	Next-generation simplified models
$\frac{m_q}{\Lambda^3}\,\bar{\chi}\chi\bar{q}q$	$g_\chi\bar{\chi}\chi S + \frac{g_q y_q}{\sqrt{2}}\,\bar{q}qS$	$g_\chi\bar{\chi}\chi s + Y_q\,\bar{q}Hq + \mu s\lvert H\rvert^2$

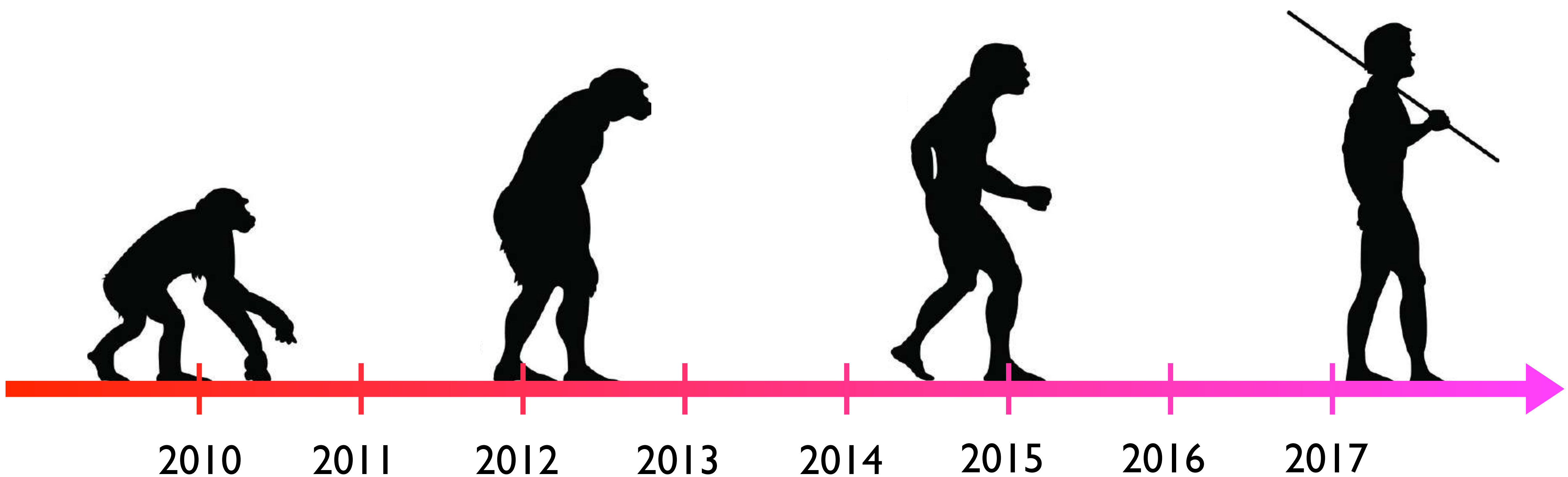

[idea & artwork adopted from Bauer]

Does DM EFT work at LHC?

Name	Operator	Coefficient
D1	$\bar{\chi}\chi\bar{q}q$	m_q/M_*^3
D2	$\bar{\chi}\gamma^5\chi\bar{q}q$	im_q/M_*^3
D3	$\bar{\chi}\chi\bar{q}\gamma^5 q$	im_q/M_*^3
D4	$\bar{\chi}\gamma^5\chi\bar{q}\gamma^5 q$	m_q/M_*^3
D5	$\bar{\chi}\gamma^\mu\chi\bar{q}\gamma_\mu q$	$1/M_*^2$
D6	$\bar{\chi}\gamma^\mu\gamma^5\chi\bar{q}\gamma_\mu q$	$1/M_*^2$
D7	$\bar{\chi}\gamma^\mu\chi\bar{q}\gamma_\mu\gamma^5 q$	$1/M_*^2$
D8	$\bar{\chi}\gamma^\mu\gamma^5\chi\bar{q}\gamma_\mu\gamma^5 q$	$1/M_*^2$
D9	$\bar{\chi}\sigma^{\mu\nu}\chi\bar{q}\sigma_{\mu\nu} q$	$1/M_*^2$
D10	$\bar{\chi}\sigma_{\mu\nu}\gamma^5\chi\bar{q}\sigma_{\alpha\beta} q$	i/M_*^2
D11	$\bar{\chi}\chi G_{\mu\nu}G^{\mu\nu}$	$\alpha_s/4M_*^3$
D12	$\bar{\chi}\gamma^5\chi G_{\mu\nu}G^{\mu\nu}$	$i\alpha_s/4M_*^3$
D13	$\bar{\chi}\chi G_{\mu\nu}\tilde{G}^{\mu\nu}$	$i\alpha_s/4M_*^3$
D14	$\bar{\chi}\gamma^5\chi G_{\mu\nu}\tilde{G}^{\mu\nu}$	$\alpha_s/4M_*^3$

One way to check:

(i) Pick one operator

(ii) Construct simplified model that leads to operator in heavy mediator limit

(iii) Calculate $E_{T,\text{miss}}$ & other distributions in both EFT & simplified model

(iv) If shapes of distributions are similar, can use EFT as proxy for simplified model, otherwise not

[Zhang et al., 0912.4511; Beltran et al., 1002.4137;
Goodman et al., 1005.1286, 1008.1783, 1009.0008;
Bai et al., 1005.3797; Rajaraman et al., 1108.1196;
Fox et al., 1109.4398; …]

Tree-level example

Vector operator:

$$\mathrm{D5} = \bar{\chi}\gamma^{\mu}\chi\bar{q}\gamma_{\mu}q$$

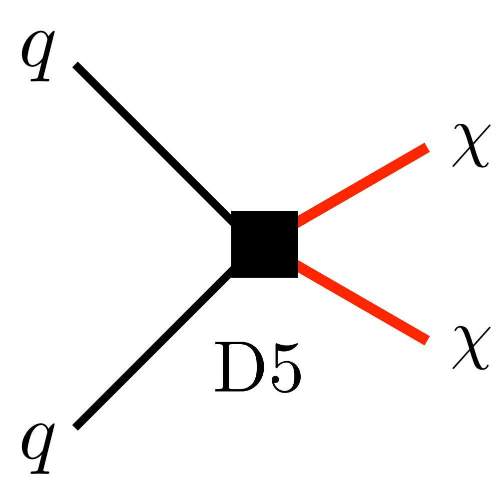

Spin-1 simplified model:

$$\mathcal{L}_V \supset g_{\chi}\bar{\chi}\gamma^{\mu}\chi V_{\mu} + \sum_q g_q\bar{q}\gamma^{\mu}qV_{\mu}$$

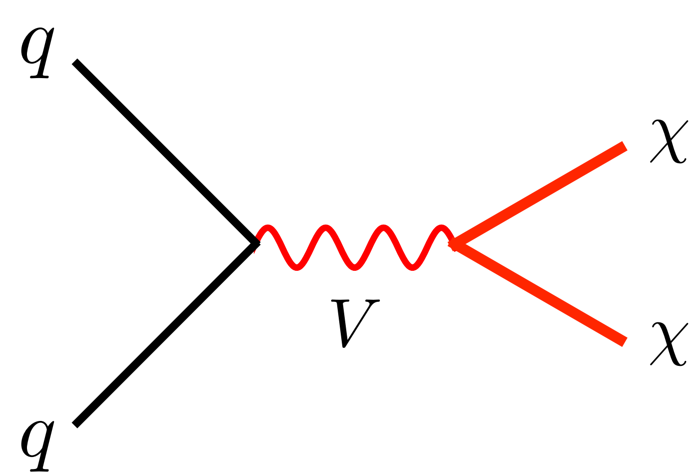

[Dudas et al., 0904.1745; Fox et al., 1104.4127; Frandsen et al., 1204.3839; …]

D5: EFT vs. simplified model

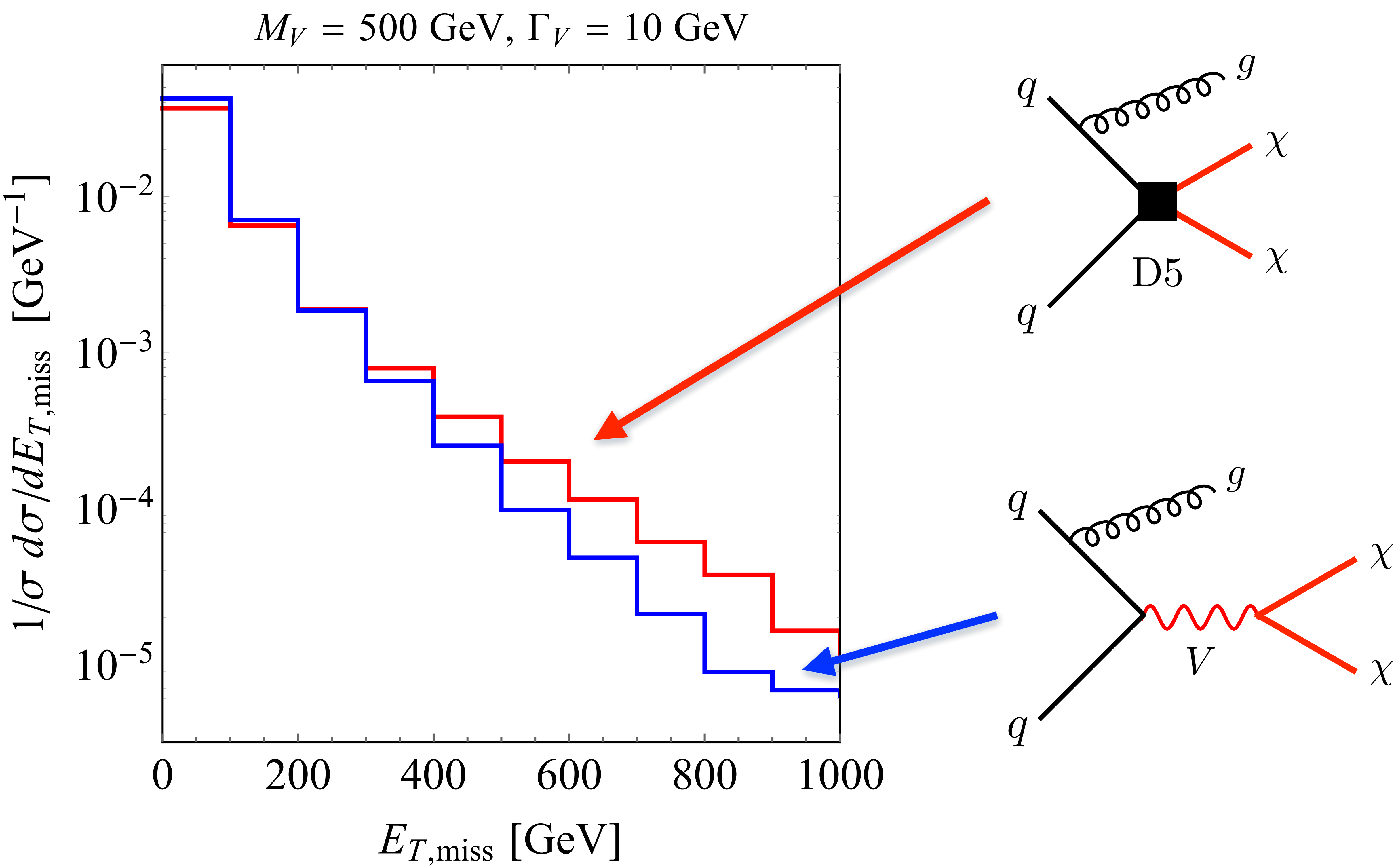

Loop-level example

Gluonic operator:

$$\mathrm{D11} = \bar{\chi}\chi G_{\mu\nu}G^{\mu\nu}$$

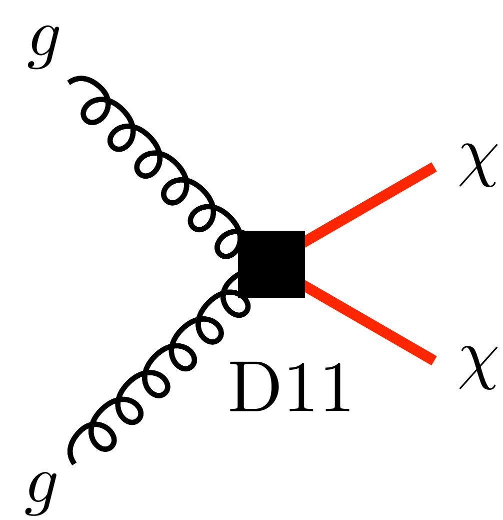

Spin-0 simplified model:

$$\mathcal{L}_S \supset g_\chi \bar{\chi}\chi S + \sum_q \frac{g_q y_q}{\sqrt{2}}\,\bar{q}qS$$

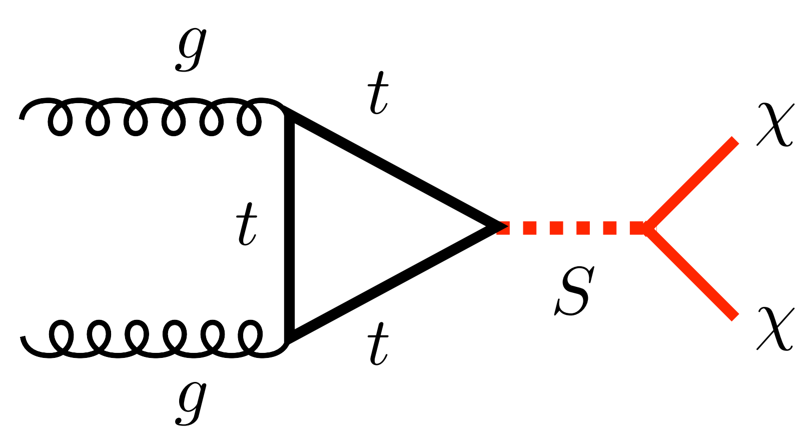

[UH et al., 1208.4605, 1311.713, 1503.00691; Buckley et al.,1410.6497; Harris et al., 1411.0535; …]

D11: EFT vs. simplified model

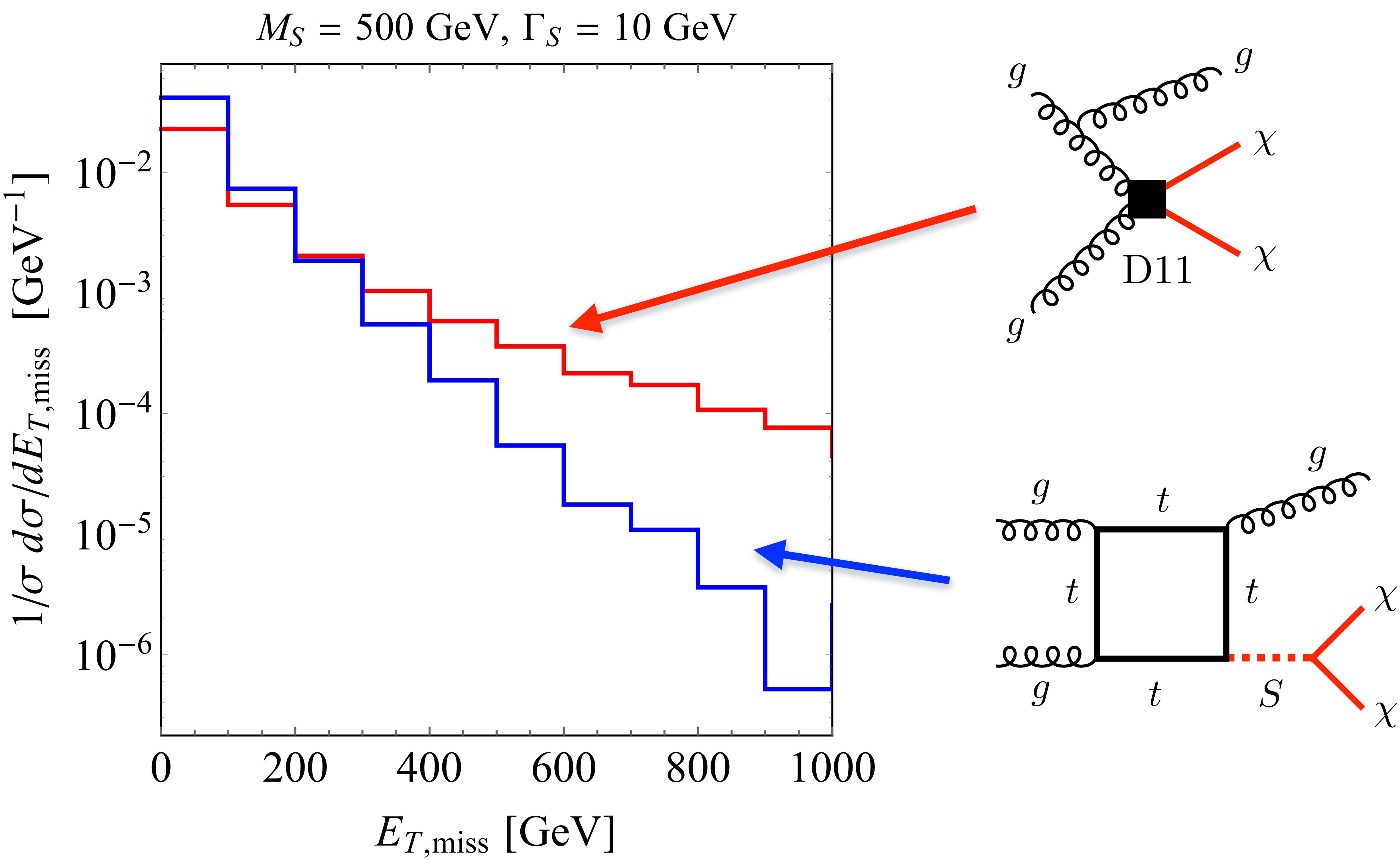

EFT vs. simplified models: verdict

EFT often fails to correctly describe kinematical distributions of weakly-coupled simplified models with weak- or TeV-scale mediators. This flaw prompted ATLAS & CMS to move from EFT to simplified models when interpret $E_{T,\,\mathrm{miss}}$ searches in LHC Run-2

But in case of strongly-coupled DM candidates — composite fermions, pseudo-Nambu-Goldstone bosons, Goldstini, … — EFT appropriate & sometimes even necessary to describe most important interactions at LHC

[see e.g. Bruggisser, Riva & Urbano, 1607.02474 & 1607.02475 for EFT discussion of strongly-coupled DM]

Spin-1 DM simplified models

$$\mathcal{L}_V \supset g_{\rm SM} \sum_q \bar{q}\gamma^\mu q V_\mu + g_{\rm DM} \bar{\chi}\gamma^\mu \chi V_\mu$$

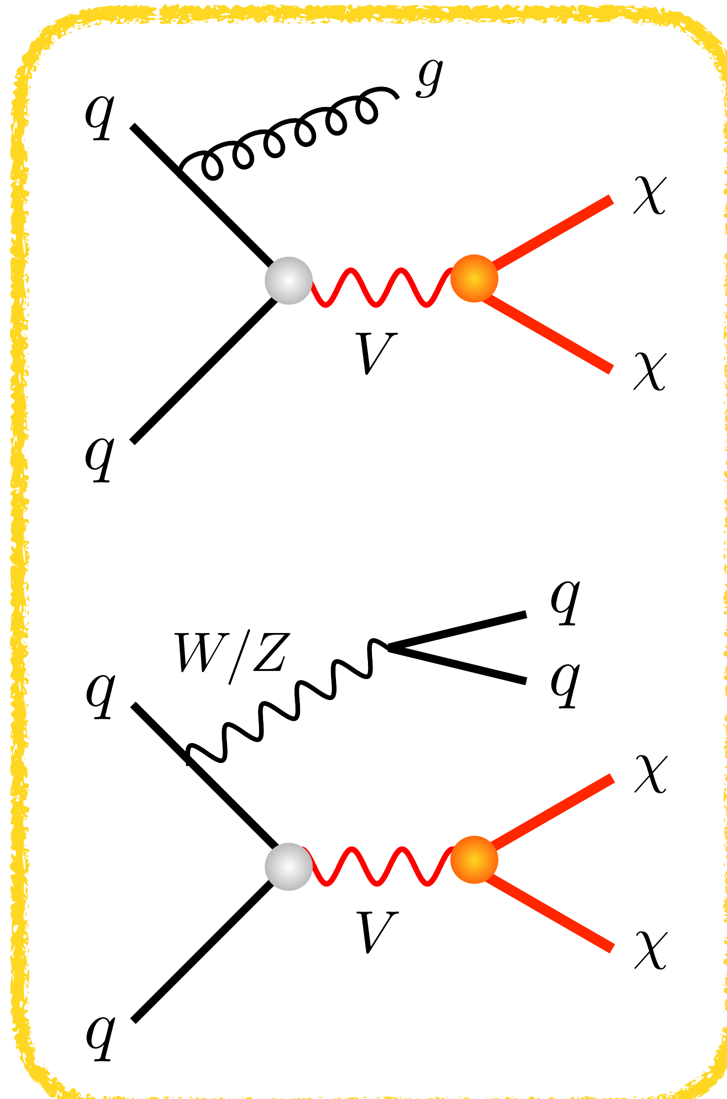

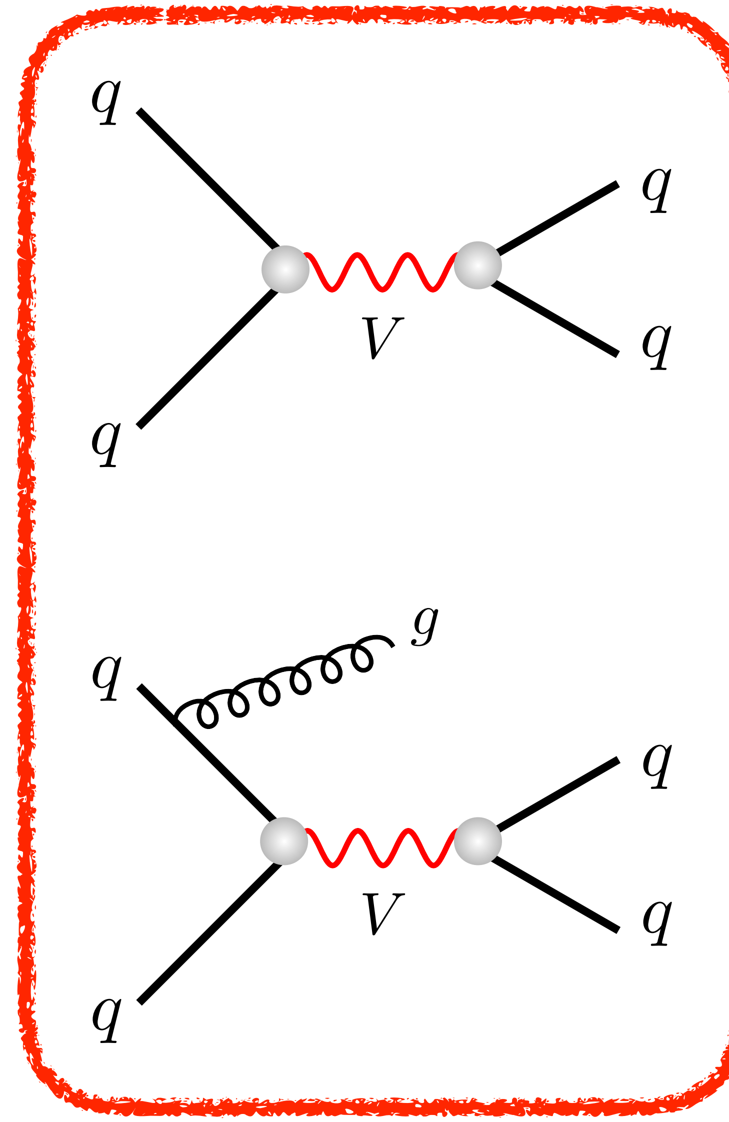

dominant $E_{T,\,miss}$ signal: mono-jet

dominant non-$E_{T,\,miss}$ signal: dijet+X

LHC constraints on spin-1 mediators

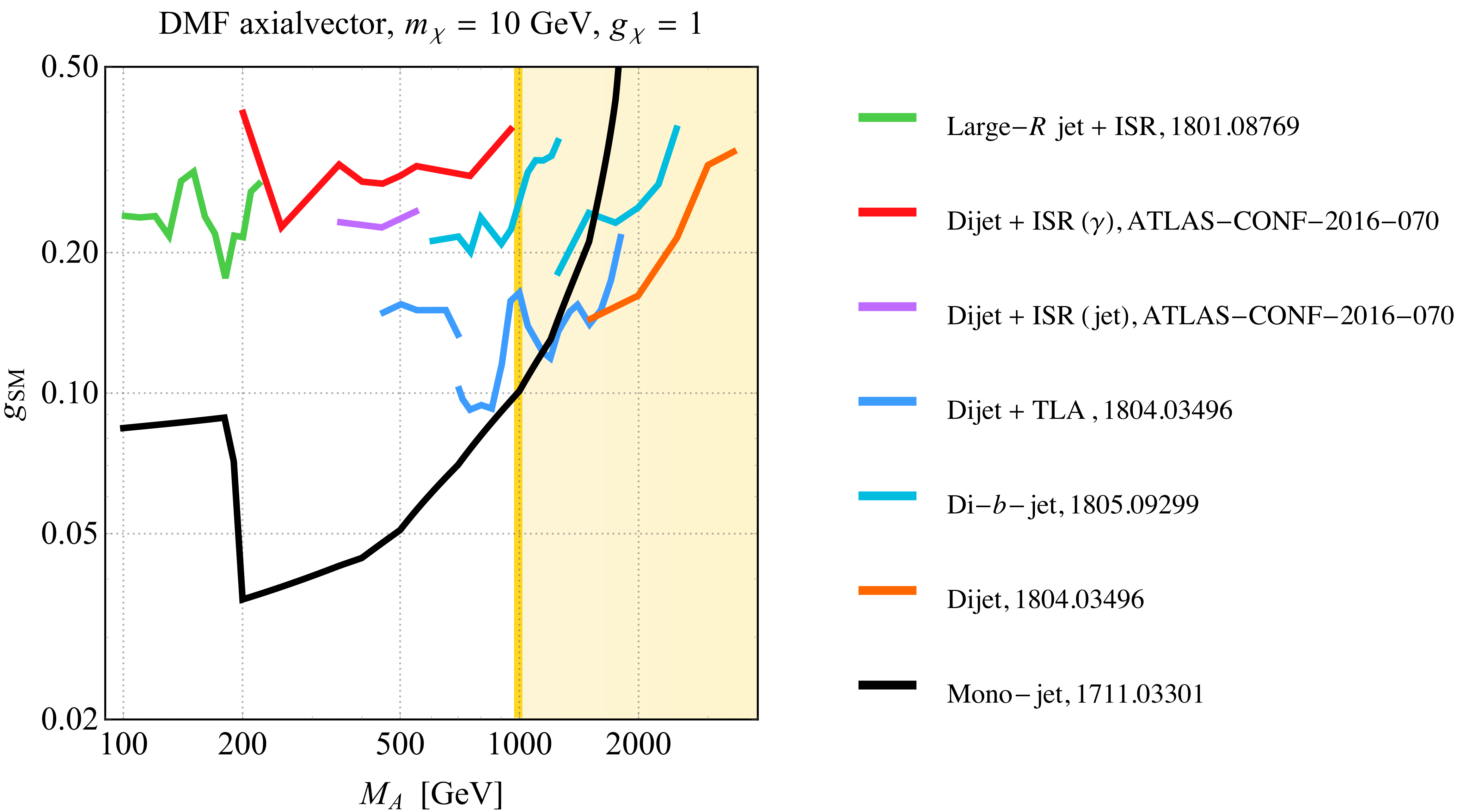

LHC dijet+X searches generically provide strongest limits on TeV-scale spin-1 mediators appearing in DM Forum (DMF) simplified models

LHC constraints on spin-1 mediators

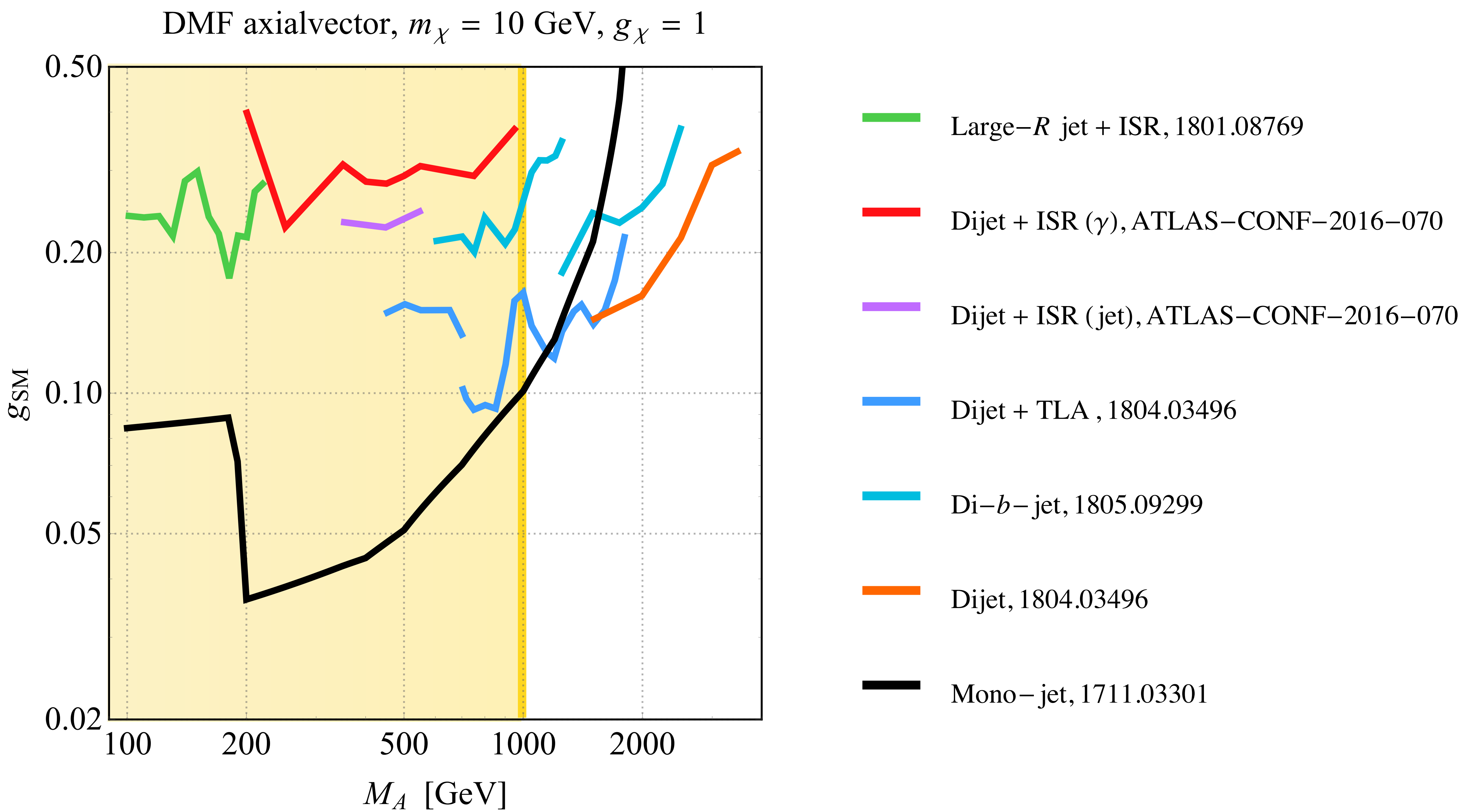

Mono-jet searches superior for lighter mediators, unless model has non-zero lepton couplings which leads to strong dimuon constraints

From LHC bounds …

[ATLAS-CONF-2018-051]

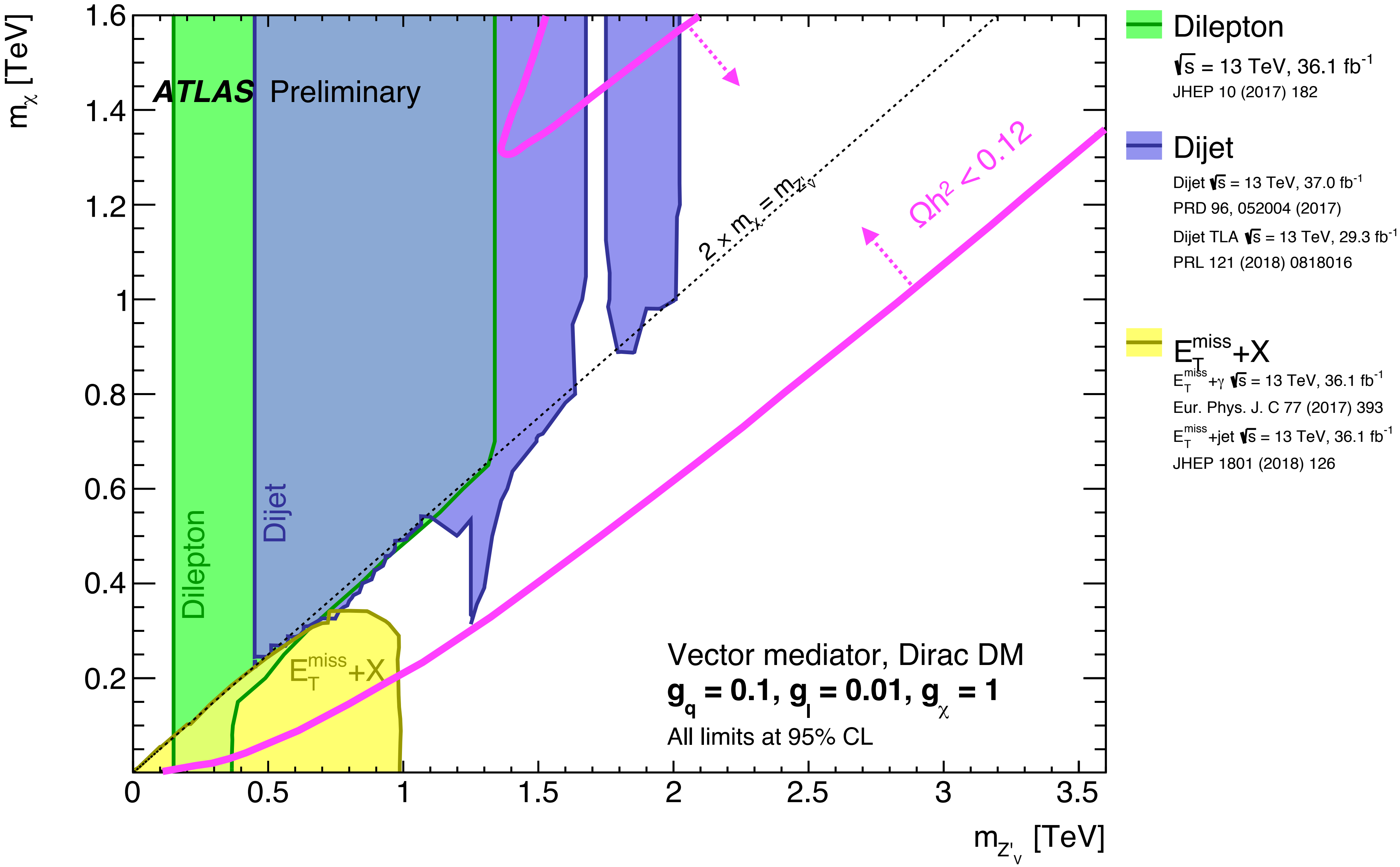

… using an EFT …

Most general EFT needed to describe χ-N interactions contains up to 14 different operators that induce 6 types of nuclear response functions:

$$\boxed{\mathcal{O}_1 = 1_\chi 1_N}$$
$$\mathcal{O}_3 = i\vec{S}_N \cdot \left[\frac{\vec{q}}{m_N} \times \vec{v}^\perp\right]$$
$$\boxed{\mathcal{O}_4 = \vec{S}_\chi \cdot \vec{S}_N}$$
$$\mathcal{O}_5 = i\vec{S}_\chi \cdot \left[\frac{\vec{q}}{m_N} \times \vec{v}^\perp\right]$$
$$\mathcal{O}_6 = \left[\vec{S}_\chi \cdot \frac{\vec{q}}{m_N}\right]\left[\vec{S}_N \cdot \frac{\vec{q}}{m_N}\right]$$
$$\mathcal{O}_7 = \vec{S}_N \cdot \vec{v}^\perp$$
$$\mathcal{O}_8 = \vec{S}_\chi \cdot \vec{v}^\perp$$
$$\mathcal{O}_9 = i\vec{S}_\chi \cdot \left[\vec{S}_N \times \frac{\vec{q}}{m_N}\right]$$
$$\mathcal{O}_{10} = i\vec{S}_N \cdot \frac{\vec{q}}{m_N}$$
$$\mathcal{O}_{11} = i\vec{S}_\chi \cdot \frac{\vec{q}}{m_N}$$
$$\mathcal{O}_{12} = \vec{S}_\chi \cdot \left[\vec{S}_N \times \vec{v}^\perp\right]$$
$$\mathcal{O}_{13} = i\left[\vec{S}_\chi \cdot \vec{v}^\perp\right]\left[\vec{S}_N \cdot \frac{\vec{q}}{m_N}\right]$$
$$\mathcal{O}_{14} = i\left[\vec{S}_\chi \cdot \frac{\vec{q}}{m_N}\right]\left[\vec{S}_N \cdot \vec{v}^\perp\right]$$
$$\mathcal{O}_{15} = -\left[\vec{S}_\chi \cdot \frac{\vec{q}}{m_N}\right]\left[\left(\vec{S}_N \times \vec{v}^\perp\right) \cdot \frac{\vec{q}}{m_N}\right]$$

spin-independent (SI)

spin-dependent (SD)

[Fitzpatrick et al., 1203.3542, 1211.2818; Anand et al., 1308.2288, 1405.6690; …]

… to direct detection (DD) limits …

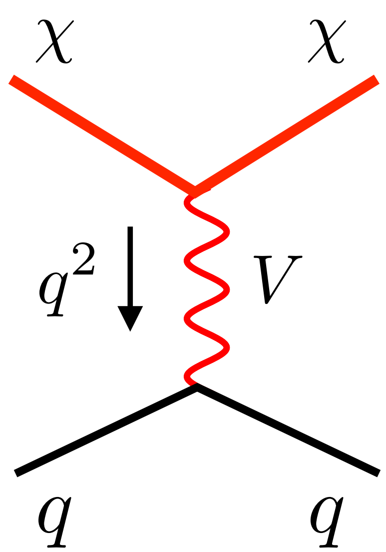

$$= \; -\frac{g_\chi g_q}{M_V^2} \cdot$$

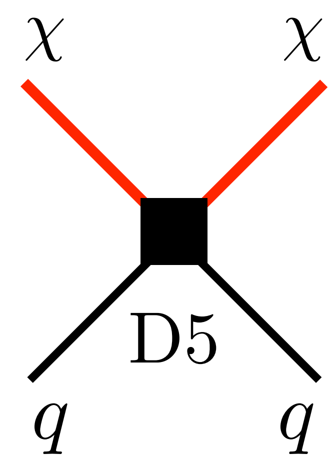

$$+ \; \mathcal{O}(q^2/M_V^2)$$

$$\mathrm{D5} = \bar{\chi}\gamma^\mu\chi\bar{q}\gamma_\mu q \quad \longrightarrow \quad \mathcal{O}_1 = 1_\chi \, 1_N$$

$$\sigma_{\mathrm{SI}} \simeq 6.9 \cdot 10^{-41}\,\mathrm{cm}^2 \left(\frac{g_\chi g_q}{0.25}\right)^2 \left(\frac{1\,\mathrm{TeV}}{M_V}\right)^4 \left(\frac{\mu_{n\chi}}{1\,\mathrm{GeV}}\right)^2$$

… & finally to a plot

[Boveia et al., 1603.04156]

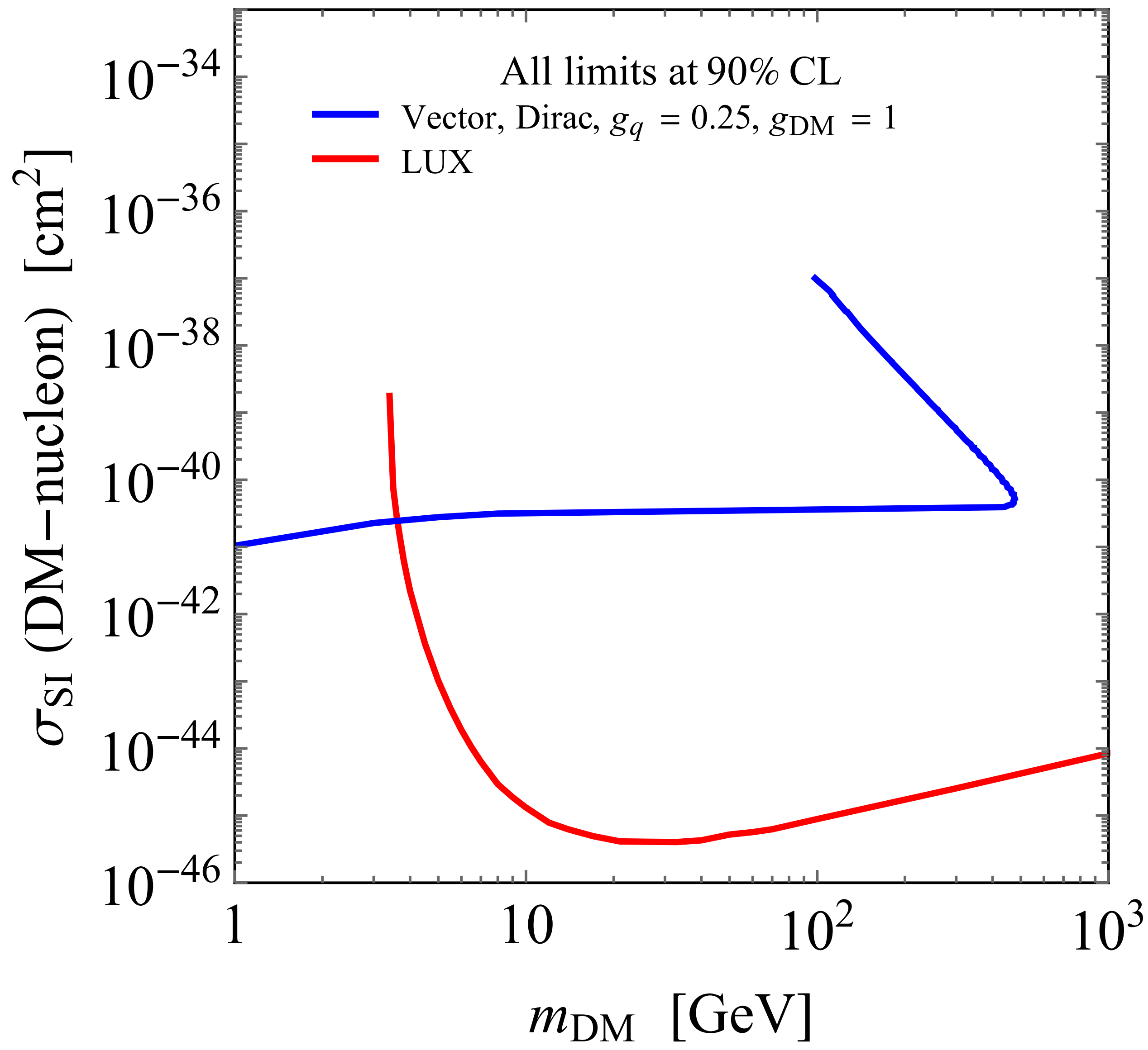

For SI interactions, LHC only competitive for low DM mass, where DD is challenging due to small nuclear recoil

… & finally to a plot

[Boveia et al., 1603.04156]

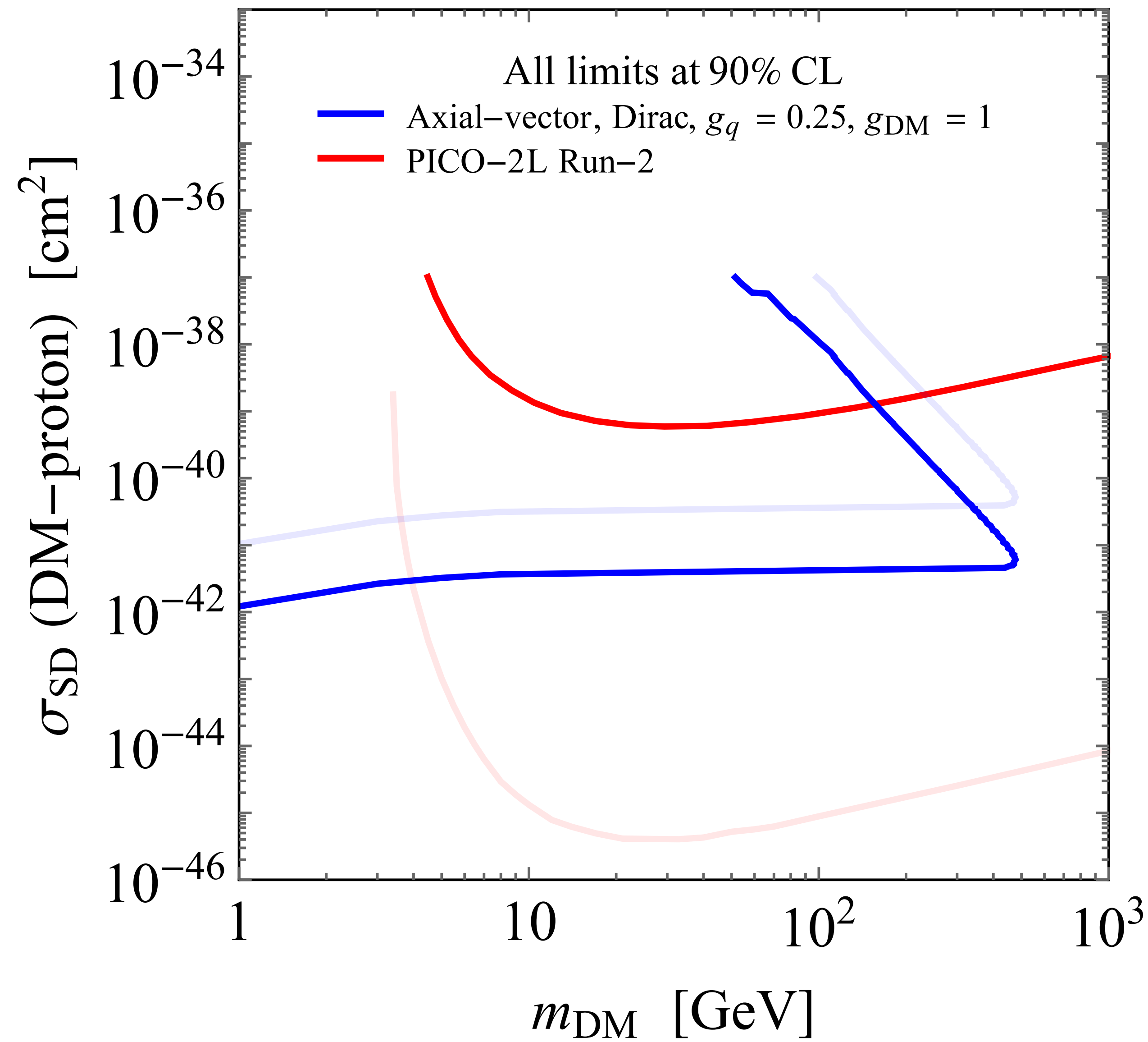

$$\boxed{\mathcal{L}_A} \longrightarrow \bar{\chi}\gamma_\mu\gamma_5\chi\bar{q}\gamma^\mu\gamma_5 q \longrightarrow \boxed{\mathcal{O}_4 = \vec{S}_\chi \cdot \vec{S}_N}$$

… & finally to a plot

[Boveia et al., 1603.04156]

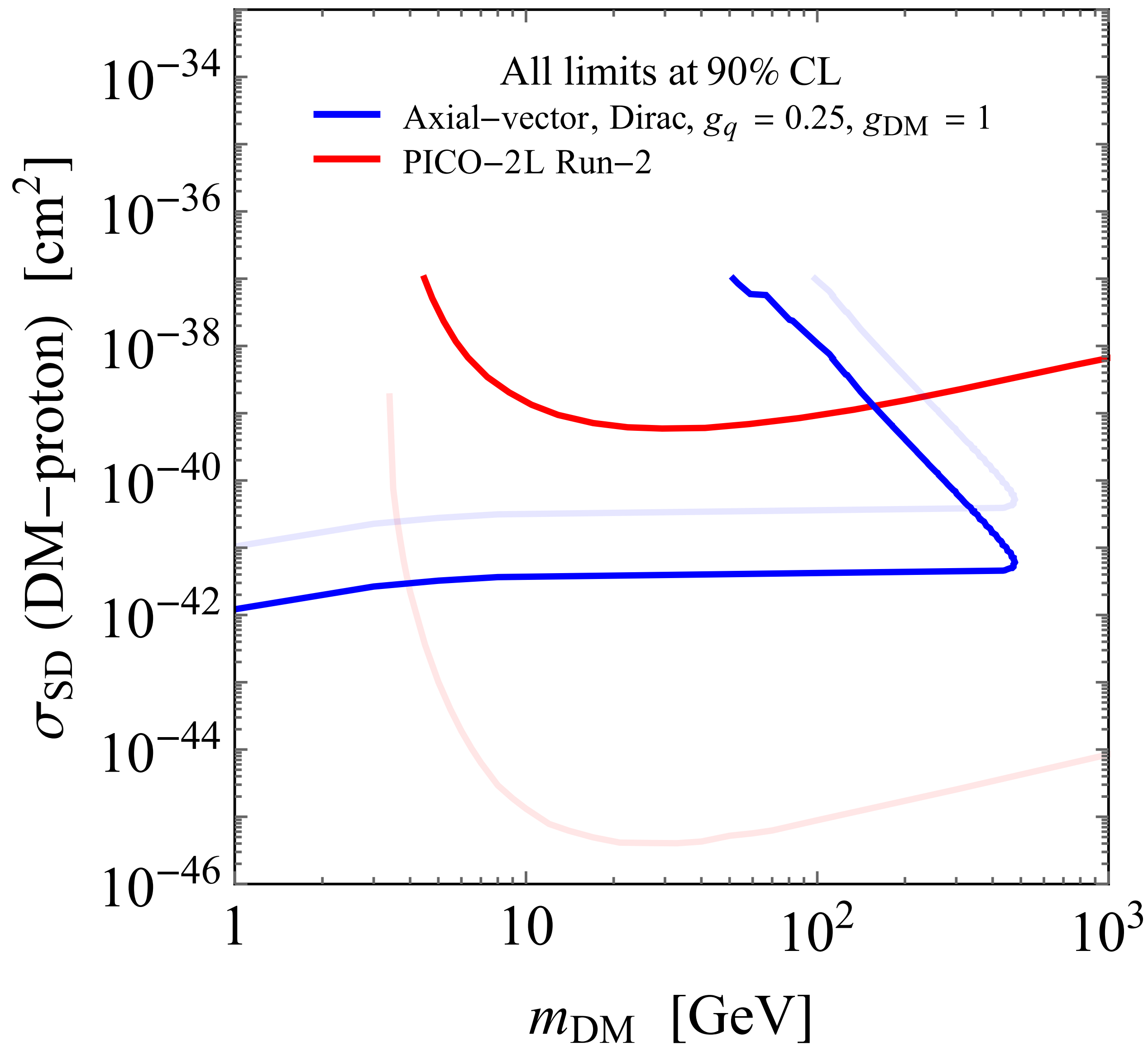

For not too heavy DM, LHC superior to any SD search, because DM-nucleon scattering is incoherent in this case

Spin-0 DM simplified models

$$\mathcal{L}_S \supset g_{\rm SM} \sum_q \frac{y_q}{\sqrt{2}}\, \bar{q} q S$$

$$+\, g_{\rm DM}\, \bar{\chi}\chi S$$

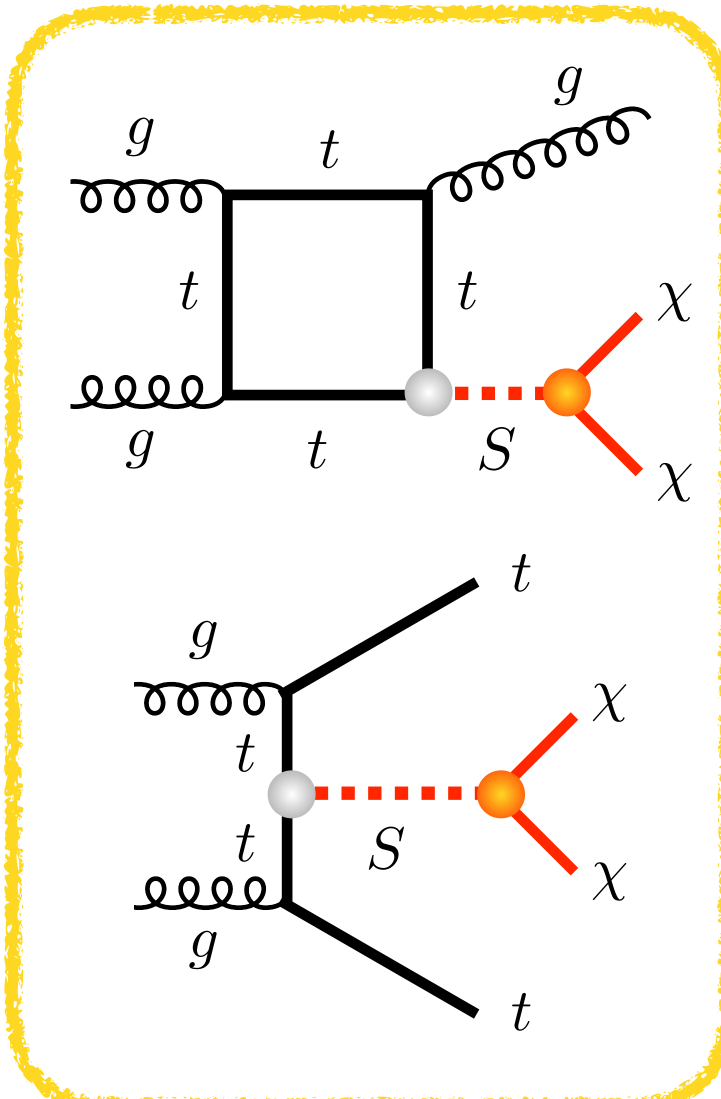

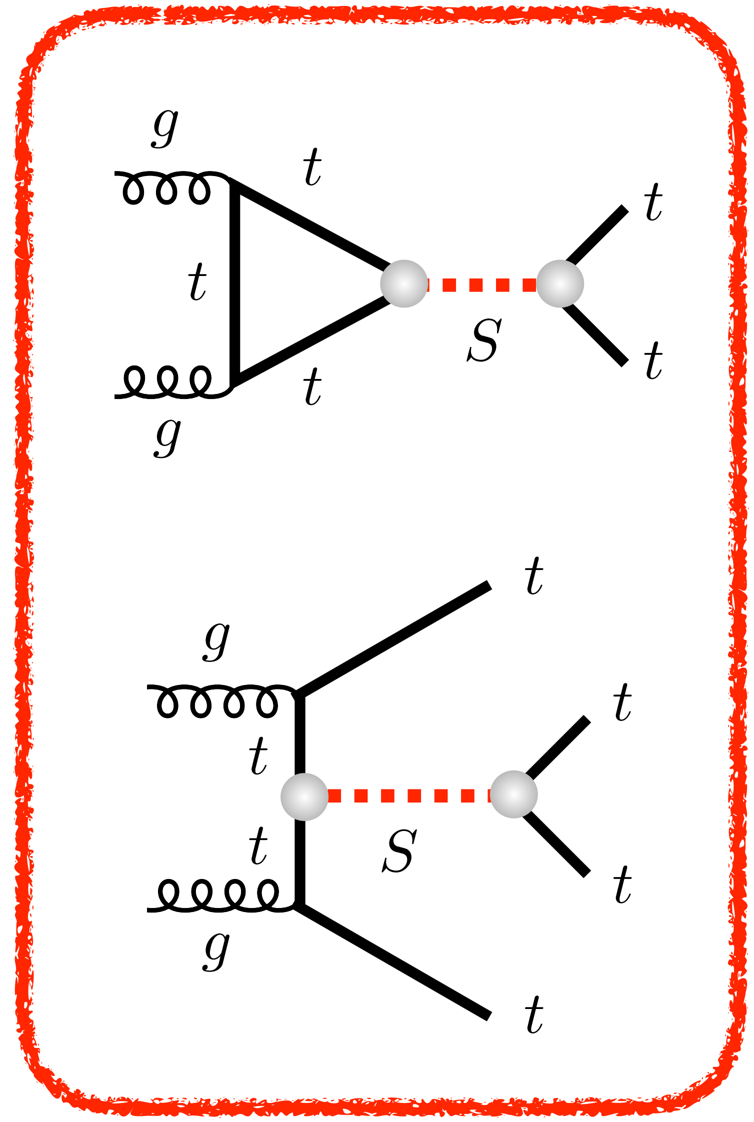

dominant $E_{T,\,\rm miss}$ signal: mono-jet & $t\bar{t}$+$E_{T,\,\rm miss}$

dominant non-$E_{T,\,\rm miss}$ signal: ditop & 4-top production

LHC constraints on spin-0 mediators

[CMS, 1712.02345]

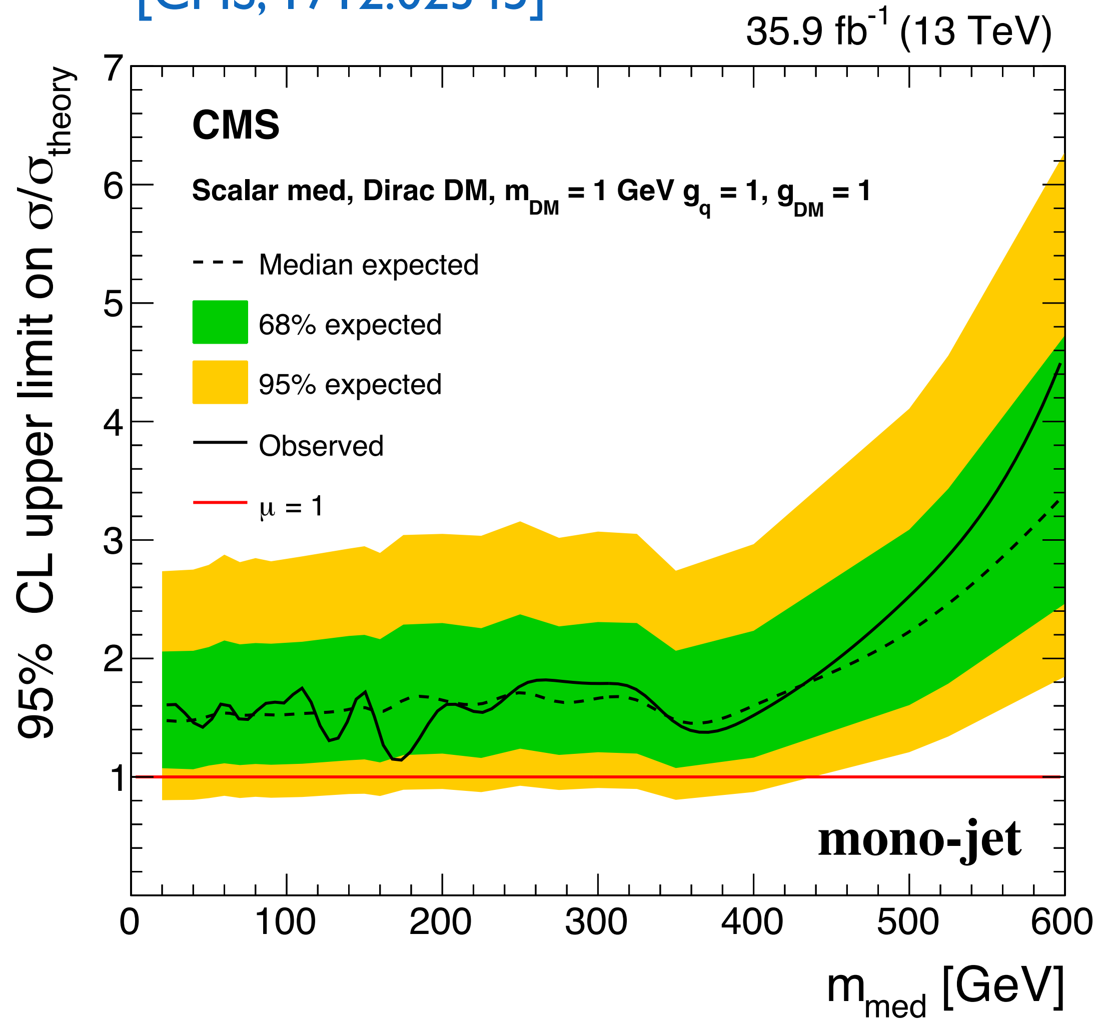

[CMS, 1706.02581]

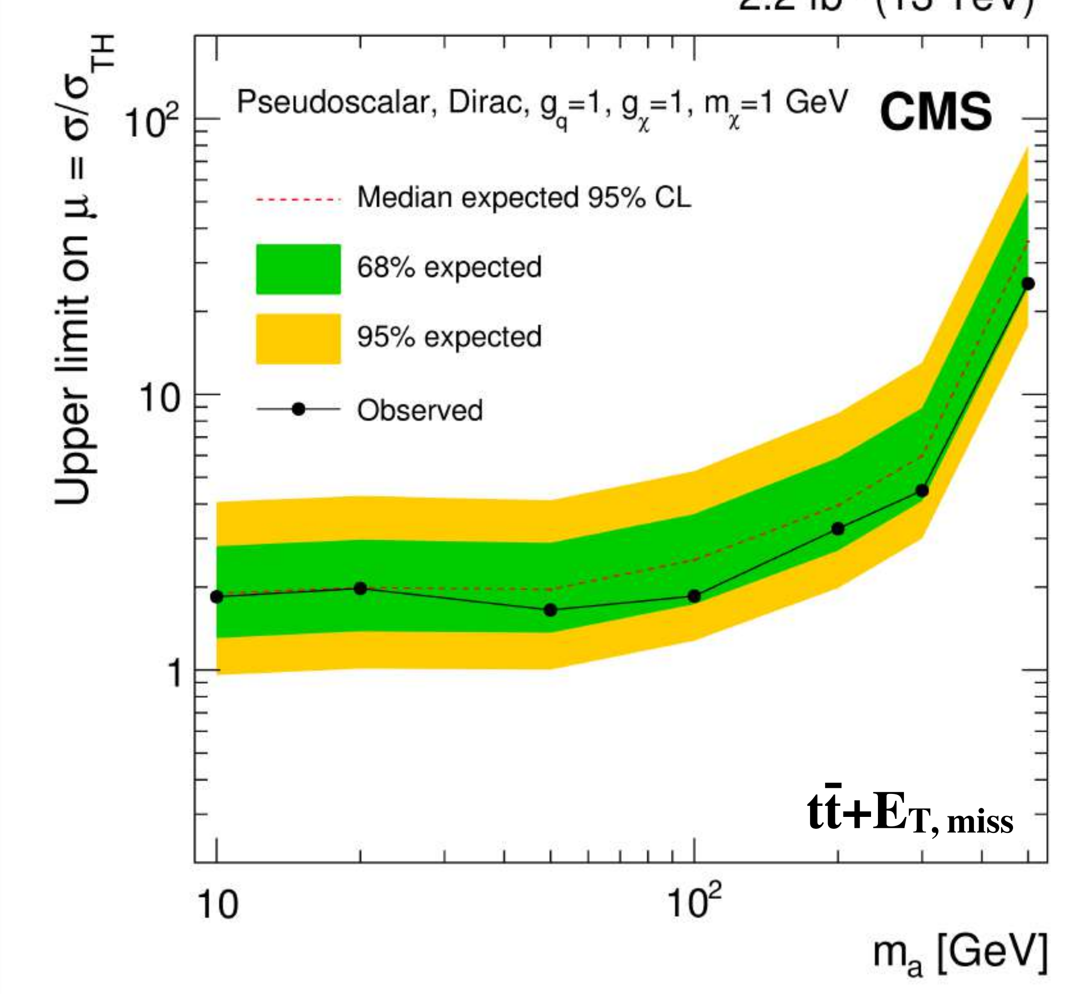

At present, LHC mono-jet & $t\bar{t}+E_{T,\,\mathrm{miss}}$ analyses have limited sensitivity to parameter space of spin-0 DM simplified models. Same statement applies to ditop & 4-top searches. Can one improve sensitivity of $E_{T,\,\mathrm{miss}}$ searches?

Searching for tX+$E_{T, miss}$ production

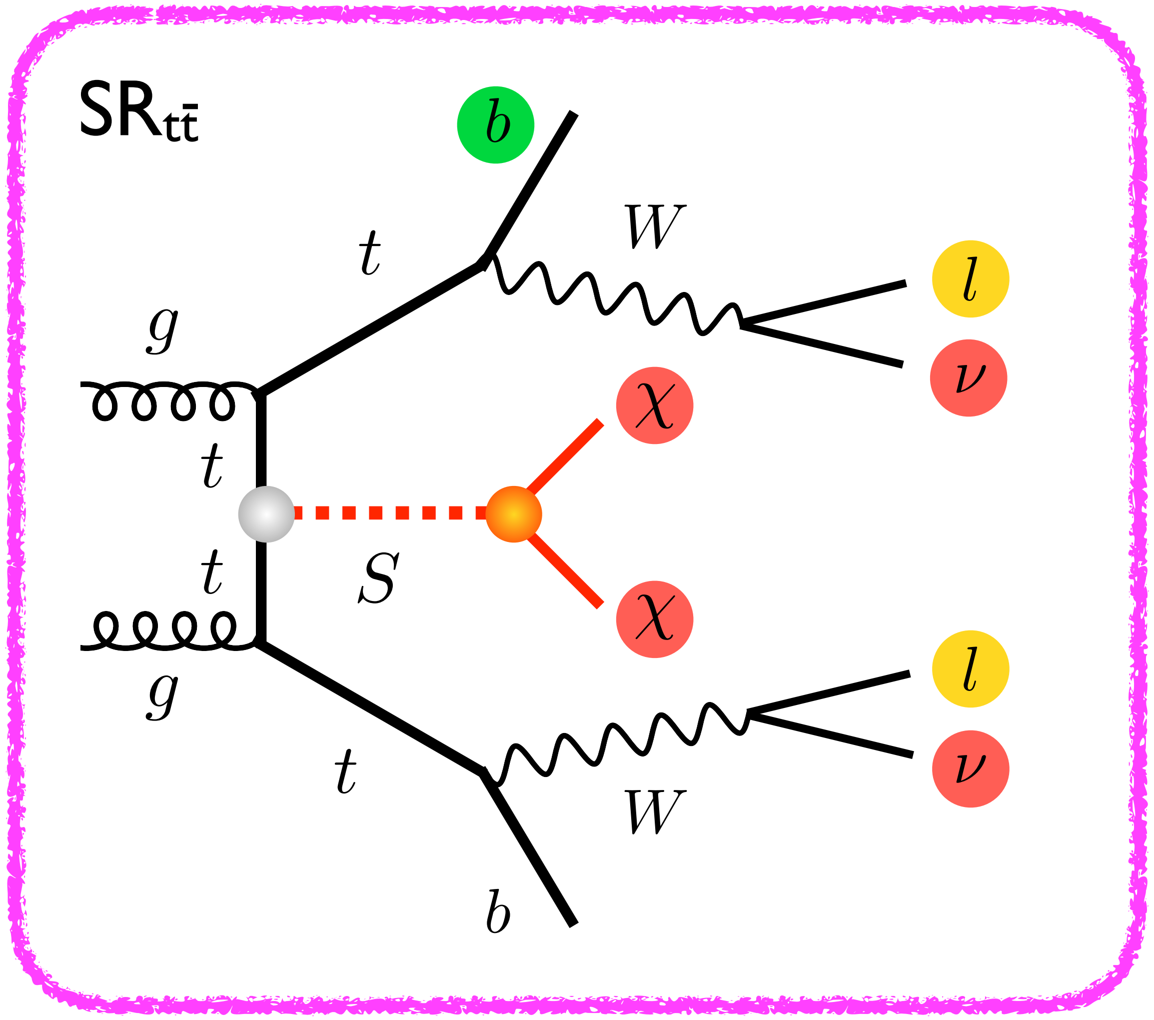

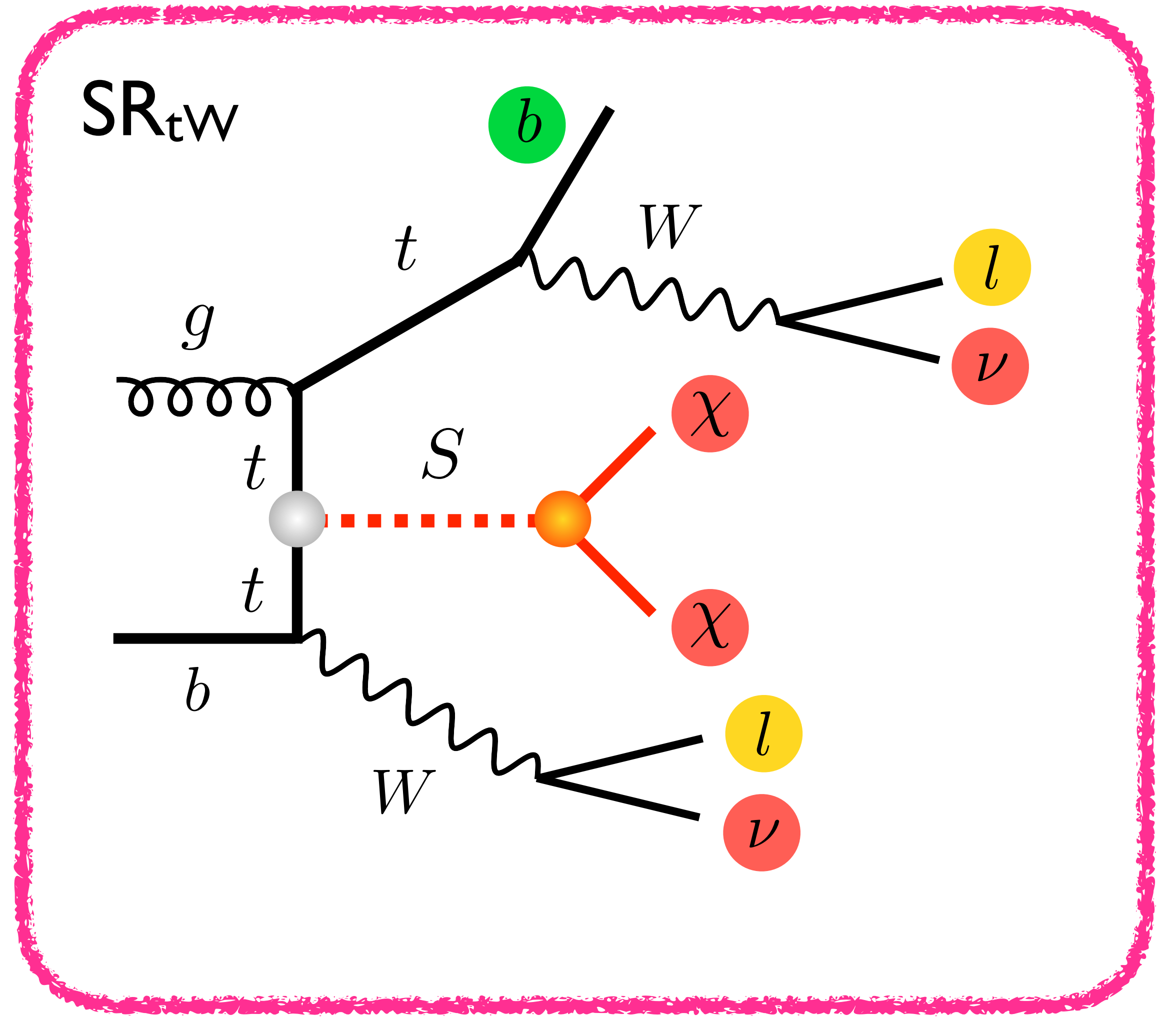

2lb+$E_{T, miss}$ final state receives contributions from $t\bar{t}$+$E_{T, miss}$ & tW+$E_{T, miss}$ channel. To enhance sensitivity of search, design two orthogonal signal regions $SR_{t\bar{t}}$ & SR_{tW} that target the different production mechanisms

Searching for tX+$E_{T,\,\text{miss}}$ production

Invariant mass of b-jet in semi-leptonic top decay bounded by:

$$\sqrt{m_t^2 - m_W^2} \simeq 153\,\text{GeV}$$

Events compatible with two semi-leptonic top decays can hence be selected by using:

$$m_{bl}^t = \min\left(\max\left(m_{l_1 j_a}, m_{l_2 j_b}\right)\right)$$

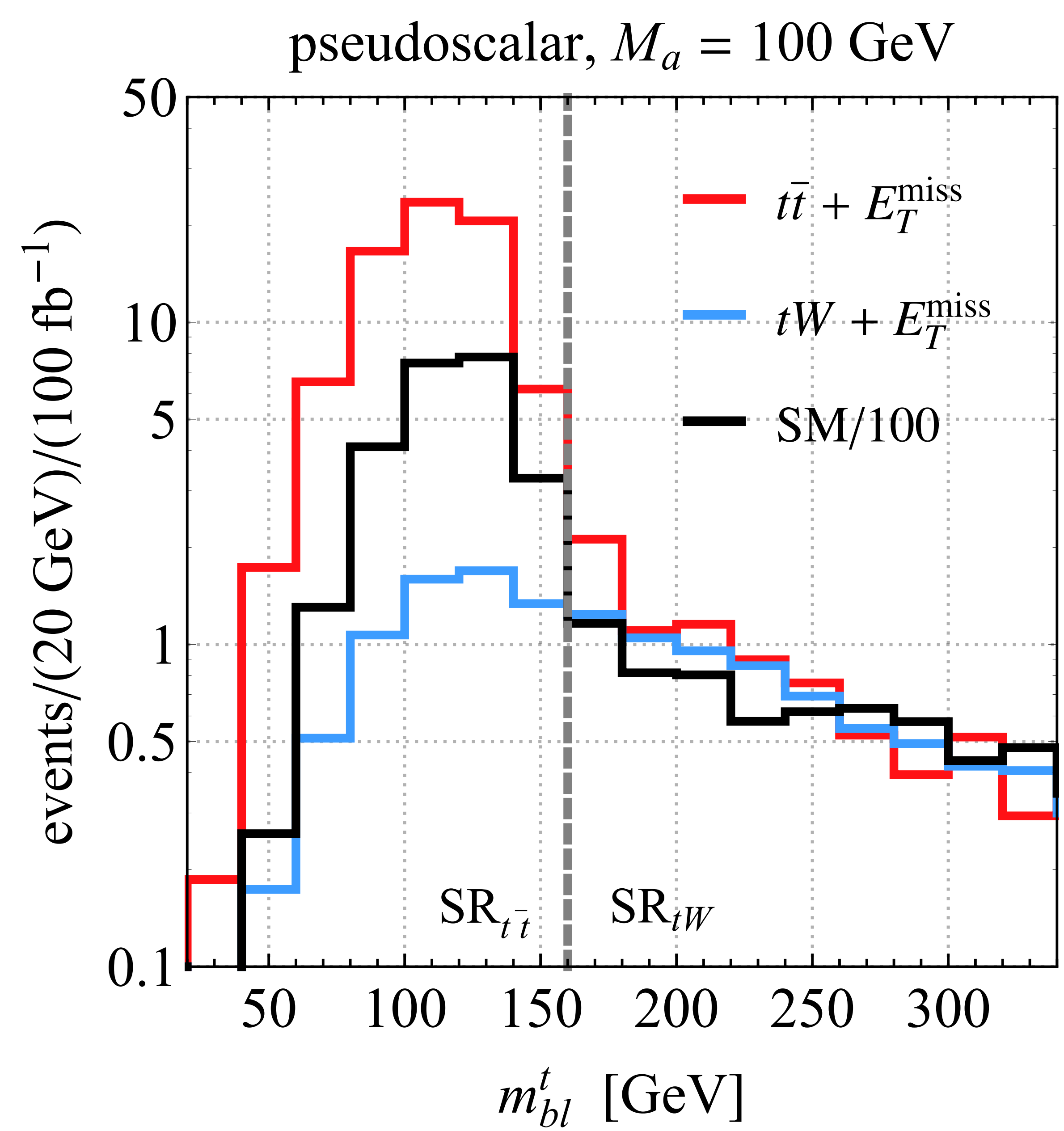

[UH & Polesello, 1812.00694]

Searching for $tX+E_{T,\text{miss}}$ production

	$\mathrm{SR}_{t\bar{t}}$	SR_{tW}
N_l	$= 2, \quad p_{T,l_1} > 25\,\mathrm{GeV}, \quad p_{T,l_2} > 20\,\mathrm{GeV}, \quad \lvert\eta_l\rvert < 2.5$	
m_{ll}	> 20 GeV, Z-boson veto for opposite-sign leptons	
N_b	$> 0, \quad p_{T,b} > 30\,\mathrm{GeV}, \quad \lvert\eta_b\rvert < 2.5$	
m_{T2}	$> 100\,\mathrm{GeV}$	
m^t_{bl}	$< 160\,\mathrm{GeV}$	$> 160\,\mathrm{GeV} \quad \Vert \quad N_j = 1$
$\lvert\Delta\phi_{min}\rvert$	> 0.8	> 0.8
$\lvert\Delta\phi_{\mathrm{boost}}\rvert$	< 1.2	n/a
M_{scal}	n/a	$< 500\,\mathrm{GeV}$
C_{em}	$> 200\,\mathrm{GeV}$	$> 200\,\mathrm{GeV}$
$\lvert\cos\theta_{ll}\rvert$	shape fit	shape fit

[UH & Polesello, 1812.00694]

Searching for tX+$E_{T, miss}$ production

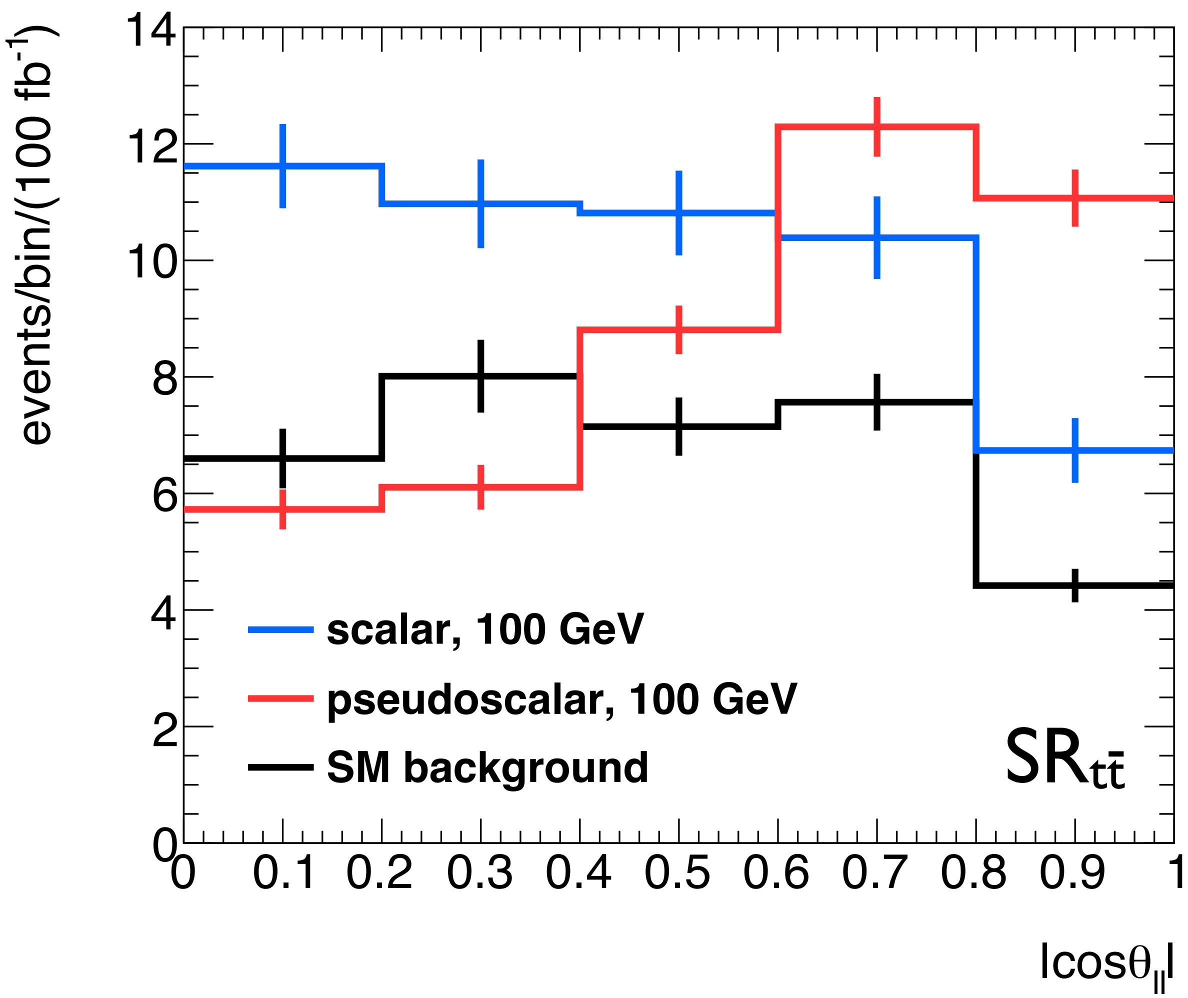

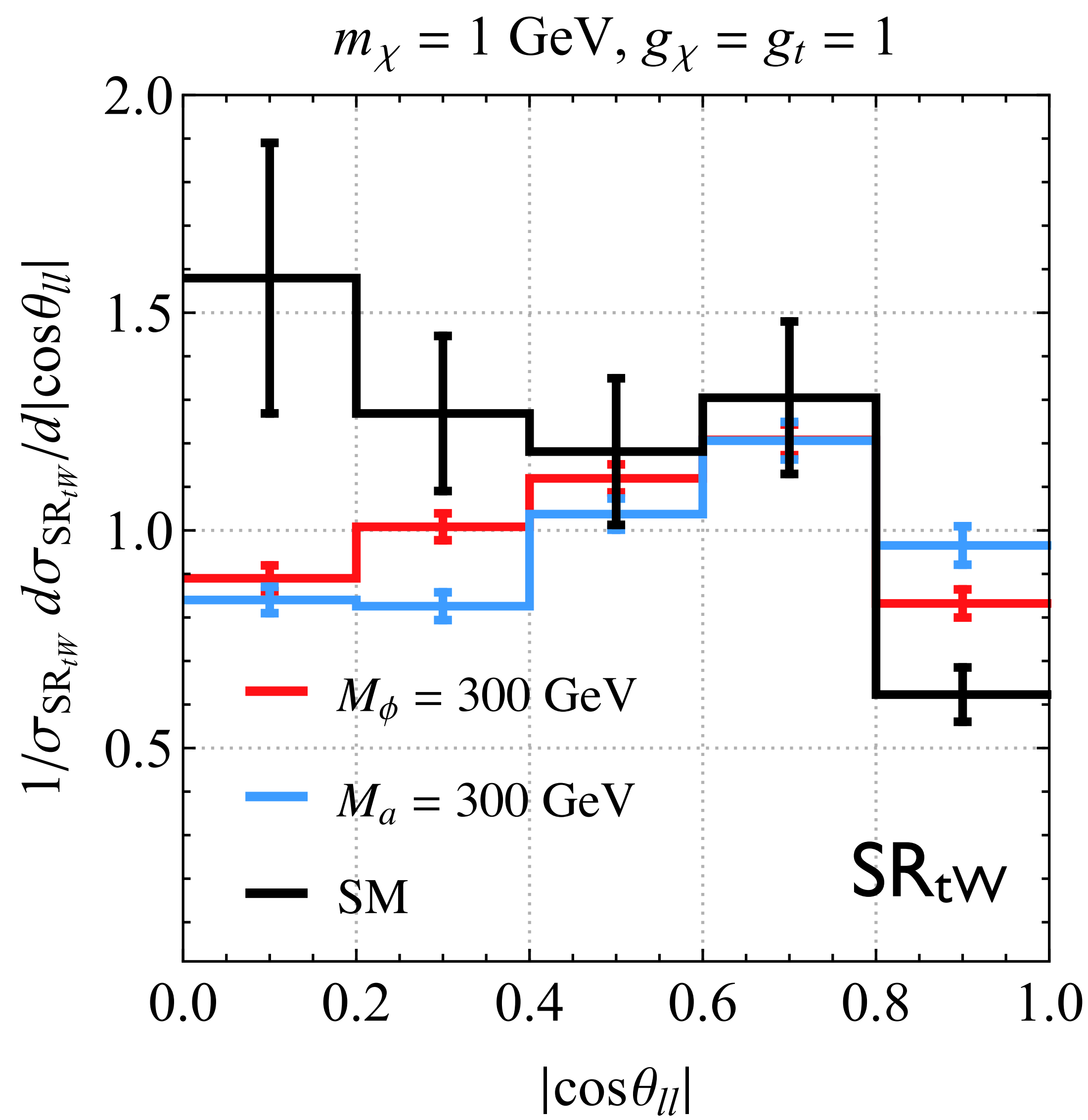

Shape fit to pseudorapidity difference of two leptons $\cos\theta_{ll} = \tanh(\Delta\eta_{ll}/2)$ allows to significantly improve search sensitivity in both signal regions

[UH, Pani & Polesello, 1611.09841; UH & Polesello, 1812.00694]

tX+$E_{T,\text{miss}}$ LHC Run-3 projections

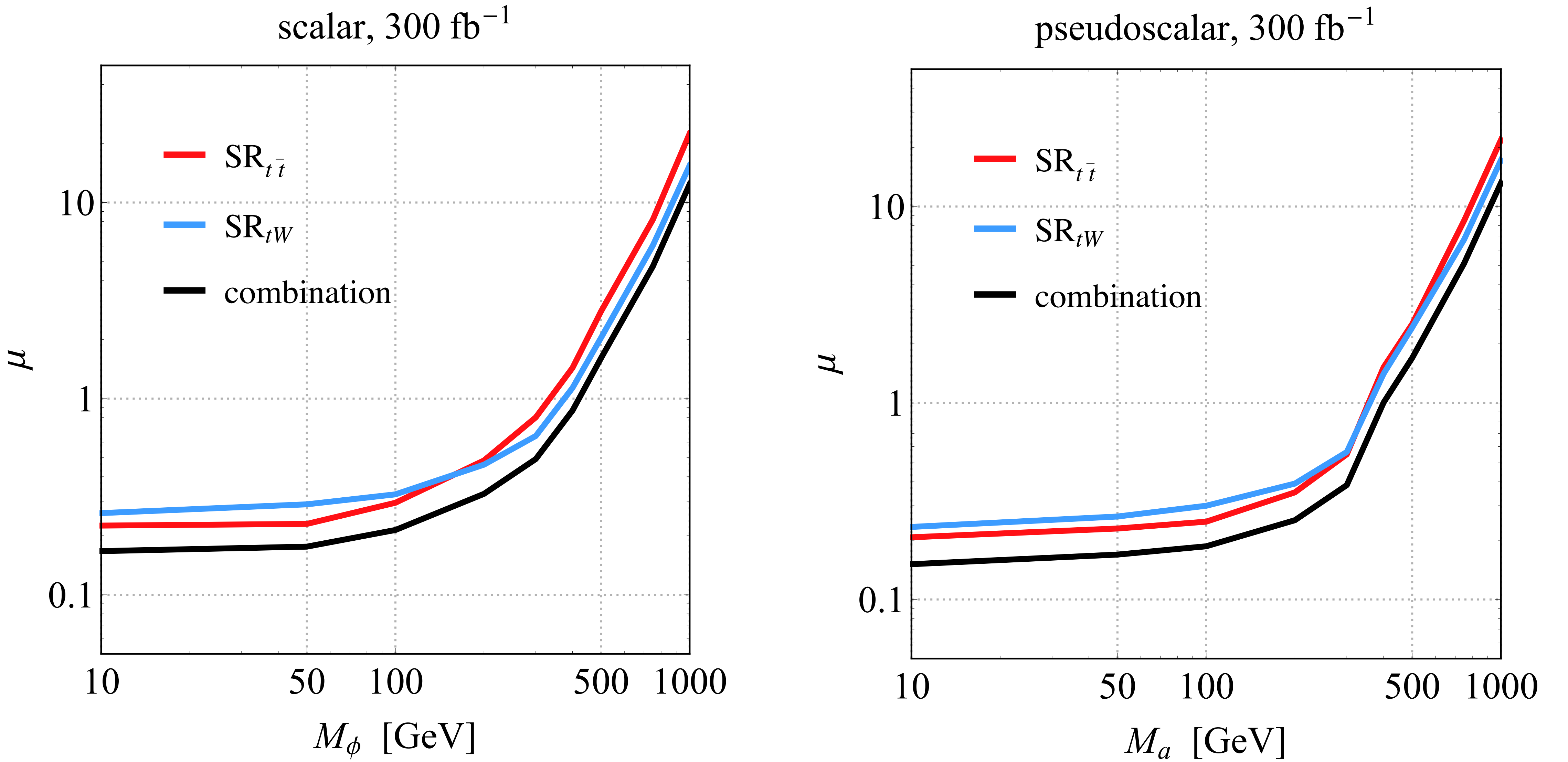

Compared to standard $SR_{t\bar{t}}$ search, sensitivity of combined $SR_{t\bar{t}}$ & SR_{tW} analysis higher by around 20% (80%) at low (high) mediator masses

[UH & Polesello, 1812.00694]

tX+$E_{T,\,miss}$ LHC Run-3 projections

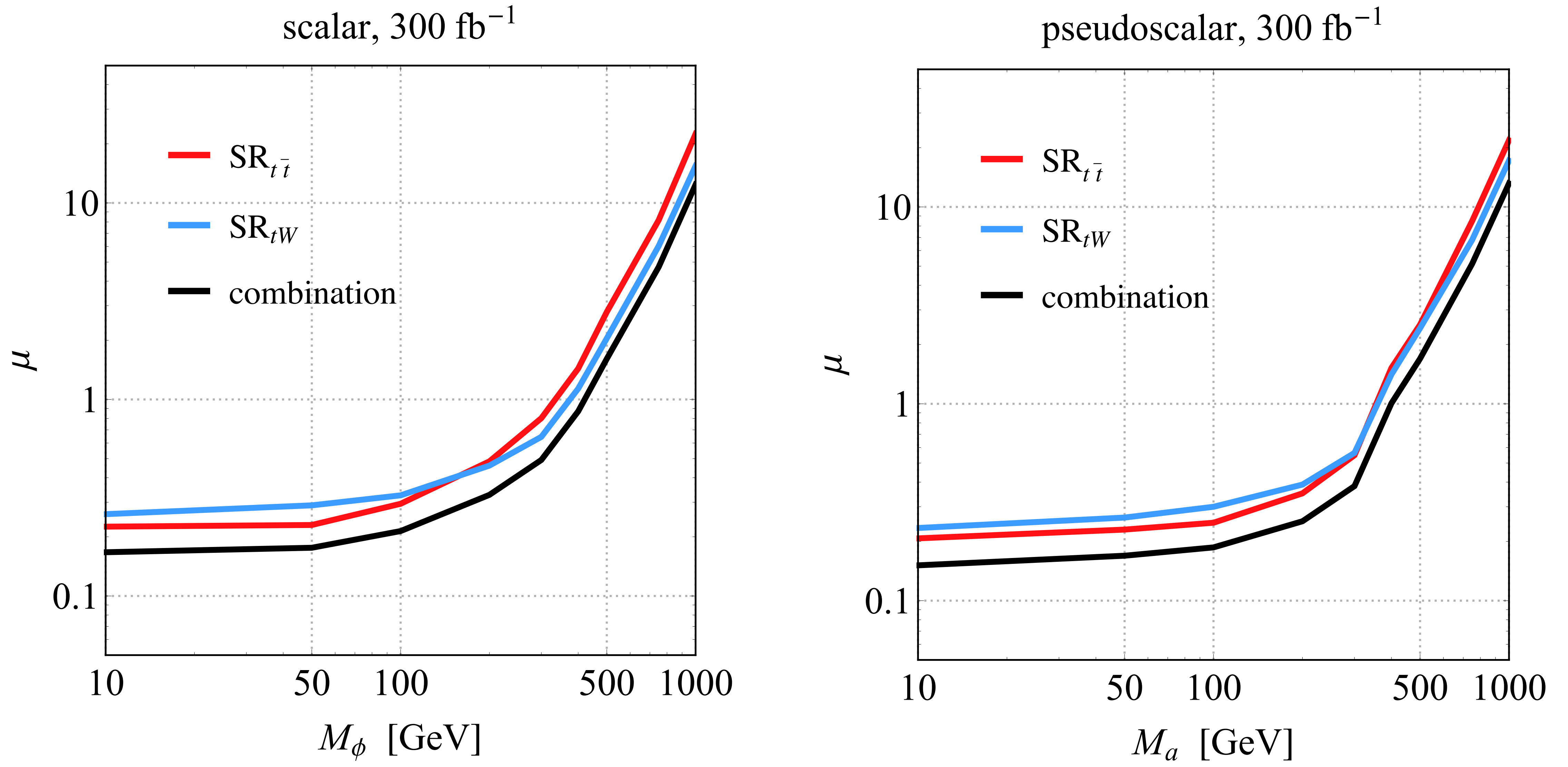

For m_{DM} = 1 GeV & g_{SM} = g_{DM} = 1, combination of SR$_{t\bar{t}}$ & SR$_{tW}$ strategies leads to 95% CL limit $M_{\phi,a} \lesssim$ 410 GeV for 300 fb^{-1} of 14 TeV LHC data

[UH & Polesello, 1812.00694]

Mono-jet production

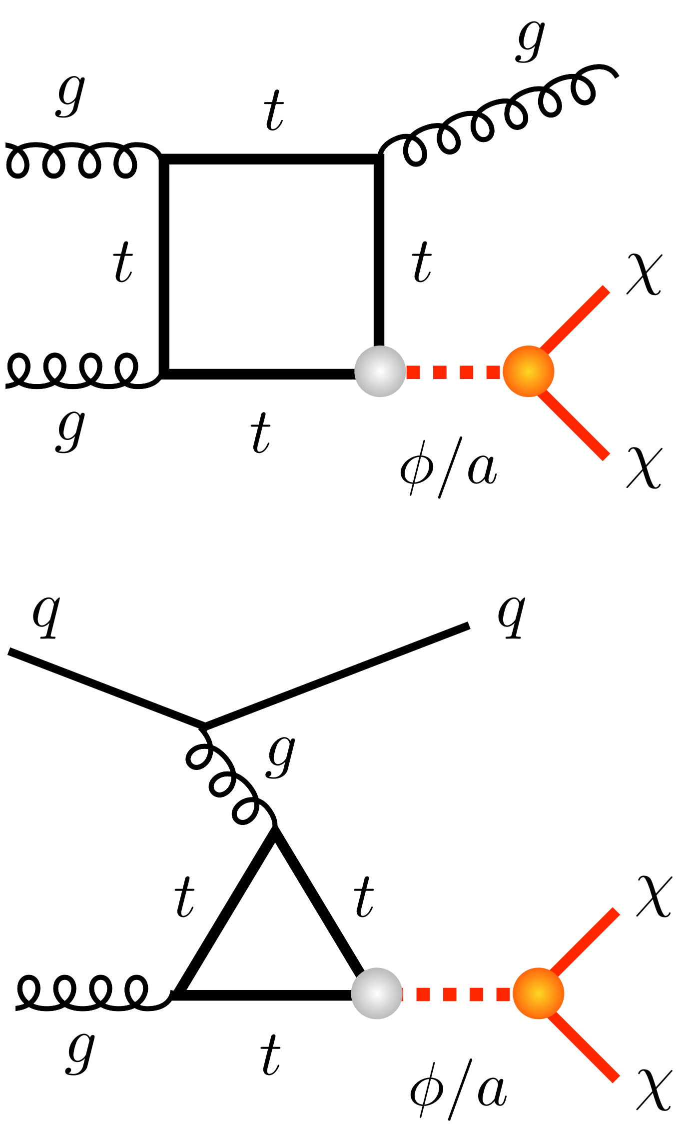

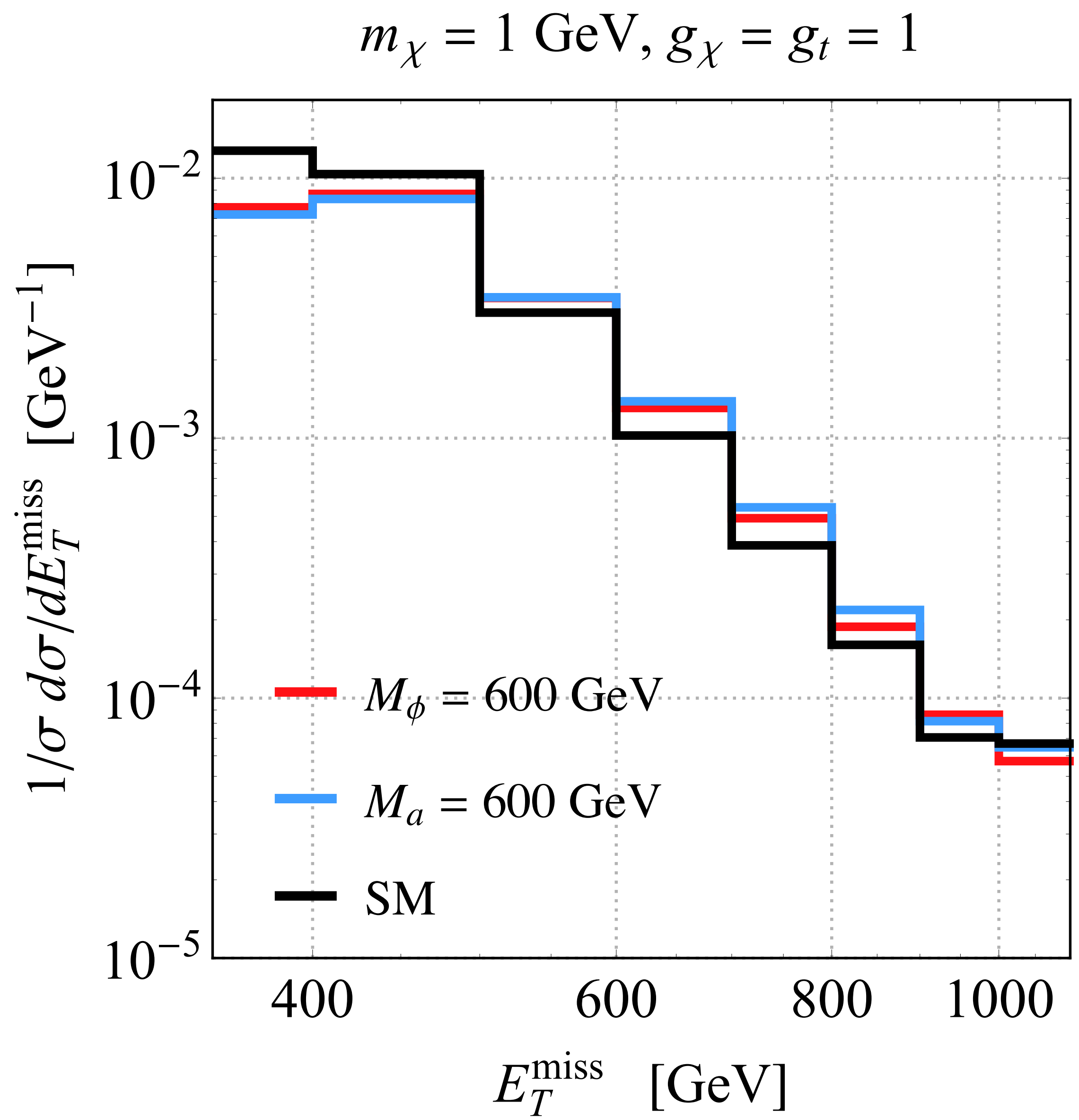

$E_{T,\,miss}$ spectra of scalar & pseudoscalar mediators almost identical. Mono-jet searches seem to be insensitive to CP nature of DM-SM interactions

Searching for 2j+$E_{T, miss}$ production

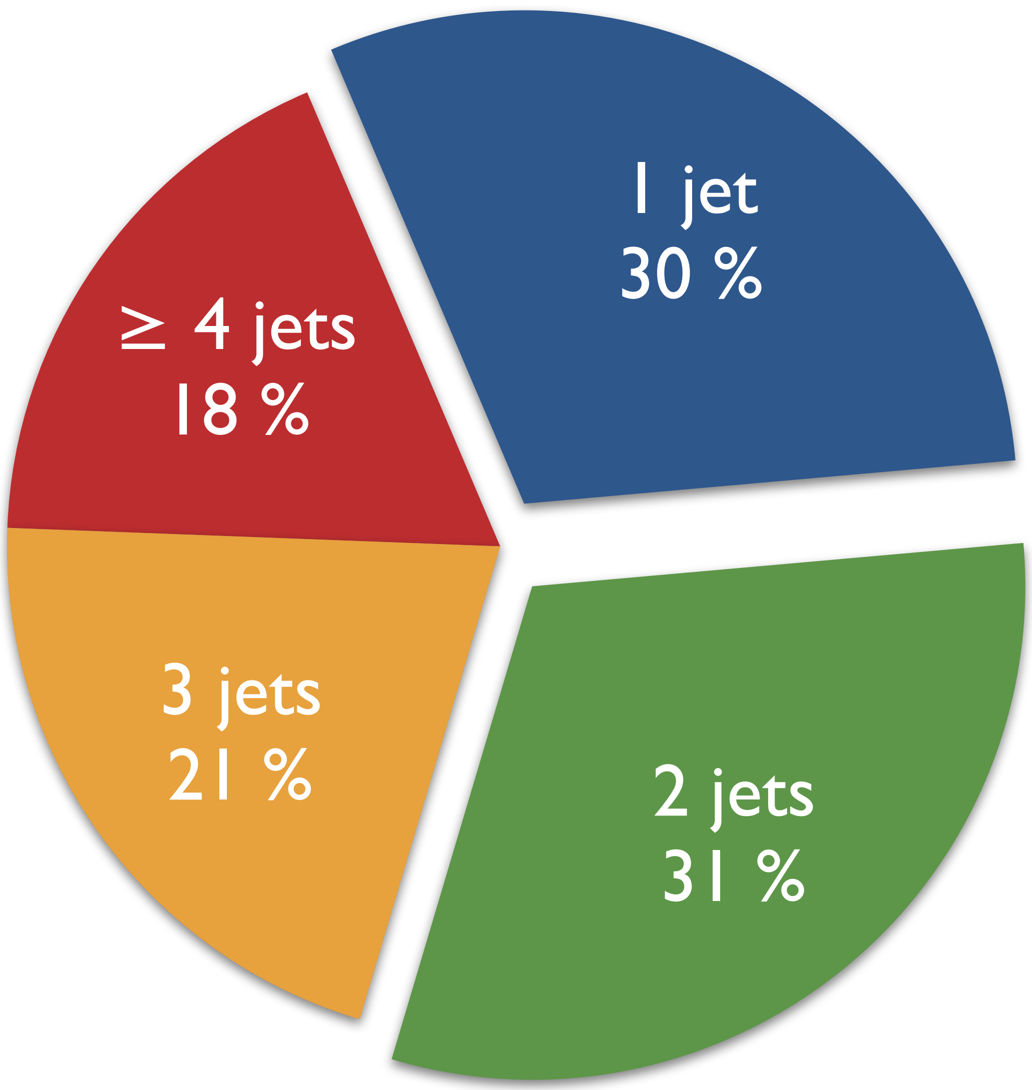

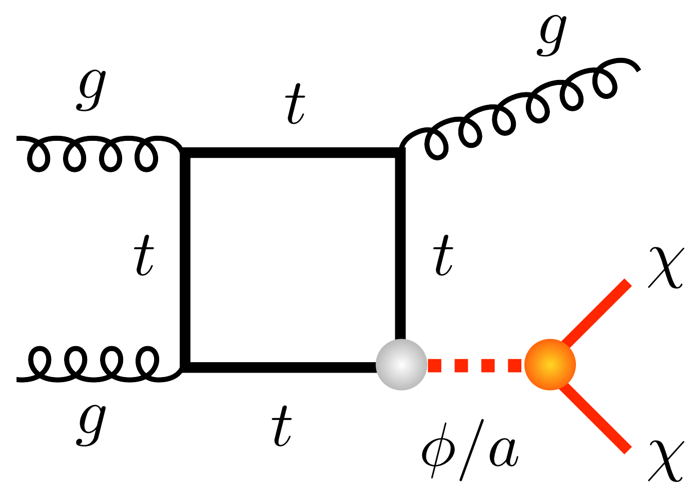

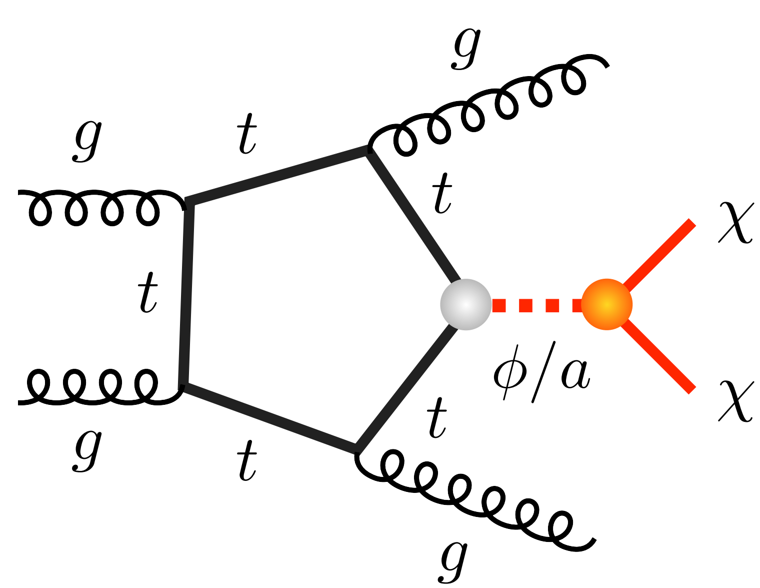

In gluon-fusion induced $E_{T,miss}$ processes such as spin-0 mono-jet production there is a large fraction of events with more than a single jet

Searching for 2j+$E_{T,\text{miss}}$ production

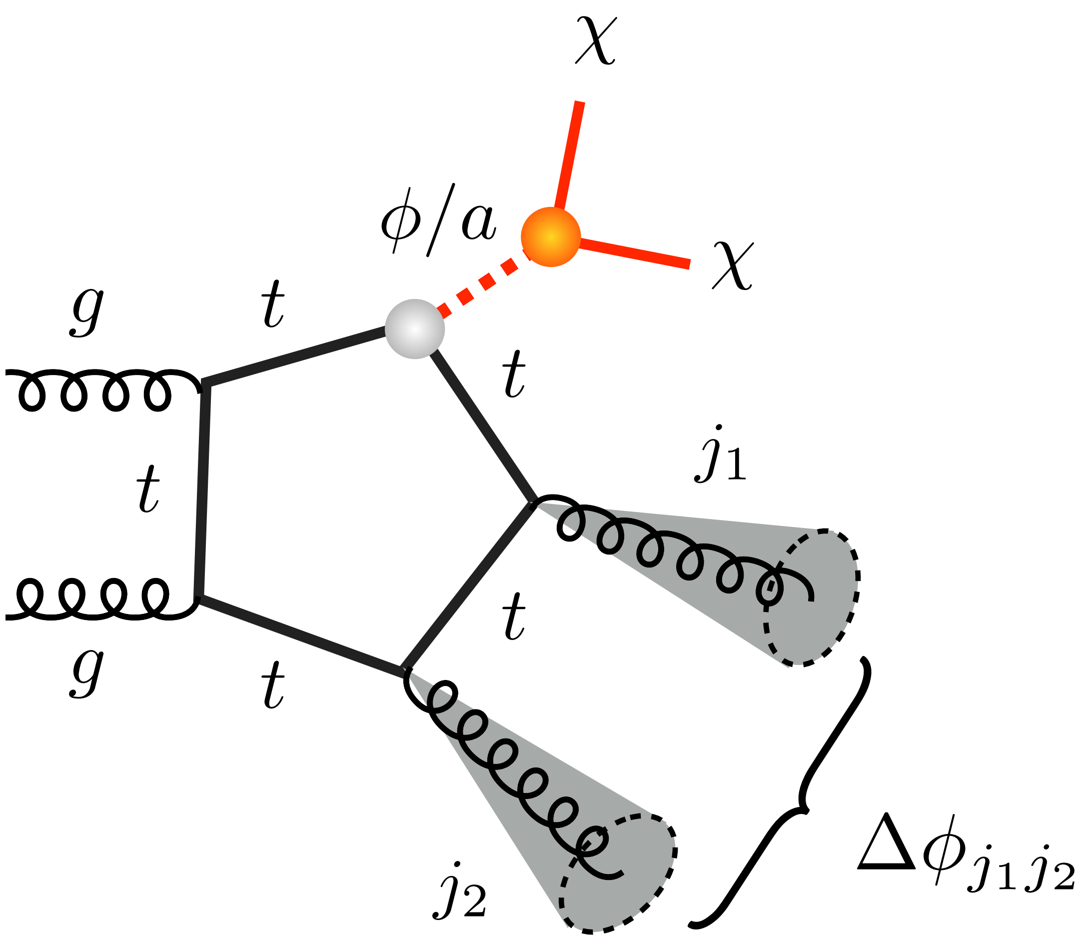

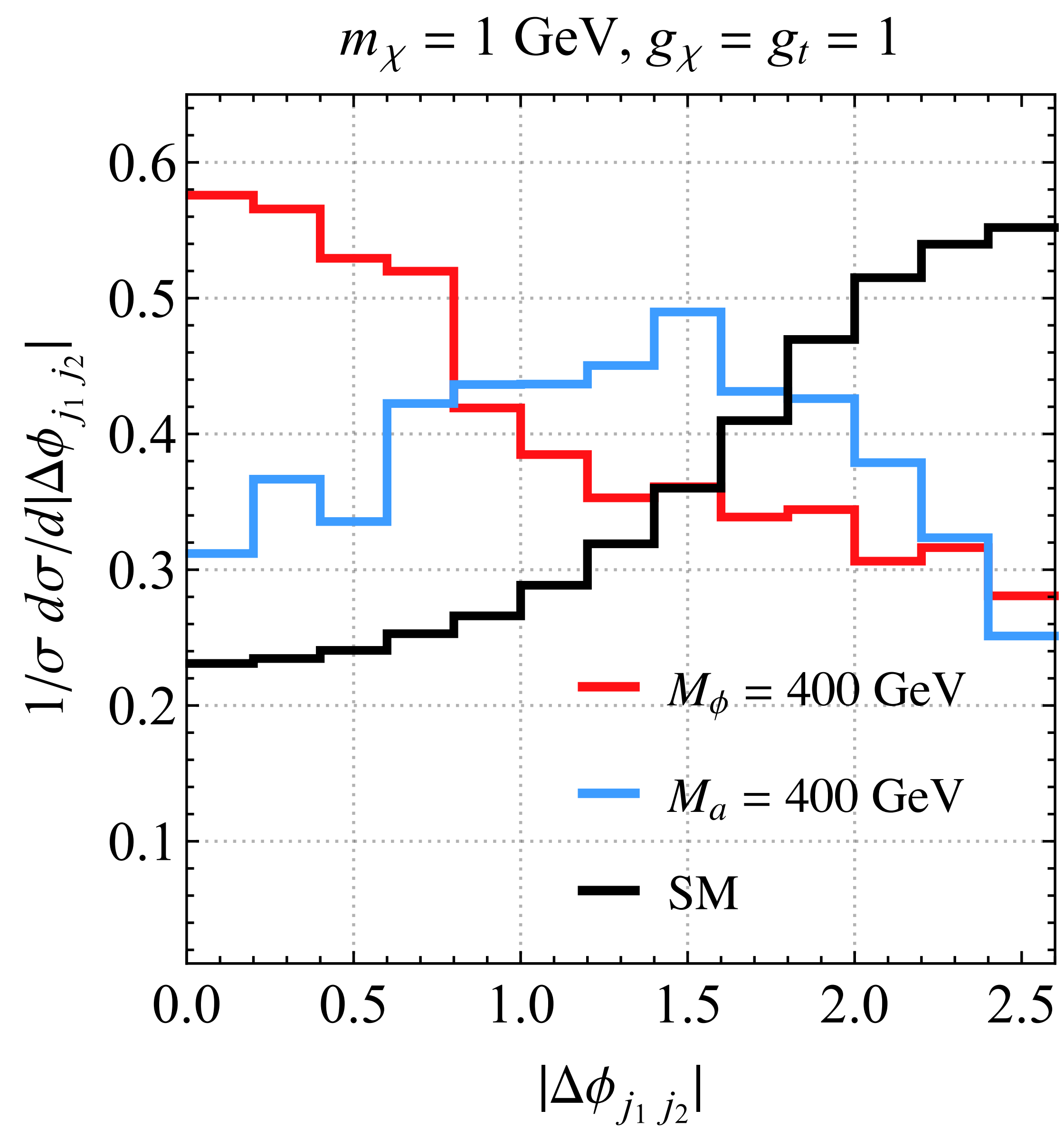

Azimuthal angle difference $\Delta\phi_{j1j2}$ in 2j+$E_{T,\text{miss}}$ events gold-plated observable to disentangle DM spin-0 signals from each other & SM background

[UH, Hibbs & Re, 1311.7131; UH & Polesello, 1812.08129]

Searching for 2j+$E_{T,\text{miss}}$ production

	SR_j	SR_{2j}
E_T^{miss} $\Delta\phi_{\vec{p}_T^{\,\text{miss}}\, j}$	$> 350\,\text{GeV}$ > 0.4	
leading jet	$\lvert\eta_{j_1}\rvert < 2.4\,, \quad p_{T,j_1} > 250\,\text{GeV}$	$\lvert\eta_{j_1}\rvert < 2.4\,, \quad p_{T,j_1} > 100\,\text{GeV}$
subleading jet	$\begin{cases} \text{n/a}\,, & N_j = 1\,, \\ \lvert\eta_{j_2}\rvert < 2.8\,, \quad p_{T,j_2} > 30\,\text{GeV}\,, & N_j > 1 \end{cases}$	$\lvert\eta_{j_2}\rvert < 2.8\,, \quad p_{T,j_2} > 50\,\text{GeV}$
$m_{j_1 j_2}$	$\begin{cases} \text{n/a}\,, & N_j = 1\,, \\ < 500\,\text{GeV}\ (800\,\text{GeV})\,, & N_j > 1 \end{cases}$	$> 500\,\text{GeV}\ (800\,\text{GeV})$

Define signal regions SR_j & SR_{2j} to select one-jet like & two-jet like events & use $\Delta\phi_{j1j2}$ shape to improve signal-to-background separation

[UH & Polesello, 1812.08129]

Mono-jet HL-LHC prospects

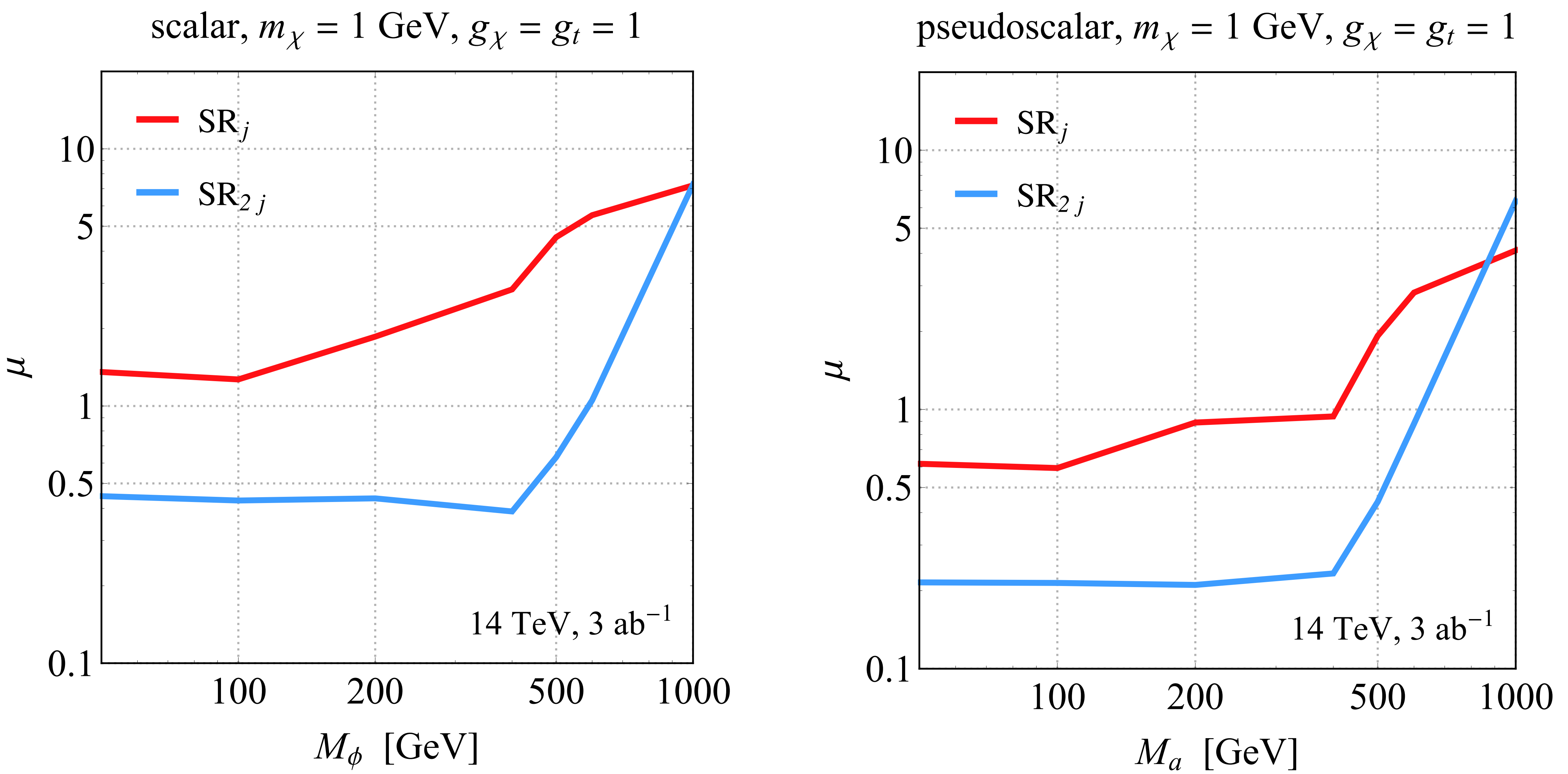

Shape fit to $\Delta\phi_{j1j2}$ observable in SR_{2j} has a significantly better reach than standard SR_j search based on $E_{T,\text{miss}}$ shape analysis

[UH & Polesello, 1812.08129]

Mono-jet HL-LHC prospects

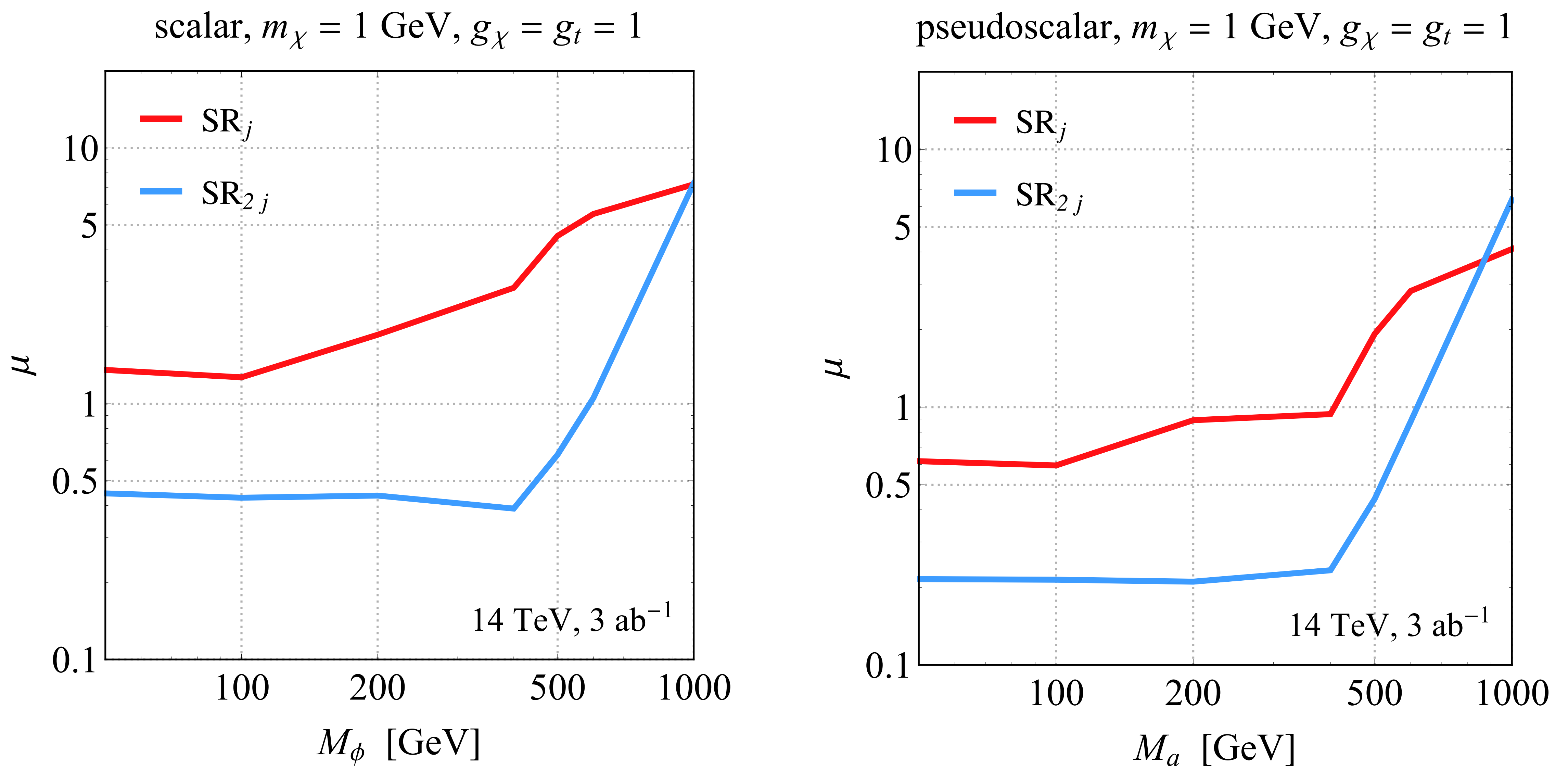

For $m_{DM} = 1$ GeV & $g_{SM} = g_{DM} = 1$, search strategy SR_{2j} leads to 95% CL limits $M_\phi \lesssim 580$ GeV & $M_a \lesssim 600$ GeV for 3 ab^{-1} of 14 TeV data

[UH & Polesello, 1812.08129]

Are simplified models perfect?

Simplified models are minimal extensions of EFT that besides DM typically contain a single mediator. Standard model (SM)- & DM-mediator couplings are treated as free parameters & mechanism that provides mass to mediator & DM is unspecified

In ultraviolet (UV) complete model such as SM, couplings are usually not random but fixed by for example gauge invariance & anomalies. Higgs mechanism also an important ingredient in SM

To UV complete simplified models have to add more structure to them & question is whether this will change phenomenology

Pseudoscalar mono-X amplitudes

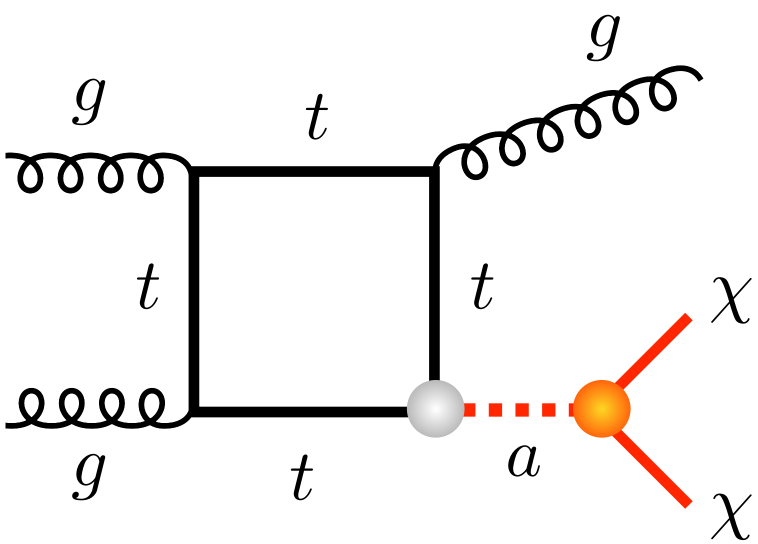

$$\sim \frac{\alpha_s}{4\pi} \, y_t \, g_{\rm SM} \, s^0$$

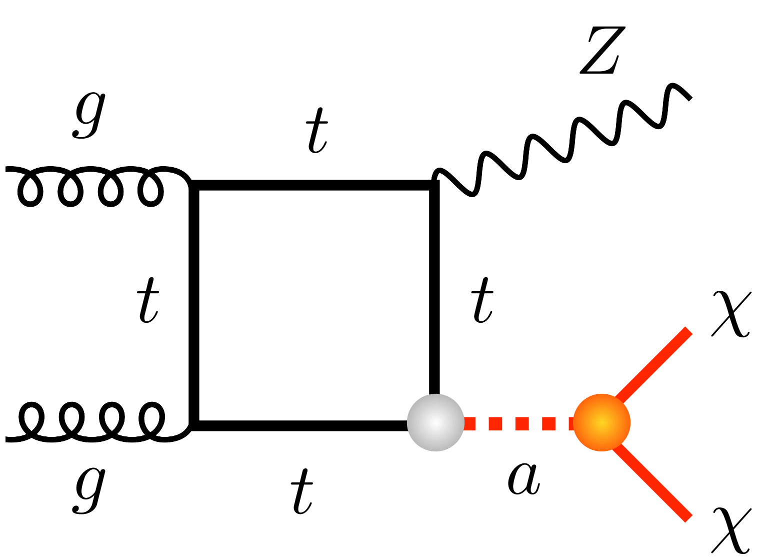

$$\sim \frac{\alpha_s}{4\pi} \, y_t \, g_{\rm SM} \, \ln^2\left(\frac{s}{m_t^2}\right)$$

Logarithmic contribution small unless g_{SM} large & $s^{1/2} \gg 14$ TeV, but …

still can ask …

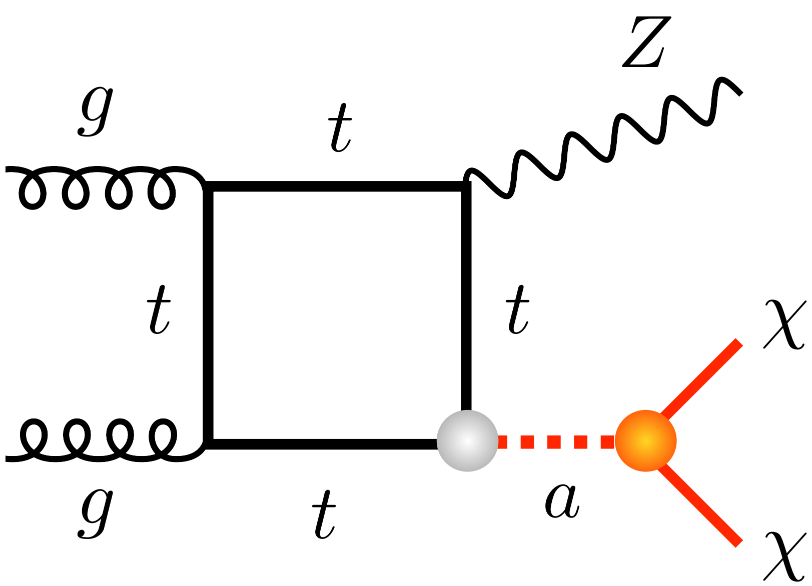

+ ? = finite

still can ask …

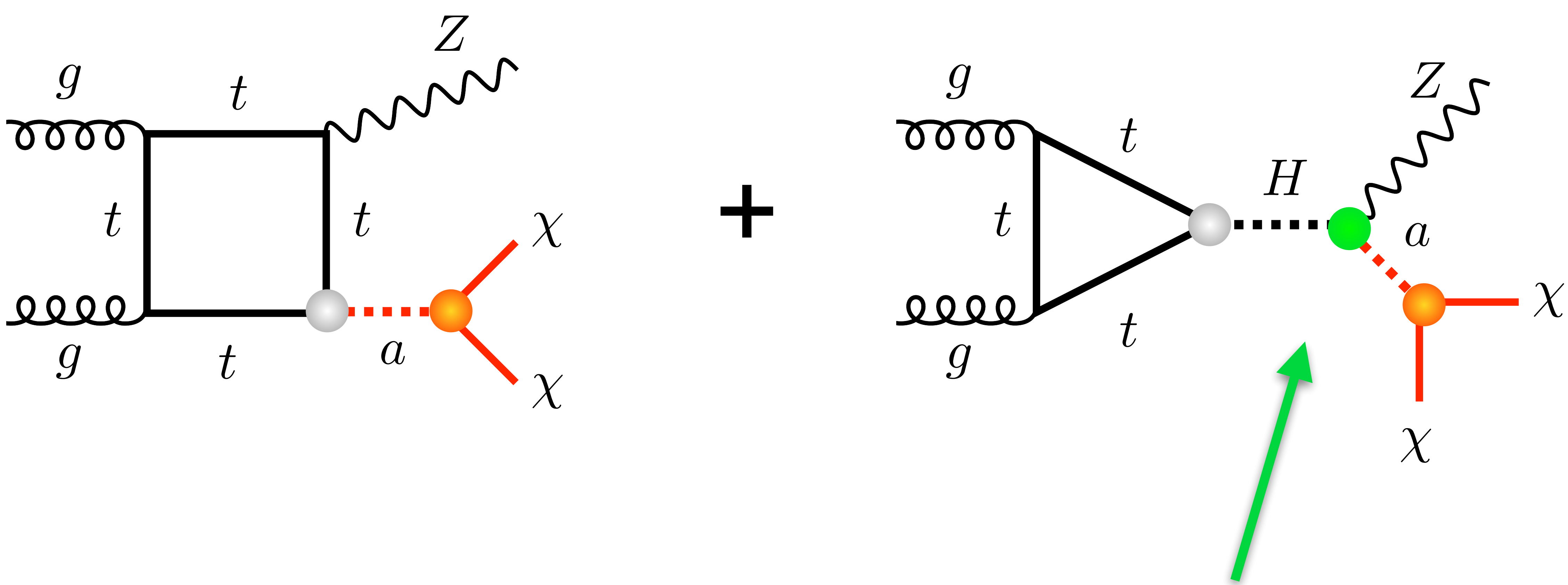

a HaZ coupling only exists in extensions of SM that feature an extended Higgs sector

Consistent spin-0 simplified models

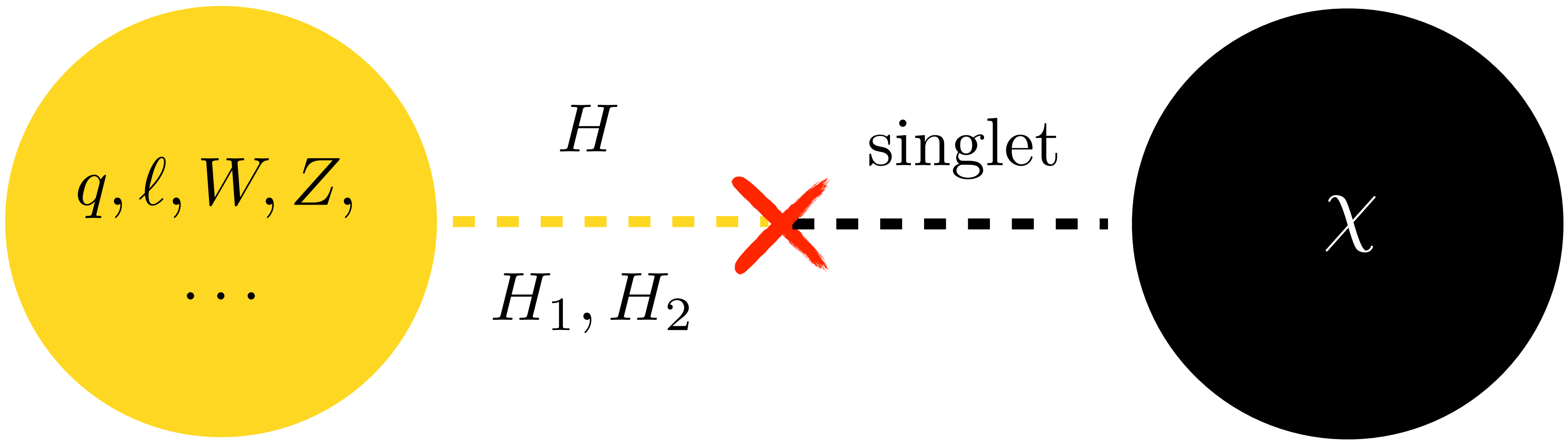

Spin-0 models with fermionic DM can be made $SU(2)_L \times U(1)_Y$ invariant by introducing a new dark Higgs that couples to visible scalar sector. If scalar sector minimal, SM Higgs is mediator & Higgs constraints are severe. But Higgs constraints avoided in decoupling or alignment limit of two-Higgs-doublet model (2HDM) extensions

[Kim et al., 0803.2932; Baek et al., 1112.1847; Lopez-Honorez et al., 1203.2064; Fairbairn & Hogan, 1305.3452; Carpenter, 1312.2592; Berlin et al., 1402.7074, 1502.06000; … ; Ko & Li, 1610.03997; Bell et al., 1612.04593; …]

2HDM+a model

$$\mathcal{L} \supset -\bar{Q} Y_u \tilde{H}_2 d_R + \bar{Q} Y_d H_1 u_R - i b_P P H_1^\dagger H_2 - i y_\chi P \bar{\chi} \gamma_5 \chi + \text{h.c.}$$

$\text{States}: h, H, A, H^\pm, a$

h is SM-like for
cos(β-α) ≃ 0

mostly P for
small θ

$\text{Angles}: \alpha, \beta, \theta$

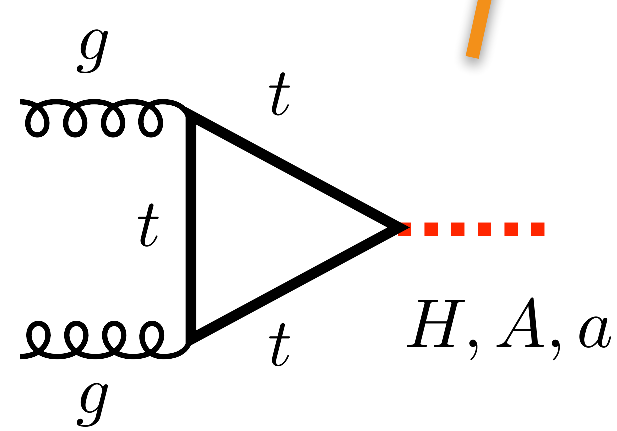

$\propto \dfrac{1}{\tan\beta}$

[Ipek et al. 1404.3716; No, 1509.01110; Goncalves et al., 1611.04593; Bauer et al., 1701.07427]

2HDM+a: constraints

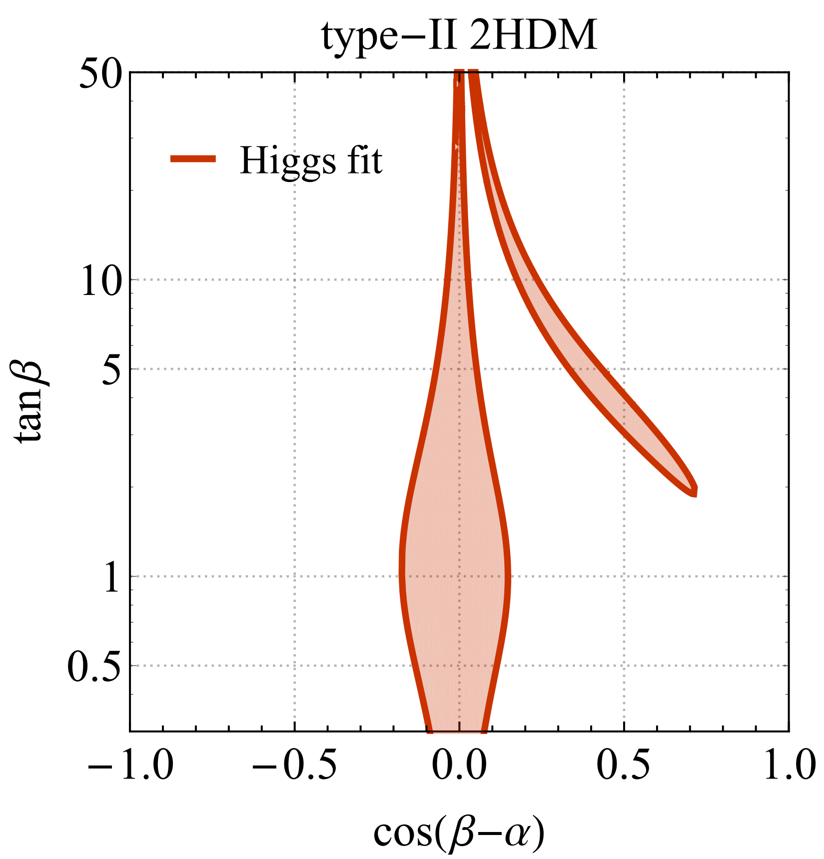

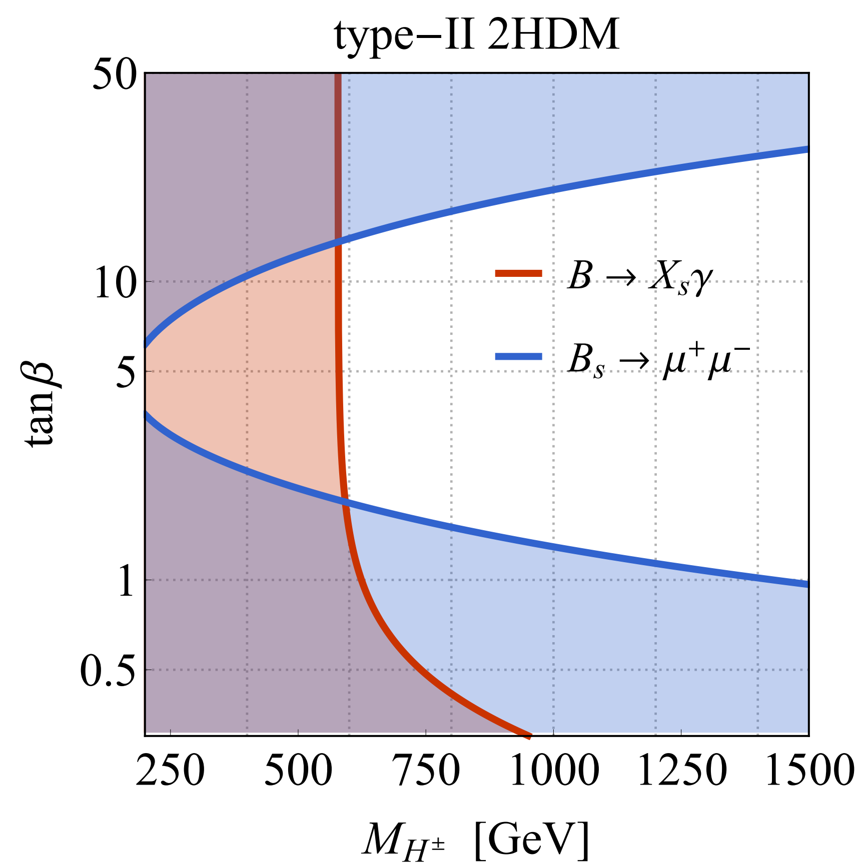

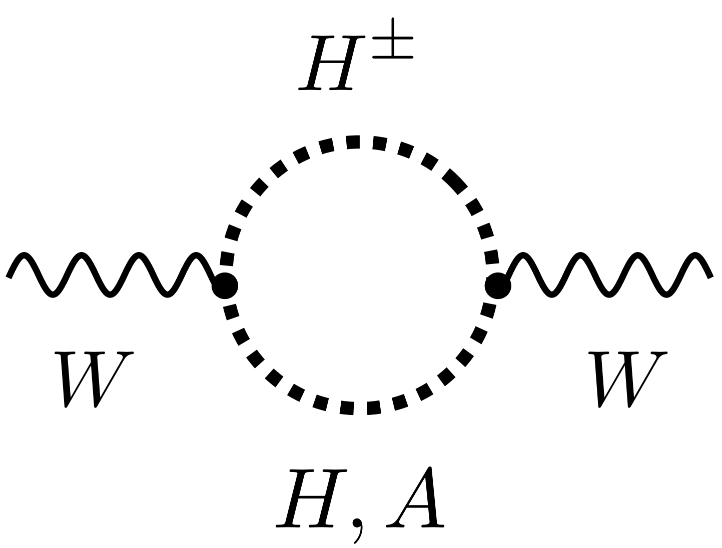

$$\cos(\beta - \alpha) \simeq 0$$

$$M_{H^\pm} > 580\,\mathrm{GeV}$$

$$M_{H^\pm} \simeq M_{H,A}$$

[see for instance LHC DMWG, 1810.09420 & references therein]

2HDM+a: resonant $E_{T,\,miss}$ signatures

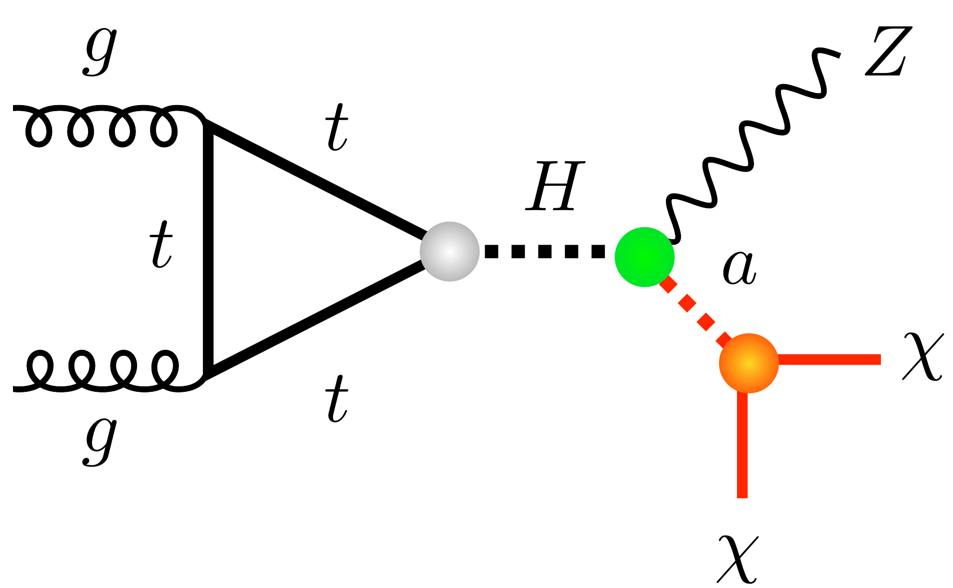

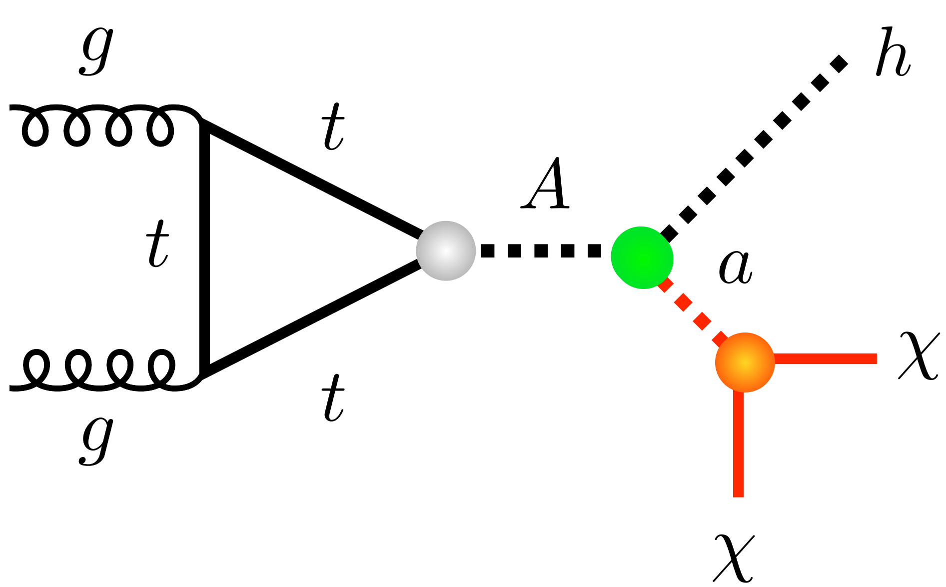

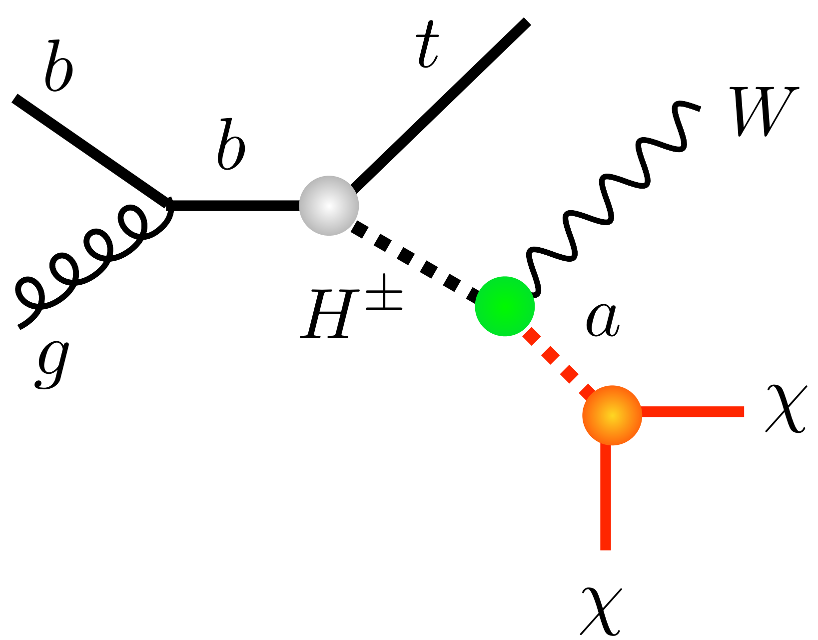

Mono-Z, mono-Higgs & tW+$E_{T,\,miss}$ channels are subleading in spin-0 DM simplified models. In 2HDM+a model, presence of H, A, & $H^{\pm}$ allows for resonant production of these mono-X signatures

[Goncalves et al., 1611.04593; Bauer et al., 1701.07427; Pani & Polesello, 1712.03874]

2HDM+a: mono-Higgs spectra

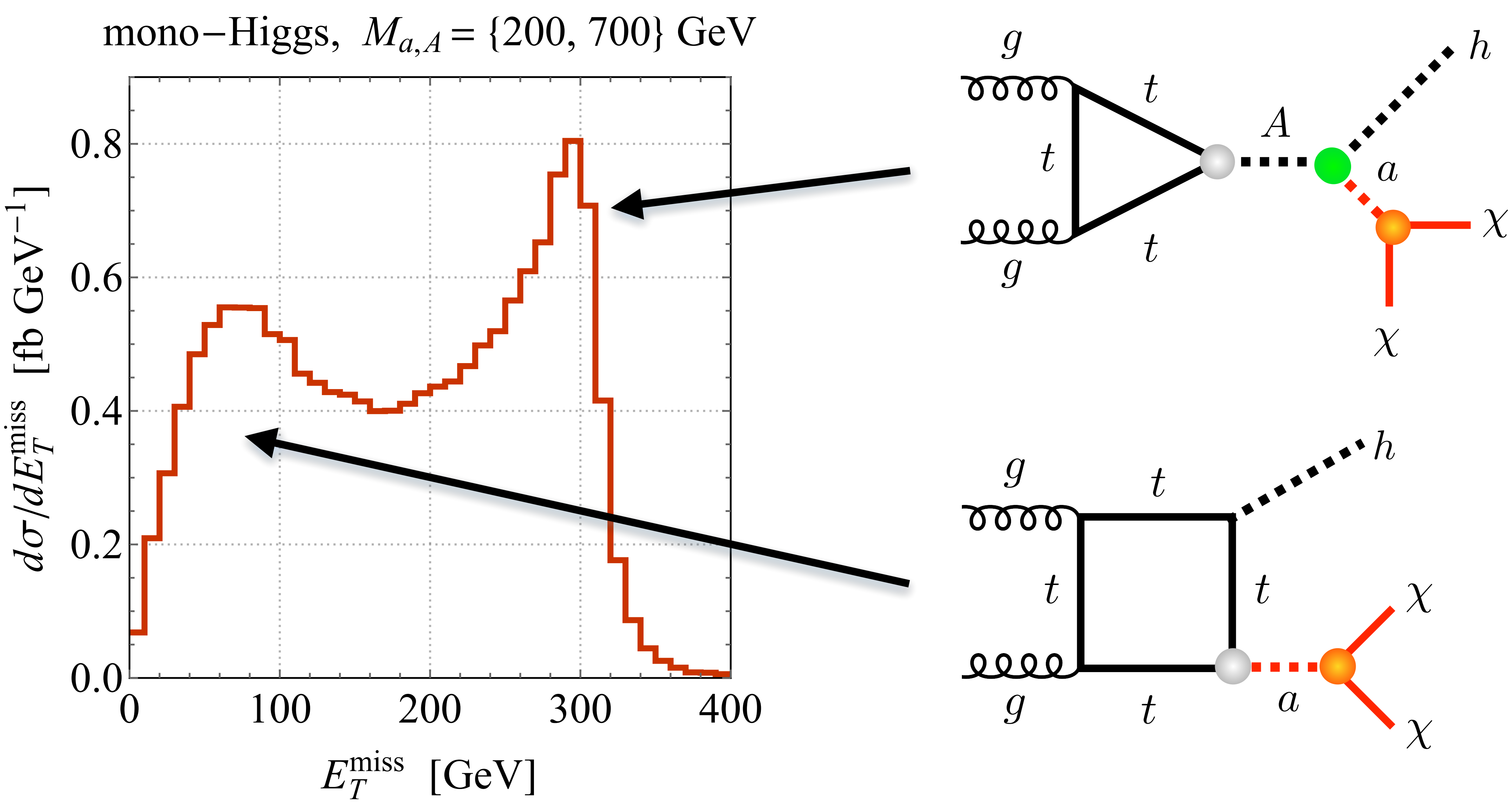

Due to interplay of resonant & non-resonant contributions,
$E_{T,\,miss}$ distributions in h+$E_{T,\,miss}$ production have non-trivial shapes

[Goncalves et al., 1611.04593; Bauer et al., 1701.07427; LHC DMWG, 1810.09420]

2HDM+a: LHC constraints

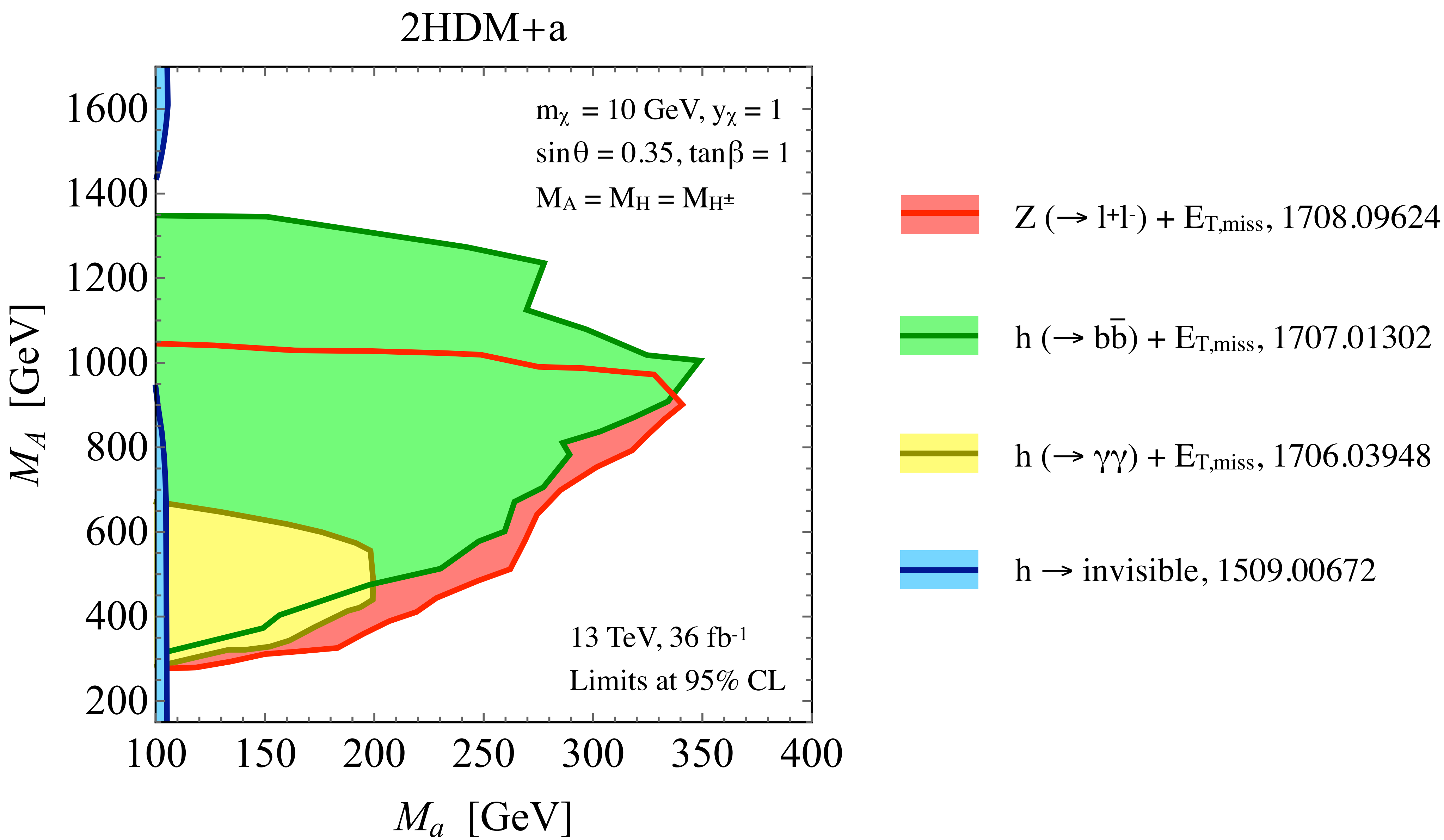

Existing mono-Z in 2l channel & mono-Higgs in 2b channel provide leading constraints. Mono-Higgs in 2γ channel interesting at LHC Run-3 & beyond

[based on ATLAS-CONF-2018-051]

2HDM+a: LHC constraints

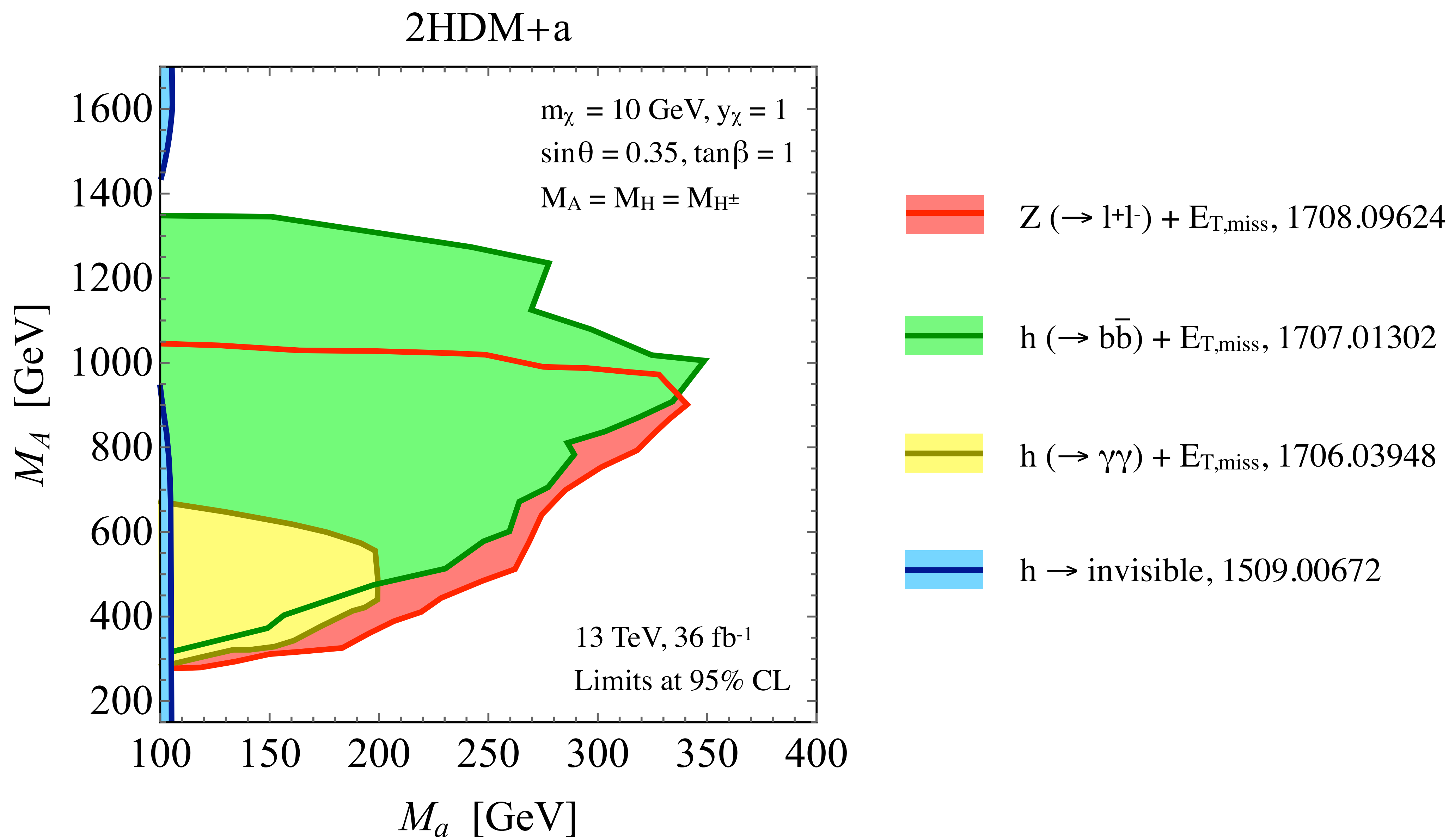

Due to resonant production mass reach significantly enhanced compared to pseudoscalar DMF model. For instance, M_a > 340 GeV for M_A = 1TeV

[based on ATLAS-CONF-2018-051]

2HDM+a: LHC constraints

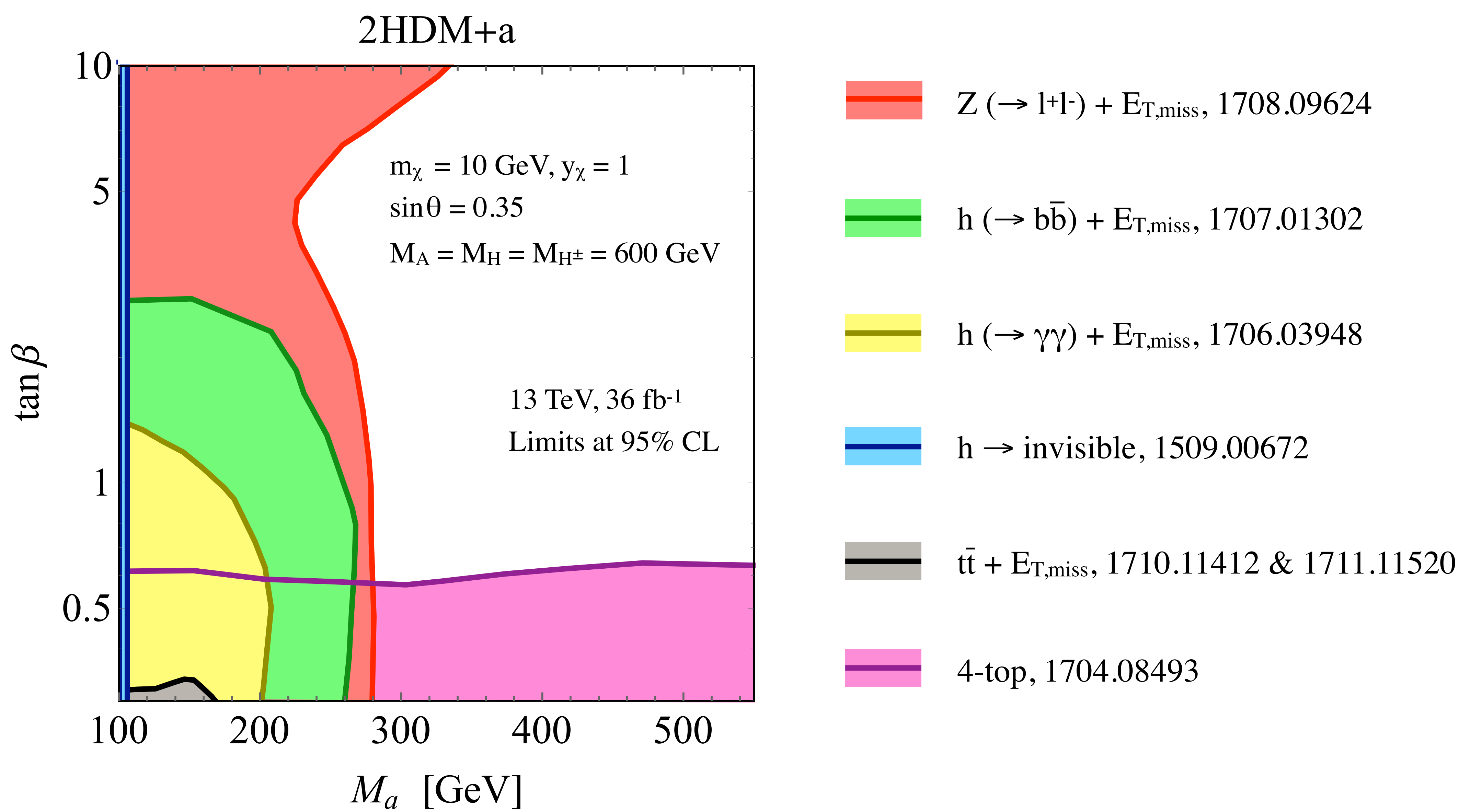

Compared to mono-Z & mono-Higgs, $t\bar{t}$+$E_{T,\text{miss}}$ searches lead to weak constraints only. 4-top production also relevant for not too heavy A & H

[based on LHC DMWG, 1810.09420 & ATLAS-CONF-2018-051]

2HDM+a: tW+$E_{T, miss}$ prospects

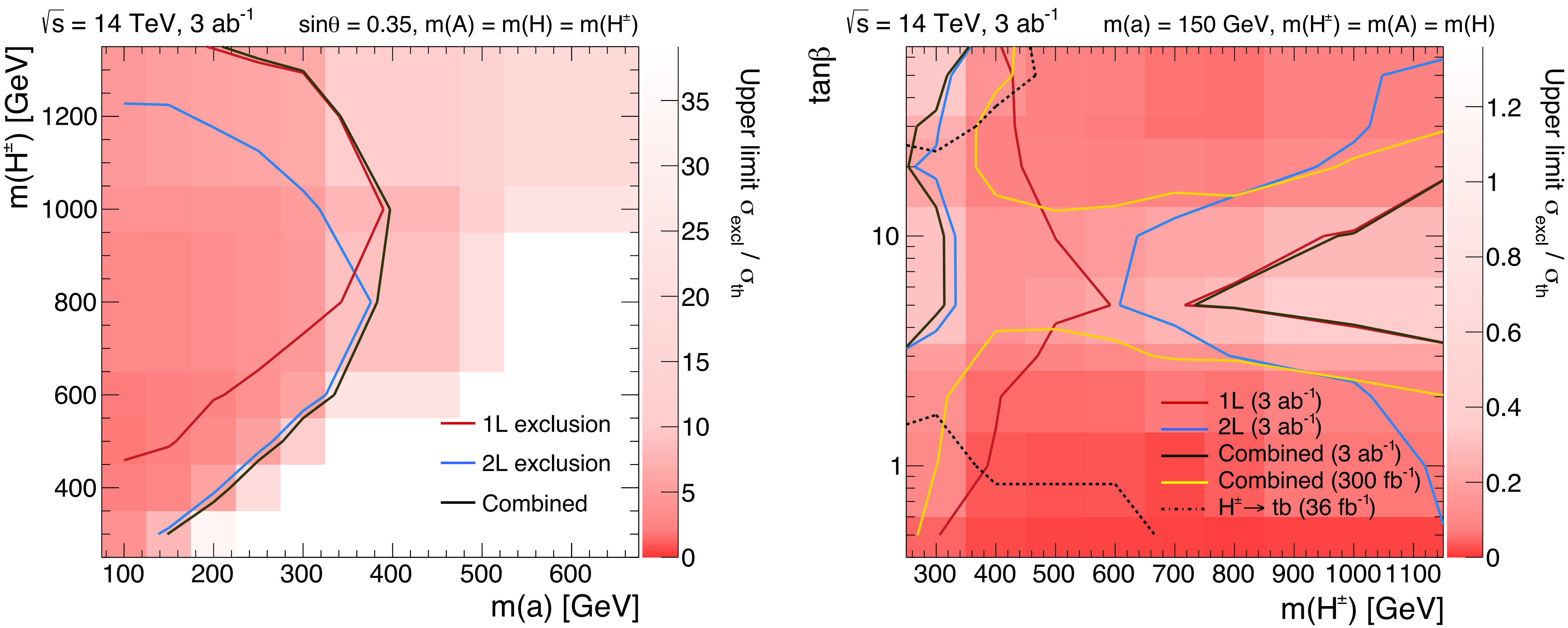

Complementary constraints on 2HDM+a parameter space can also be obtained from tW+$E_{T, miss}$ searches in future LHC runs

[Pani & Polesello, 1712.03874; UH, Pani & Polesello in 1812.07831]

2HDM+a: relic density vs. LHC

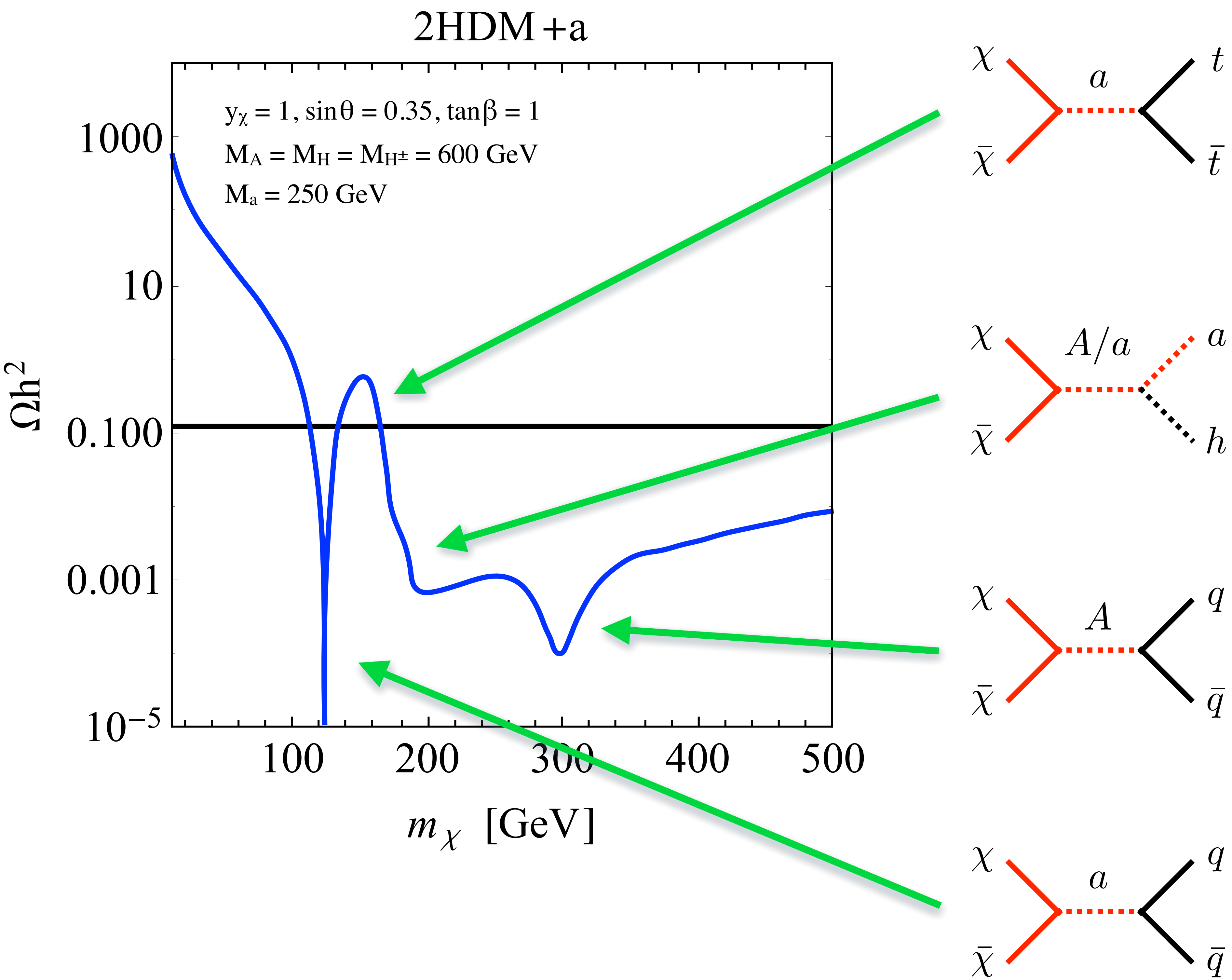

[based on ATLAS-CONF-2018-051]

2HDM+a: relic density vs. LHC

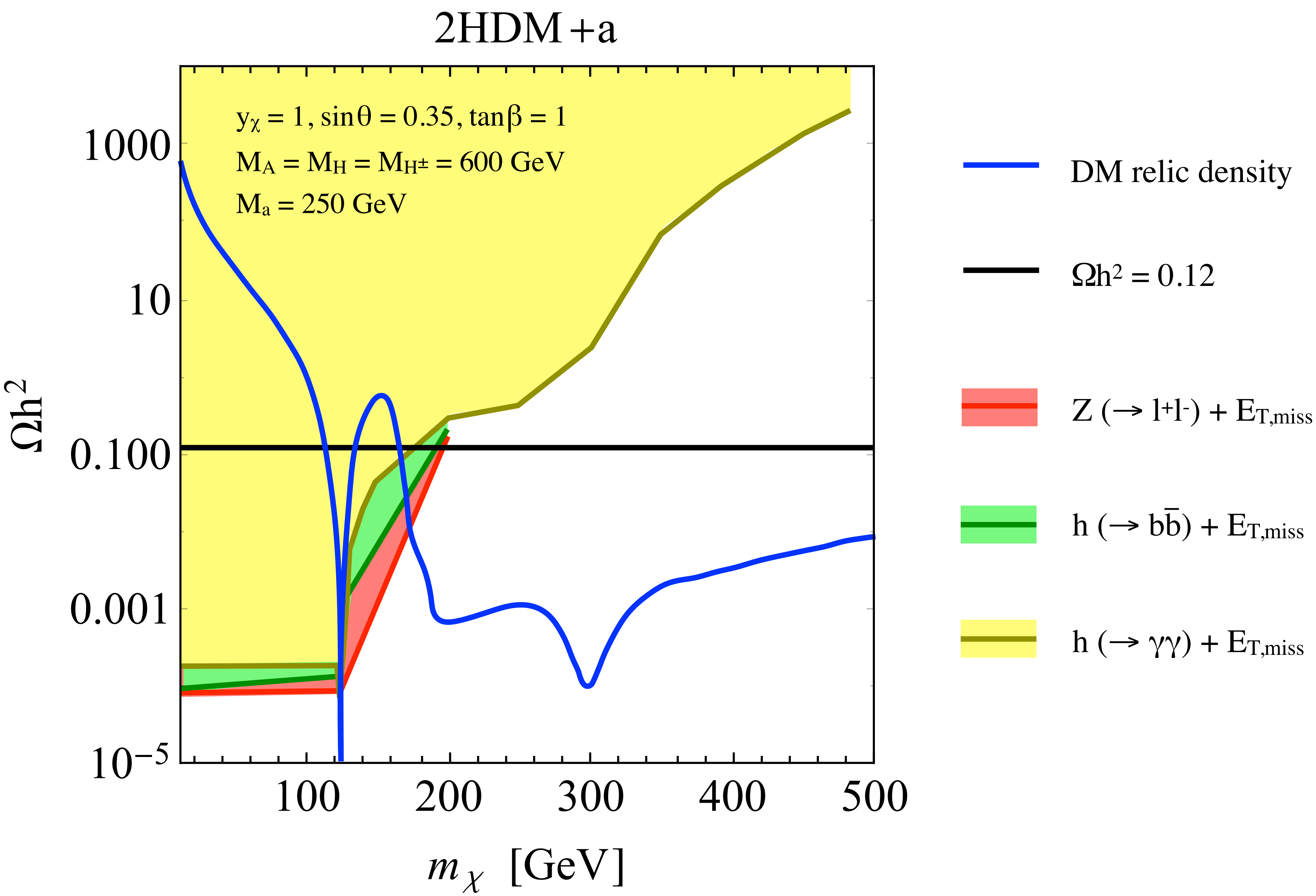

For M_a = 250 GeV, models that predict Ωh^2 = 0.12 excluded by LHC data

[based on ATLAS-CONF-2018-051]

2HDM+a: relic density vs. LHC

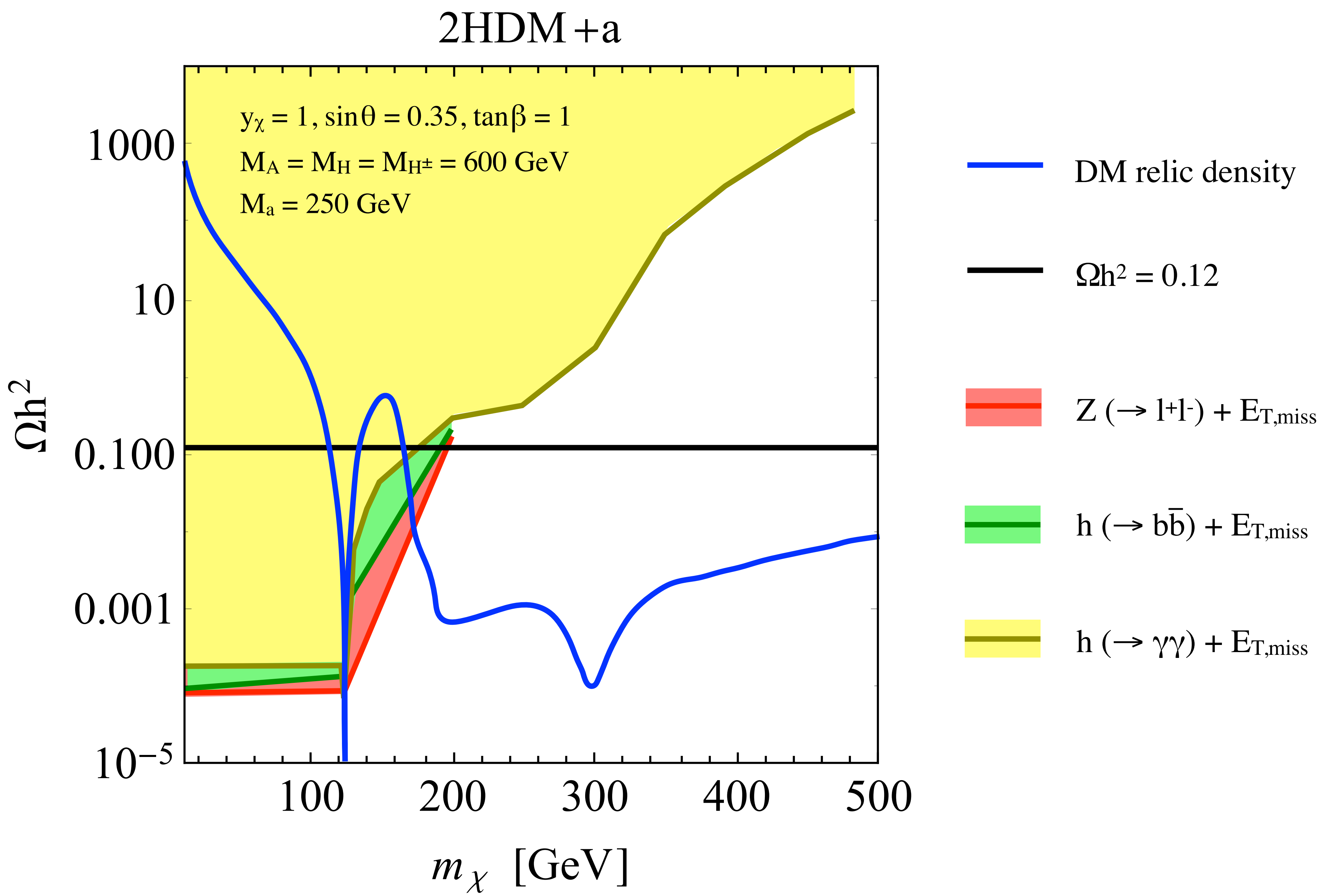

But large portions of parameter space with $\Omega h^2 < 0.12$ untested by LHC

[based on ATLAS-CONF-2018-051]

Conclusions

- ATLAS & CMS searches for DM in $X+E_{T,\,miss}$ with $X = j, \gamma, W, Z, h, t, t\bar{t}, b\bar{b}, \ldots$ & their interpretations in framework of spin-0 & spin-1 DM simplified models well established

- At future LHC runs possible to search for $X+E_{T,\,miss}$ more differential. In spin-0 case, studies of angular correlations in 2j & 2l final states can be used to enhance LHC reach & characterise portal interactions

- Mono-Z, mono-Higgs & $tW+E_{T,\,miss}$ production can furnish leading bounds in consistent spin-0 models with an extended Higgs sector. This motivates studies that have received less/little attention so far

Backup

2HDM+a: relic density

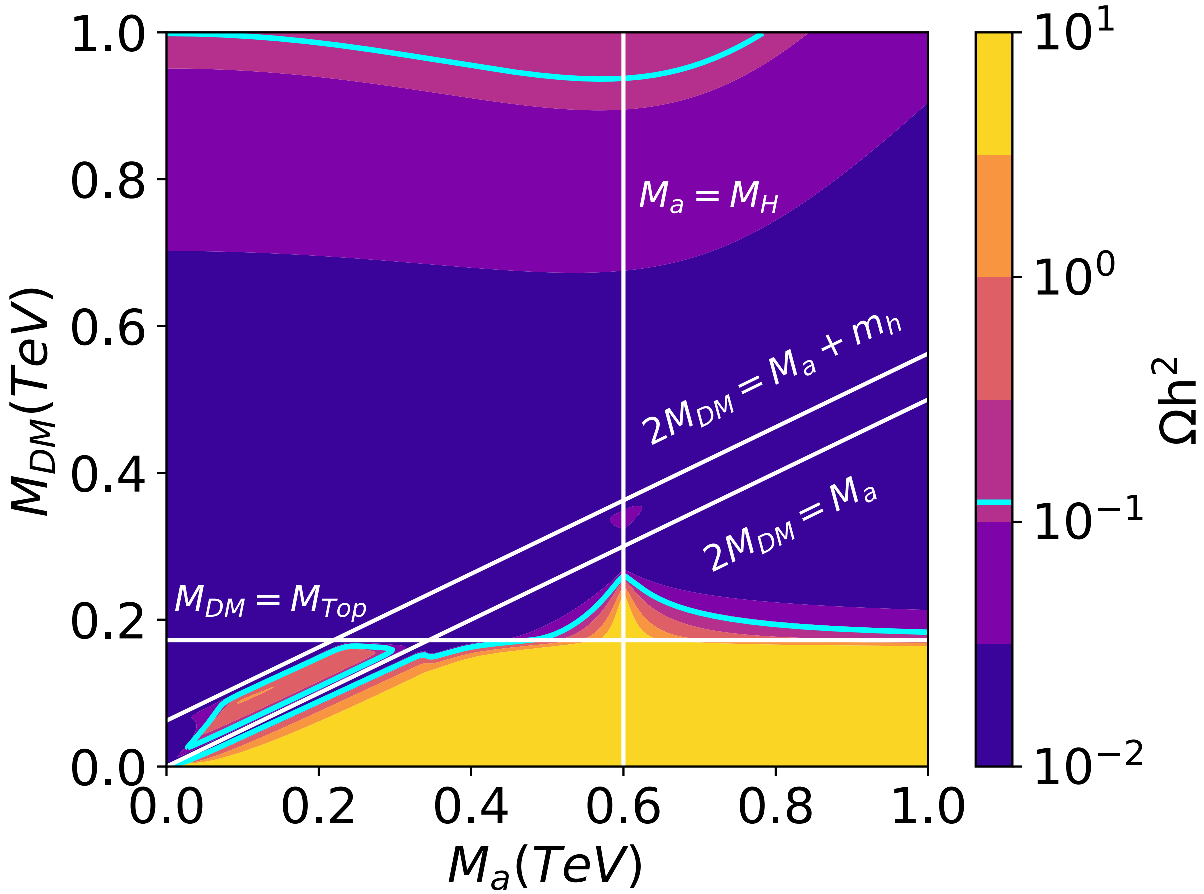

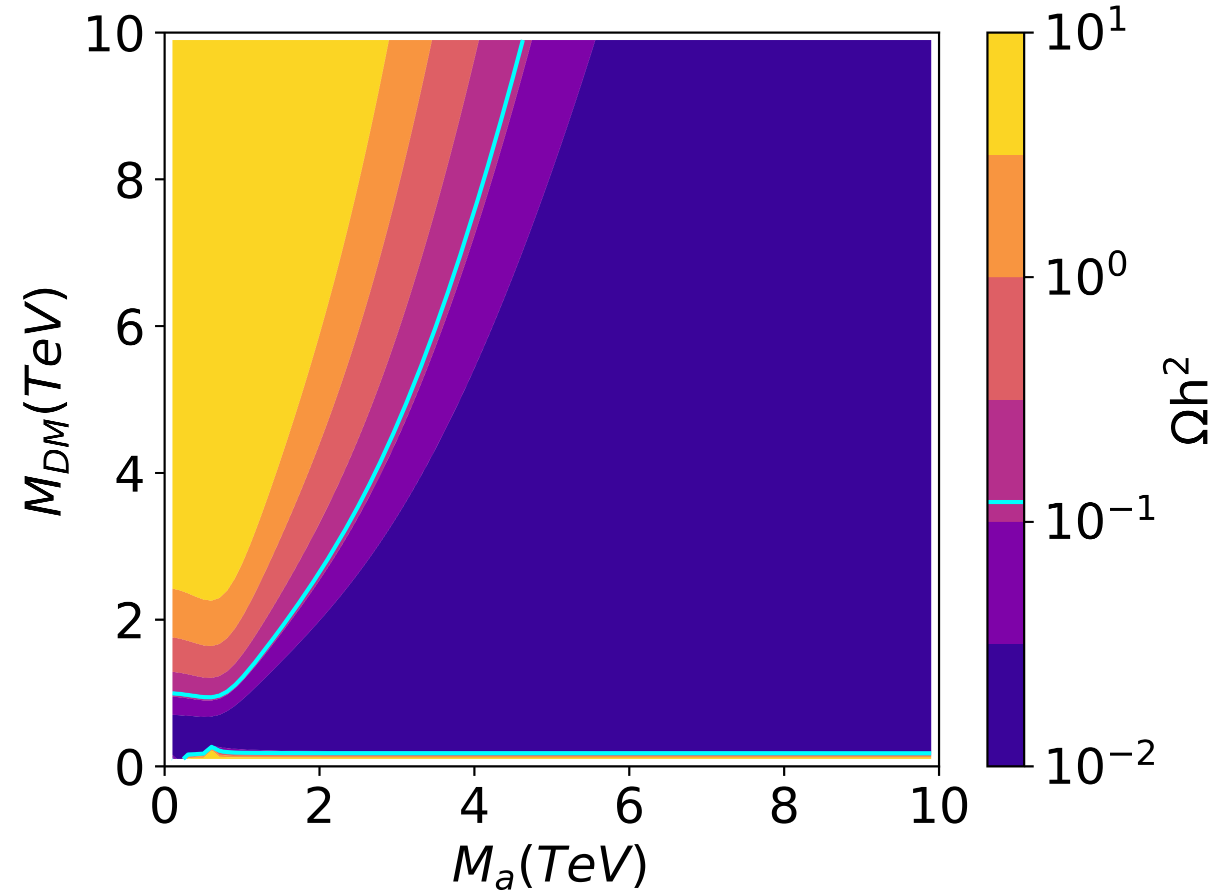

[LHC DMWG, 1810.09420]

2HDM+a: SI DM-nucleon cross section

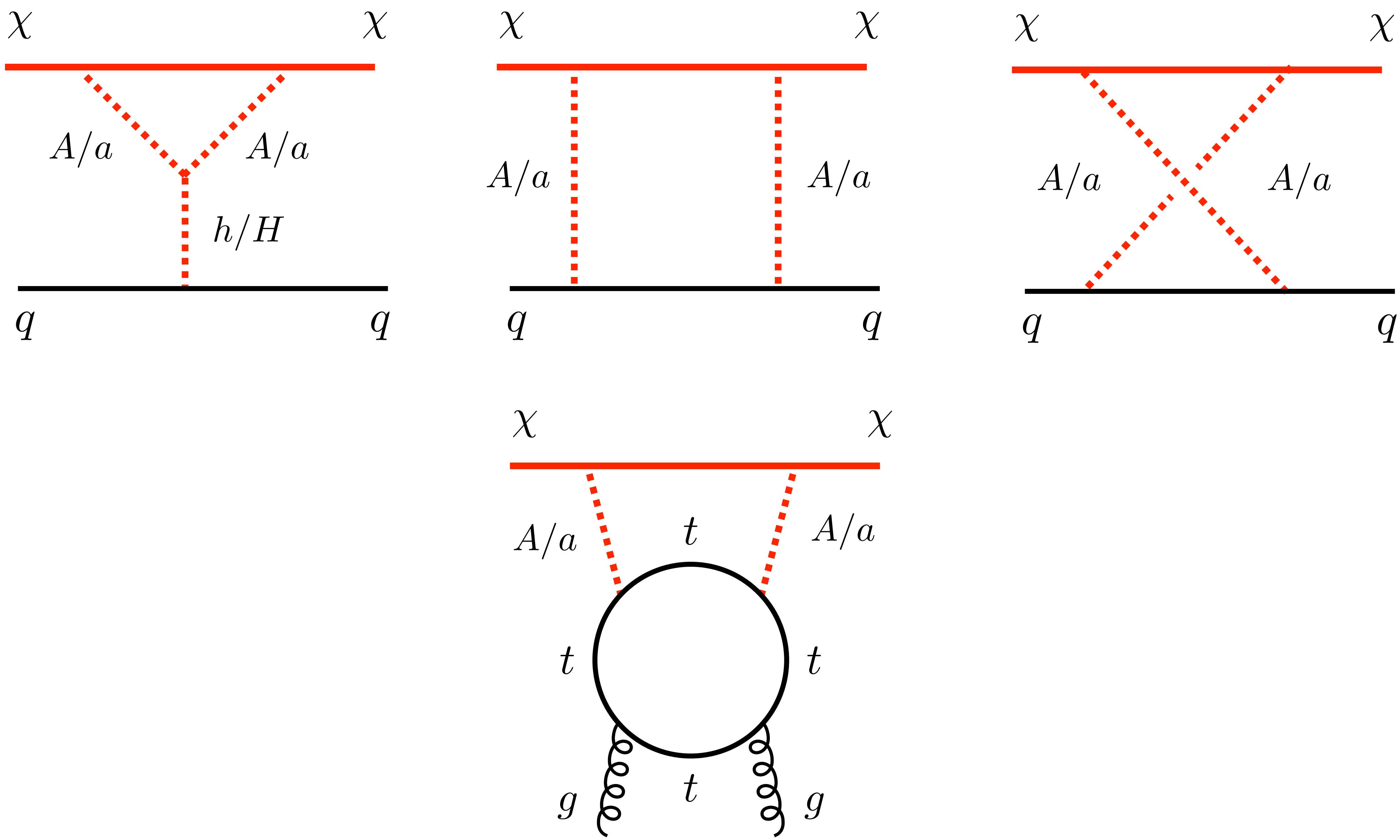

[Bell et al., 1803.01574; Abe et al., 1810.01039]

2HDM+a: DD constraints

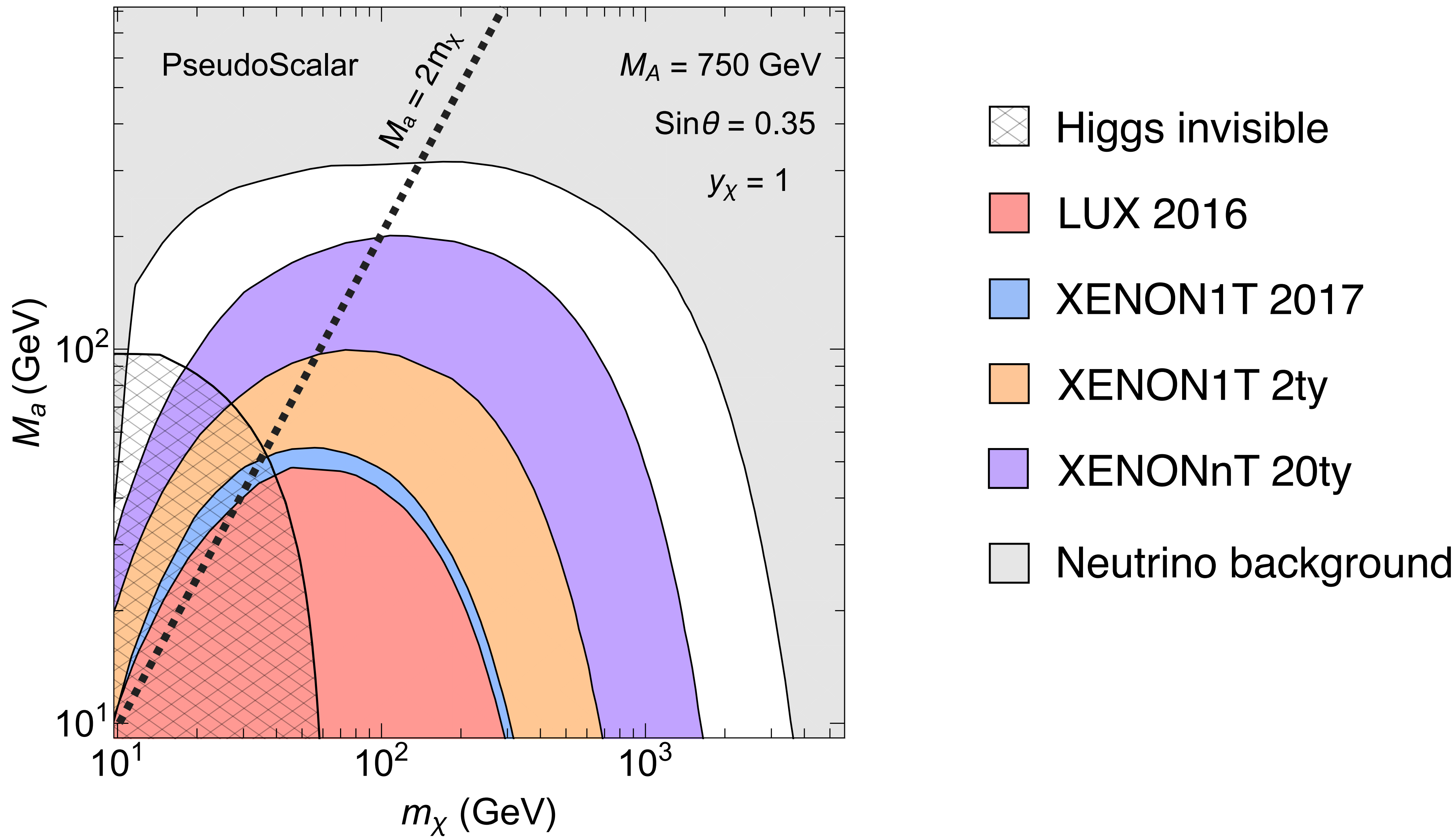

Since a SI DM-nucleon cross section arises only at loop level, DD limits are generically weak in 2HDM+a model, in particular in $M_a > 2m_\chi$ region

[Bell et al., 1803.01574; Abe et al., 1810.01039]

2HDM+a: indirect detection

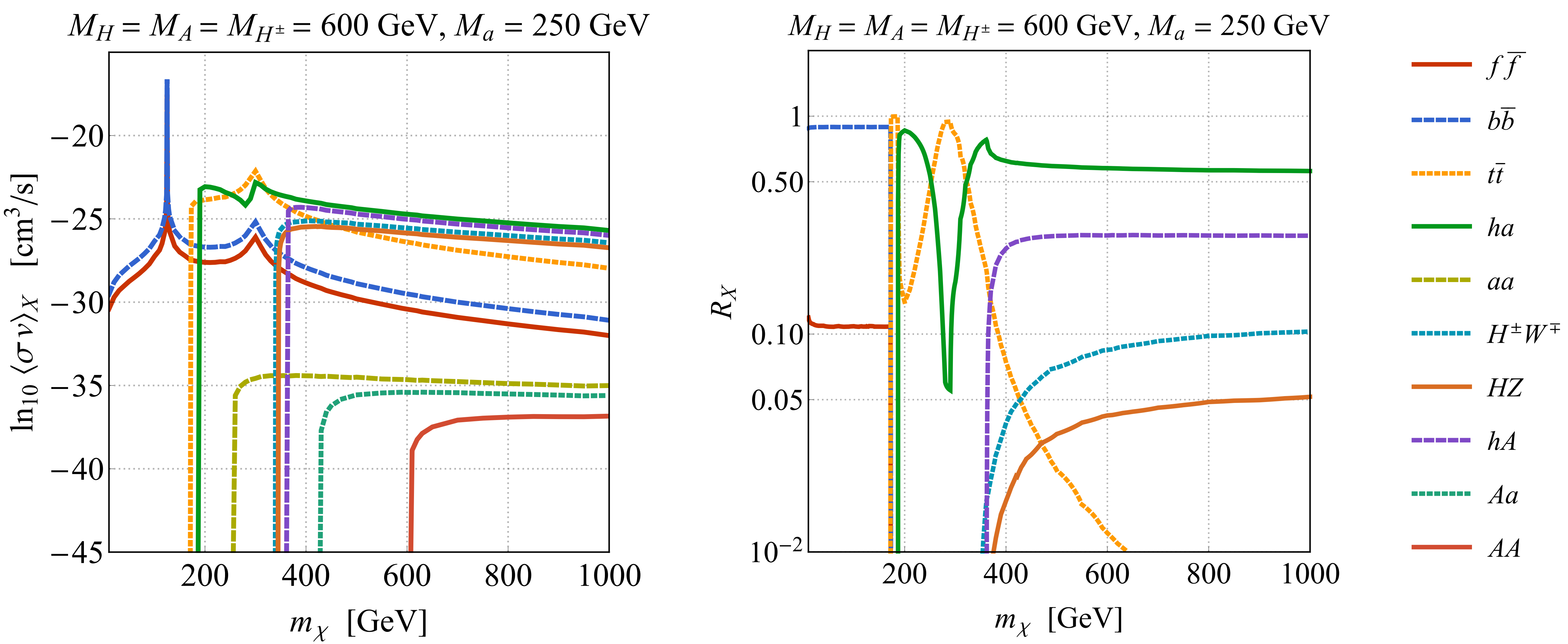

For m_{DM} = 10 GeV, velocity averaged annihilation cross section into $b\bar{b}$ is $3 \cdot 10^{-30}$ cm³/s. Corresponding Fermi-LAT bound reads $4.8 \cdot 10^{-27}$ cm³/s

[LHC DMWG, 1810.09420]

Mono-jet: recent theory progress

[Lindert et al., 1705.04664]

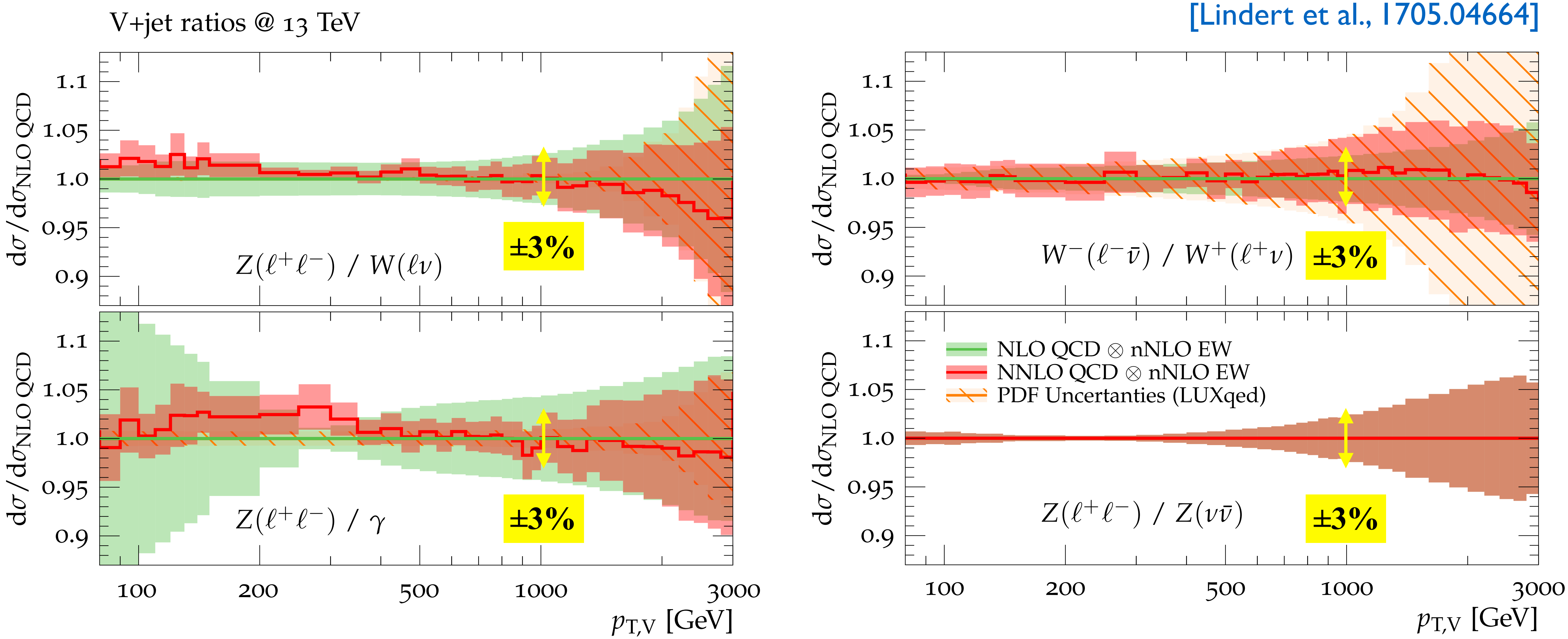

Model-dependence of exclusions

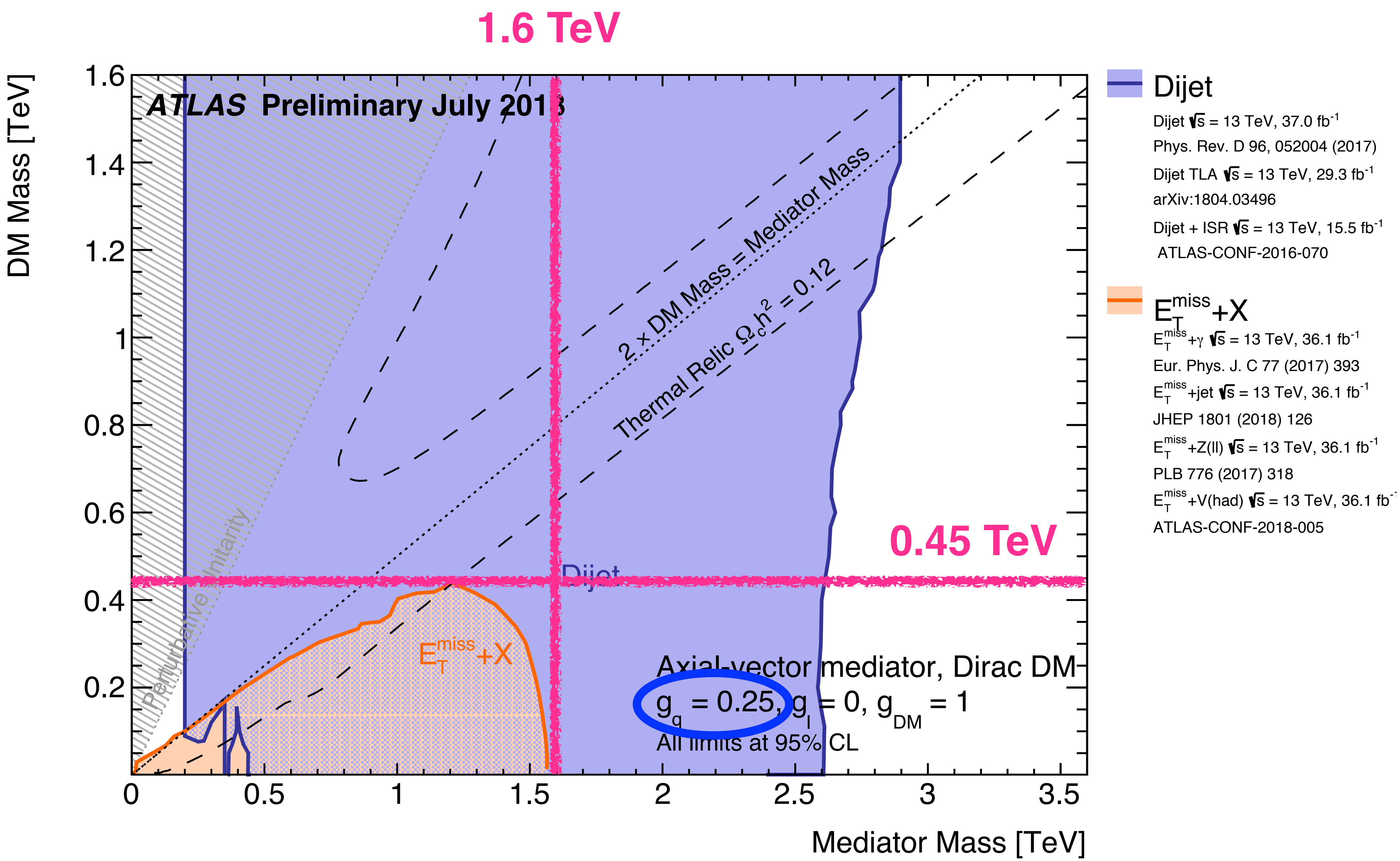

[https://atlas.web.cern.ch/Atlas/GROUPS/PHYSICS/CombinedSummaryPlots/EXOTICS/]

Model-dependence of exclusions

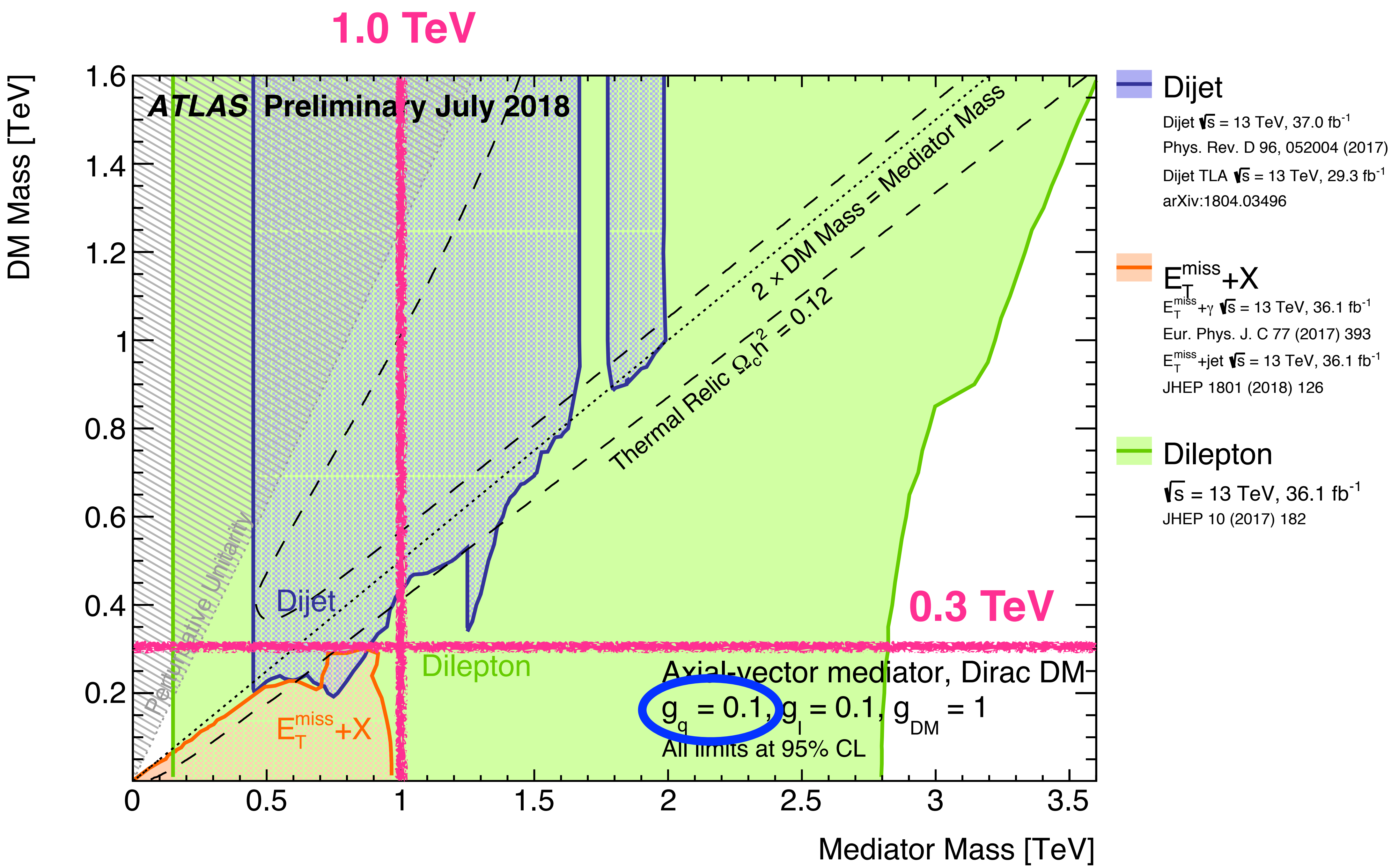

[https://atlas.web.cern.ch/Atlas/GROUPS/PHYSICS/CombinedSummaryPlots/EXOTICS/]

Model-dependence of exclusions

$$\sigma(pp \to E_{T,\mathrm{miss}} + X) \mathrel{\substack{\propto \\ \sim}} \frac{g_q^2}{M_V^4} \quad \Longrightarrow \quad M_{V,1} \simeq \sqrt{\frac{(g_q)_1}{(g_q)_0}}\, M_{V,0}$$

In example above $(g_q)_0 = 0.25$, $(g_q)_1 = 0.1$ and $M_{V,0} = 1.6\,\mathrm{TeV}$:

$$M_{V,1} \simeq \sqrt{\frac{0.1}{0.25}}\, 1.6\,\mathrm{TeV} \simeq 1.0\,\mathrm{TeV} \quad ✔$$

Model-dependence of exclusions

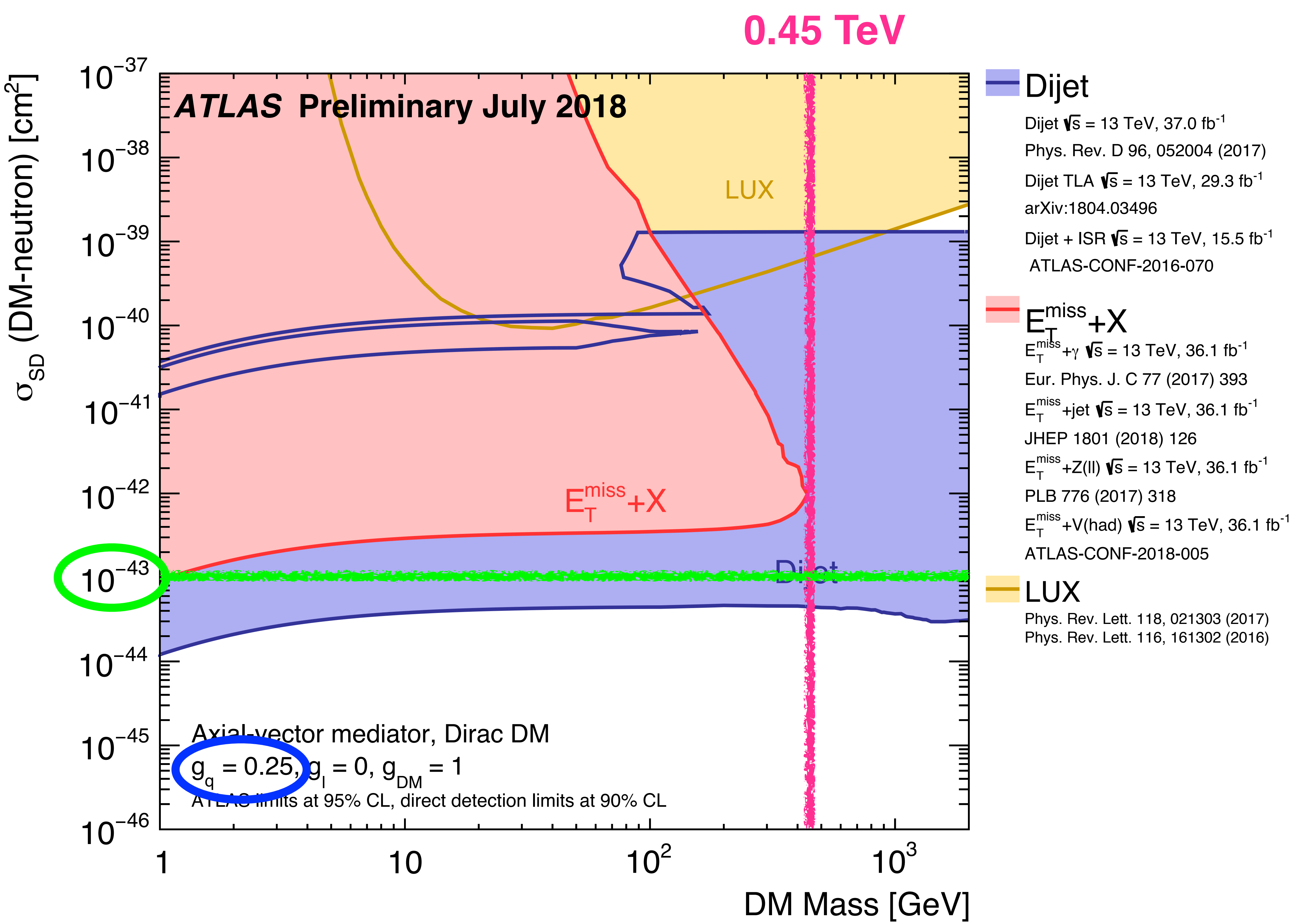

[https://atlas.web.cern.ch/Atlas/GROUPS/PHYSICS/CombinedSummaryPlots/EXOTICS/]

Model-dependence of exclusions

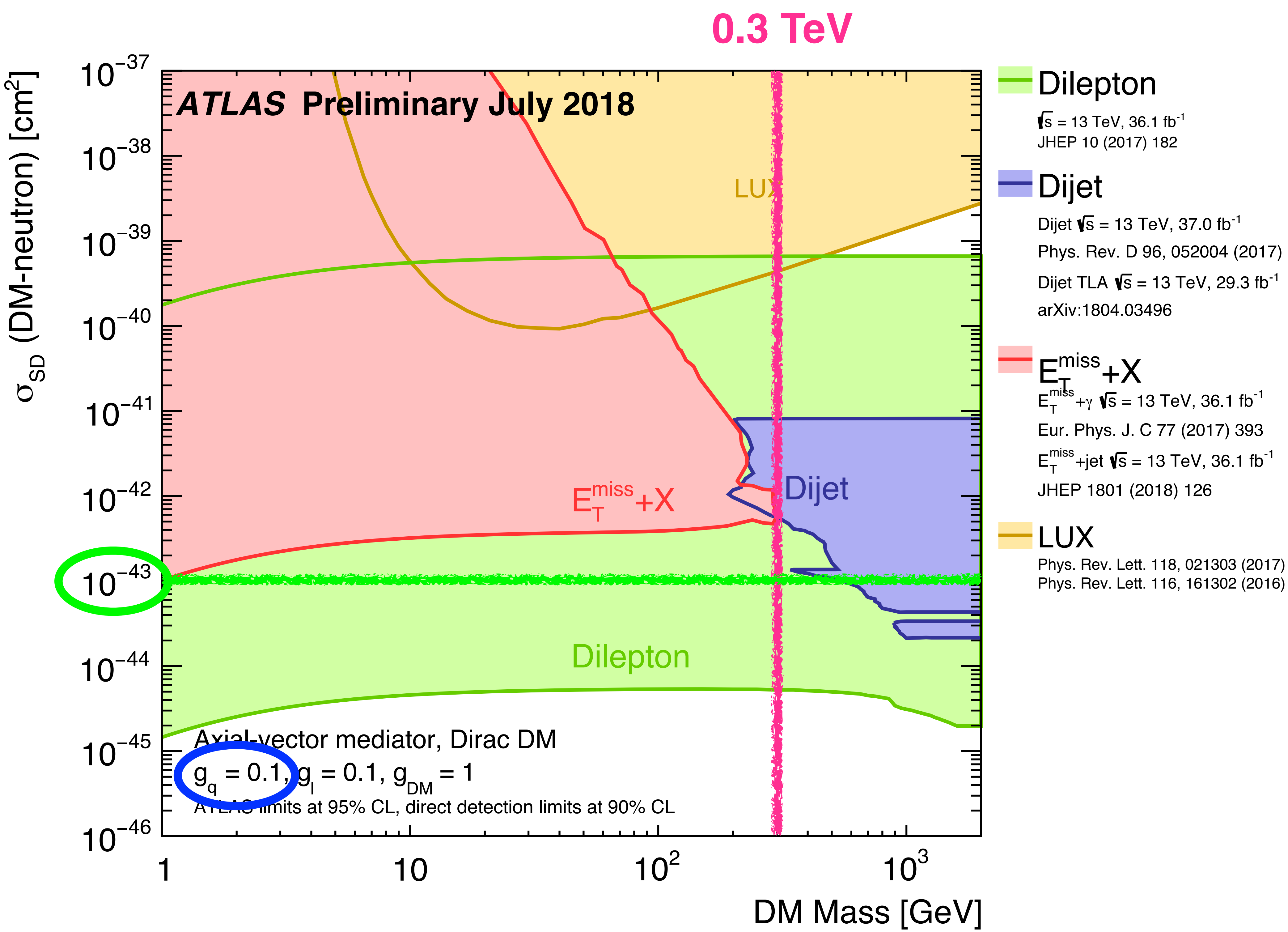

[https://atlas.web.cern.ch/Atlas/GROUPS/PHYSICS/CombinedSummaryPlots/EXOTICS/]

Model-dependence of exclusions

$\sigma_{\text{mono-jet}} =$

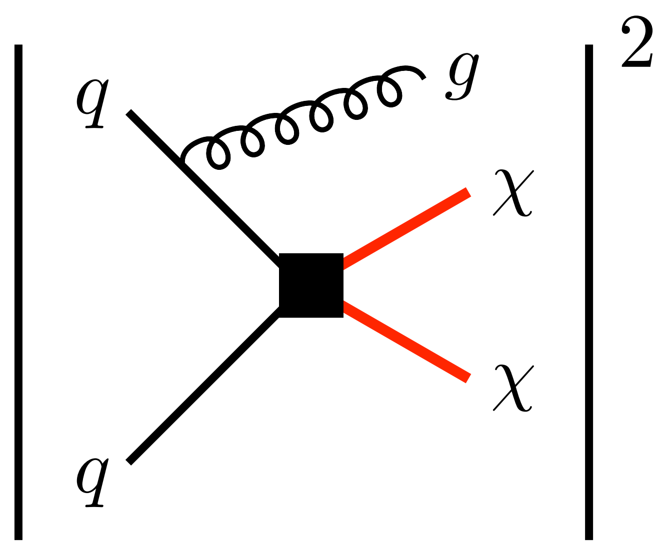

$\overset{\propto}{\sim}$

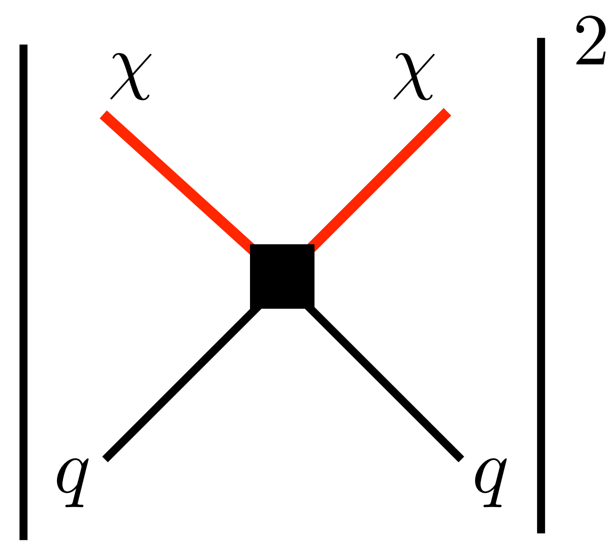

$= \sigma_{\text{DM-nucleon}}$

For light DM, above relation implies (in agreement with plots) that limit on DM-nucleon cross section from mono-X searches should become independent of parameter choices. For higher DM masses, bounds will however differ, because in this regime LHC exclusions depend on g_q etc.

Simplified models: HL-LHC prospects

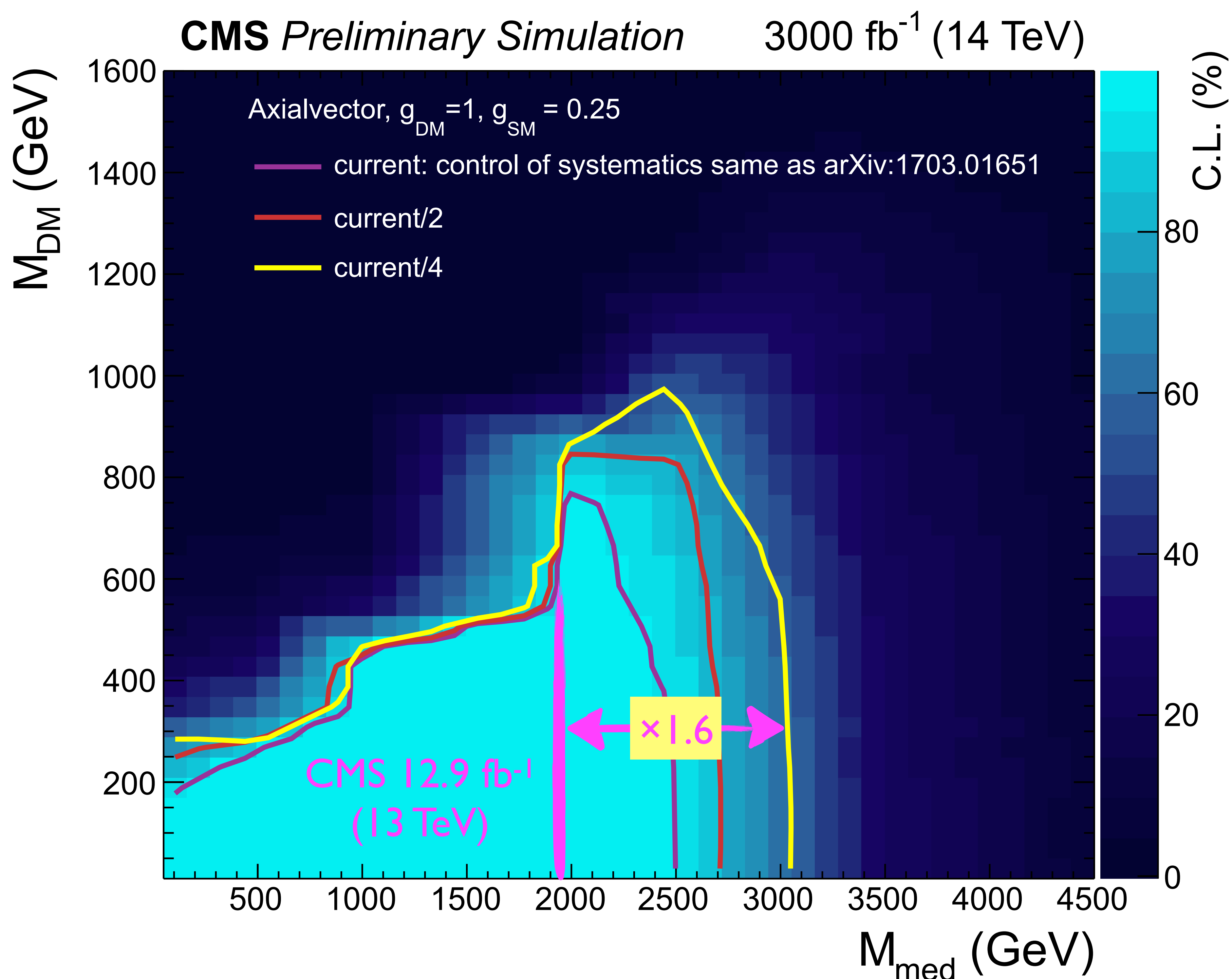

[CMS-PAS-FTR-16-005]

Simplified models: HL-LHC prospects

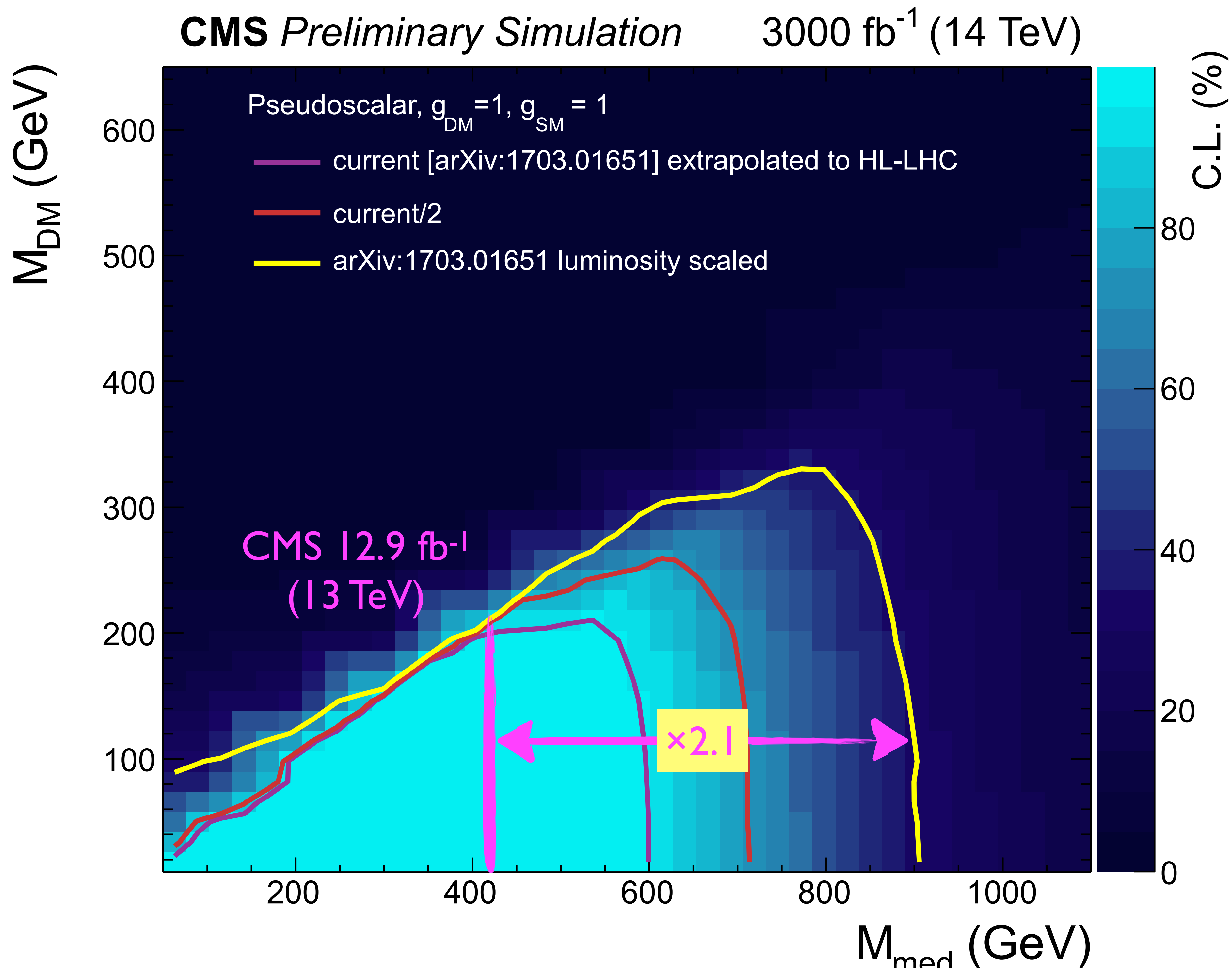

[CMS-PAS-FTR-16-005]

Scales in DM searches

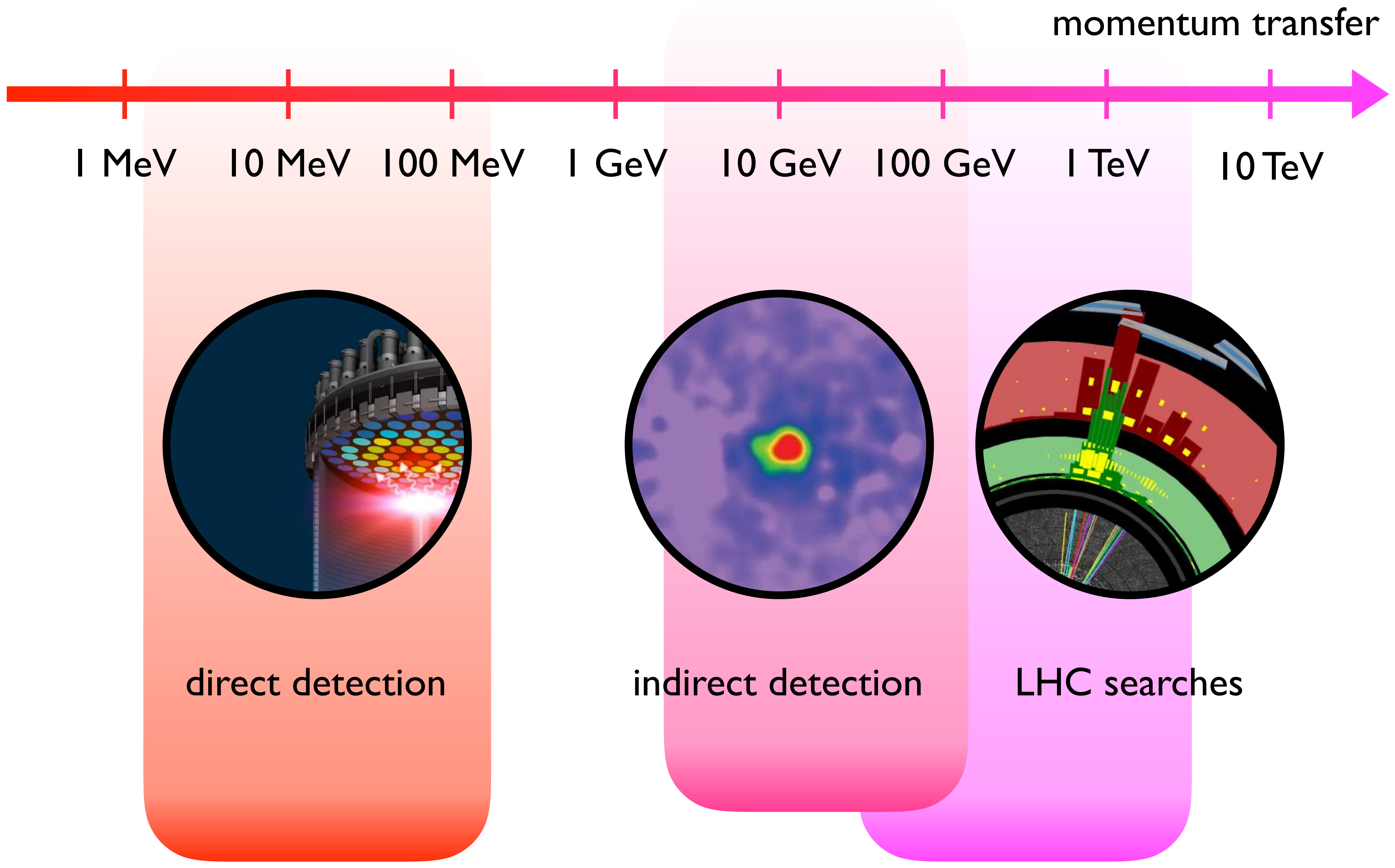

Scales in DM searches

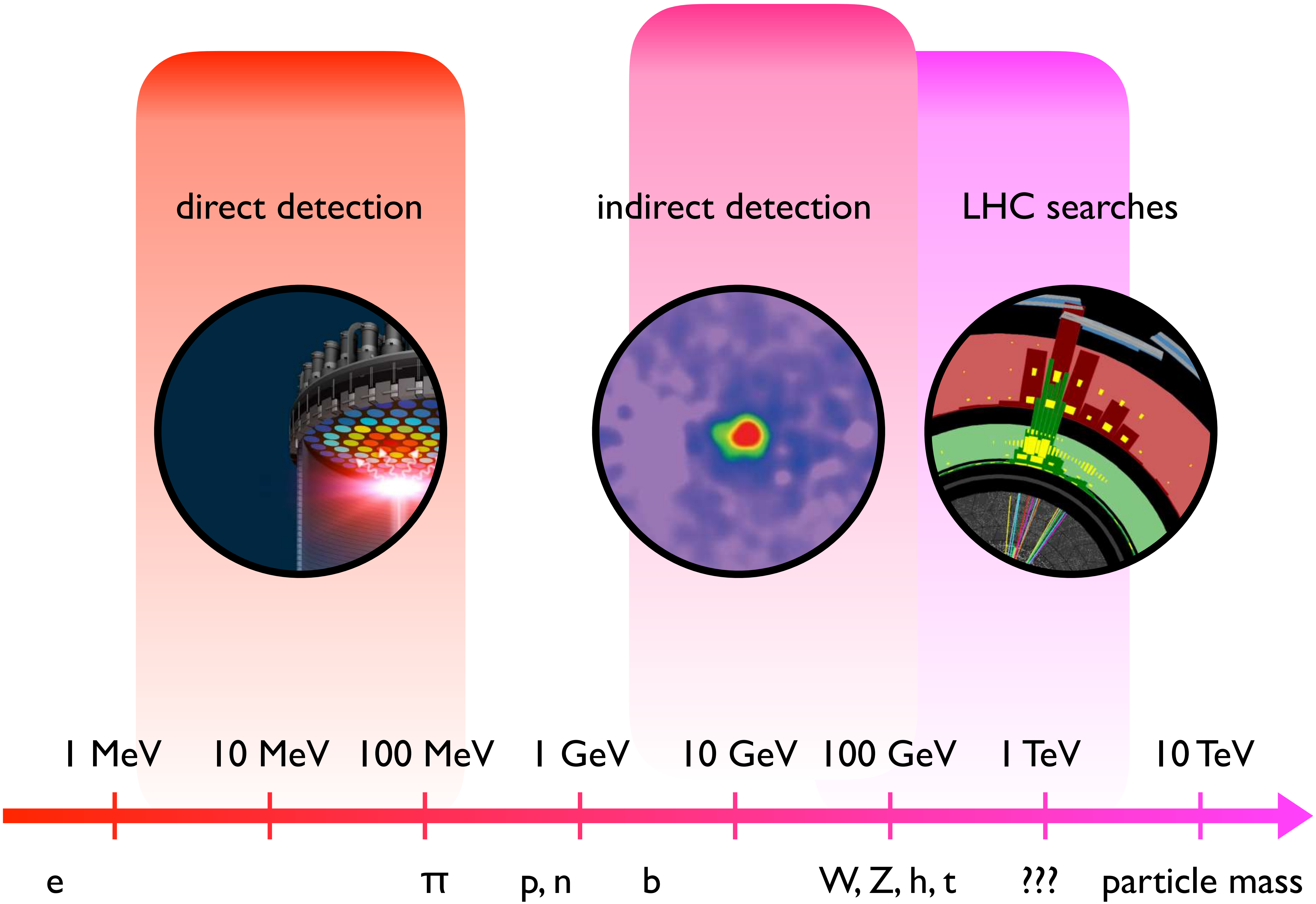

What is an EFT?

[…] An effective field theory includes the appropriate degrees of freedom to describe physical phenomena occurring at a chosen length scale or energy scale, while ignoring substructure and degrees of freedom at shorter distances (or, equivalently, at higher energies) […] Effective field theories typically work best when there is a large separation between length scale of interest and the length scale of the underlying dynamics […]

[from Wikipedia, the free encyclopedia, https://en.wikipedia.org/wiki/Effective_field_theory]

EFT for DD experiments

direct detection

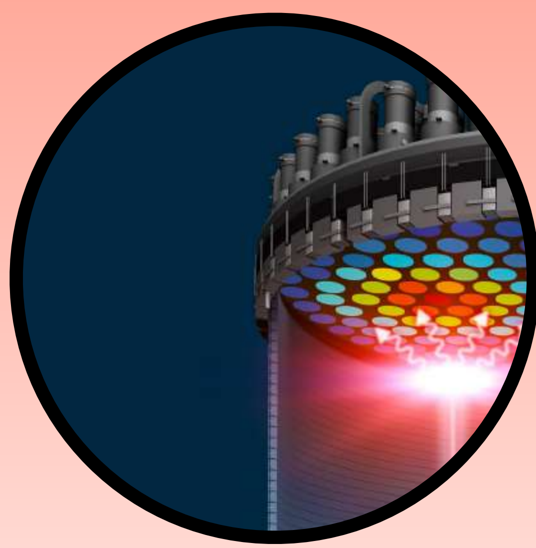

- degrees of freedom:
  DM & light quark, gluon currents; N-π interactions
- separation of scales:
  $m_p, \ldots, m_t \gg 50$ MeV

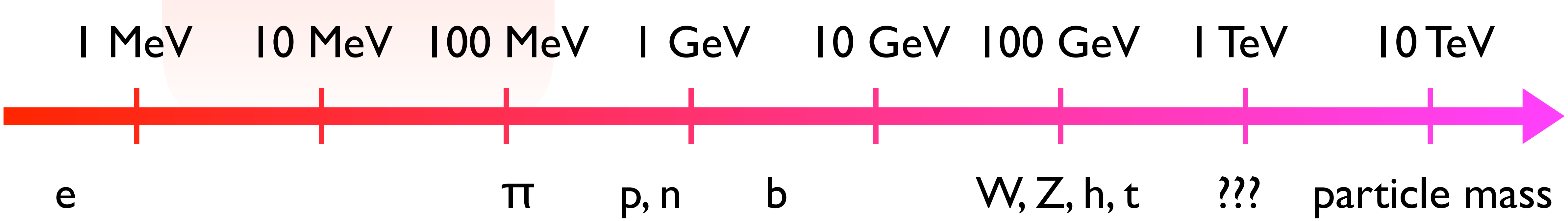

EFT for LHC DM searches

- degrees of freedom:

  DM, all SM particles, ???

- separation of scales:

  $m_{???} \overset{?}{\gg} 5$ TeV

LHC searches

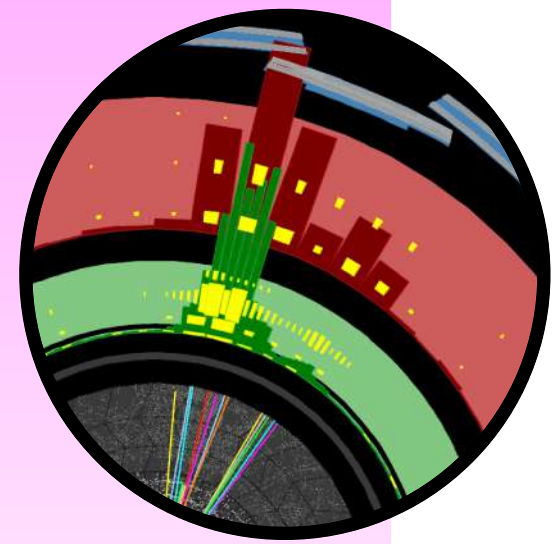

1 MeV | 10 MeV | 100 MeV | 1 GeV | 10 GeV | 100 GeV | 1 TeV | 10 TeV

e | π | p, n | b | W, Z, h, t | ??? | particle mass

Classification of χ-N interactions

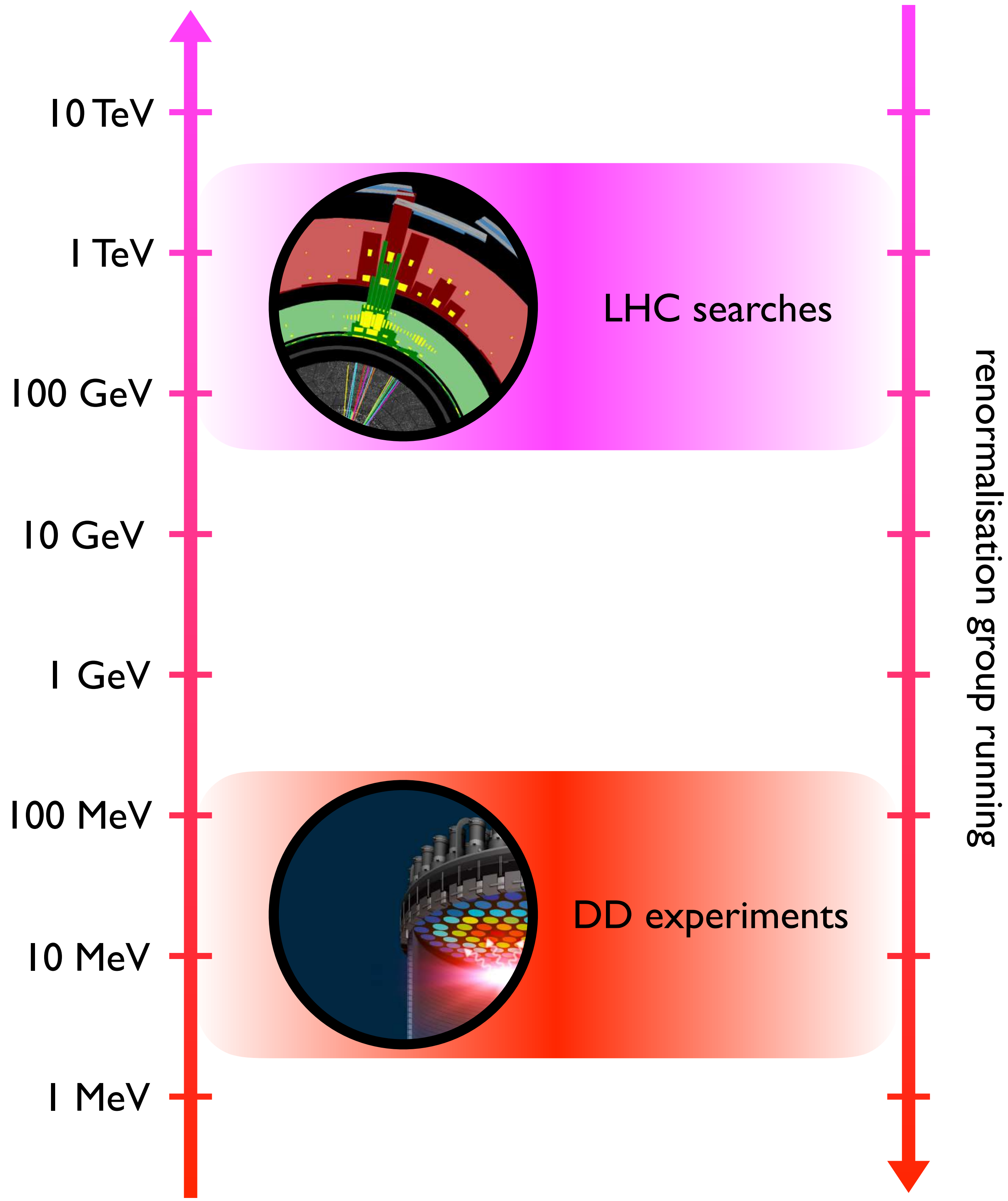

Distinction between SI & SD (or q-suppressed) χ-N couplings not stable under radiative corrections. Effects particular important for mixing of suppressed into unsuppressed operators

[Kopp et al., 0907.3159; Freytsis & Ligeti, 1012.5317;
Hill & Solon, 1111.0016; UH & Kahlhoefer 1302.4454;
Crivellin et al. 1402.1173, 1408.5046;
D'Eramo et al. 1409.2893; …]

Spin-1 simplified models: SD effects

[D'Eramo et al.,1605.04917]

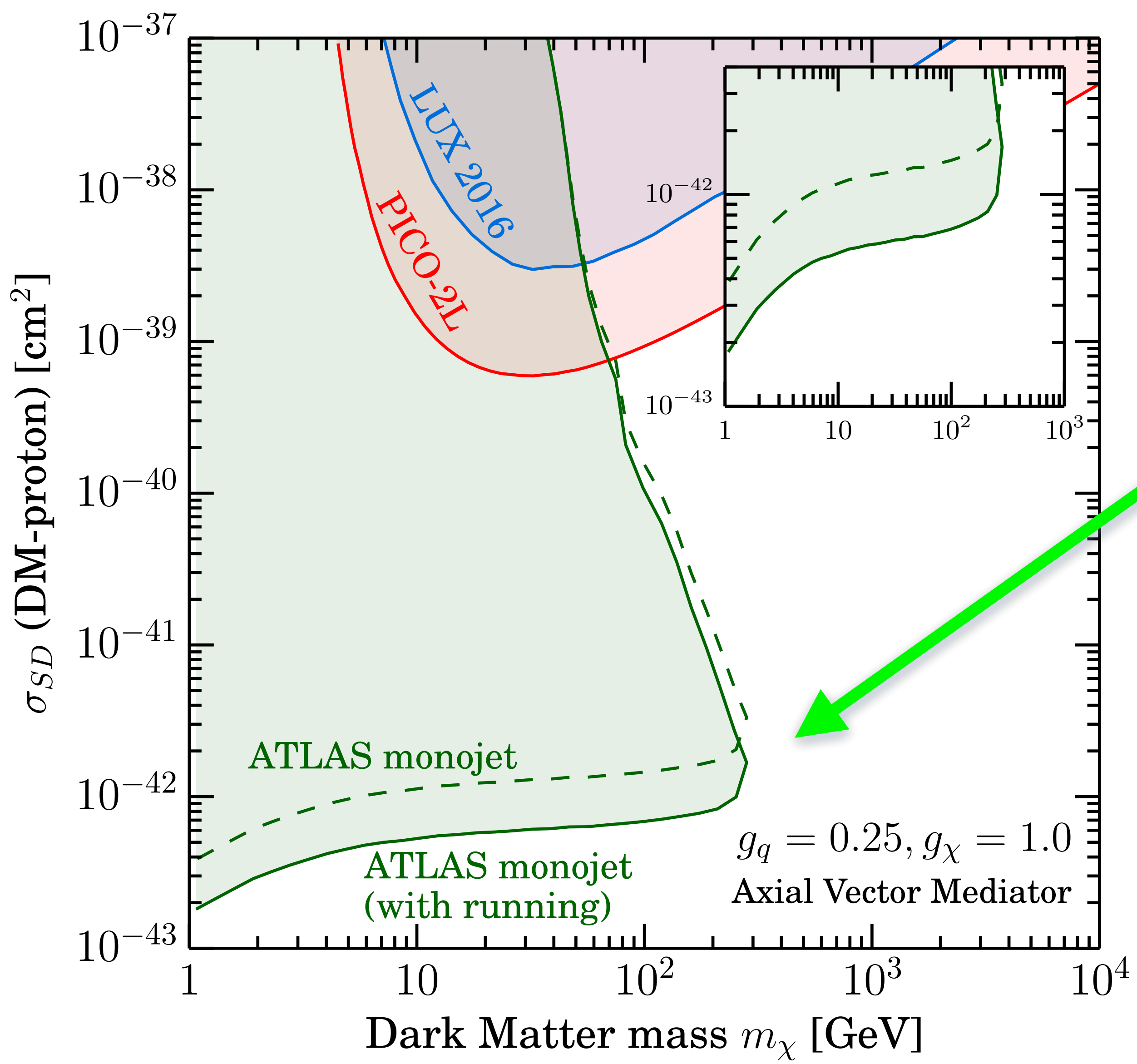

in axialvector case bounds are strengthened by a factor of around 2 by renormalisation group running

While LHC limit quite similar to SI case, DD bounds weakened significantly since DM-nucleon scattering is incoherent in SD case

χ-N scattering for spin-0 mediators

$$\mathcal{L}_S \longrightarrow \bar{\chi}\chi\bar{q}q \longrightarrow \boxed{\mathcal{O}_1 = 1_\chi \, 1_N}$$

$$\mathcal{L}_P \longrightarrow \bar{\chi}i\gamma_5\chi\bar{q}i\gamma_5 q \longrightarrow \boxed{\mathcal{O}_6 = \frac{1}{m_N^2}\left(\vec{S}_\chi \cdot \vec{q}\right)\left(\vec{S}_N \cdot \vec{q}\right)}$$

SI

SD & momentum suppressed

Due to loss of coherence & since q = O(0.1 GeV) resulting χ-N cross section O(10^{-11}) lower than σ_{SI}. As a result very poor limits from DD

DM annihilation: pseudoscalar case

$$\langle \sigma v_{\rm rel} \rangle_q = \frac{3m_q^2}{2\pi v^2} \frac{g_q^2 g_{\rm DM}^2 m_{\rm DM}^2}{(M_{\rm med}^2 - 4m_{\rm DM}^2)^2 + M_{\rm med}^2 \Gamma_{\rm med}^2} \sqrt{1 - \frac{m_q^2}{m_{\rm DM}^2}}$$

$$\langle \sigma v_{\rm rel} \rangle_g = \frac{\alpha_s^2}{2\pi^3 v^2} \frac{g_q^2 g_{\rm DM}^2}{(M_{\rm med}^2 - 4m_{\rm DM}^2)^2 + M_{\rm med}^2 \Gamma_{\rm med}^2} \left| \sum_q m_q^2 f_{\text{pseudo-scalar}} \left(\frac{m_q^2}{m_\chi^2} \right) \right|^2$$

$$f_{\text{pseudo-scalar}}(\tau) = \tau \arctan^2 \left(\frac{1}{\sqrt{\tau - 1}} \right)$$

Due to m_q^2 terms annihilation to heaviest kinematically accessible quark dominates total annihilation rate

LHC vs. indirect detection

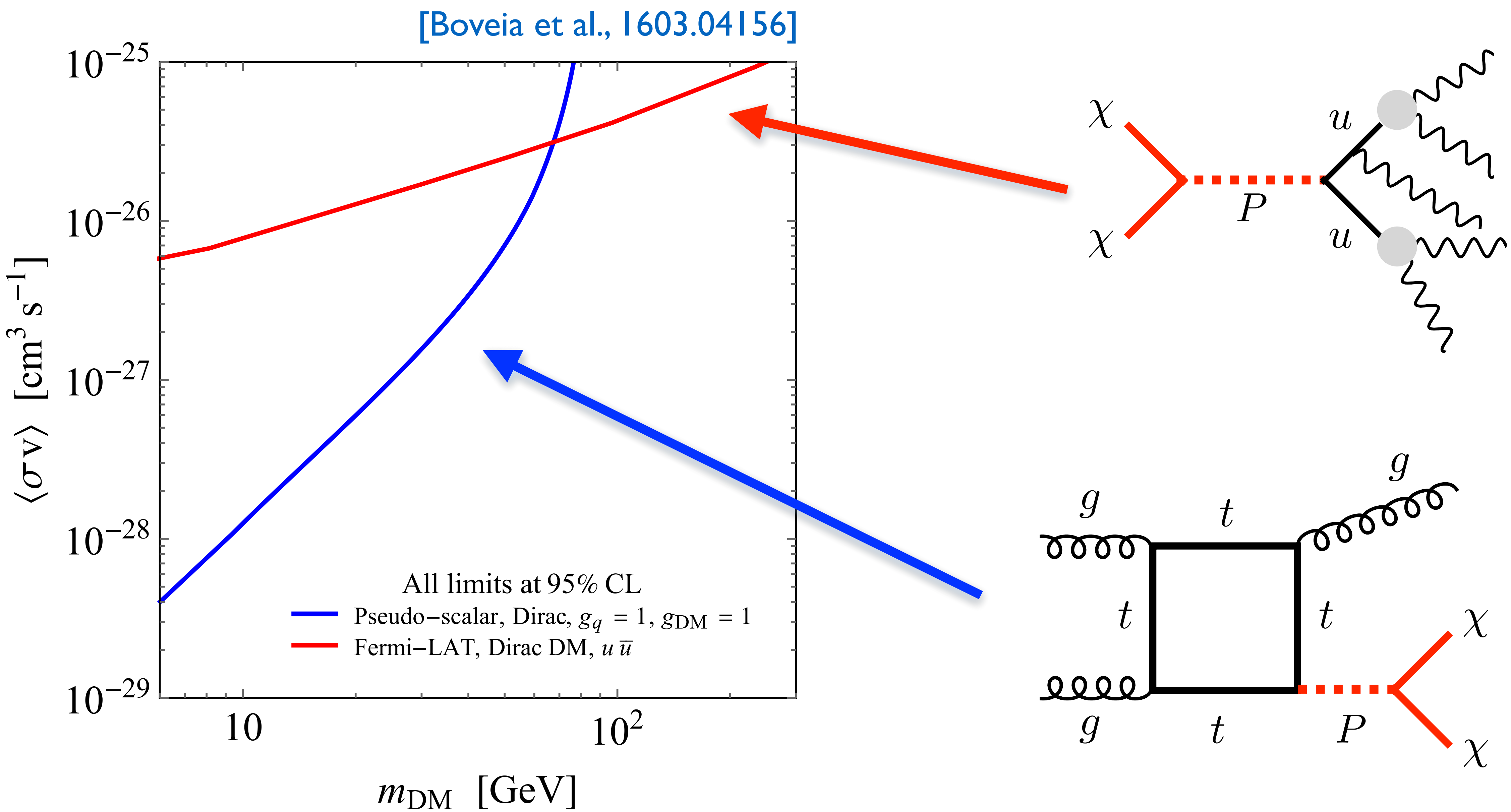

For pseudoscalar mediator model nice complementarity between LHC mono-jet bound & indirect detection limit from Fermi-LAT

γ-ray spectra from DM annihilation

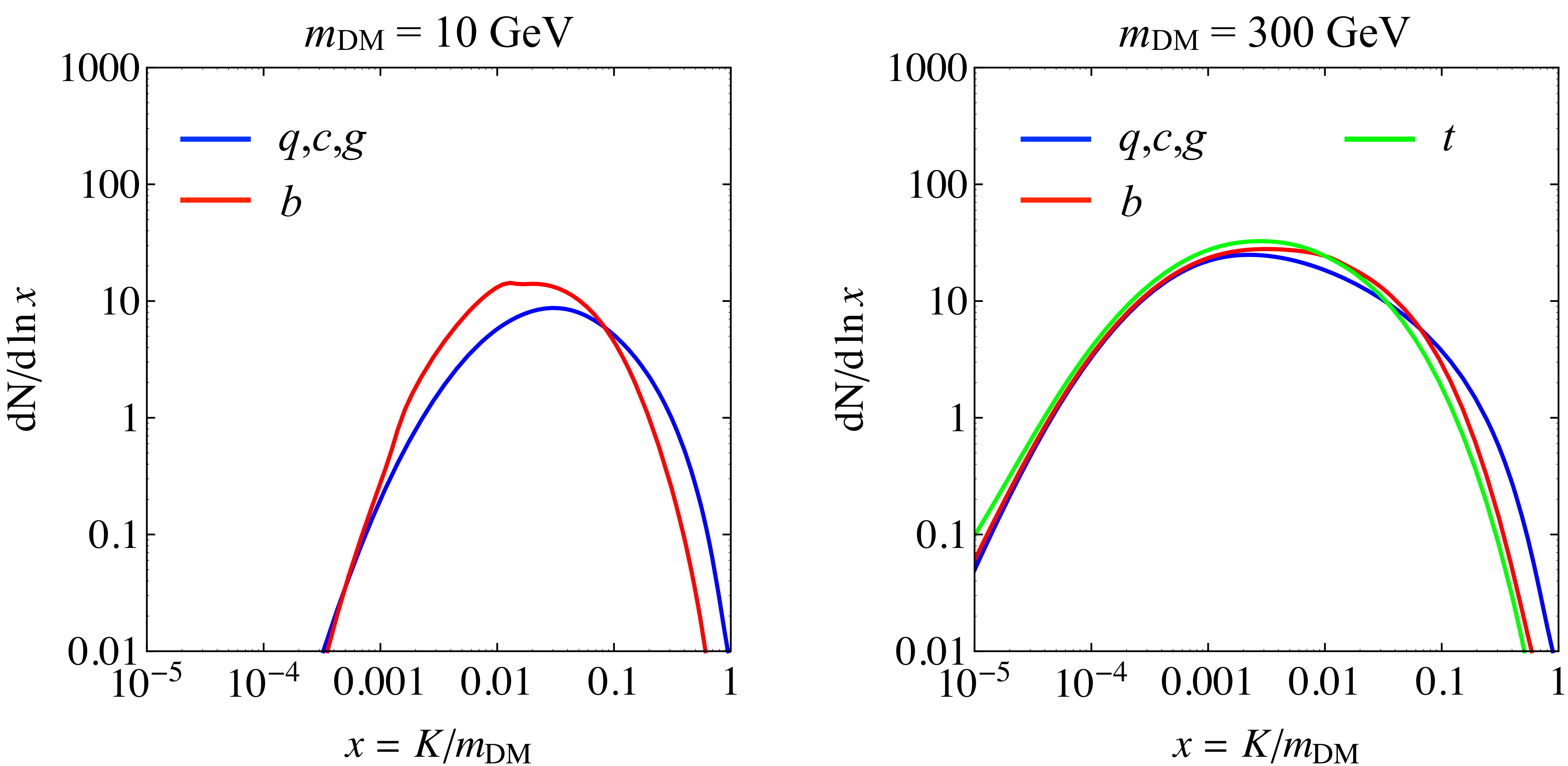

[Cirelli et al., 1012.4515; http://www.marcocirelli.net/PPPC4DMID.html]

DM annihilation bounds from dwarfs

[Fermi-LAT, 1503.02641]

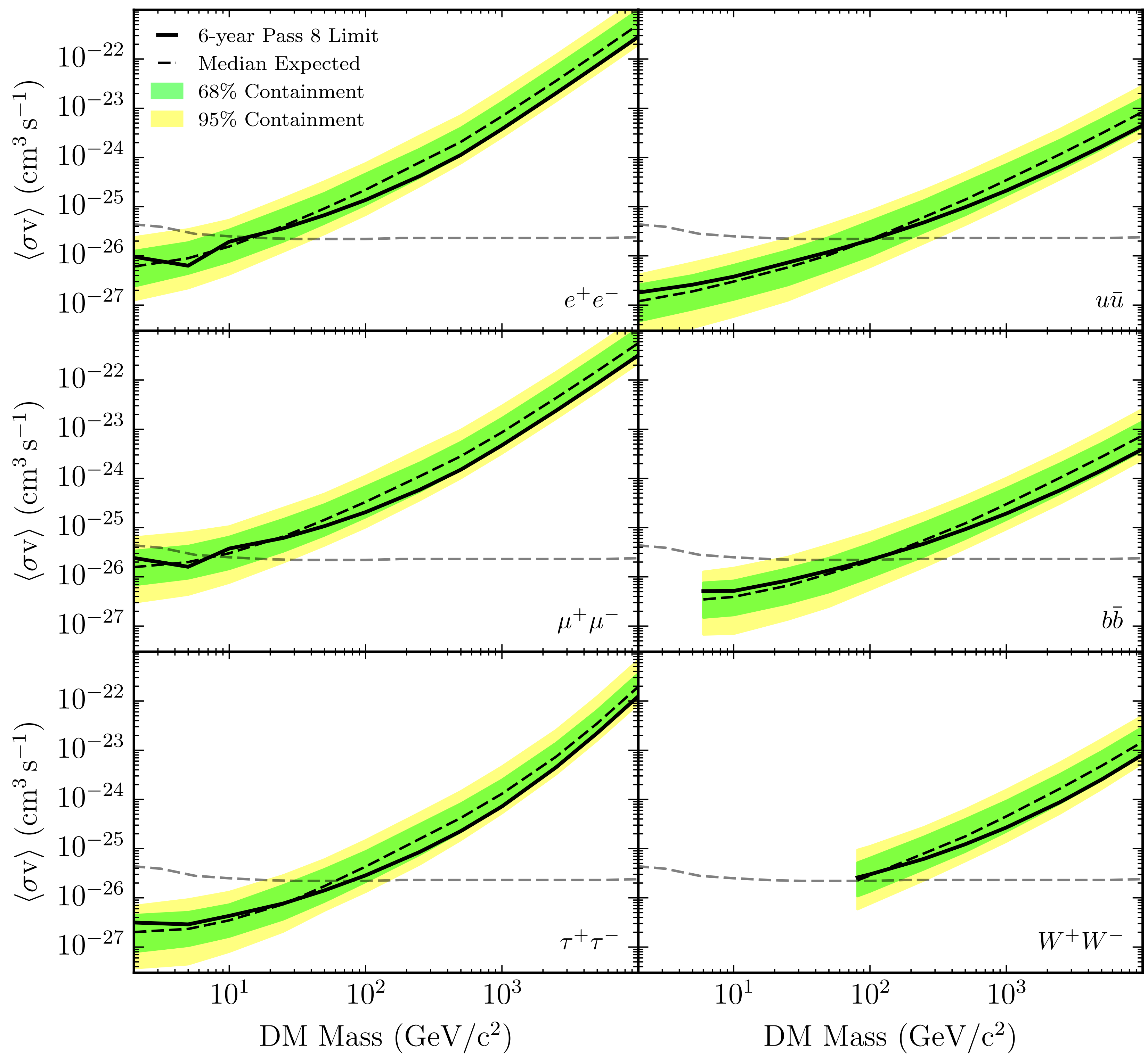

From suppressed to unsuppressed DD

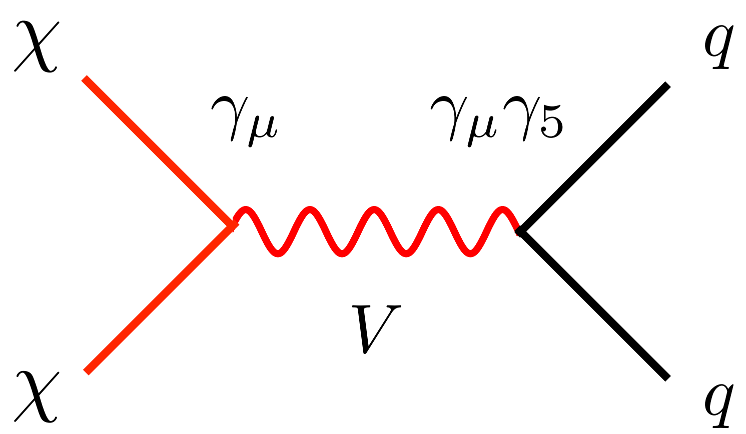

$$= C_7^q D_7^q$$

$$C_7^q = -\frac{g_\chi g_q}{M_V^2}\,, \qquad D_7^q = \bar{\chi}\gamma^\mu \chi \bar{q}\gamma_\mu \gamma_5 q$$

operator leads to SD χ-N interactions
that are both v^2 & q^2 suppressed

From suppressed to unsuppressed DD

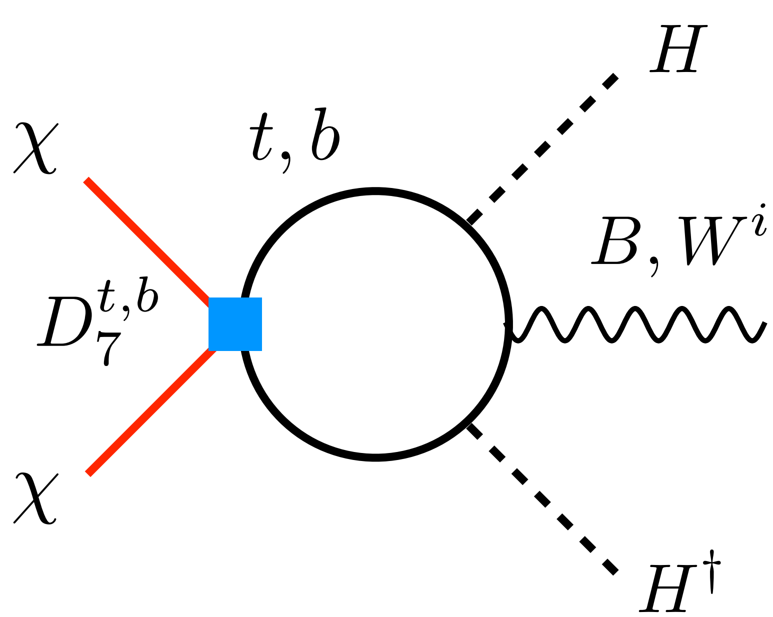

$= C_H D_H$

$$C_H = -\sum_{q=t,b} \frac{3y_q^2 T_3^q C_7^q}{2\pi^2} \ln\left(\frac{v}{M_V}\right) , \qquad D_H = \bar{\chi}\gamma^\mu\chi \left(H^\dagger i \overleftrightarrow{D}_\mu H\right)$$

[Crivellin et al. 1402.1173]

From suppressed to unsuppressed DD

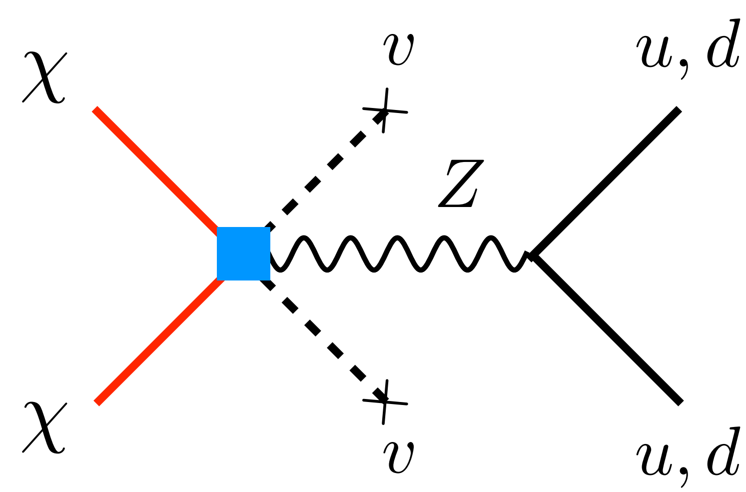

$$= C_5^{u,d} D_5^{u,d}$$

$$C_5^q = \frac{g_\chi}{M_V^2} \left(T_3^q - 2Q_q s_w^2\right) \sum_{p=t,b} \frac{3y_p^2 g_p T_3^p}{2\pi^2} \ln\left(\frac{v}{M_V}\right) , \qquad D_5^q = \bar{\chi}\gamma^\mu\chi\,\bar{q}\gamma_\mu q$$

operator leads to SI χ-N interactions

[Crivellin et al. 1402.1173]

From suppressed to unsuppressed DD

[D'Eramo et al., 1605.04917]

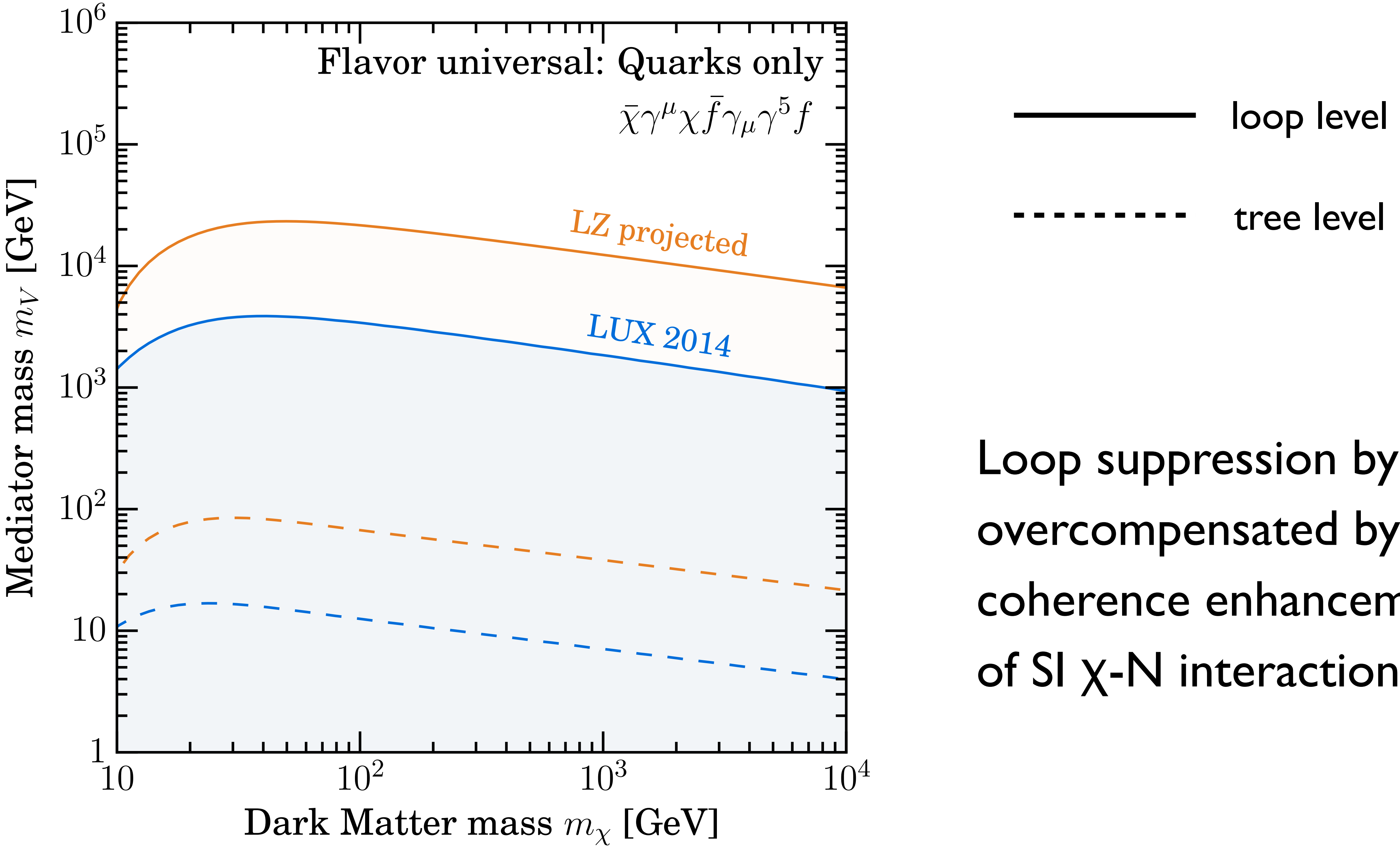

Loop suppression by far overcompensated by coherence enhancement of SI χ-N interactions

Mono-jet bounds on spin-0 models

[CMS, 1712.02345]

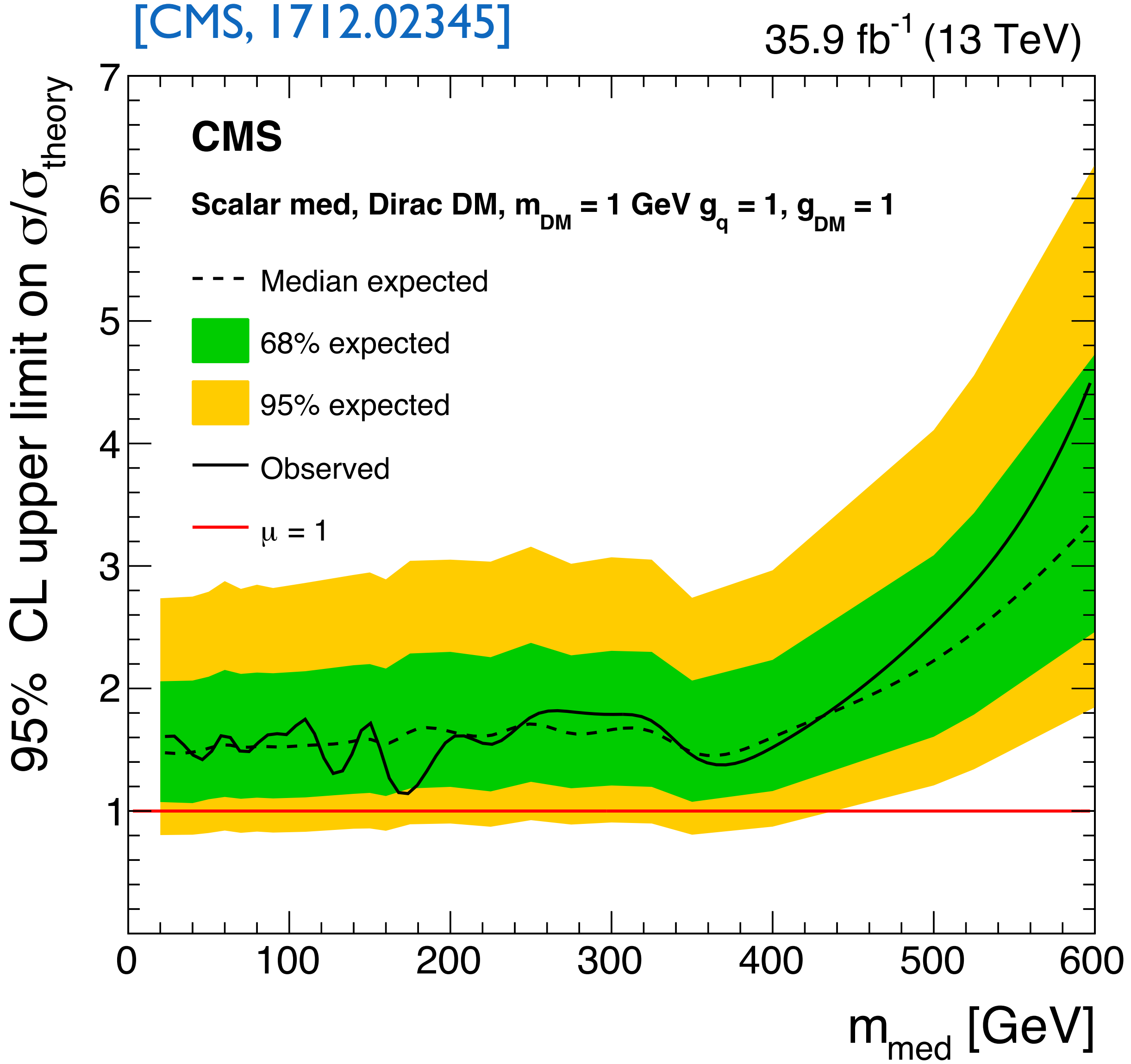

[ATLAS, 1711.03301]

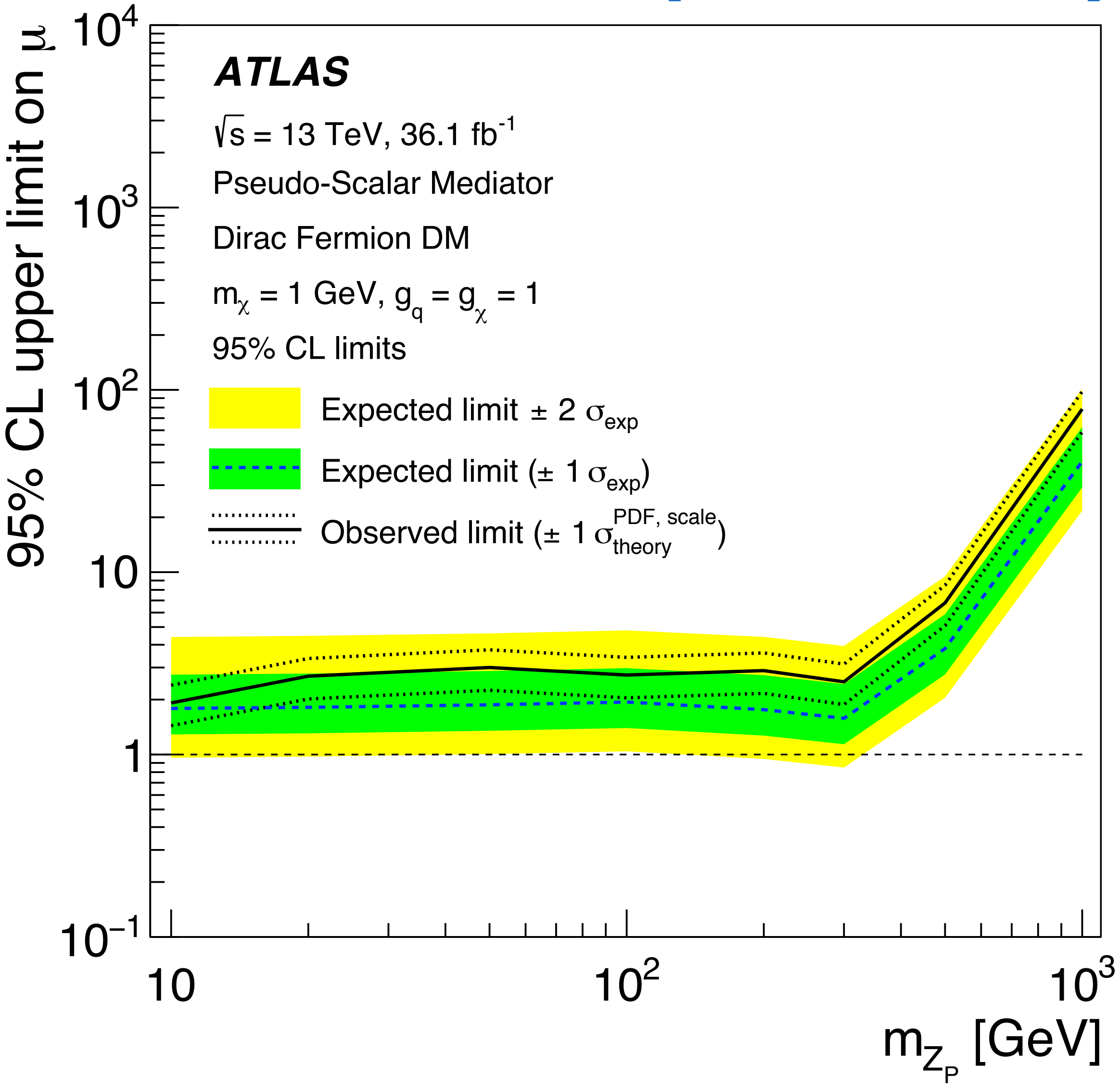

$t\bar{t}/b\bar{b}+E_{T,\,miss}$ bounds on spin-0 models

[ATLAS-CONF-2018-051]

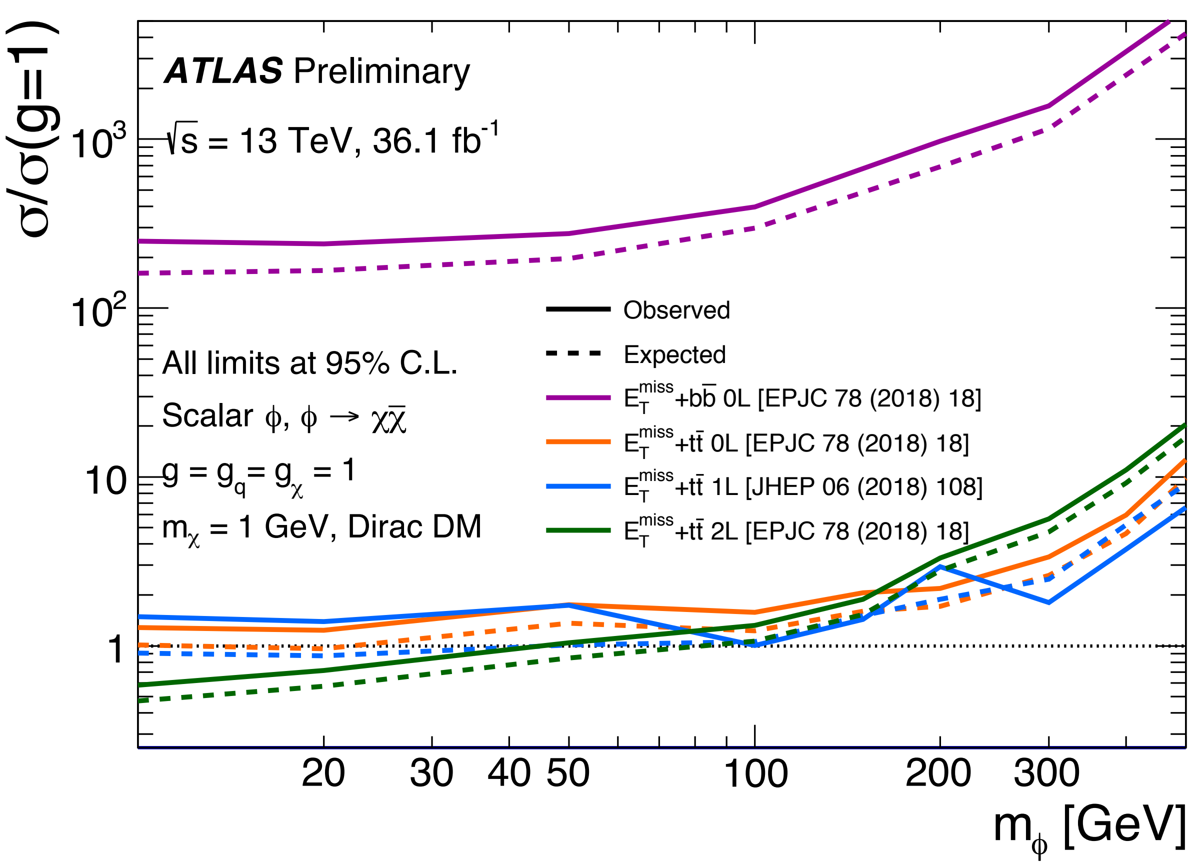

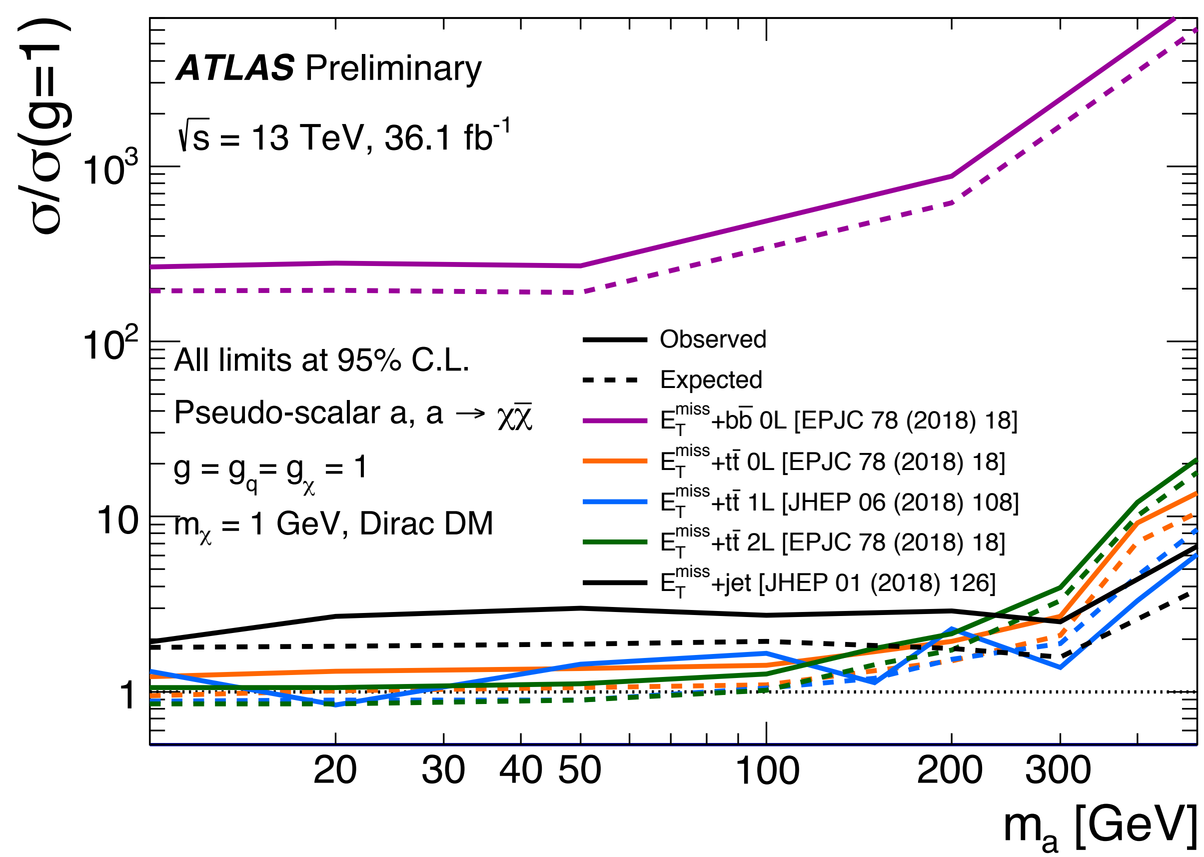

$t\bar{t}/b\bar{b}+E_{T,\,miss}$ bounds on spin-0 models

[CMS, 1706.02581]

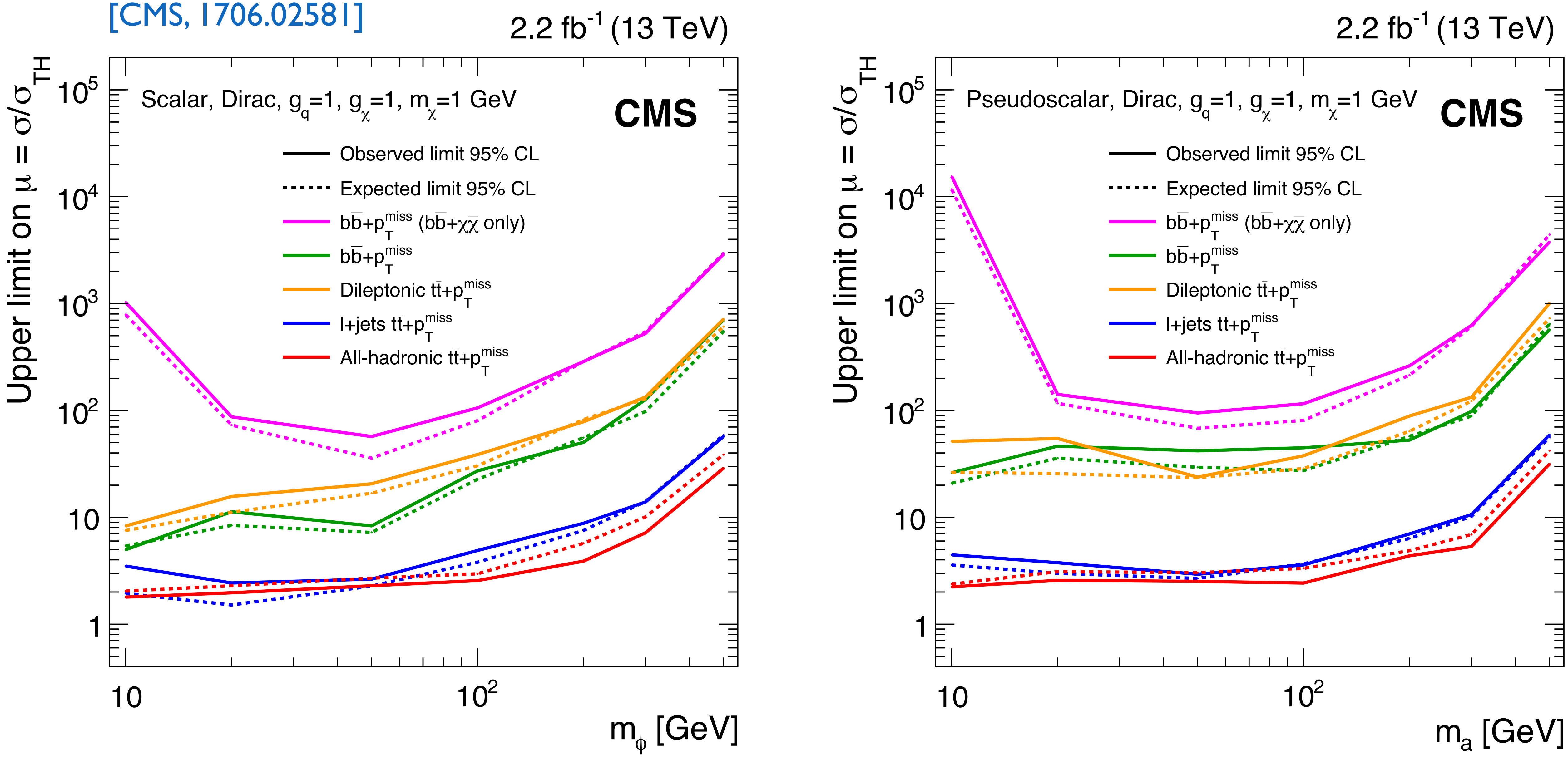

Ditop limits

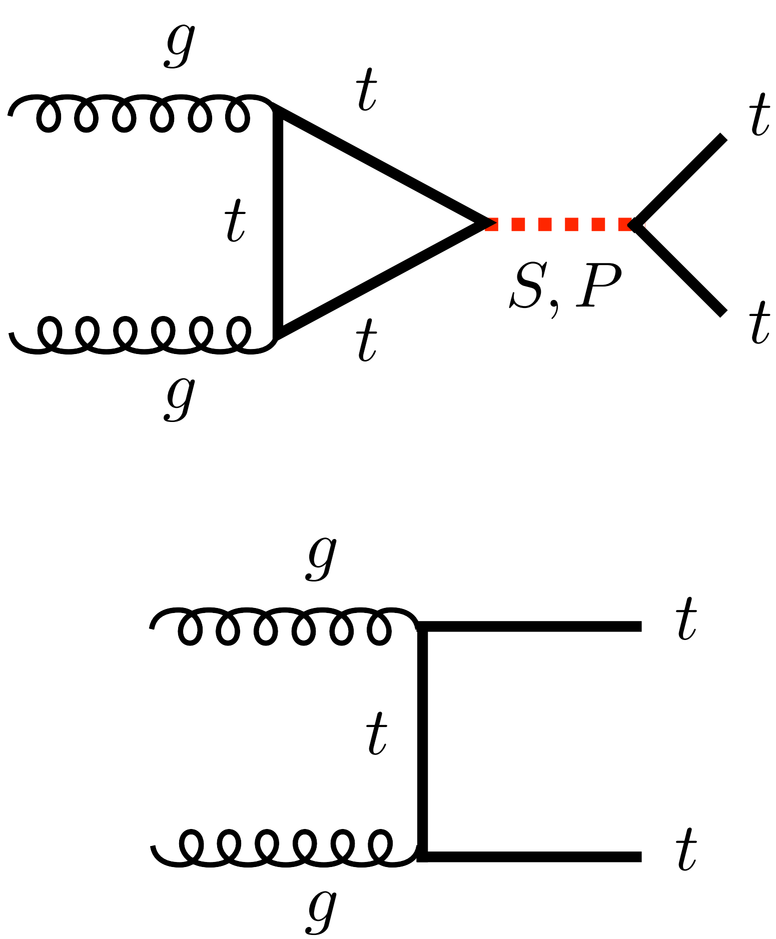

[ATLAS-CONF-2016-073]

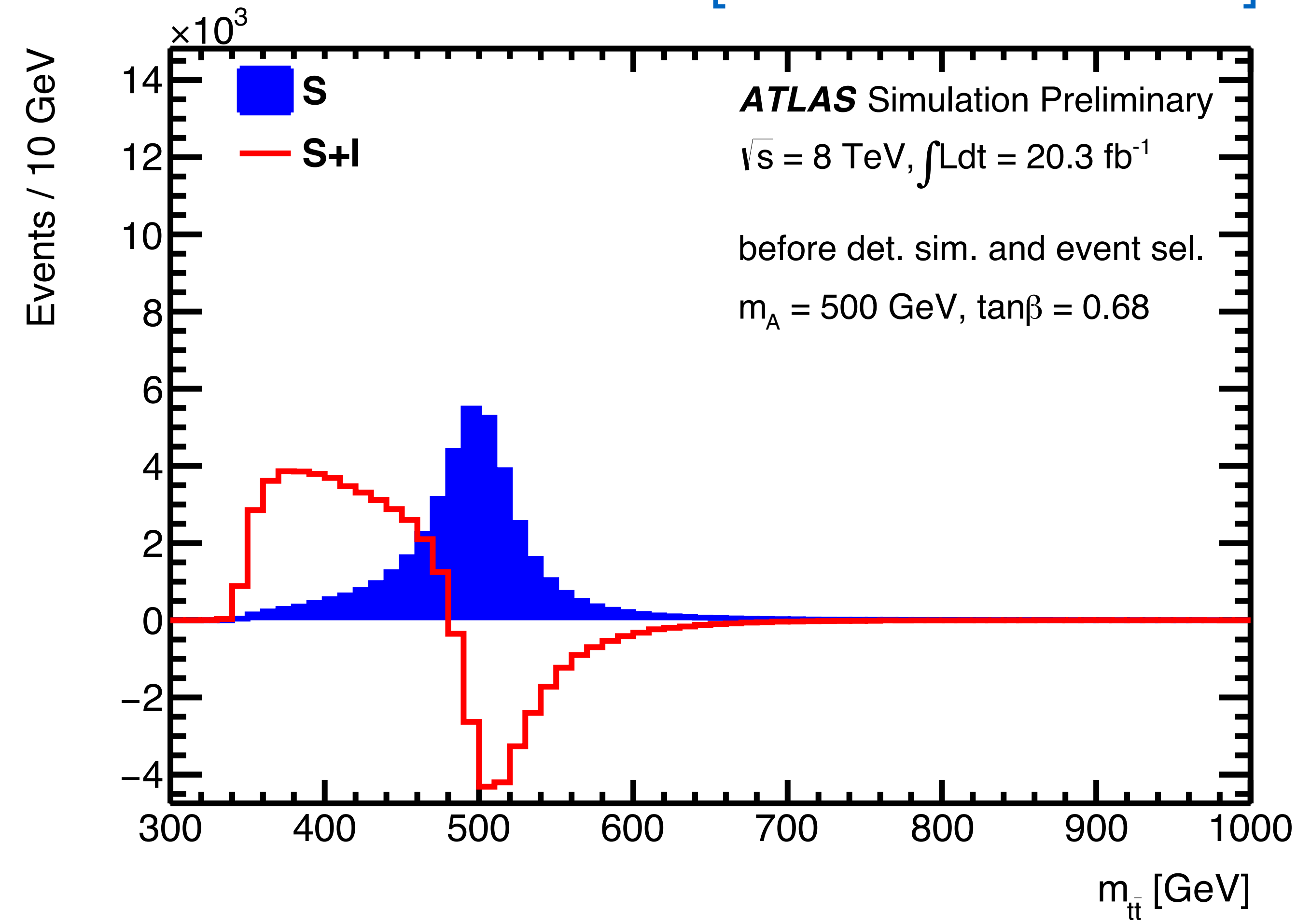

Spin-0 ditop resonances interfere maximal with SM background, which leads to a peak-dip structure in $m_{t\bar{t}}$ invariant mass spectrum

[Dicus et al., 9404359; Frederix & Maltoni, 0712.2355; Craig et al., 1504.04630; Bernreuther et al., 1511.05584; …]

Ditop limits

[ATLAS-CONF-2016-073]

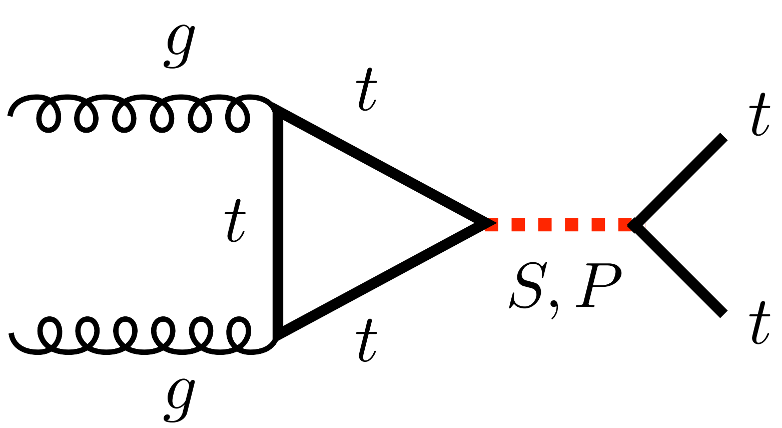

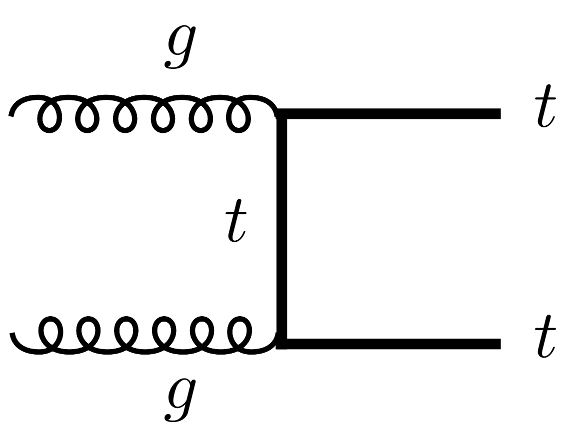

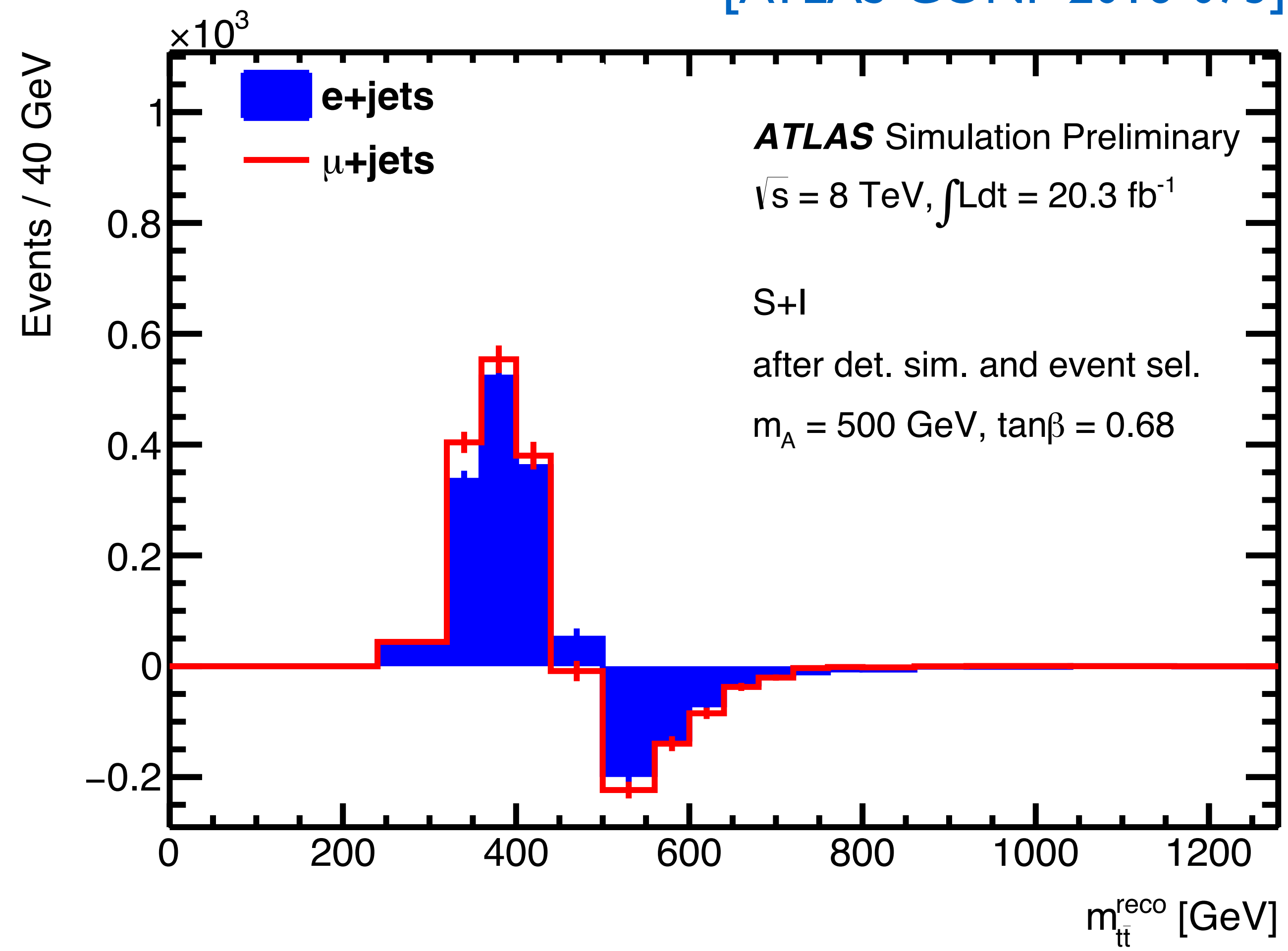

Compared to parton-level spectra, reconstructed distributions with narrower resonances are more strongly distorted due detector resolution

Ditop limits

[ATLAS, 1707.06025]

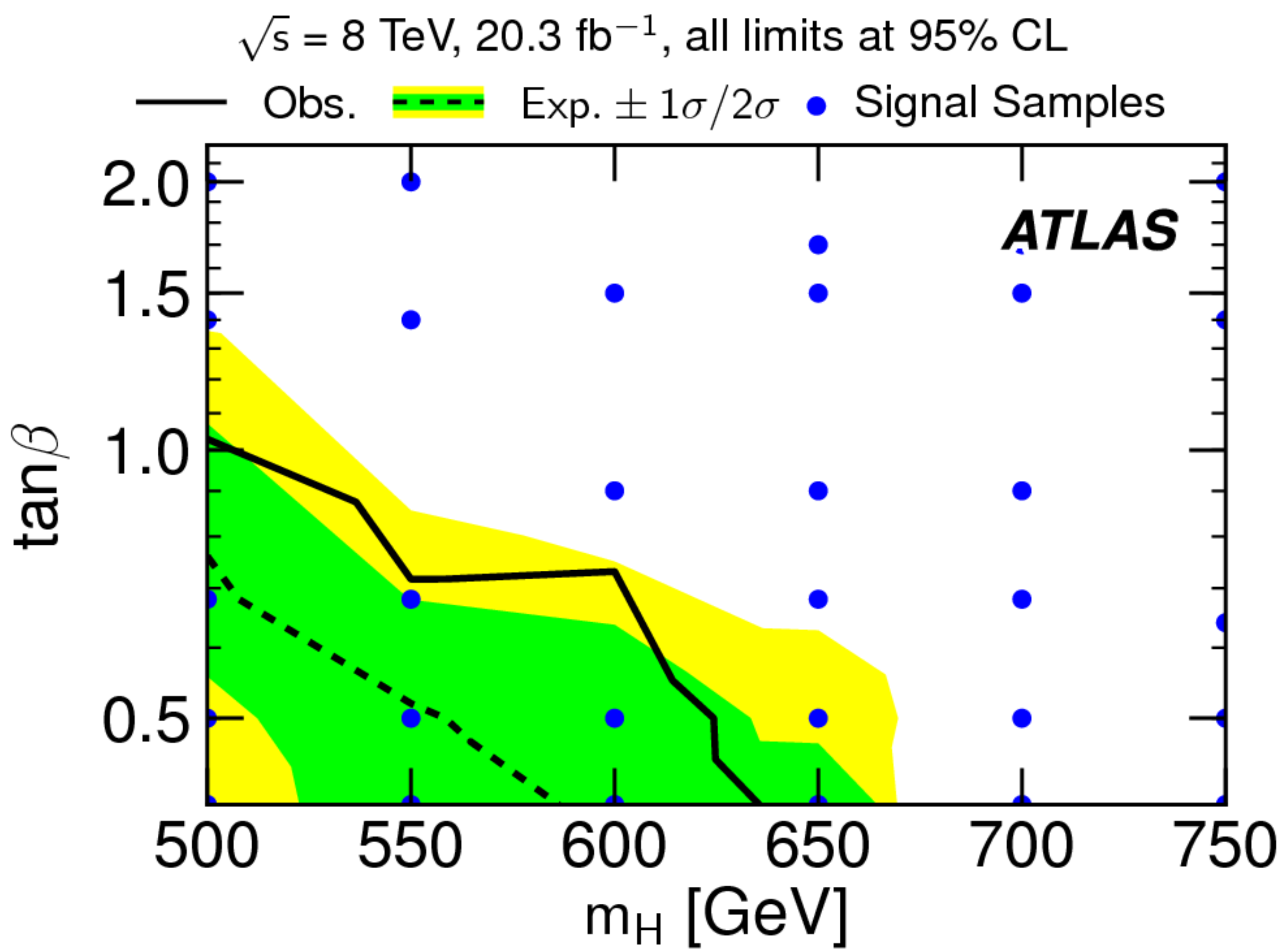

For a scalar of 500 GeV (600 GeV) values of tanβ < 1.0 (tanβ < 0.73) are excluded at 95% CL in type-II 2HDM

Ditop limits

[ATLAS, 1707.06025]

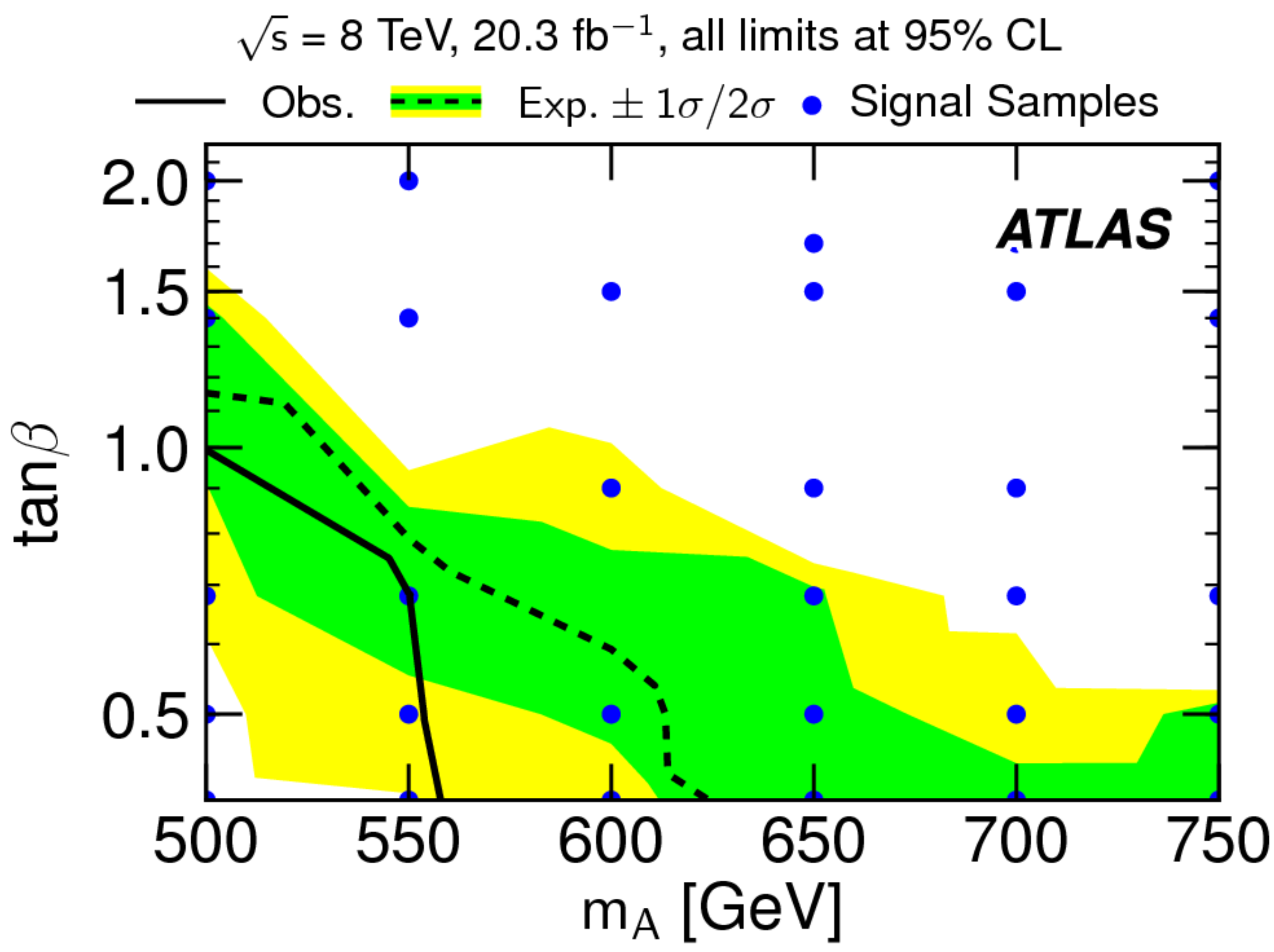

For a pseudoscalar of 500 GeV (550 GeV) values of tanβ < 1.0 (tanβ < 0.69) are excluded at 95% CL in type-II 2HDM

Ditop limits

[ATLAS, 1707.06025]

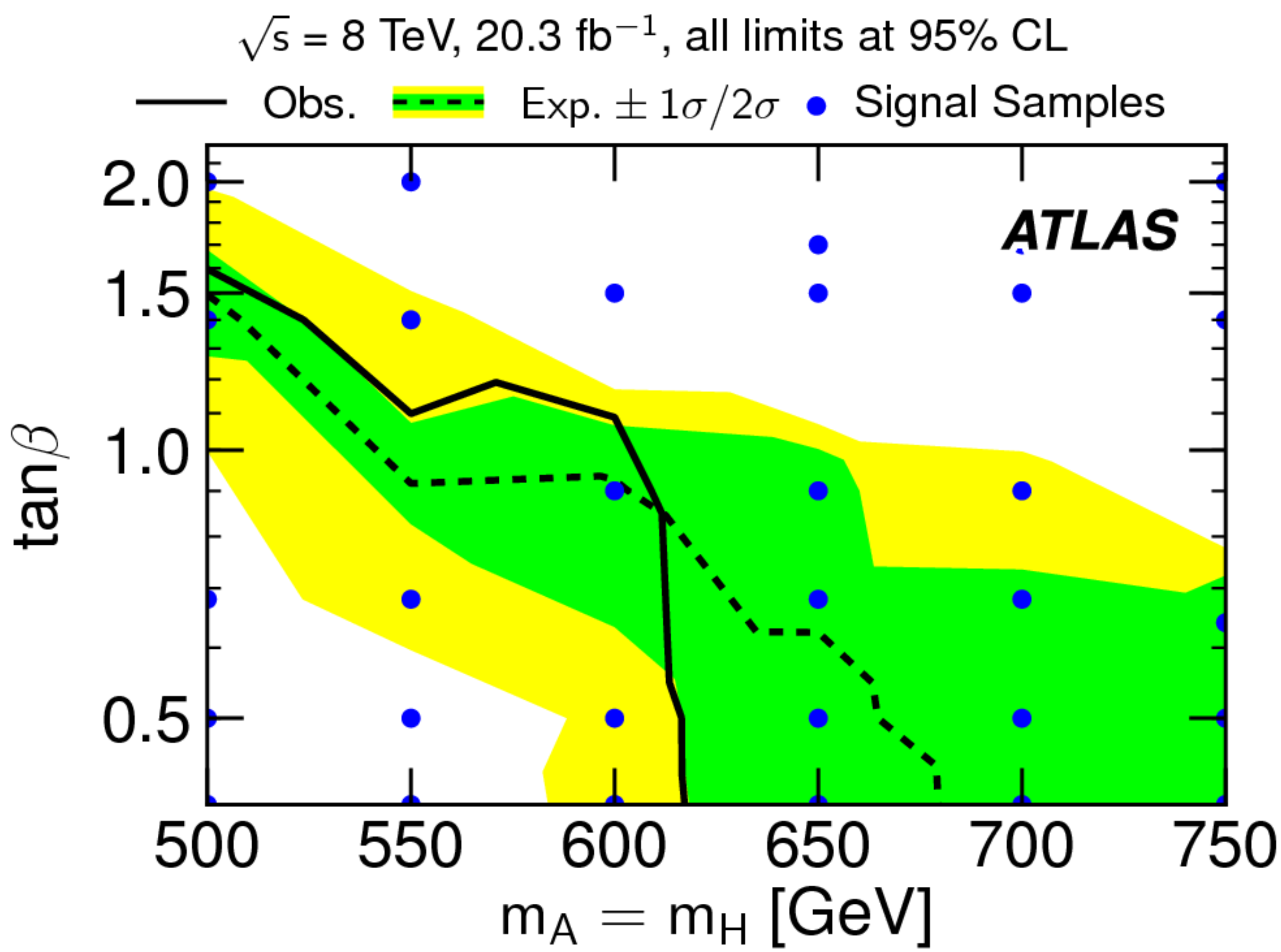

In mass degenerate case, scenarios with 500 GeV (600 GeV) & values of tanβ < 1.55 (tanβ < 1.09) are excluded at 95% CL in type-II 2HDM

$t\bar{t}+E_{T,\text{miss}}$ production

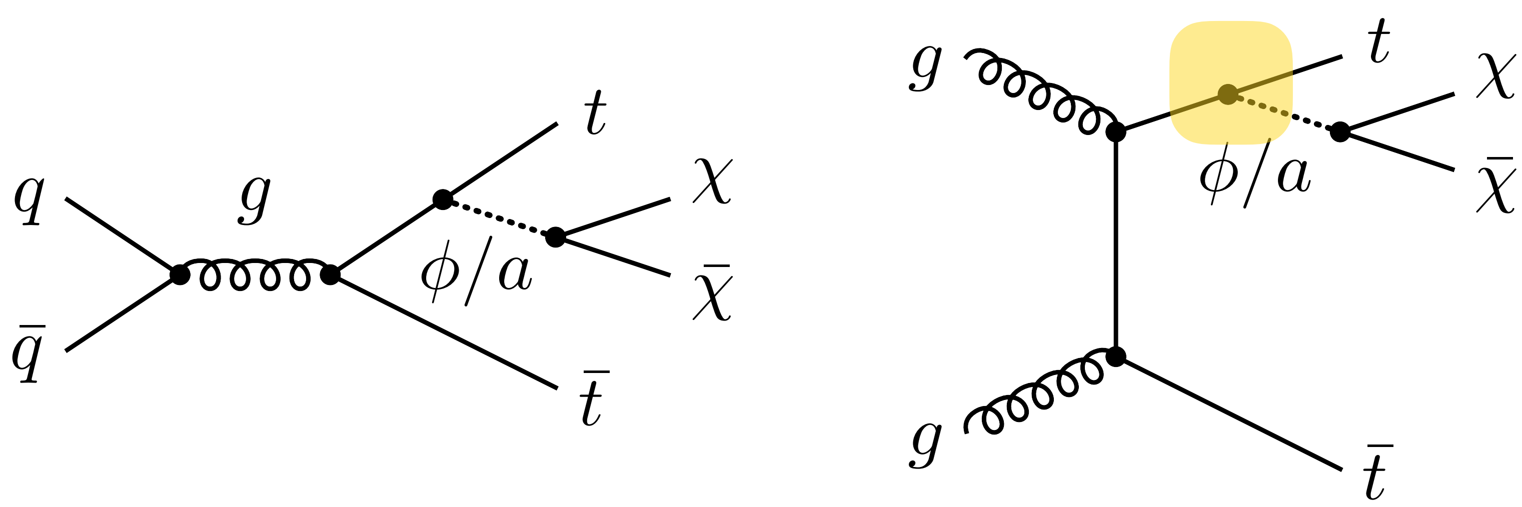

$$f_{t\to\phi}(x) = \frac{g_t^2}{(4\pi)^2}\left[\frac{4\,(1-x)}{x} + x\ln\left(\frac{s}{m_t^2}\right)\right] \qquad f_{t\to a}(x) = \frac{g_t^2}{(4\pi)^2}\left[x\ln\left(\frac{s}{m_t^2}\right)\right]$$

soft singularity enhances production cross section for light scalar compared to pseudoscalar

[UH, Pani & Polesello, 1611.09841]

$t\bar{t}+E_{T,\,\mathrm{miss}}$ production

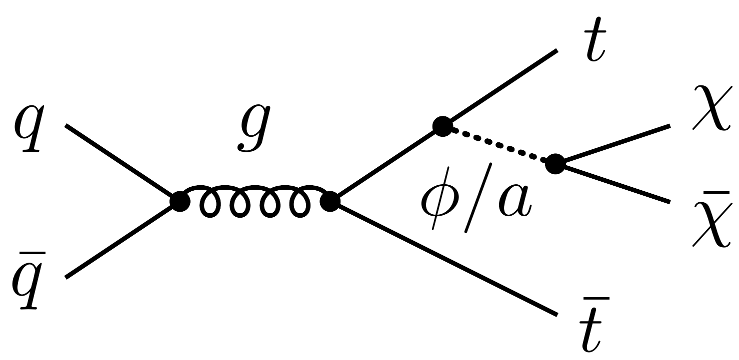

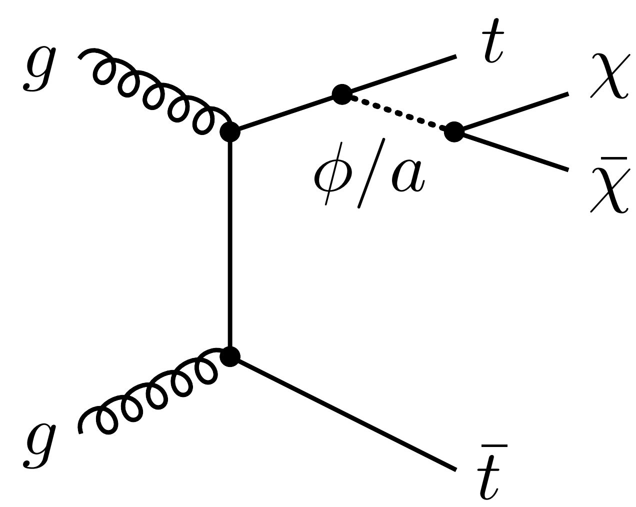

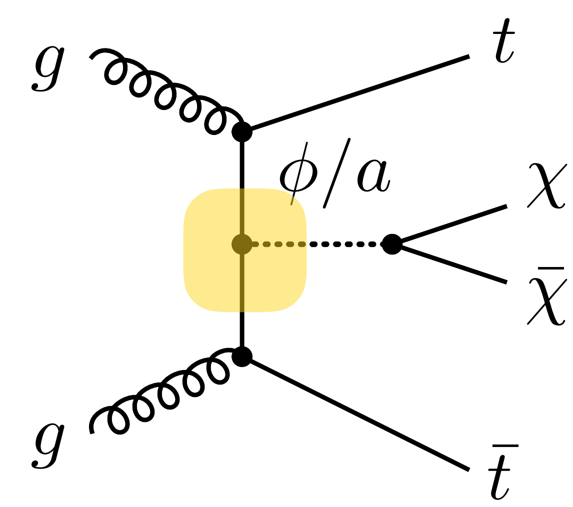

$$\overline{\sum}\left|\mathcal{M}(t\bar{t}\to\phi)\right|^2 = \frac{g_t^2\, s}{12}\,\beta^2$$

$$\overline{\sum}\left|\mathcal{M}(t\bar{t}\to a)\right|^2 = \frac{g_t^2\, s}{12}$$

scalar production in top-fusion
velocity-suppressed at threshold
compared to pseudoscalar production

[UH, Pani & Polesello, 1611.09841]

$t\bar{t}+E_{T,\,miss}$ production

[UH, Pani & Polesello , 1611.09841]

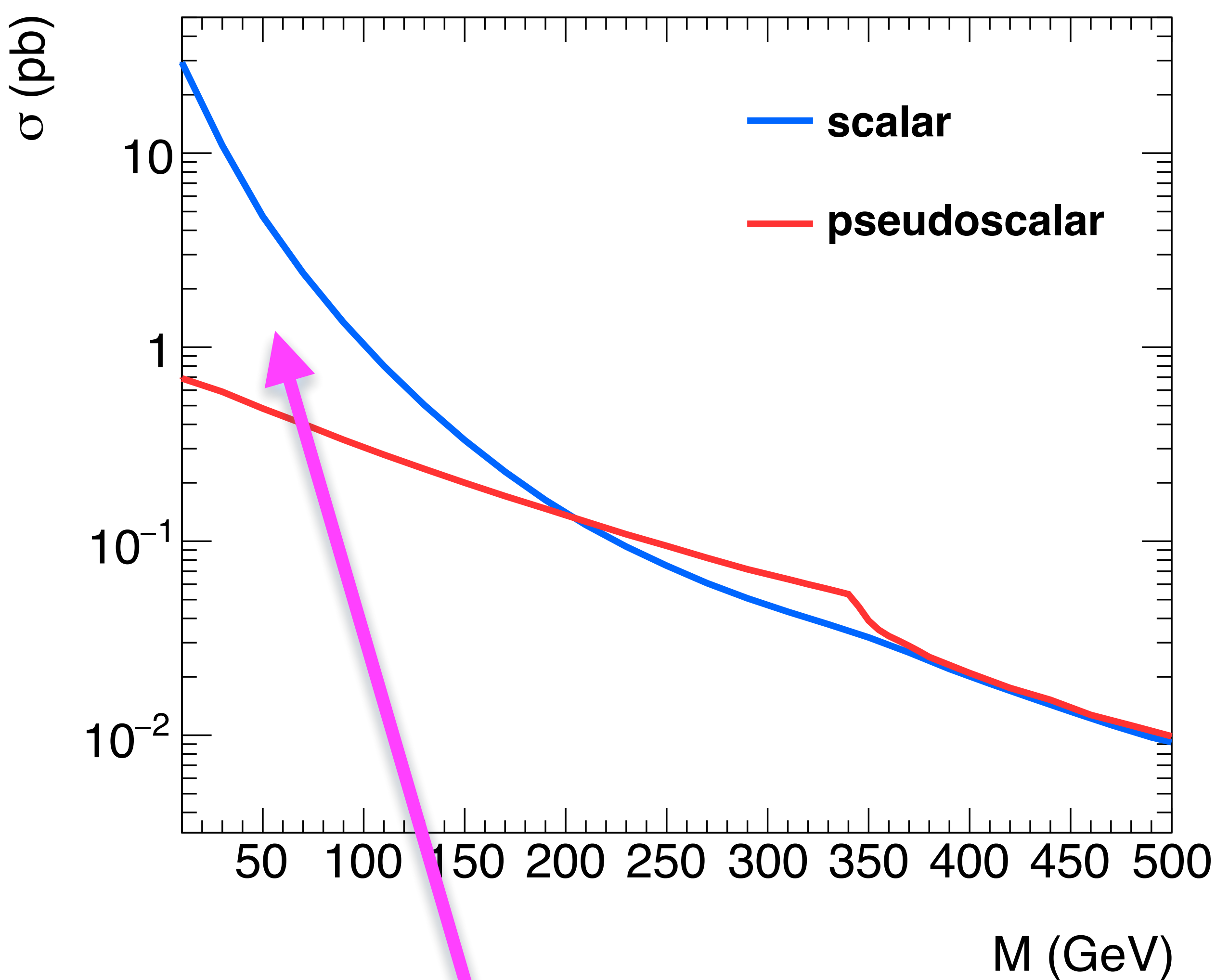

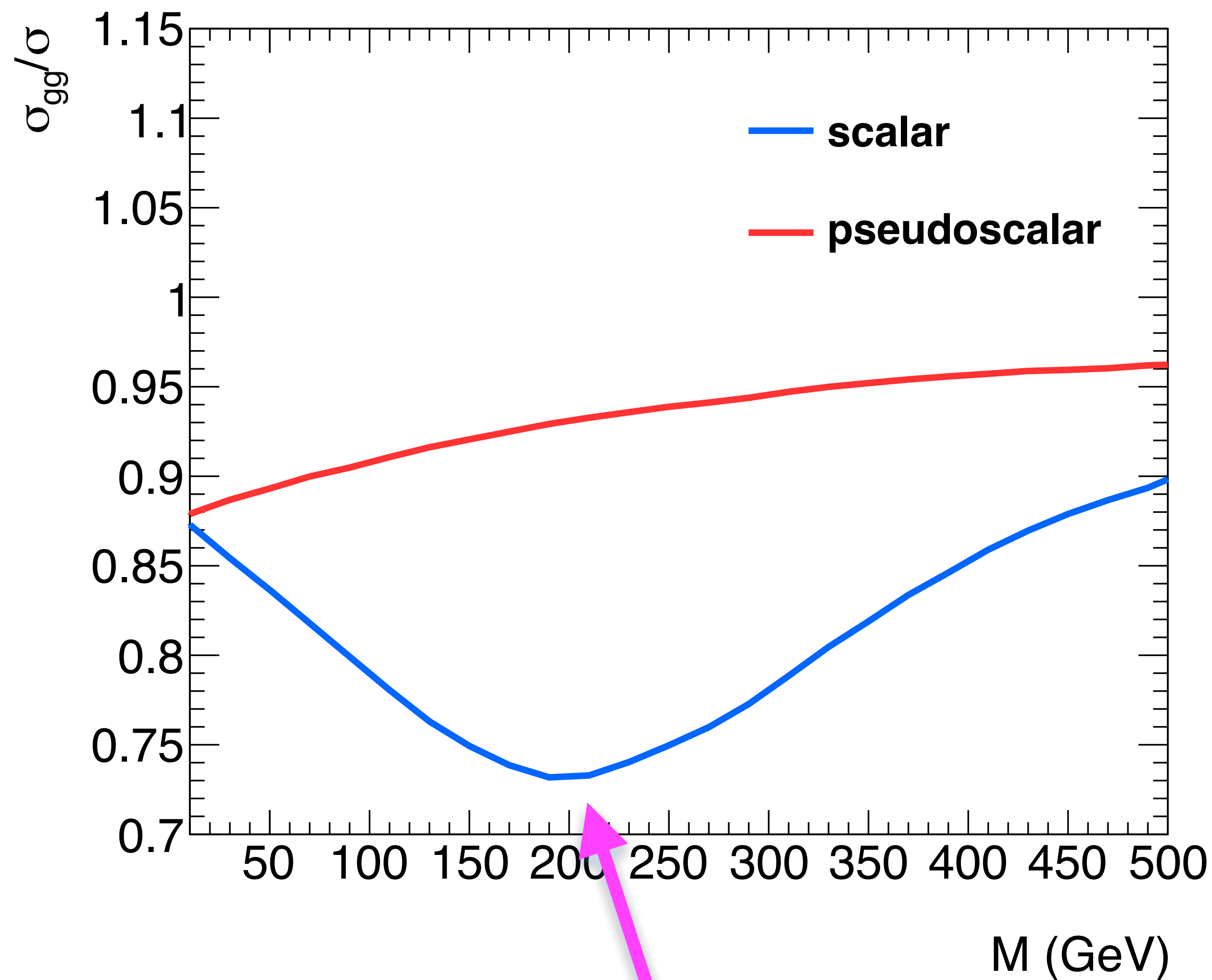

soft enhancement of scalar production in fragmentation/radiation

threshold suppression of scalar production in top-fusion

$t\bar{t}+E_{T,miss}$: signal vs. background

[UH, Pani & Polesello, 1611.09841]

top background:
$t\bar{t}$ & tW

reducible
background:
WW, WZ,
ZZ & Z+jets

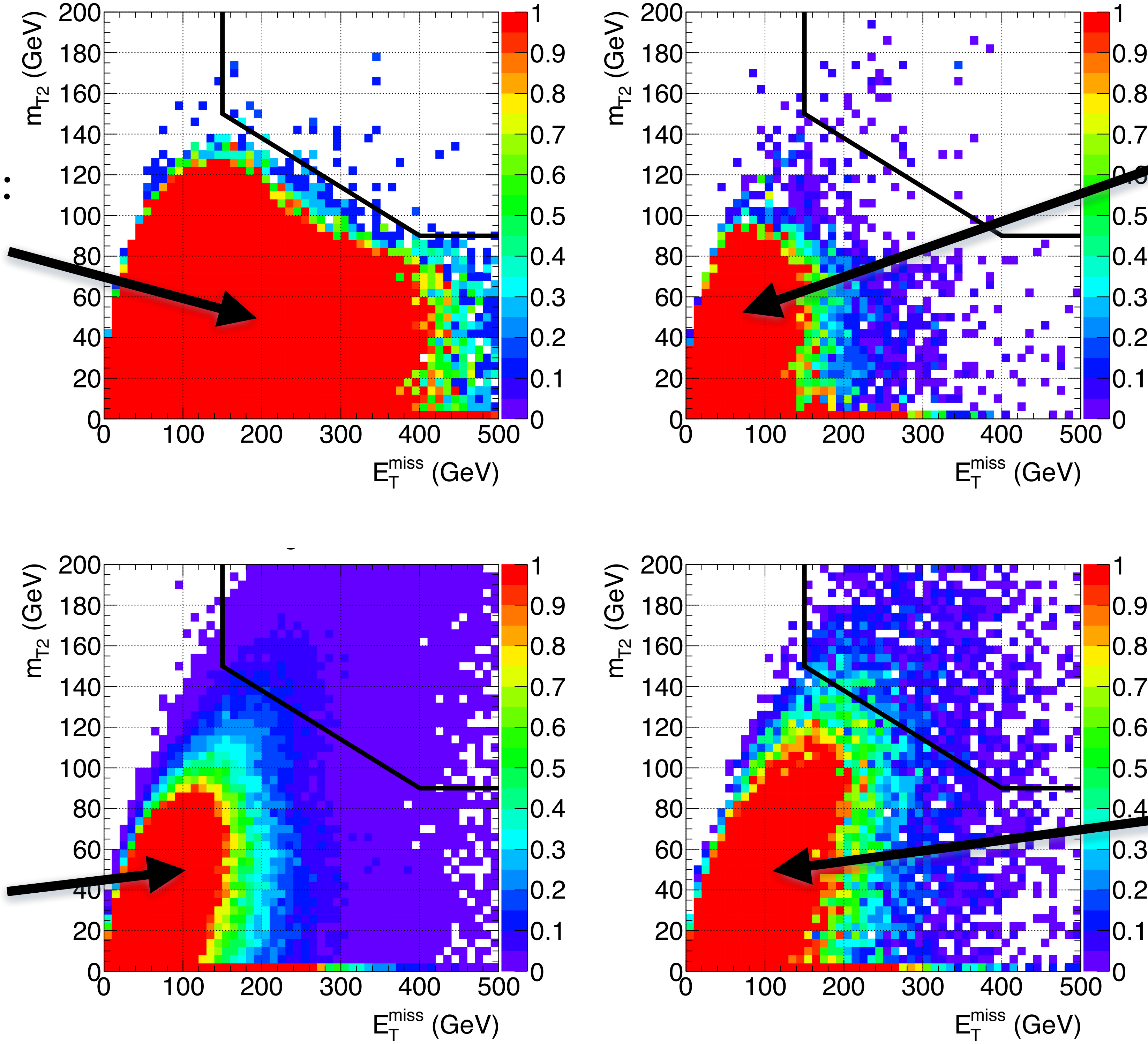

irreducible
background:
$t\bar{t}Z$ & $t\bar{t}W$

DM signal

$t\bar{t}+E_{T,\mathrm{miss}}$: background suppression

[UH, Pani & Polesello, 1611.09841]

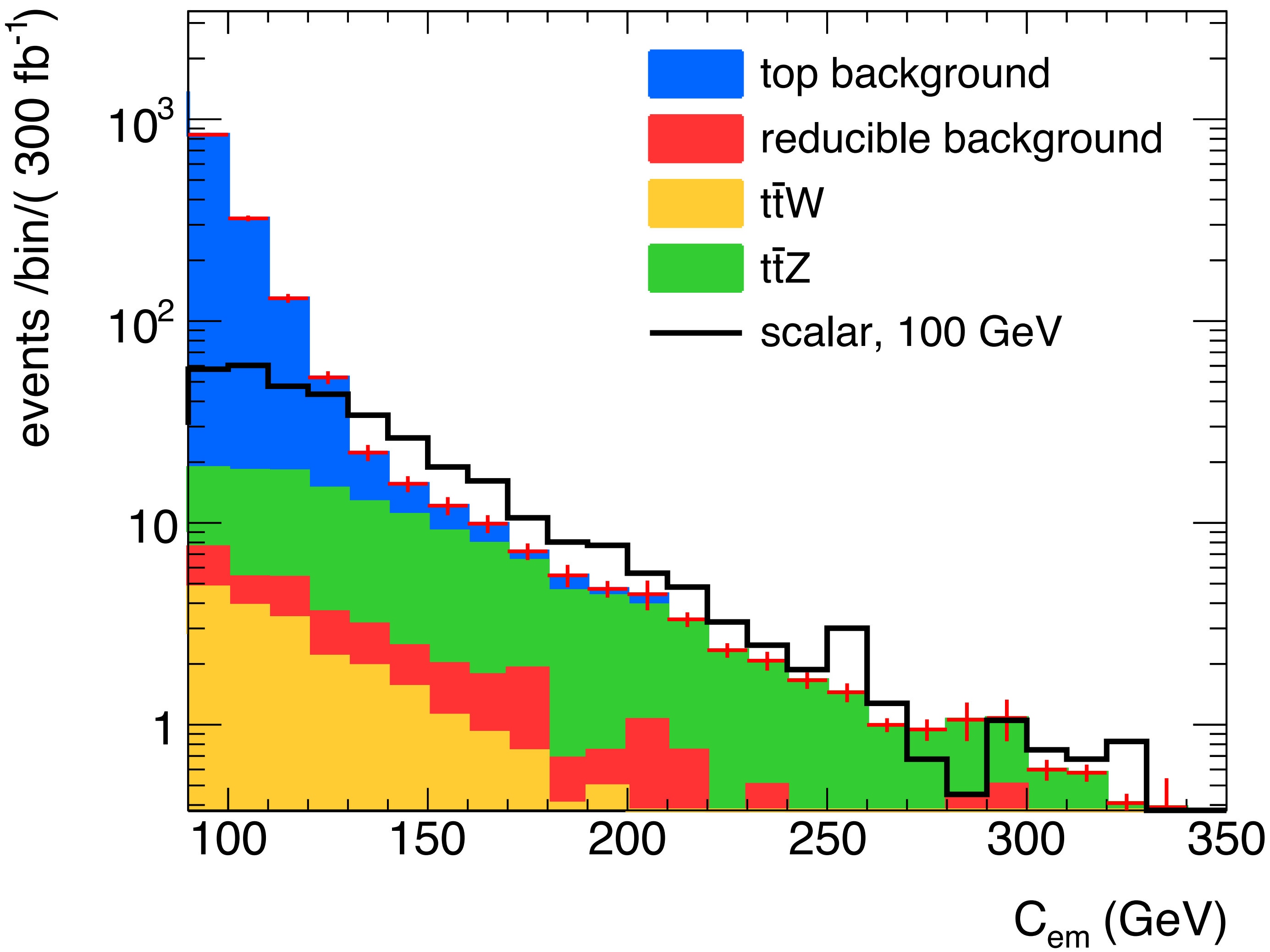

$$C_{\mathrm{em}} = m_{T2} + 0.2\ (200\,\mathrm{GeV} - E_{T,\mathrm{miss}})$$

Angular correlations in $SR_{t\bar{t}}$

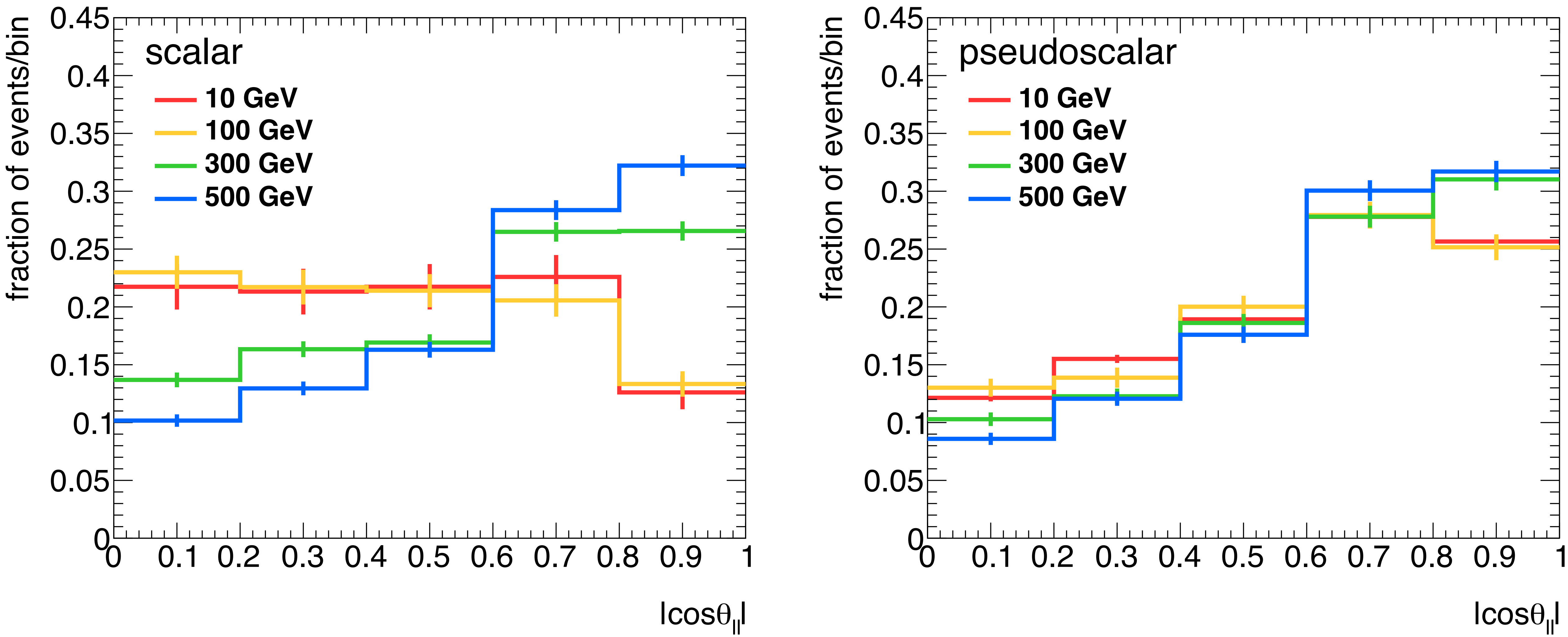

[UH, Pani & Polesello, 1611.09841]

Unitarity violation in tW+E$_{T, \text{miss}}$

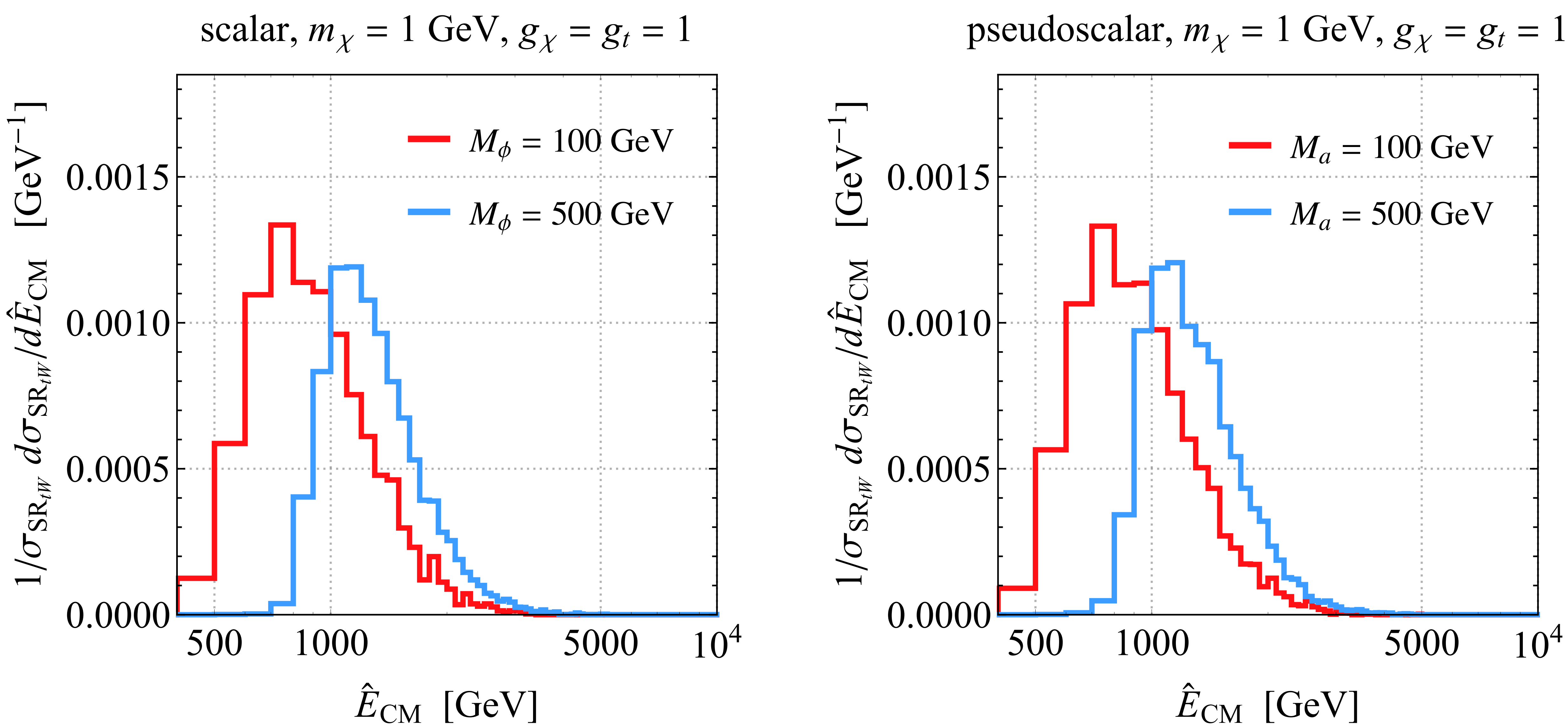

Fraction of events in tW+E$_{T, \text{miss}}$ production above cut-off of 18.6 TeV negligible at 14 TeV LHC. Unitarity violation in tX+E$_{T, \text{miss}}$ thus spurious

[UH & Polesello, 1812.00694]

Angular correlations in SR_{tW}

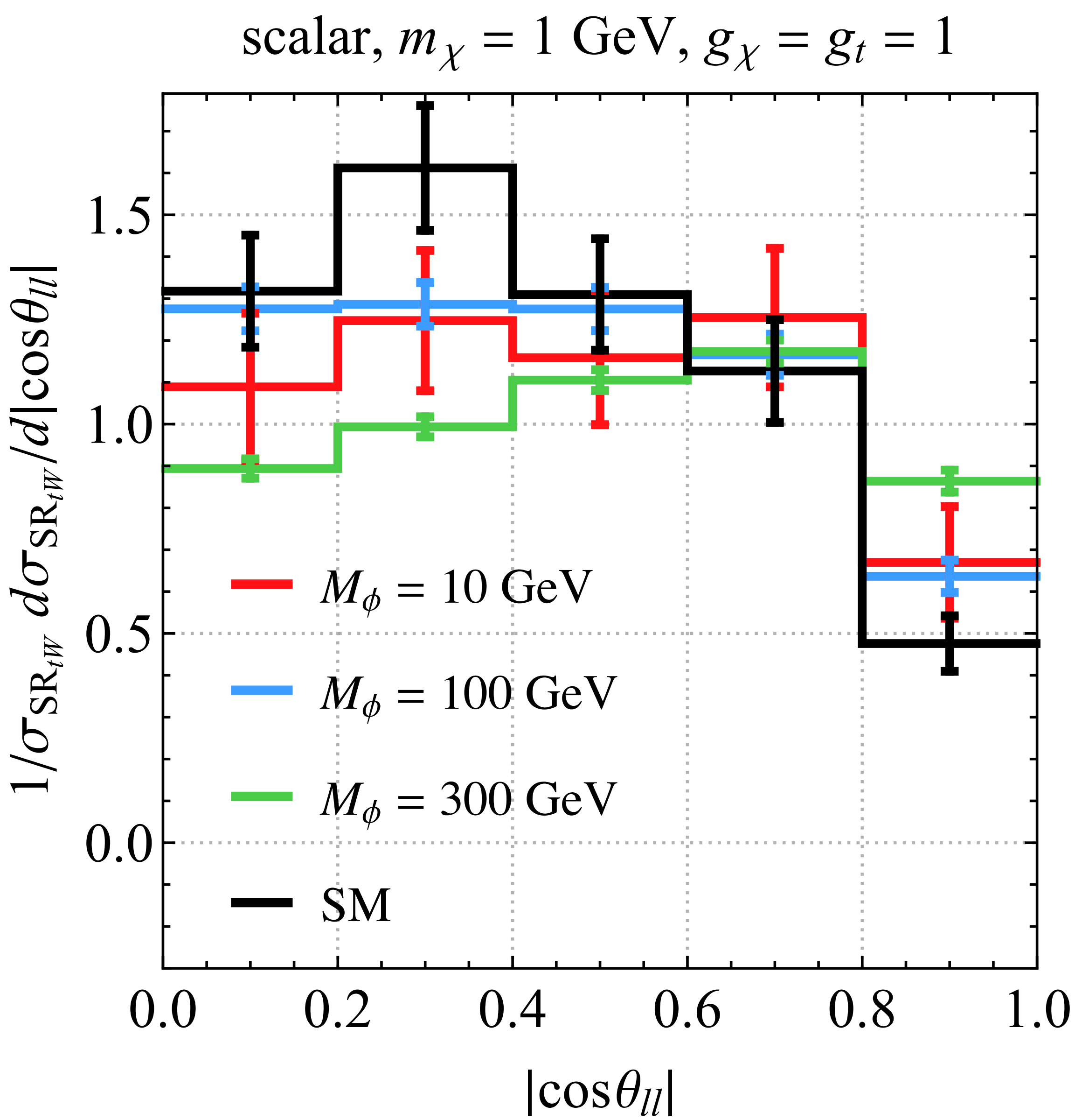

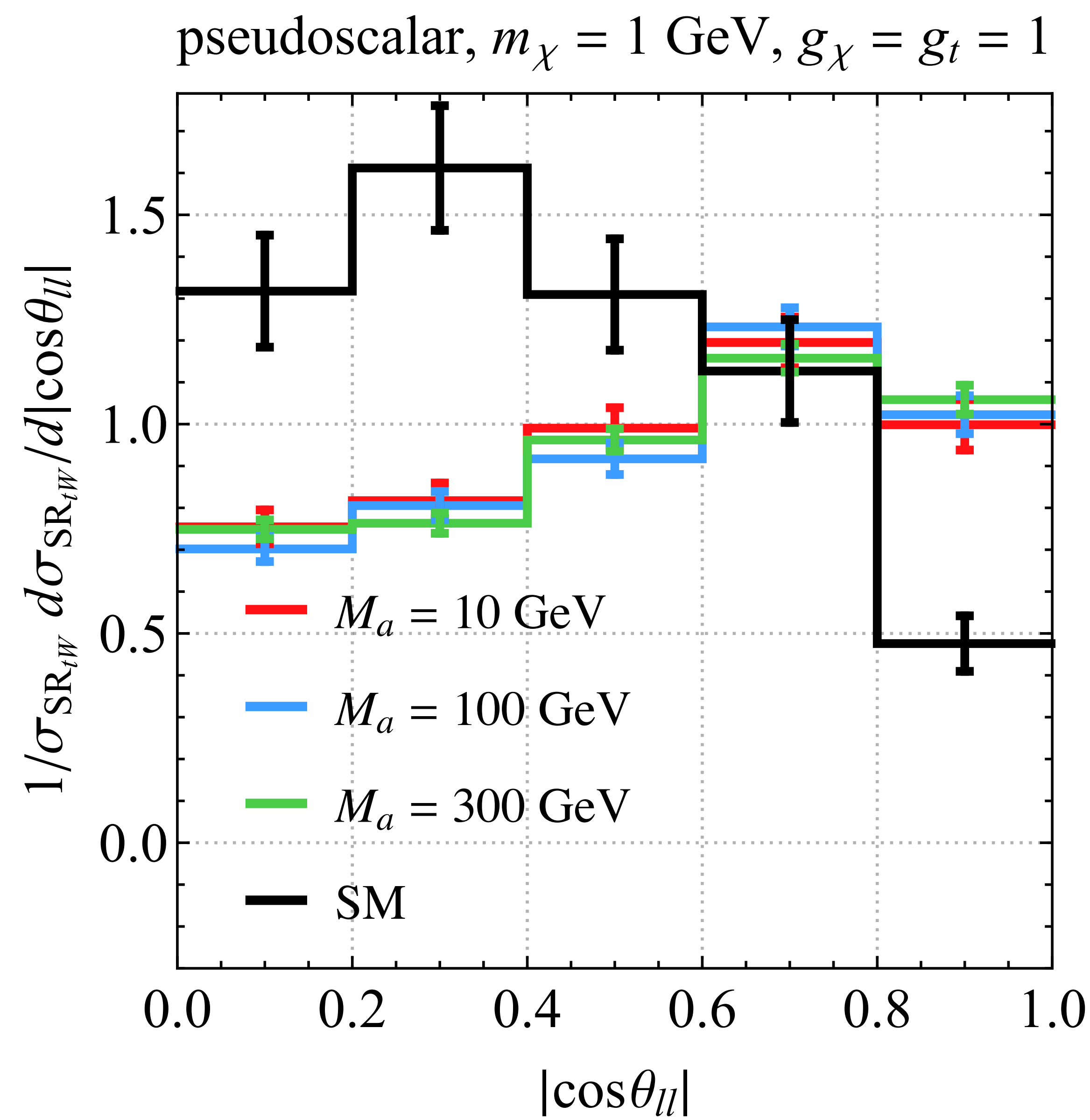

[UH & Polesello, 1812.00694]

tX+E$_{T, miss}$ HL-LHC projections

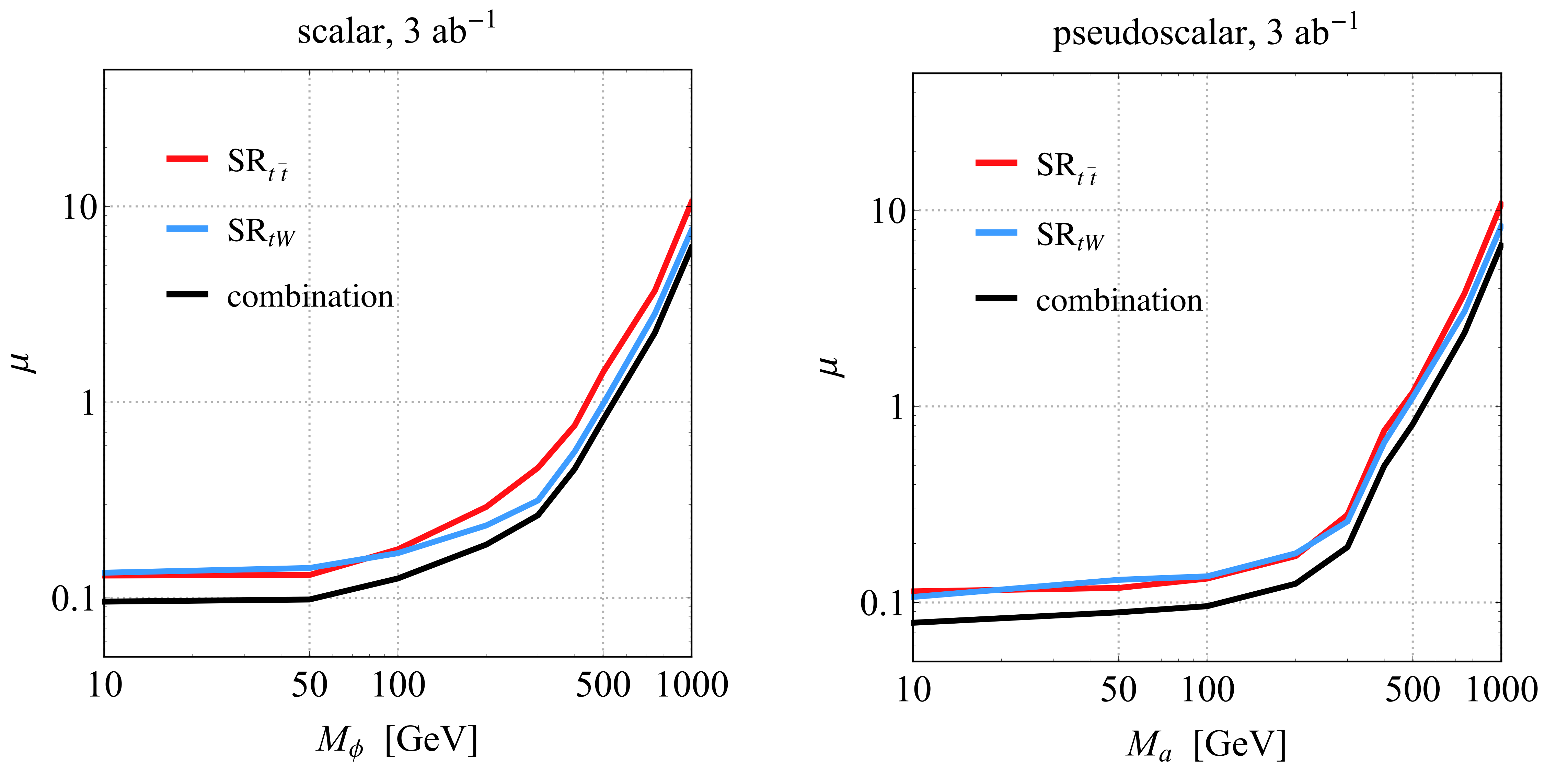

For m_{DM} = 1 GeV & $g_{SM} = g_{DM}$ = 1, combination of $SR_{t\bar{t}}$ & SR_{tW} strategies leads to 95% CL limit $M_{\phi,a} \lesssim$ 530 GeV for 3 ab^{-1} of 14 TeV LHC data

[UH & Polesello, 1812.00694]

Mono-jet shapes: $\Delta\phi_{j1j2}$ vs. $E_{T,\,miss}$

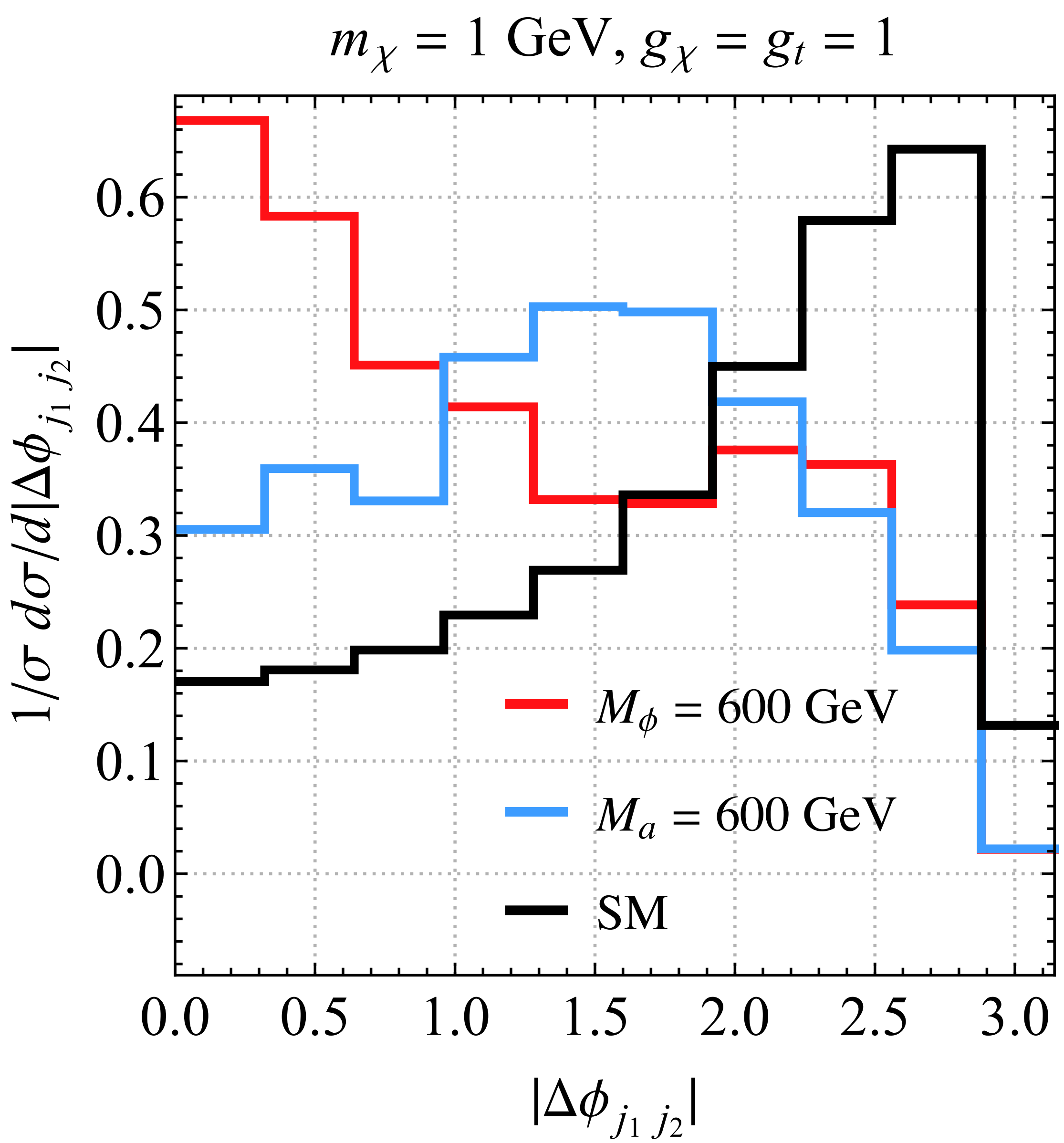

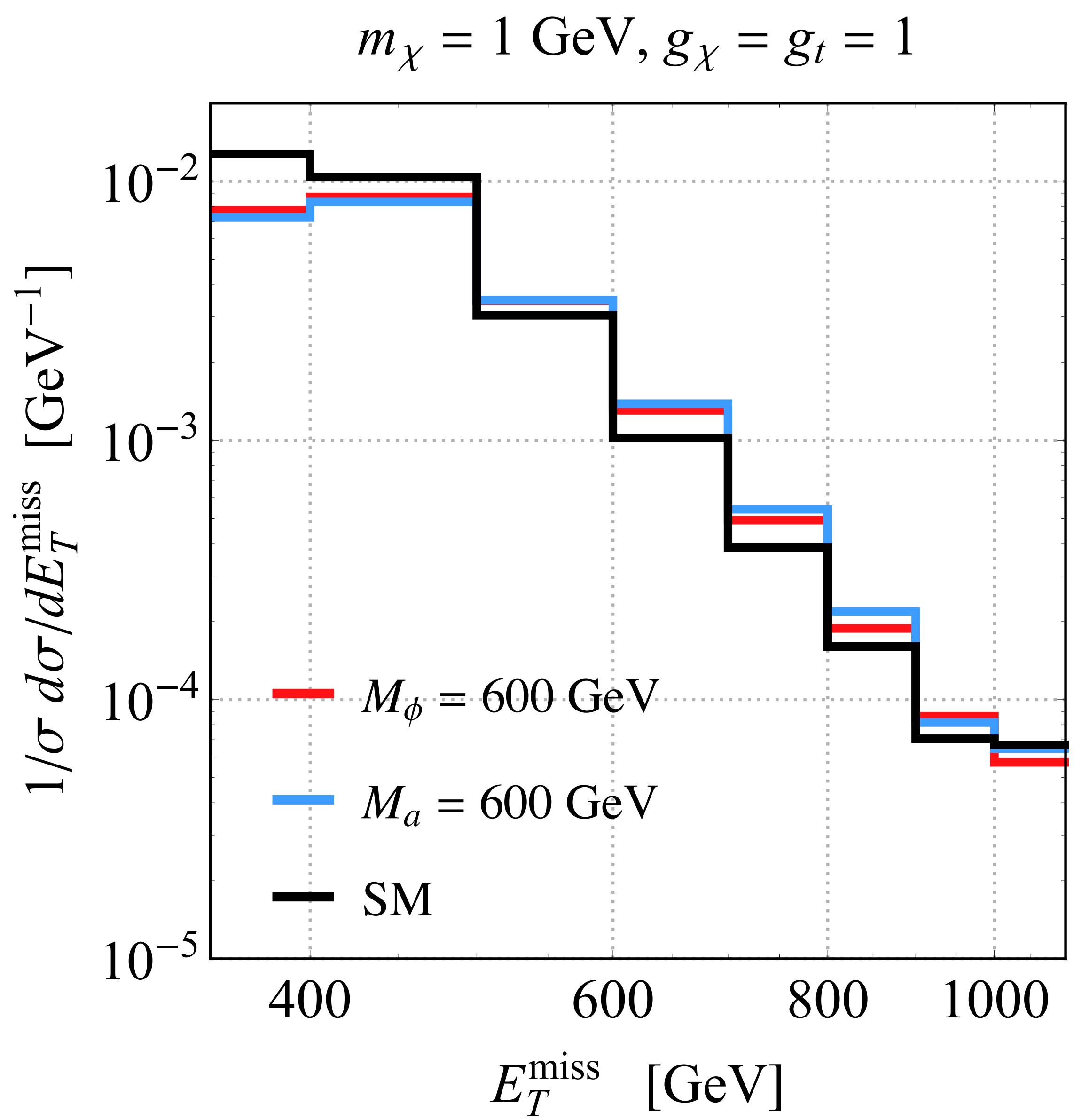

[UH & Polesello, 1812.00694]

Mono-jet LHC Run-3 prospects

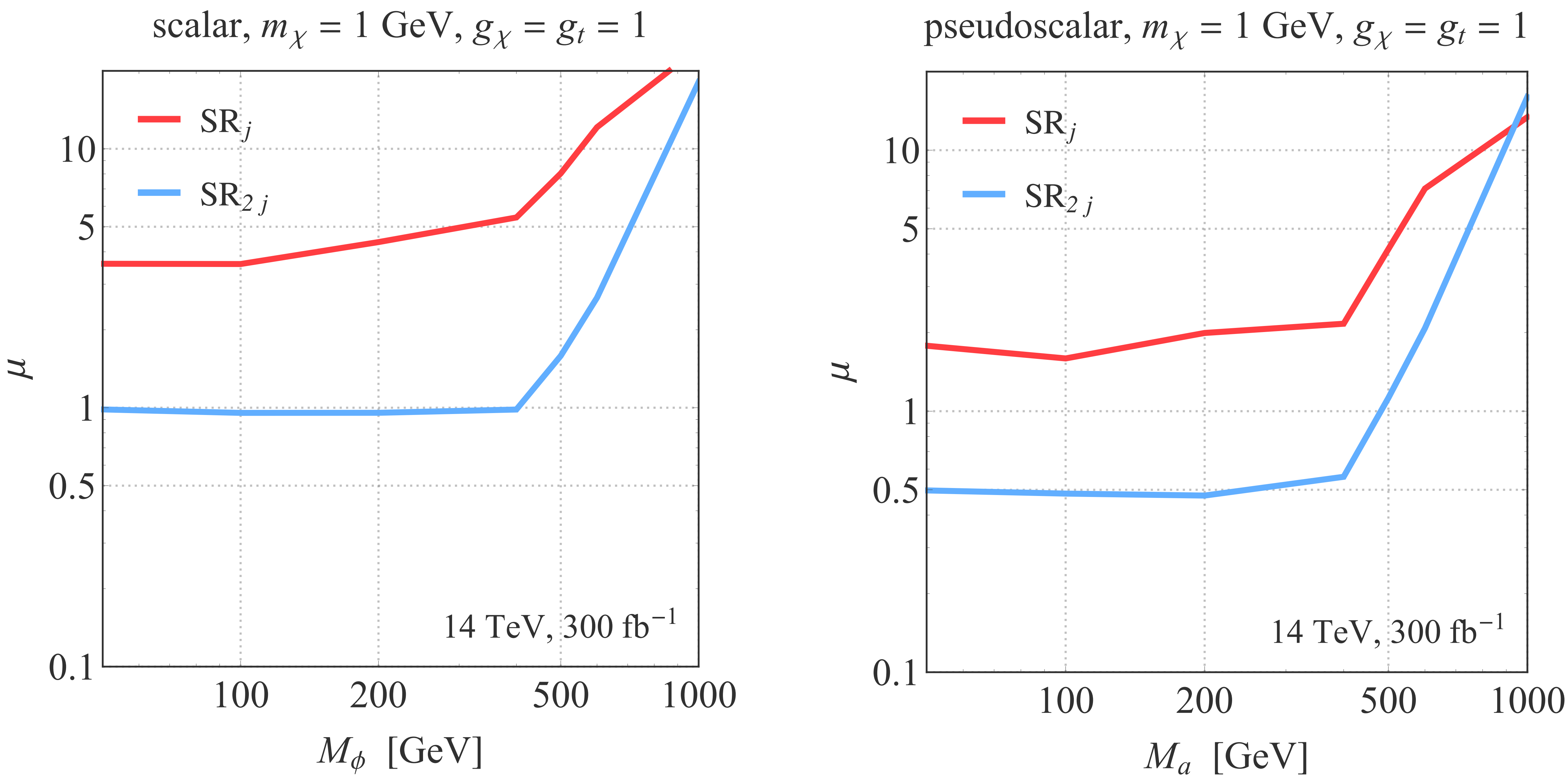

[UH & Polesello, 1812.08129]

Gain in mono-jet sensitivity

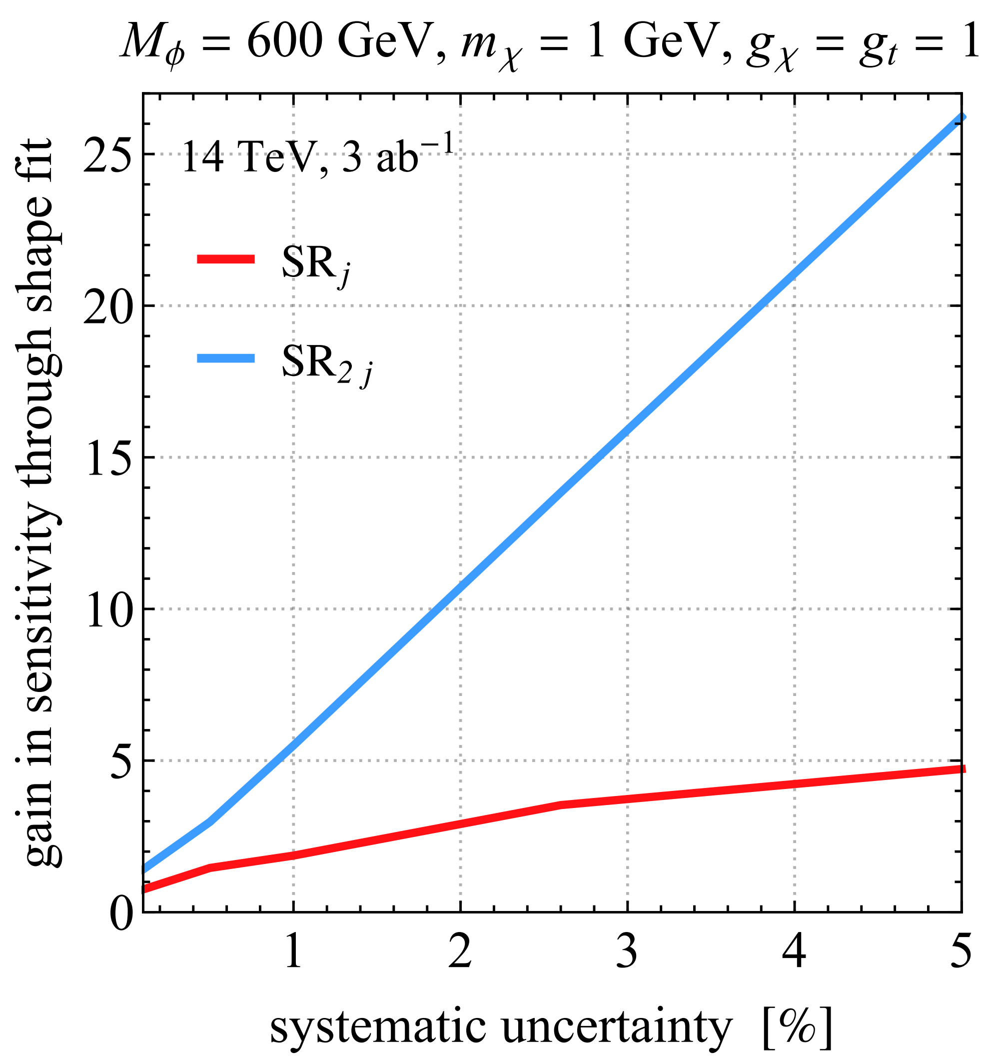

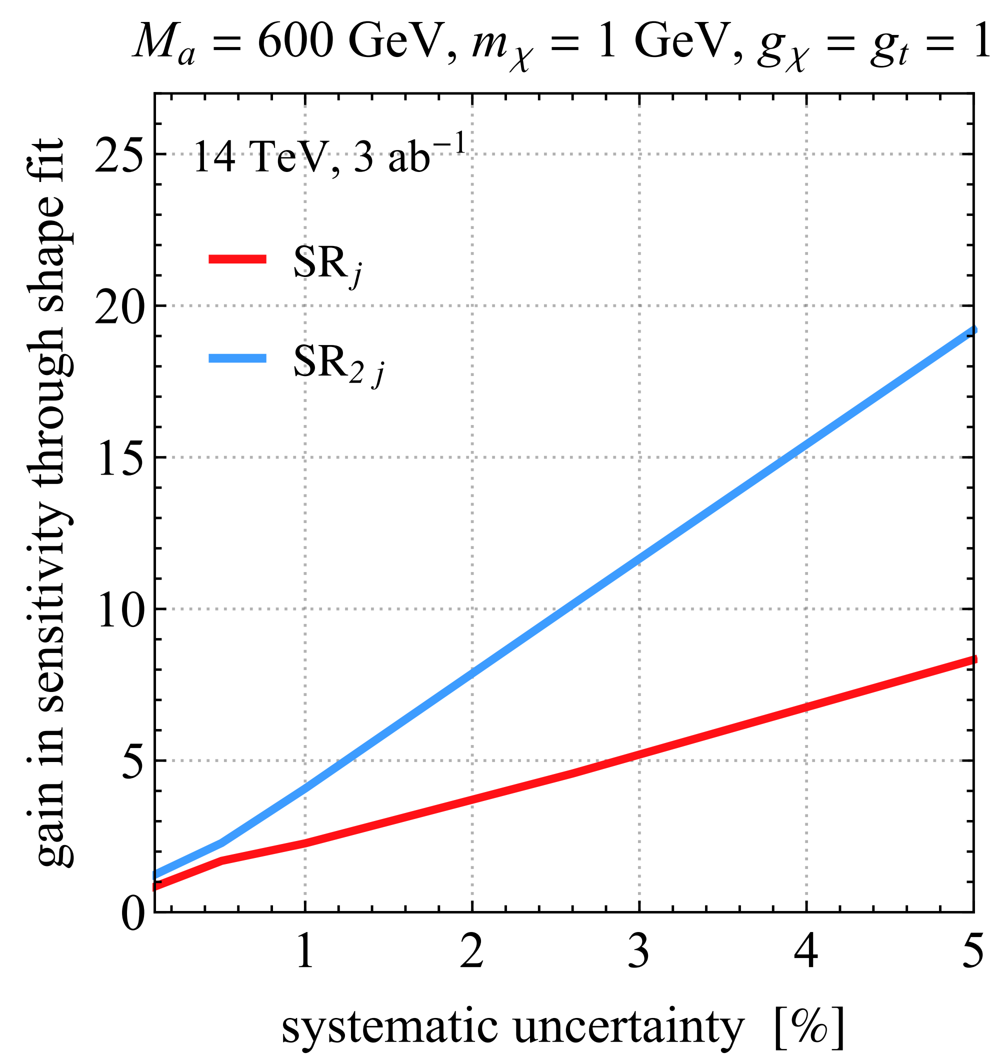

$\Delta\phi_{j1j2}$ shape fits in not only more powerful than $E_{T,\,miss}$ shape analyses, but also less dependent on hypothetical improvements of systematic errors

[UH & Polesello, 1812.08129]

Complementarity of $E_{T,miss}$ searches

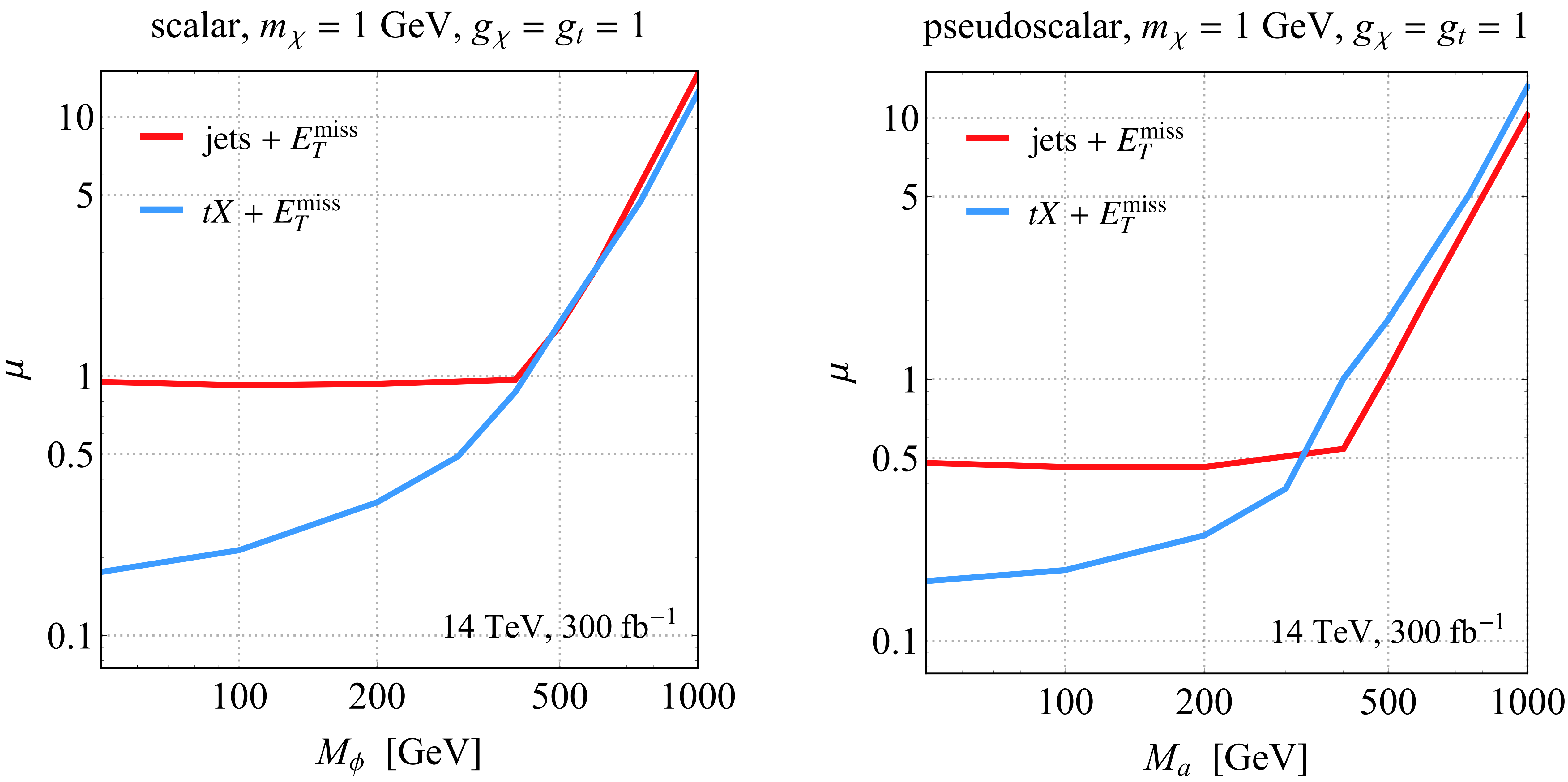

[based on UH & Polesello, 1812.00694 & 1812.08129]

Complementarity of $E_{T,miss}$ searches

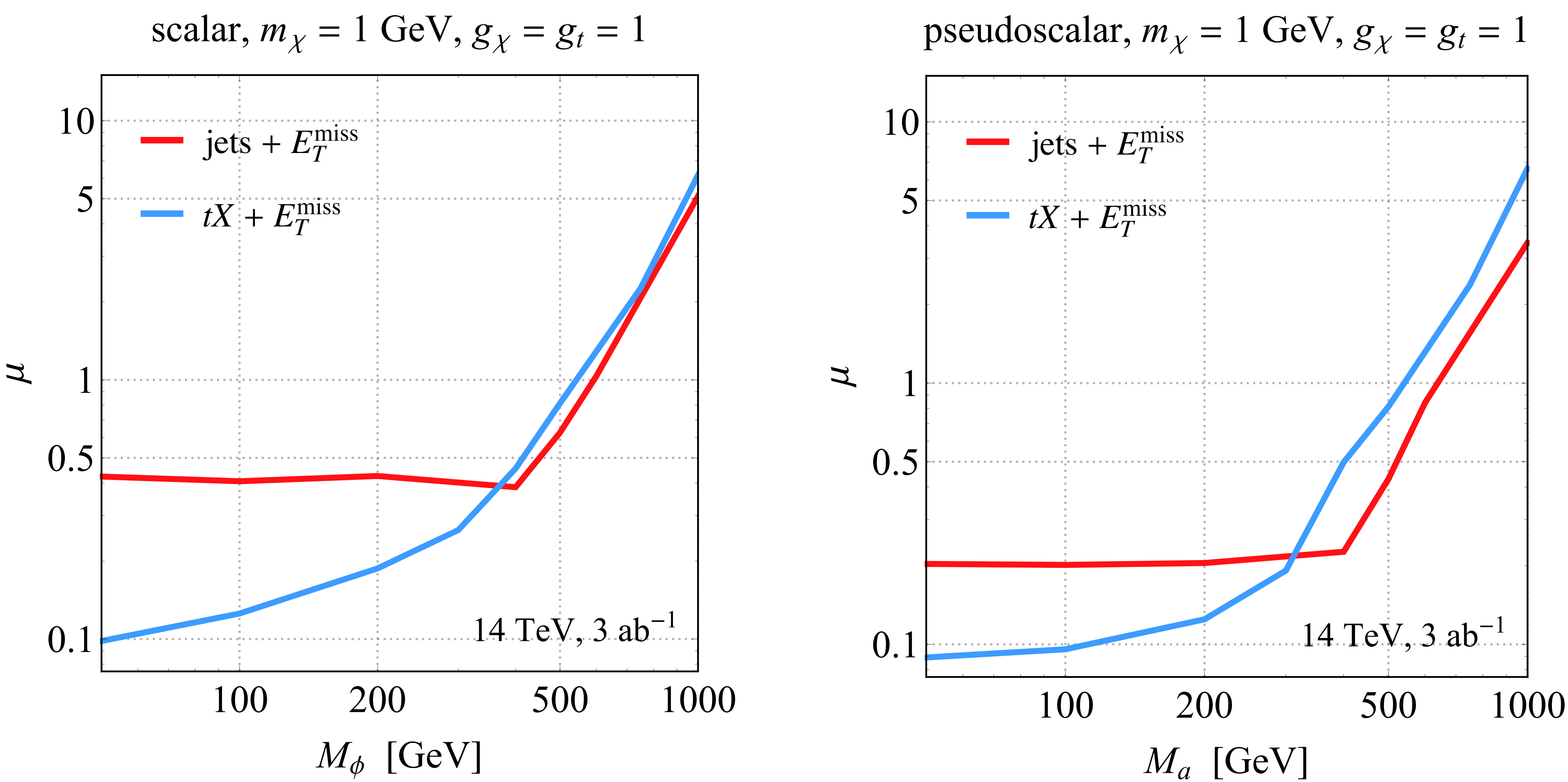

[based on UH & Polesello, 1812.00694 & 1812.08129]

2HDM+a: constraints

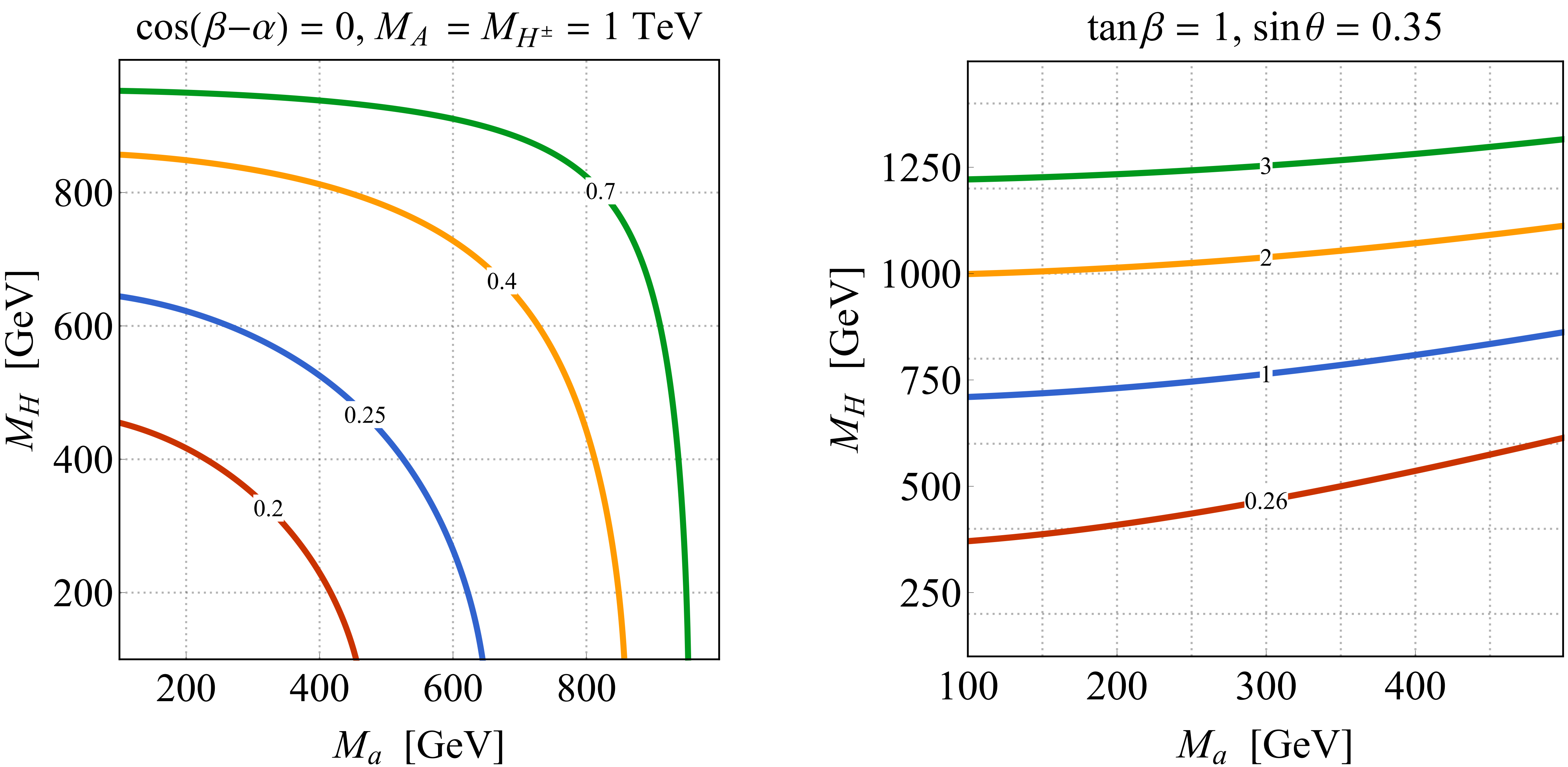

[LHC DMWG, 1810.09420]

2HDM+a: h→X branching ratios

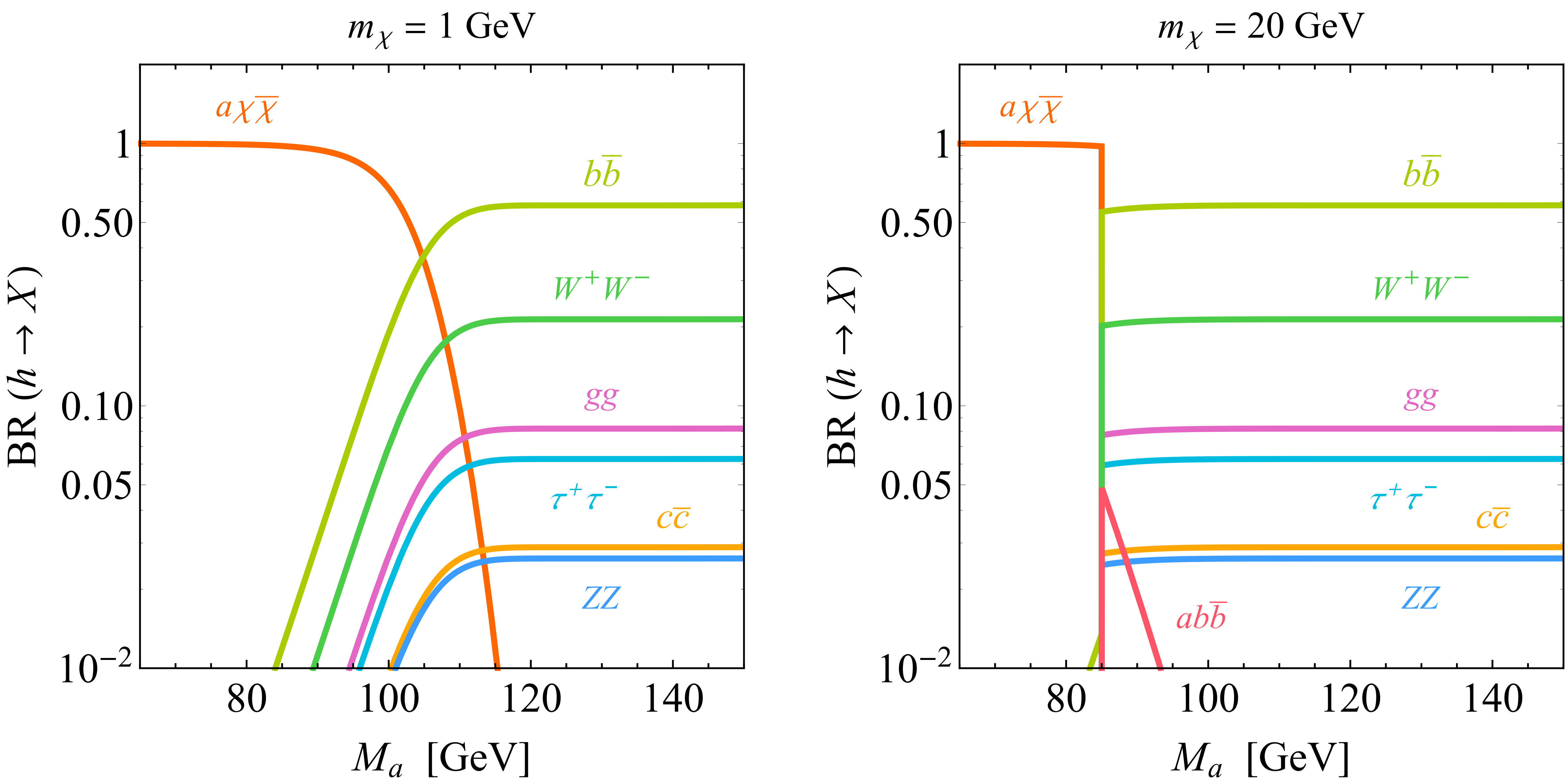

[Bauer et al., 1701.07427]

2HDM+a: H→X branching ratios

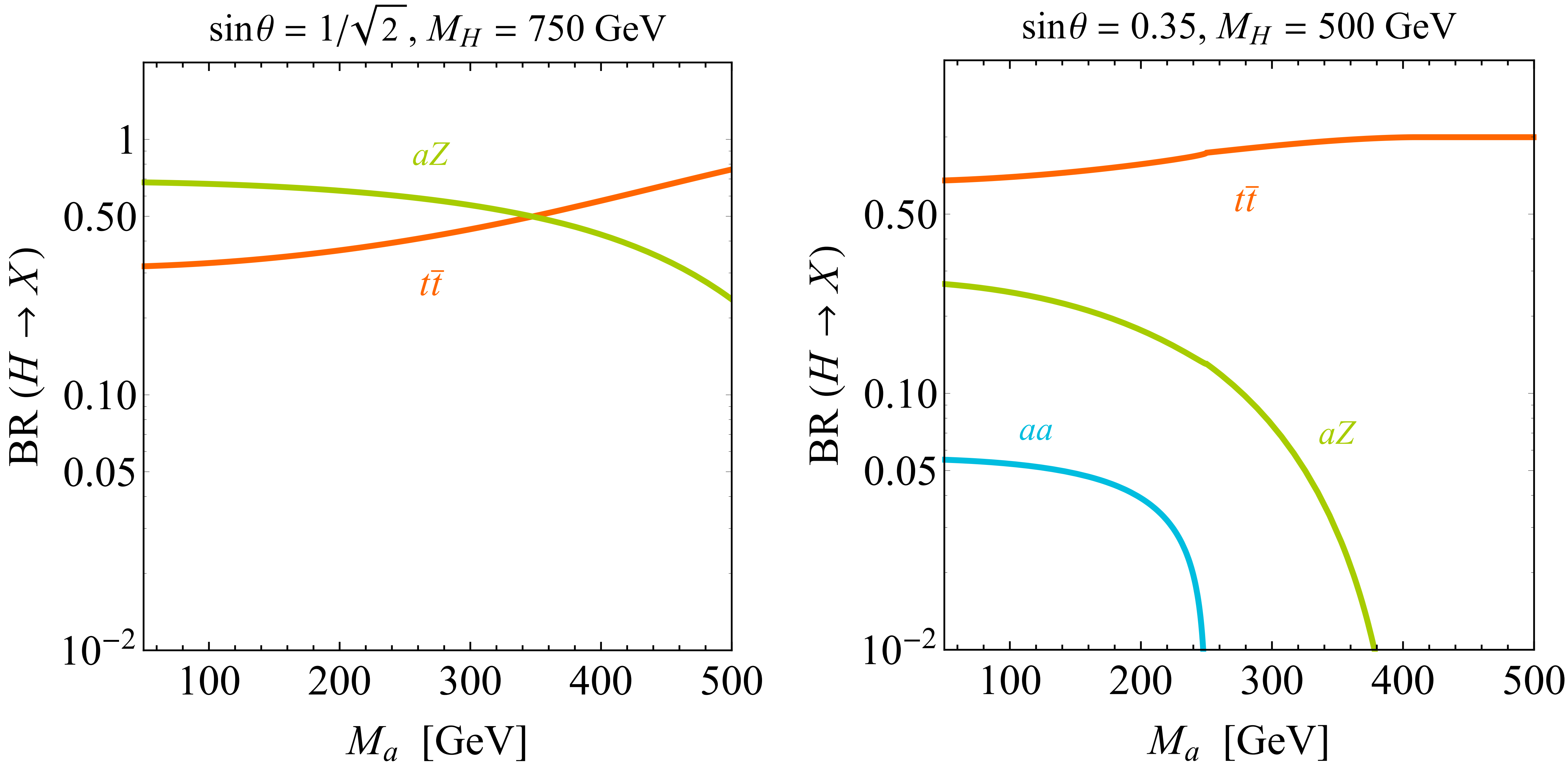

[Bauer et al., 1701.07427]

2HDM+a: A→X branching ratios

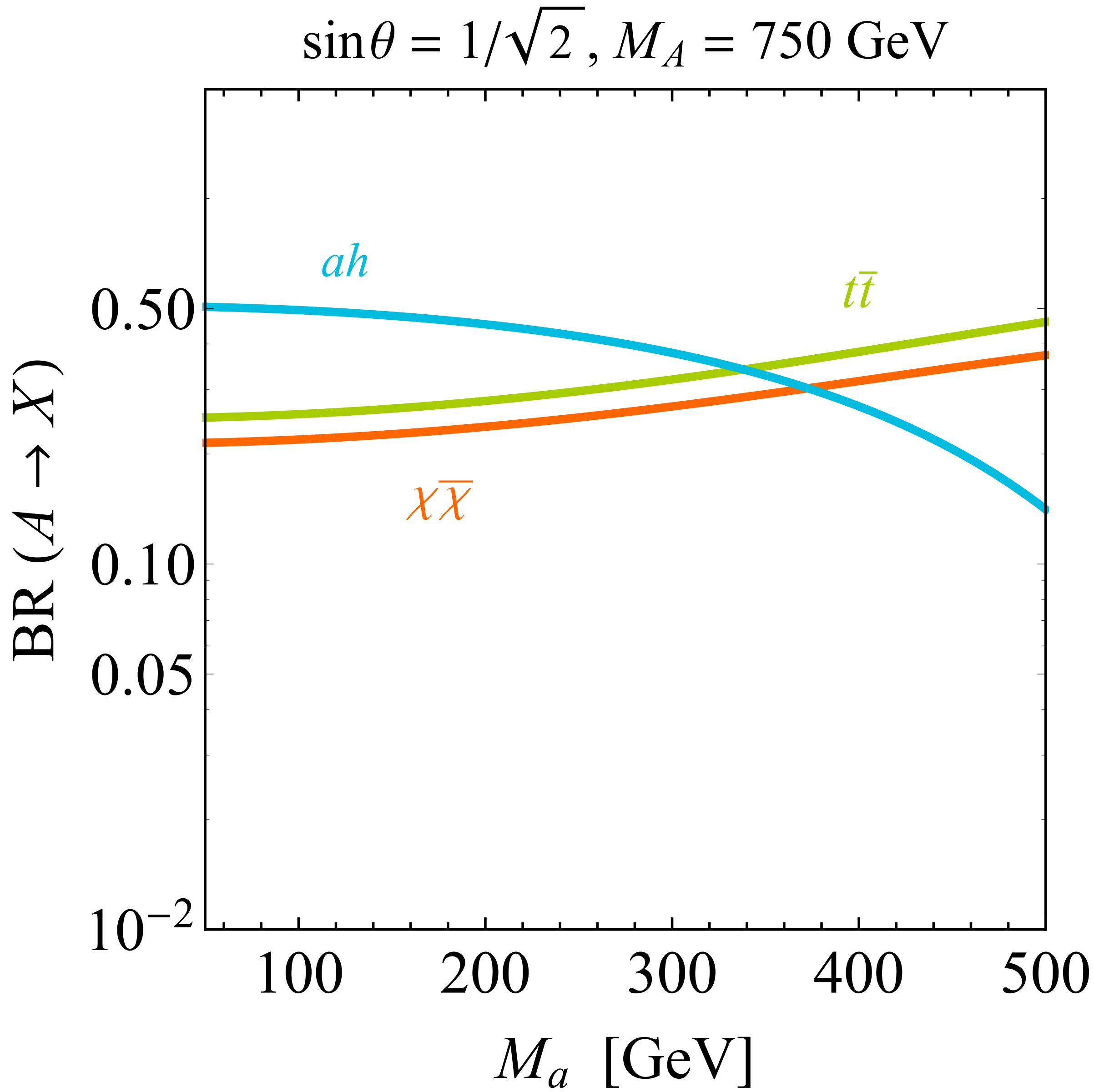

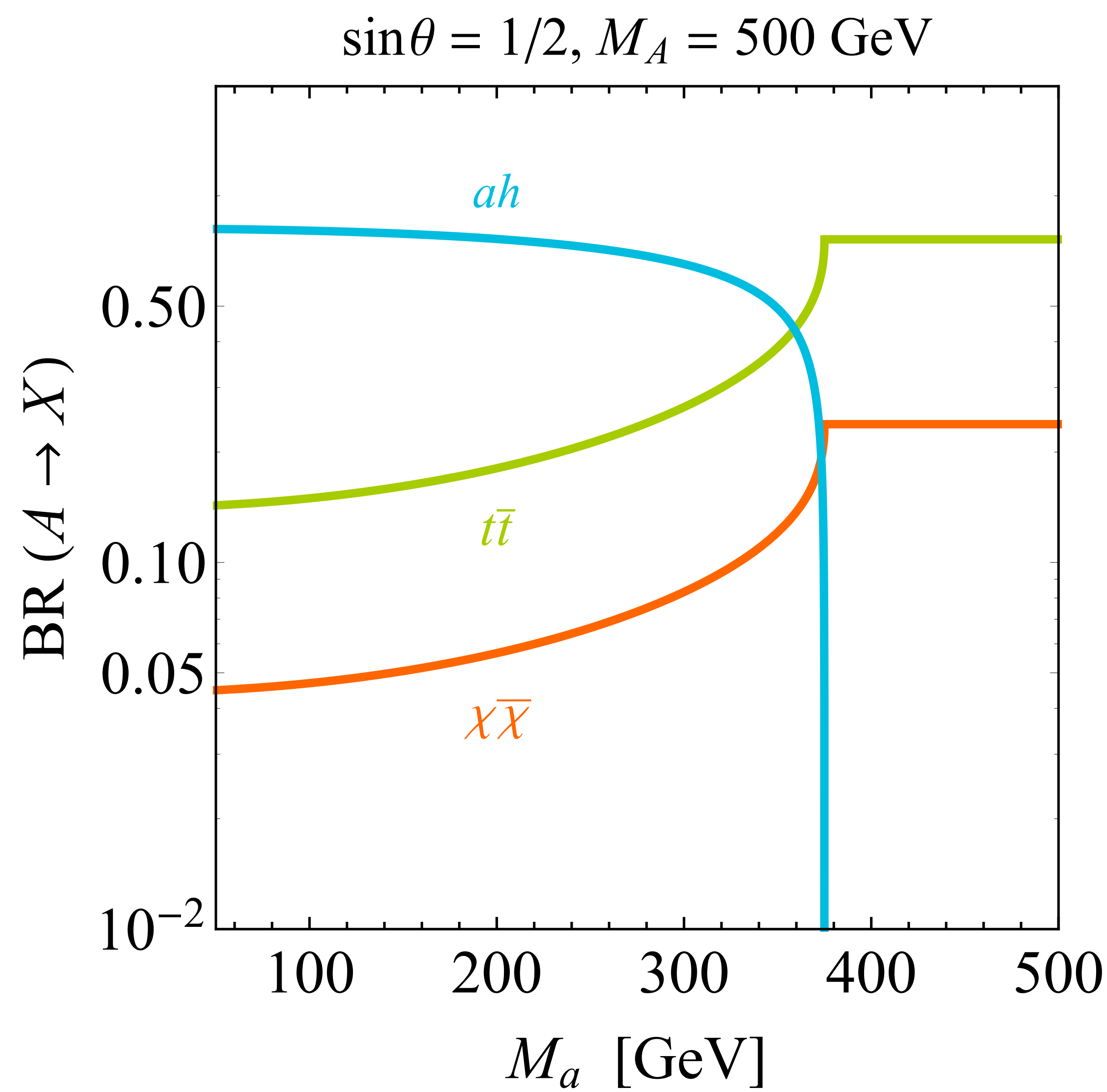

[Bauer et al., 1701.07427]

2HDM+a: a→X branching ratios

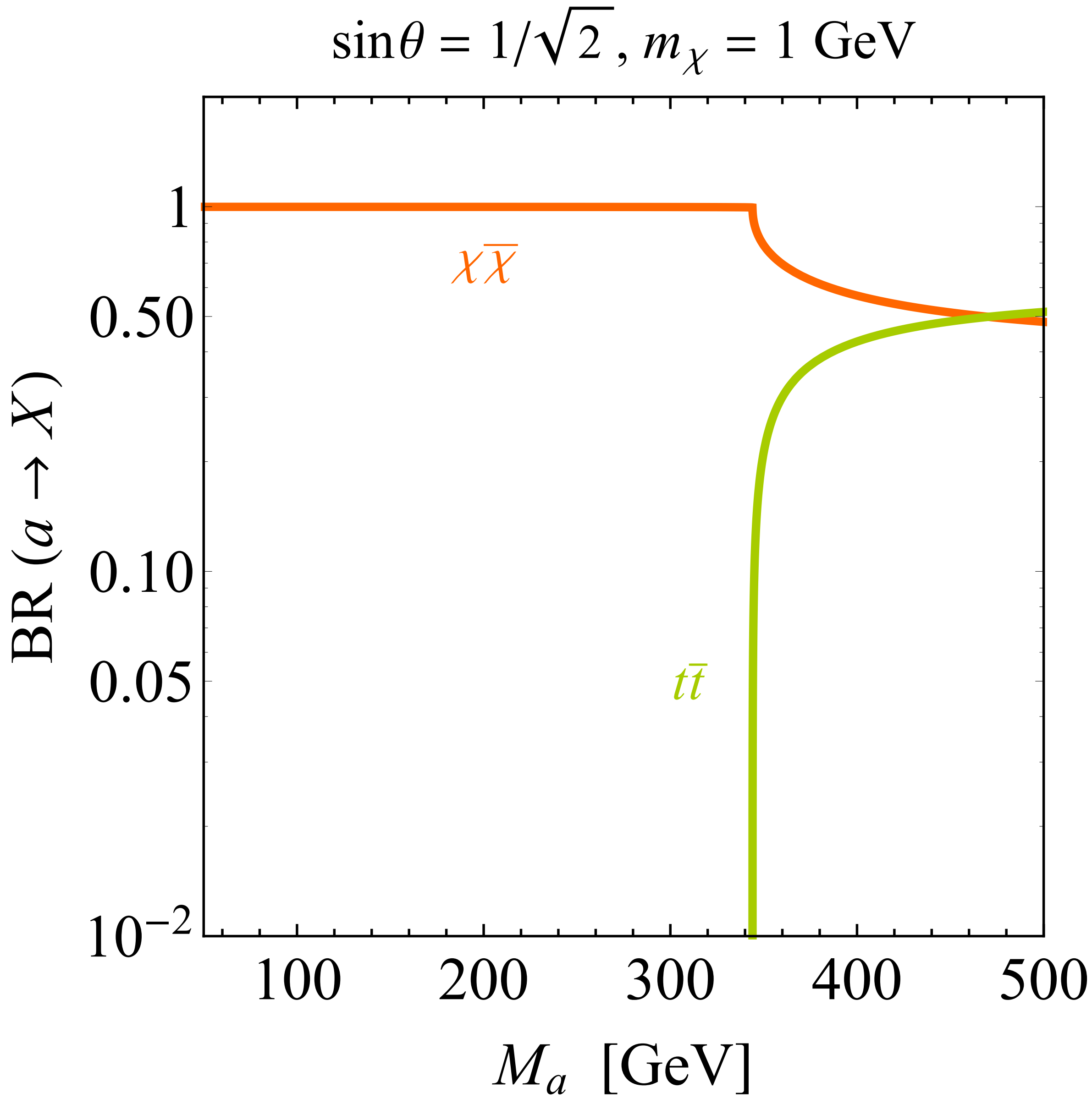

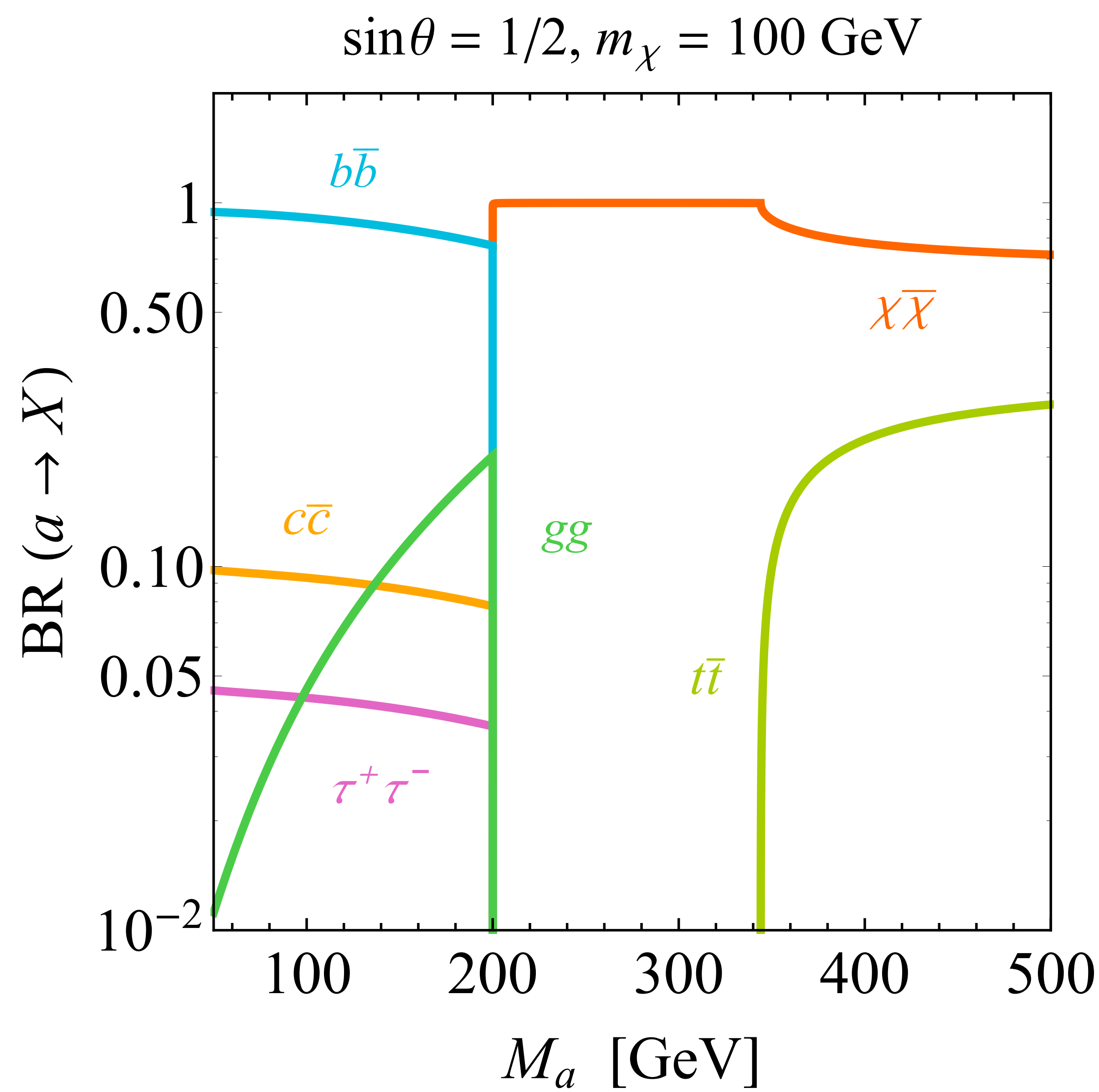

[Bauer et al., 1701.07427]

2HDM+a: $H^+ \to X$ branching ratios

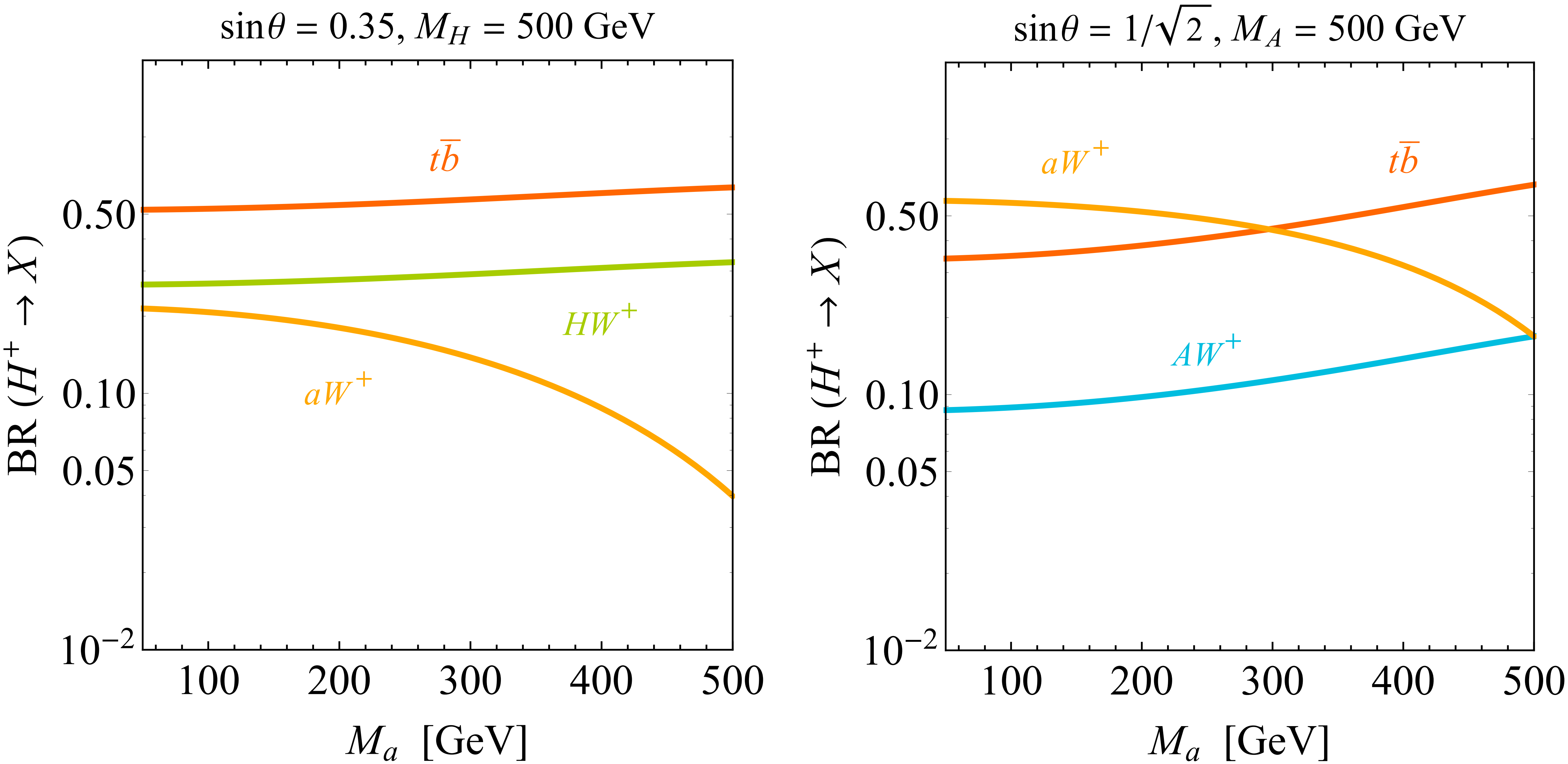

[Bauer et al., 1701.07427]

2HDM+a: mono-Higgs distributions

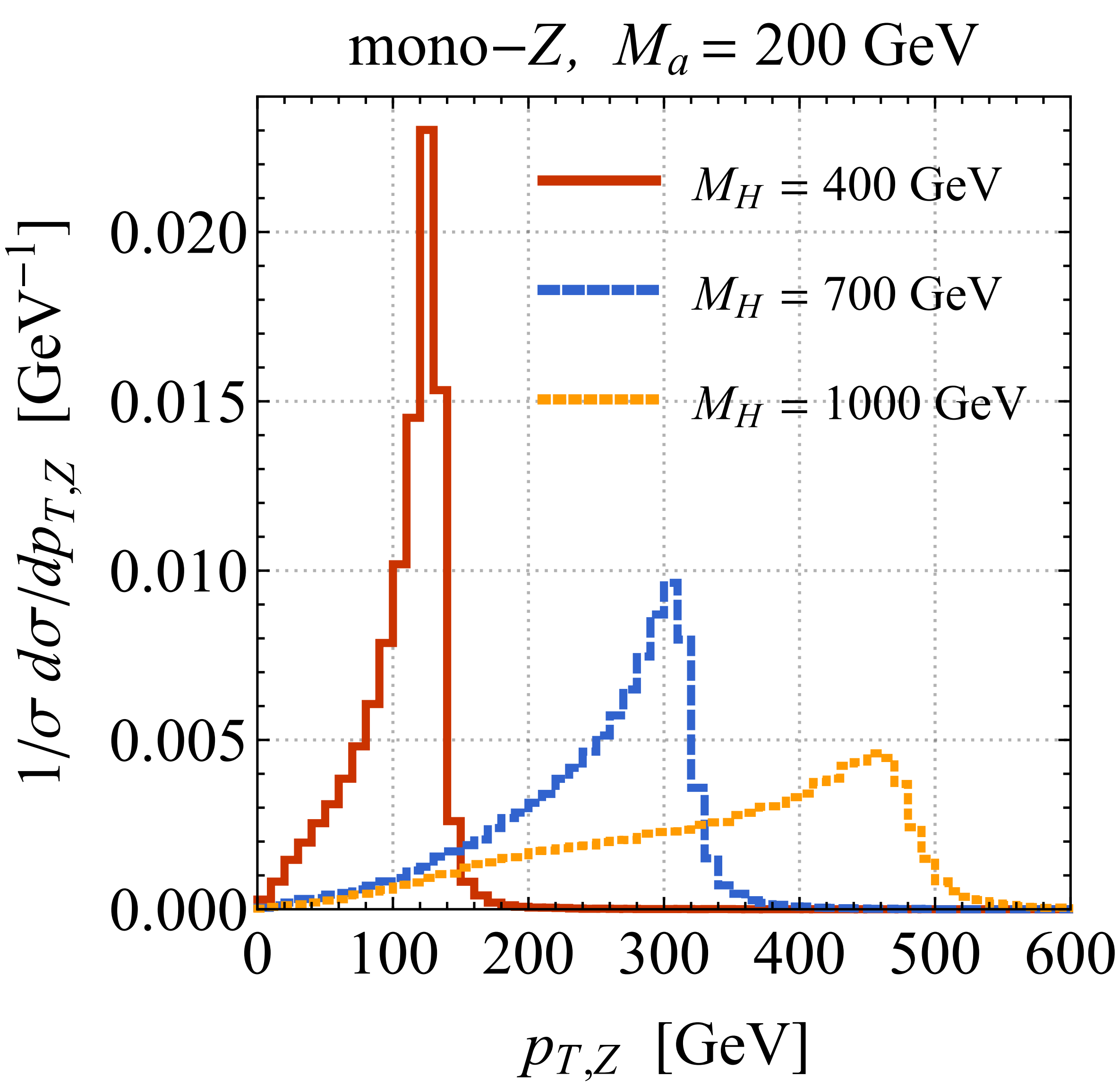

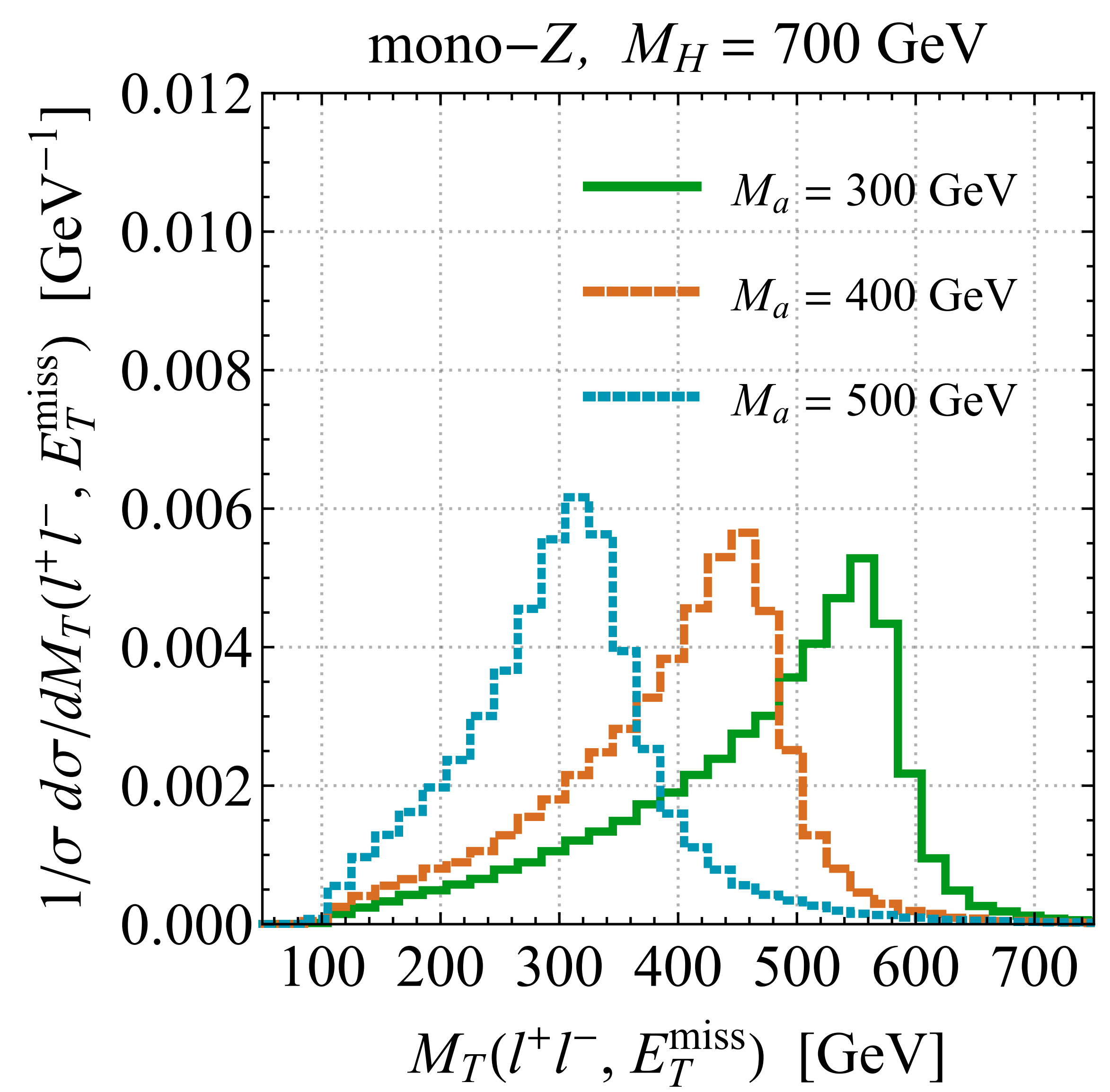

[LHC DMWG, 1810.09420]

2HDM+a: mono-Z distributions

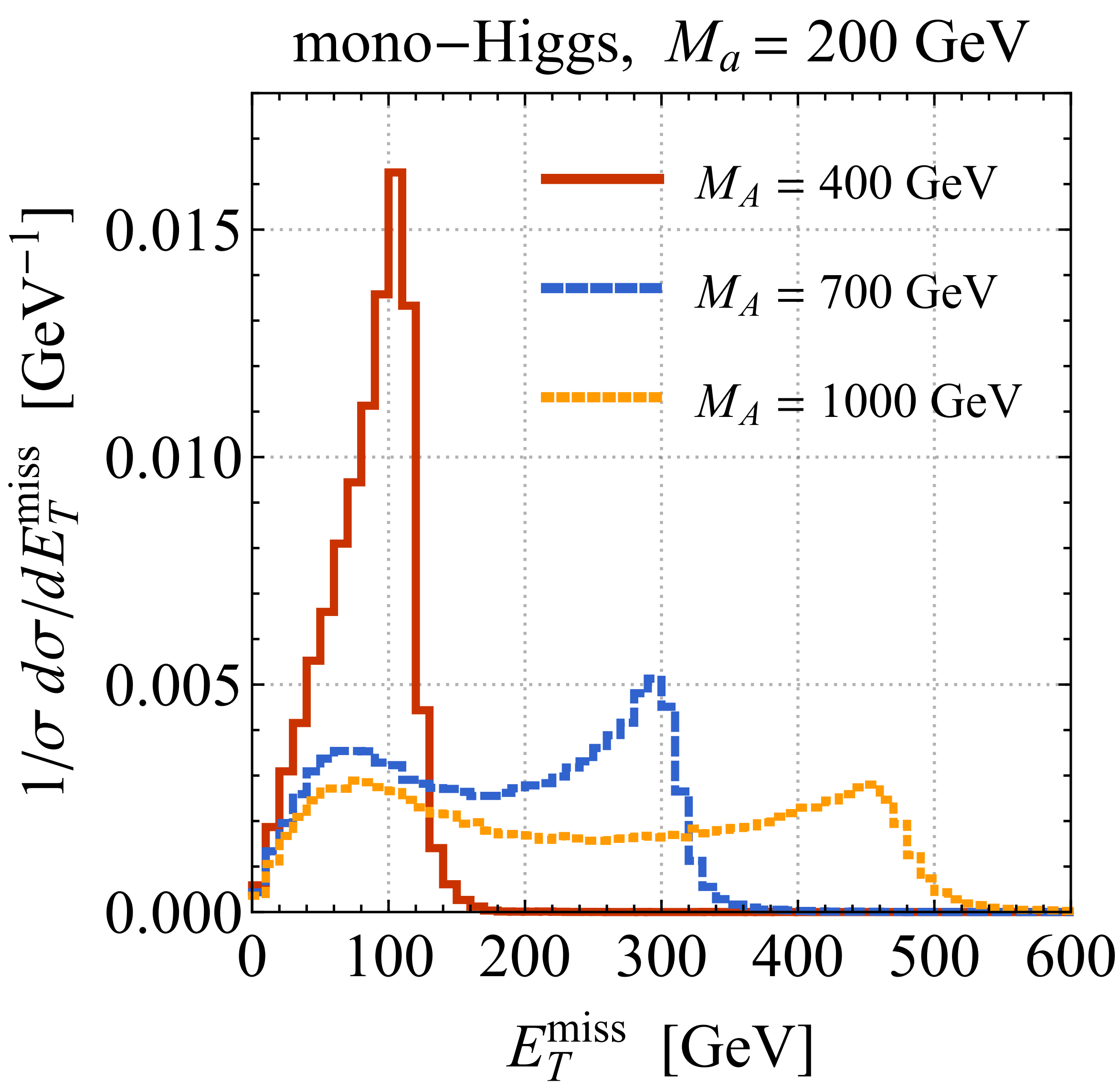

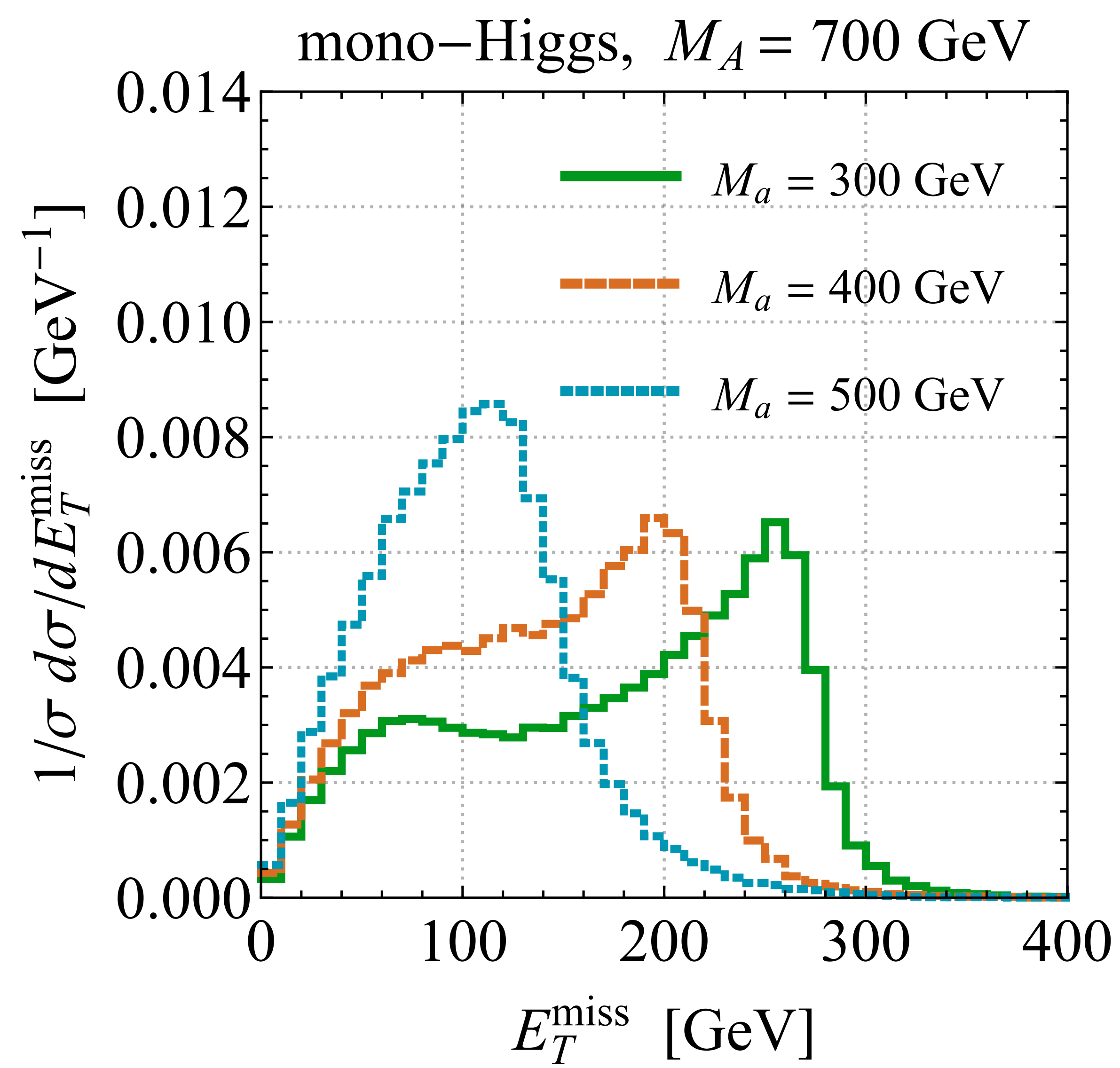

[LHC DMWG, 1810.09420]

2HDM+a: tW+$E_{T,miss}$ distributions

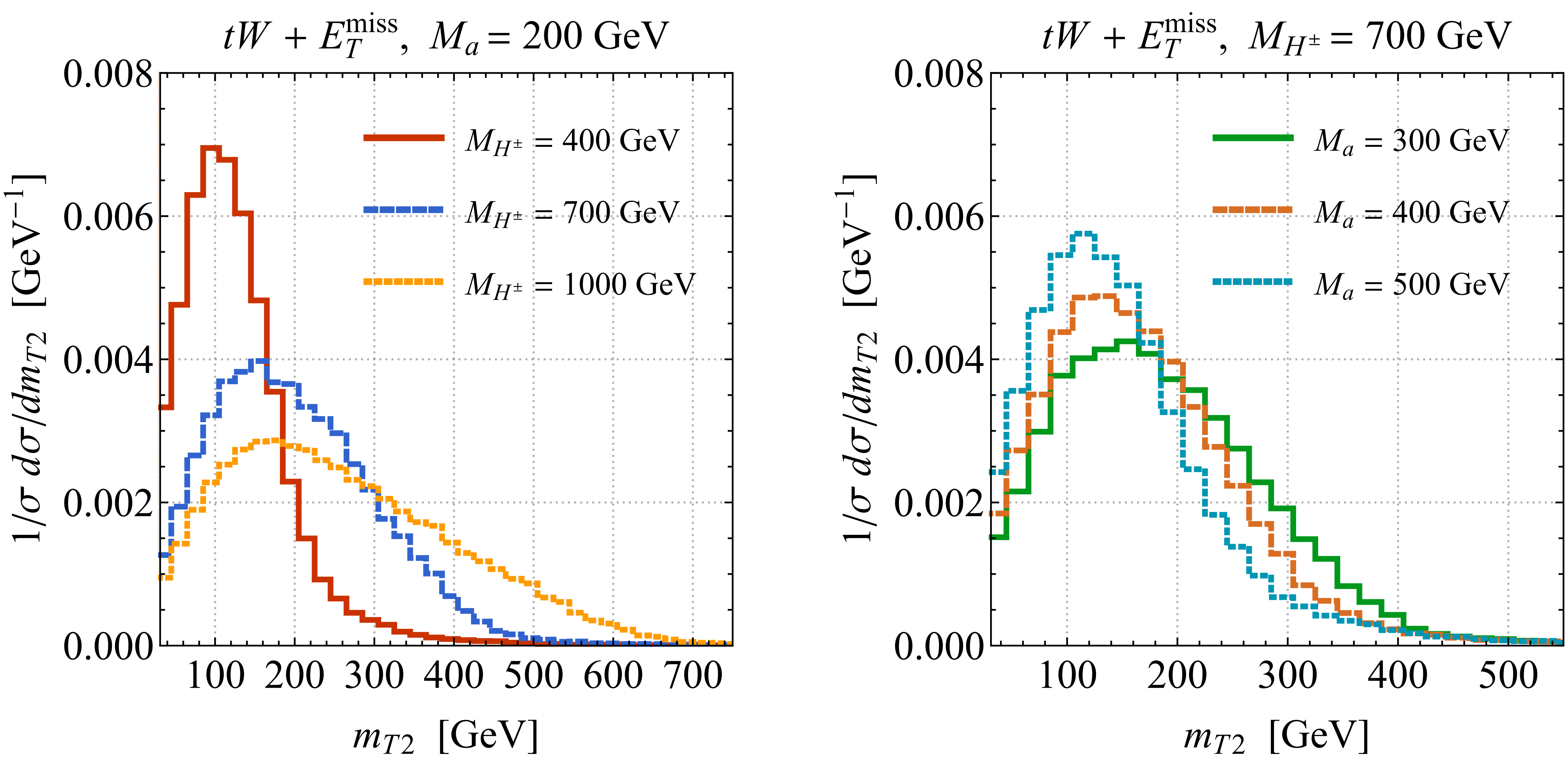

[LHC DMWG, 1810.09420]

2HDM+a: sinθ dependence

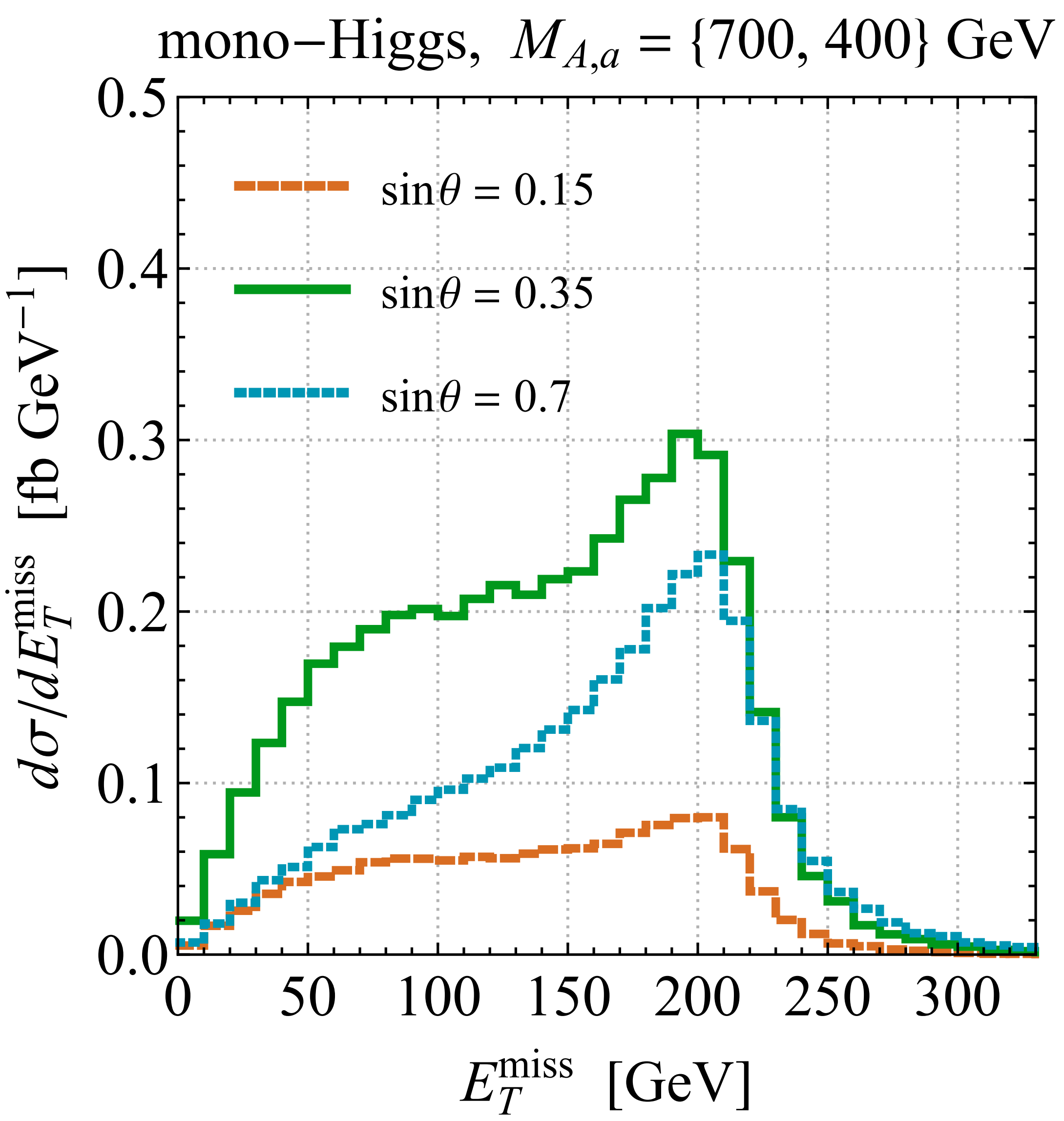

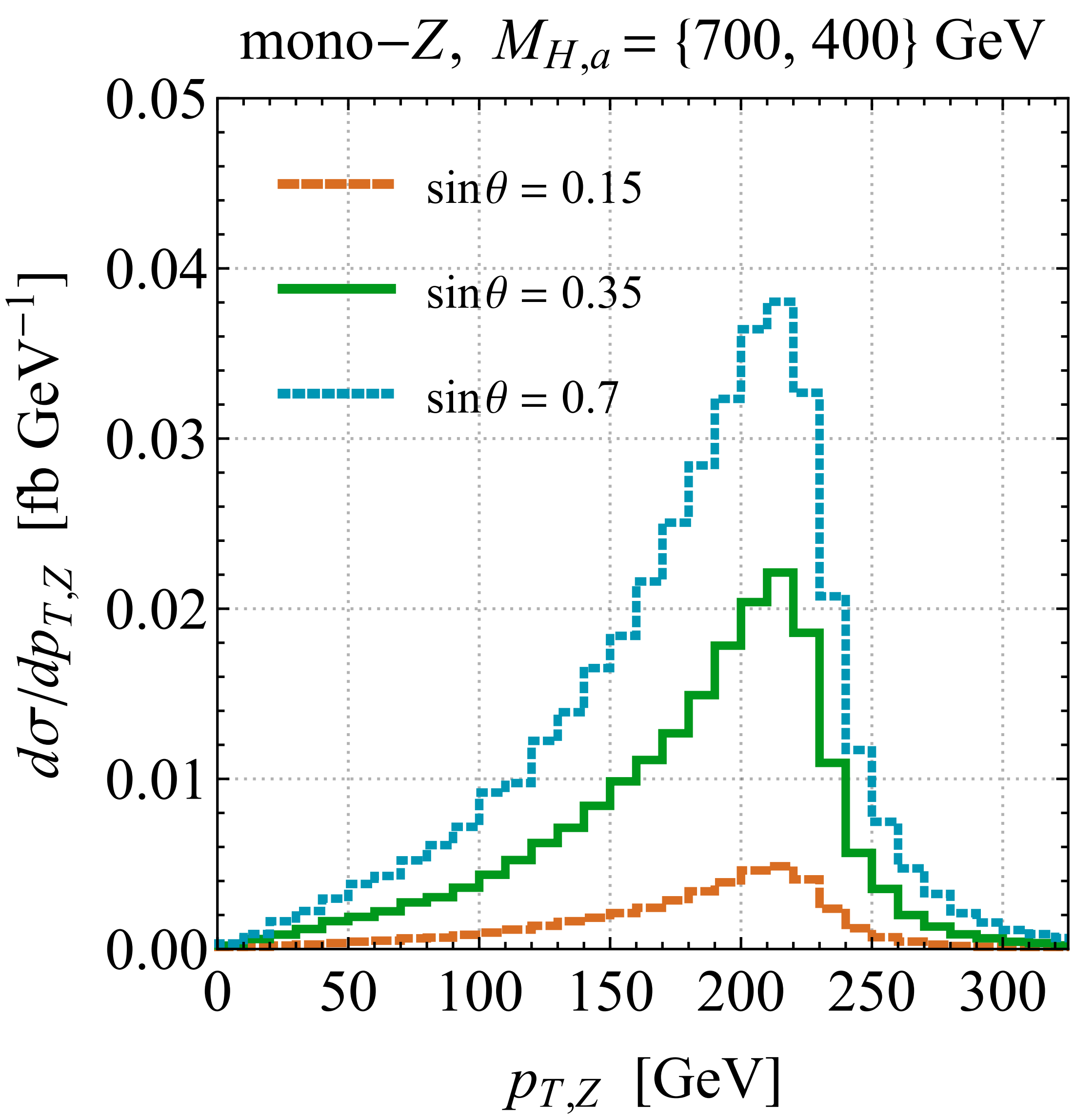

[LHC DMWG, 1810.09420]

2HDM+a: tanβ dependence

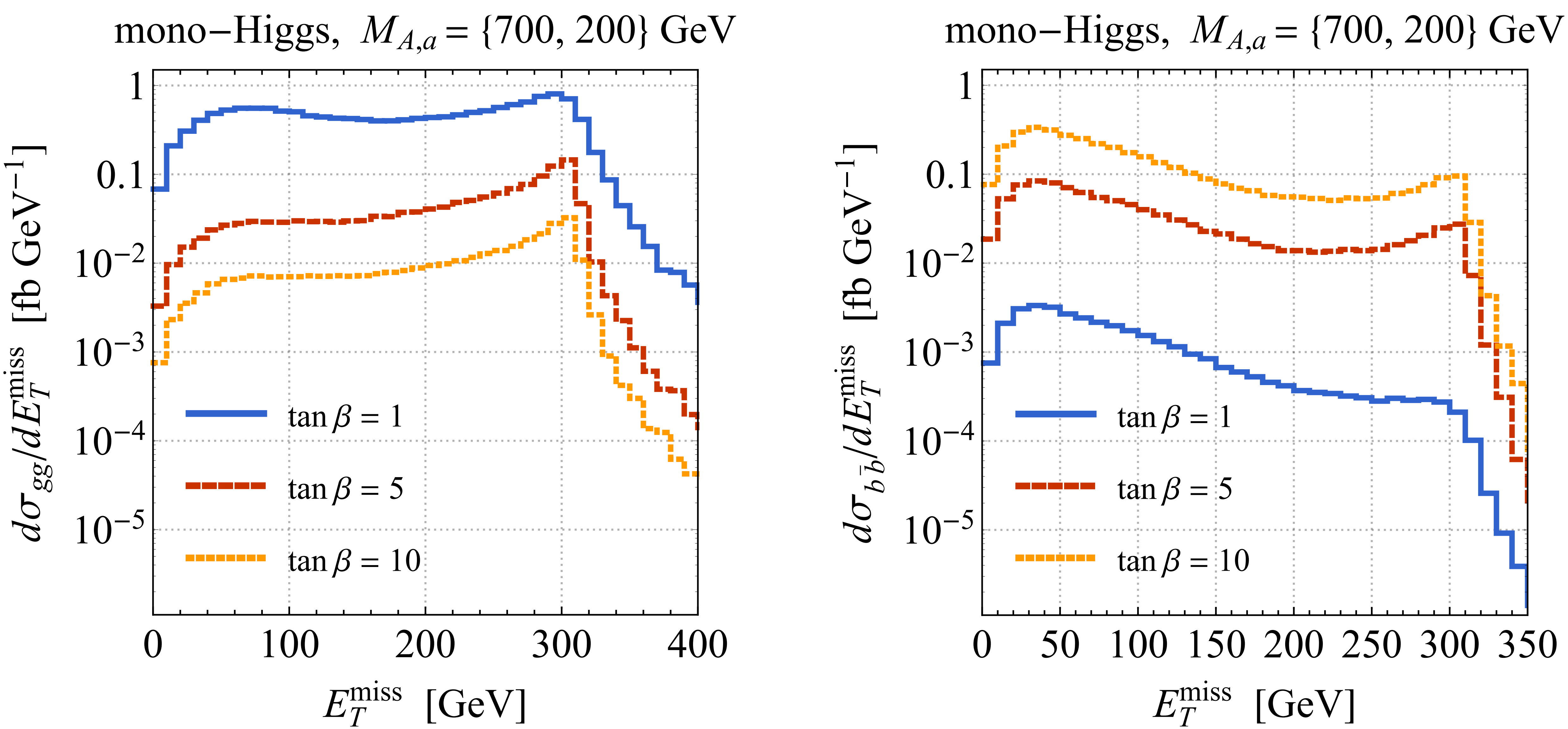

[LHC DMWG, 1810.09420]

2HDM+a: tanβ dependence

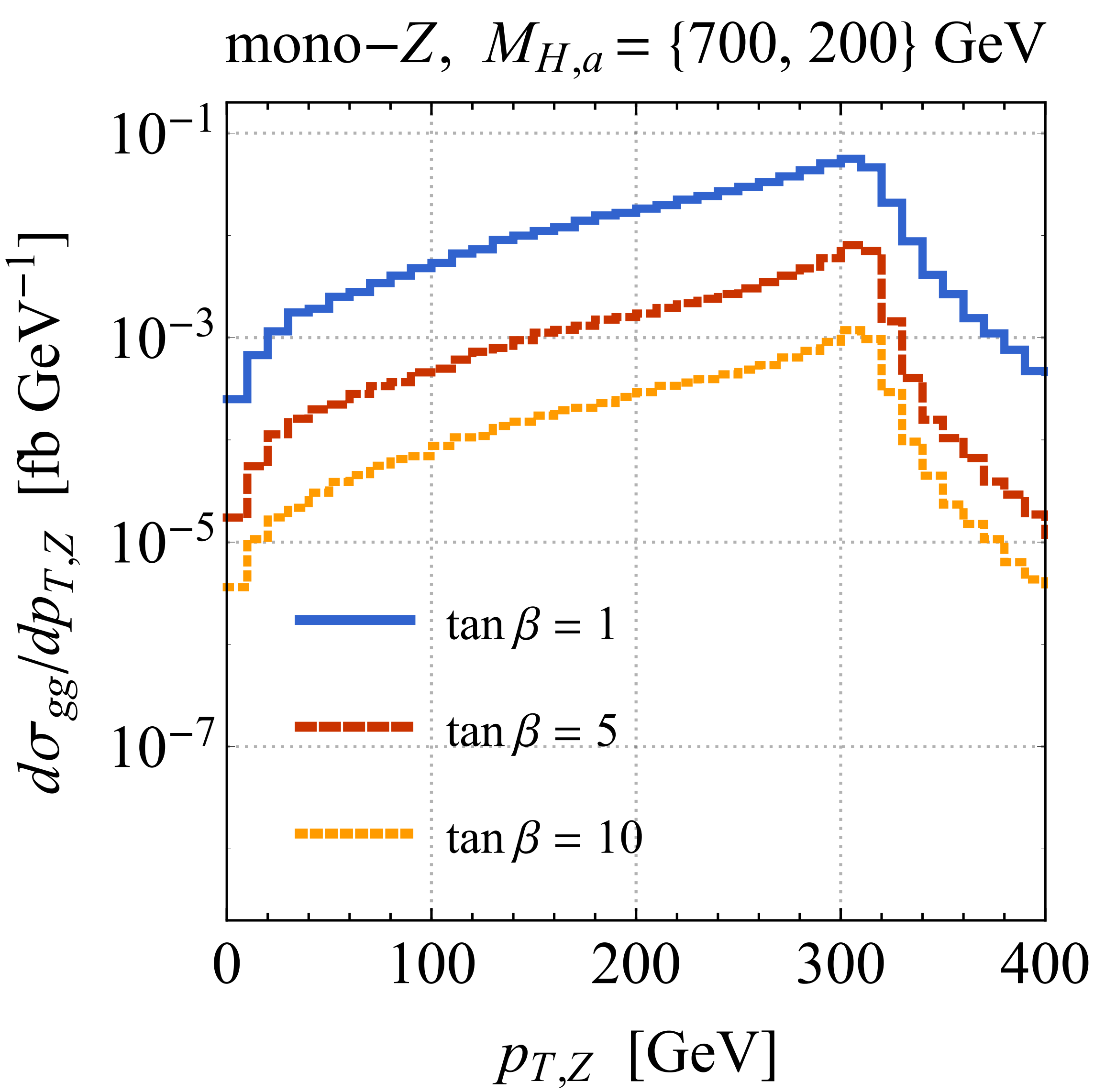

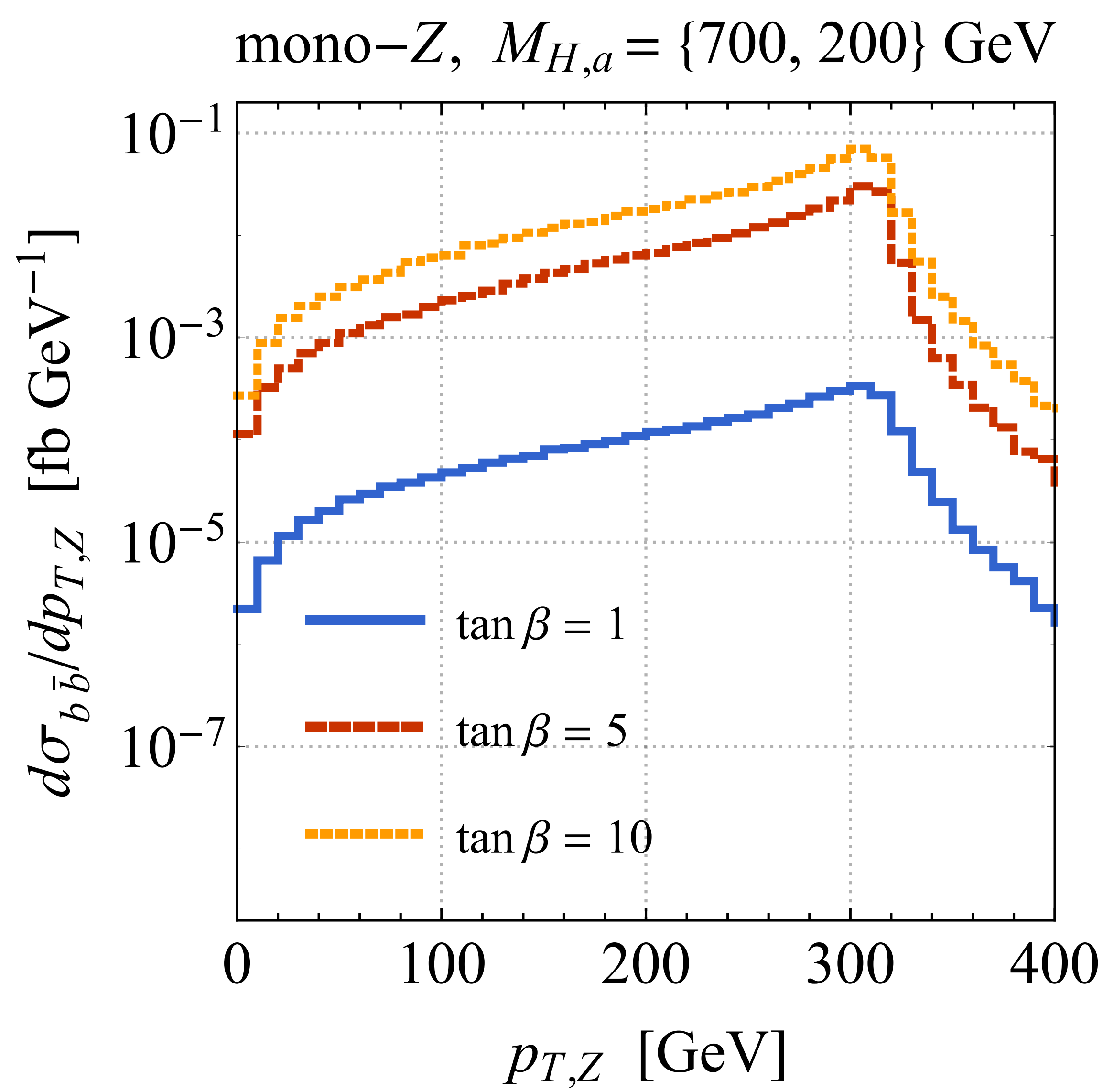

[LHC DMWG, 1810.09420]

2HDM+a: mDM dependence

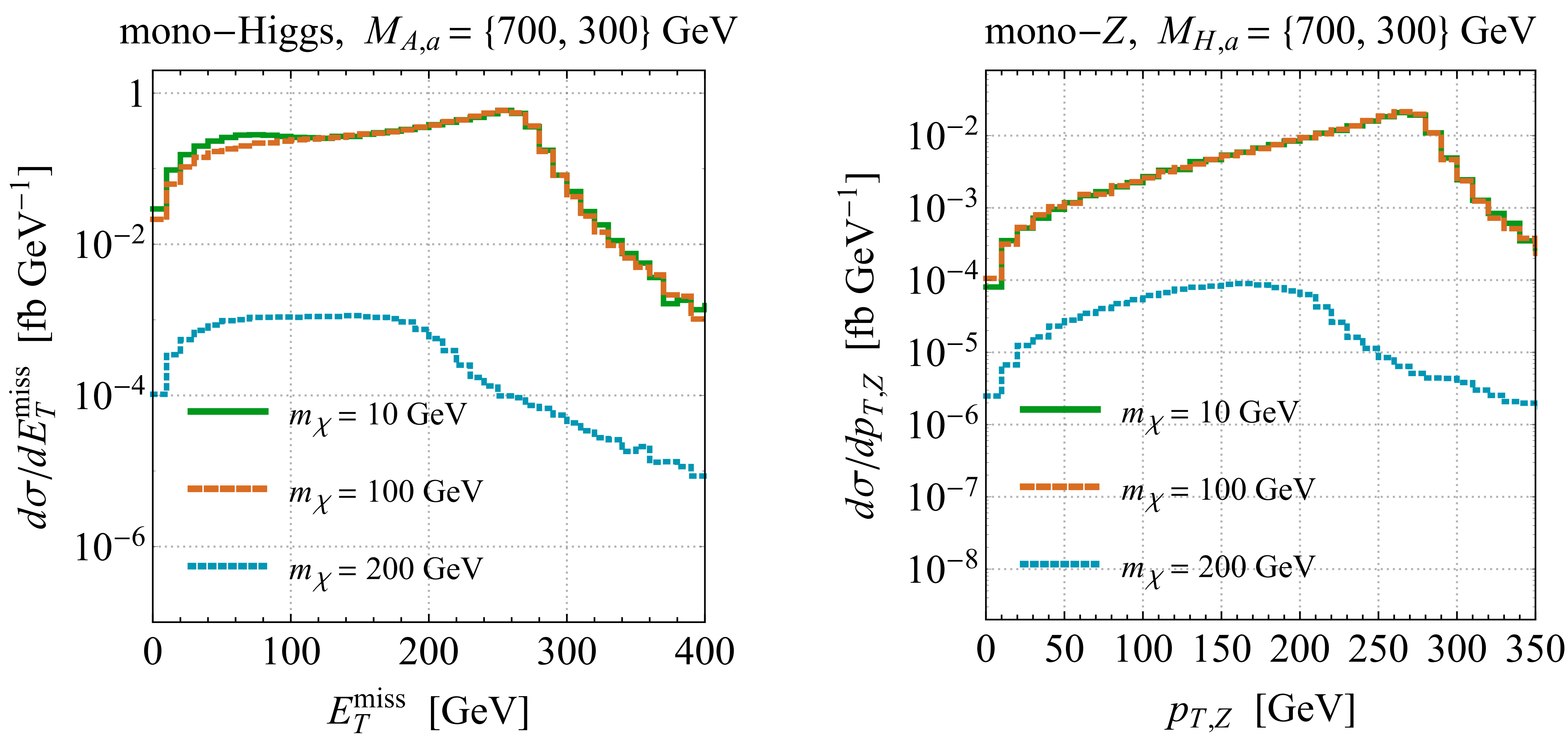

[LHC DMWG, 1810.09420]

2HDM+a: present constraints

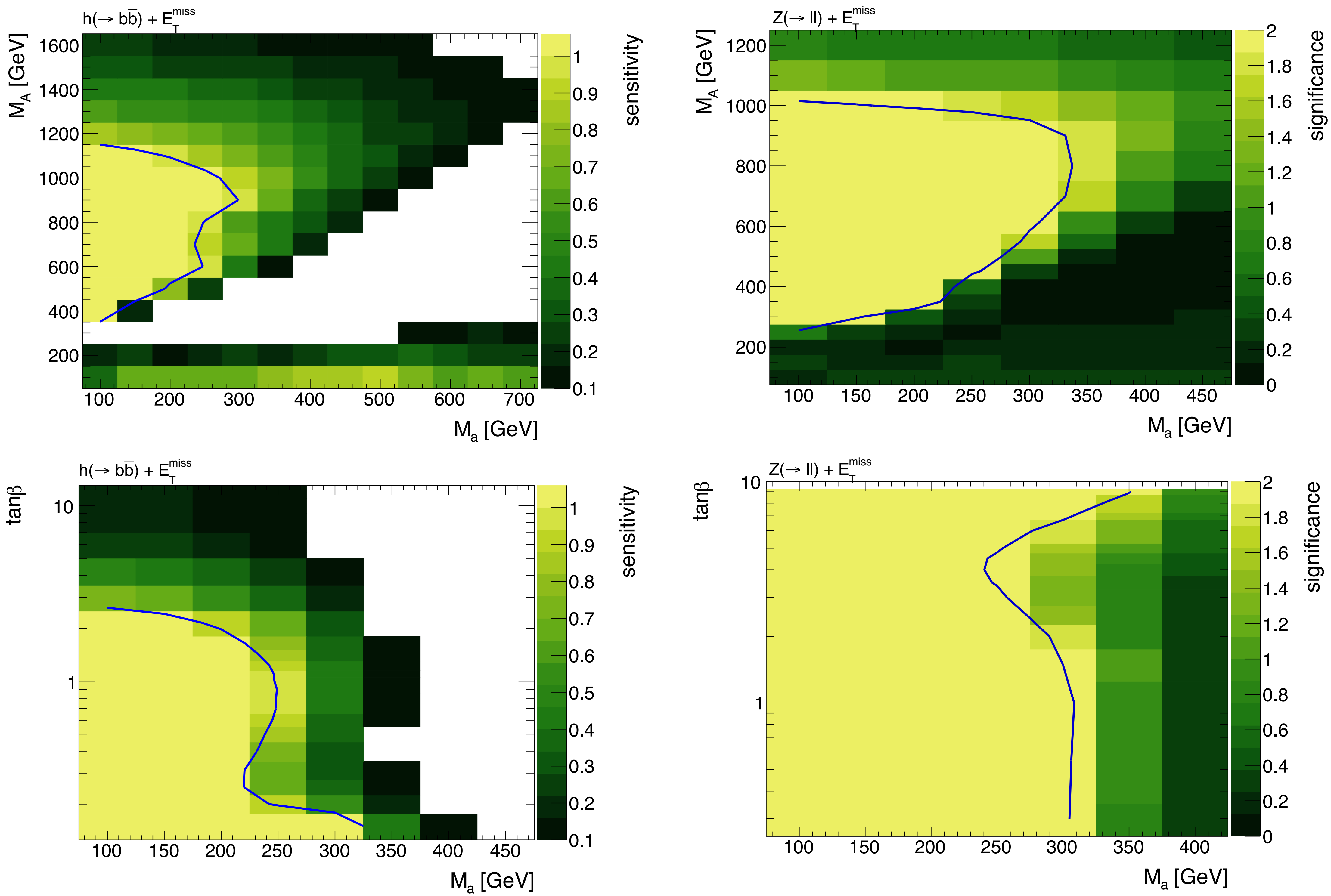

[LHC DMWG, 1810.09420]

2HDM+a: present constraints

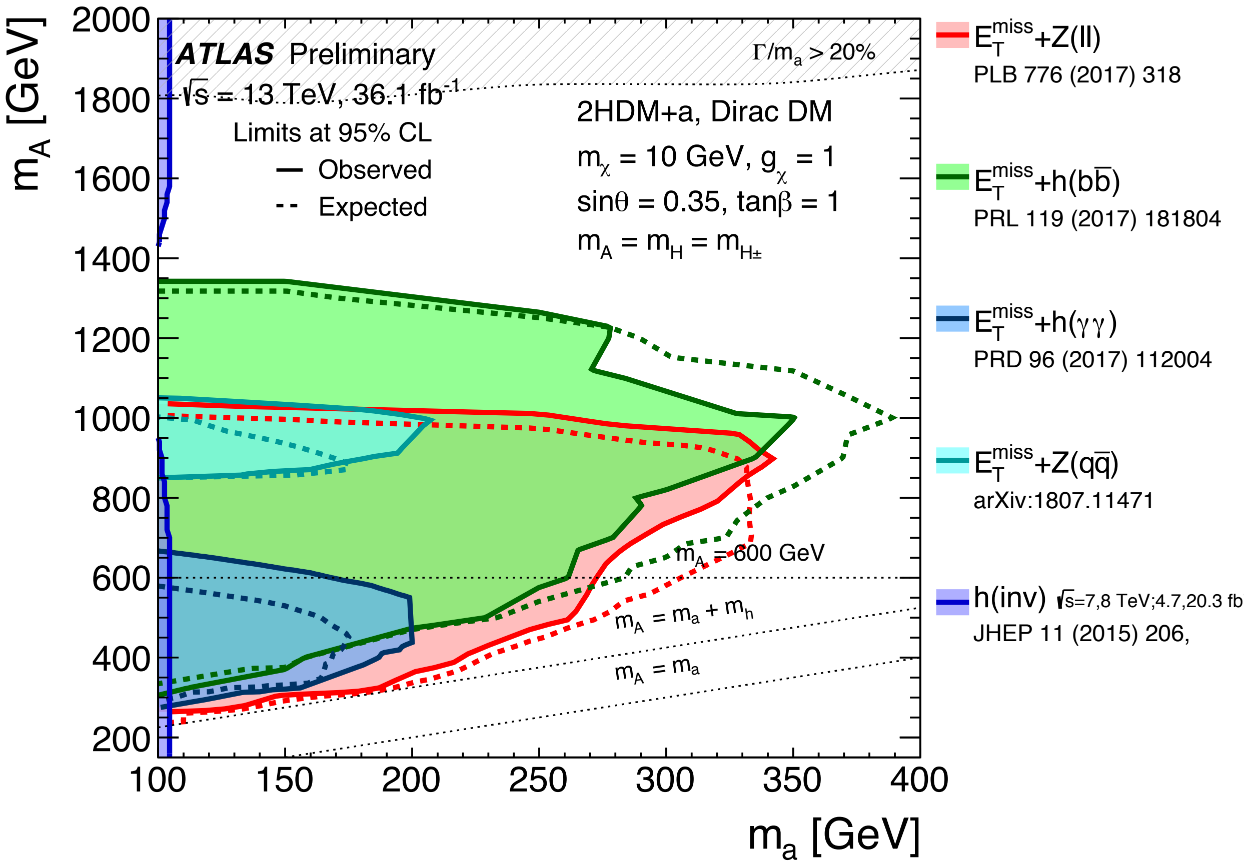

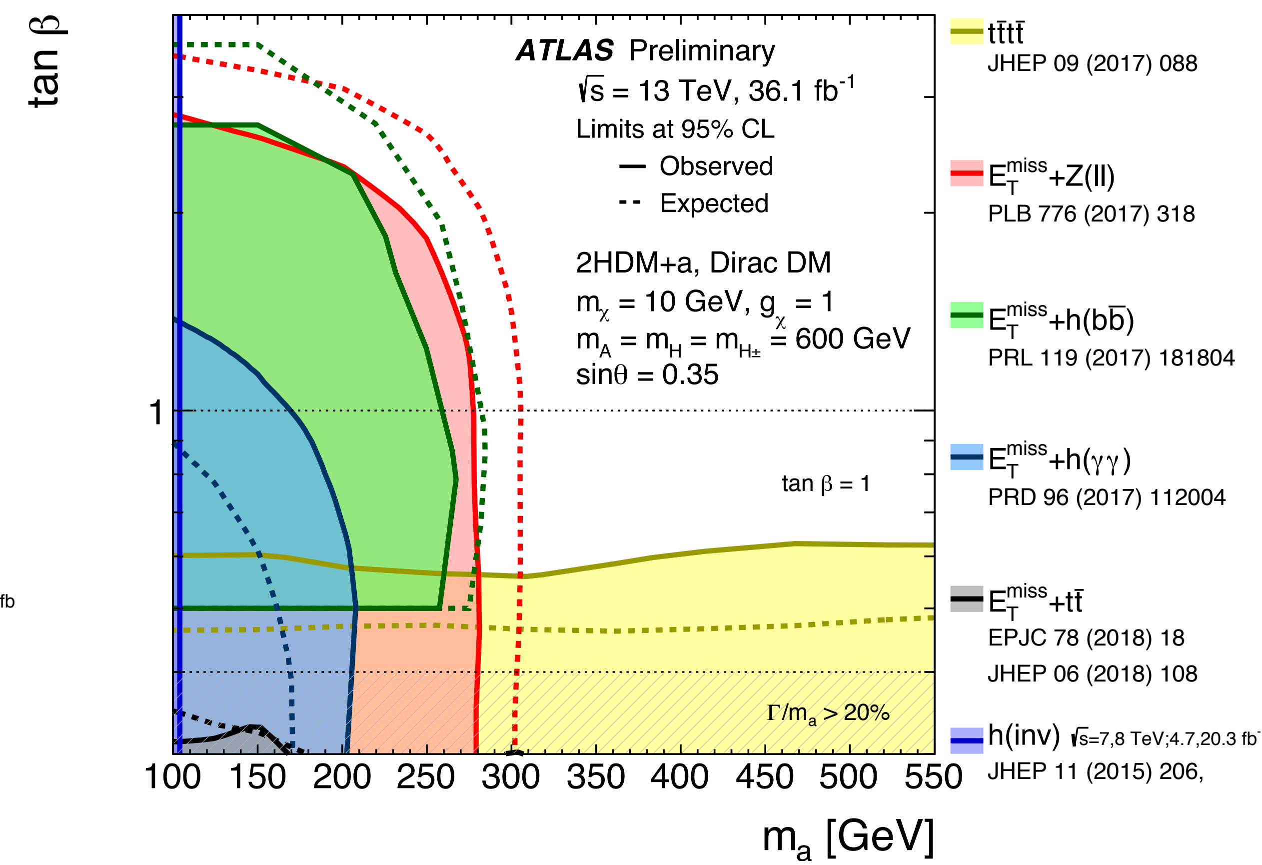

[ATLAS-CONF-2018-051]

2HDM+a: present constraints

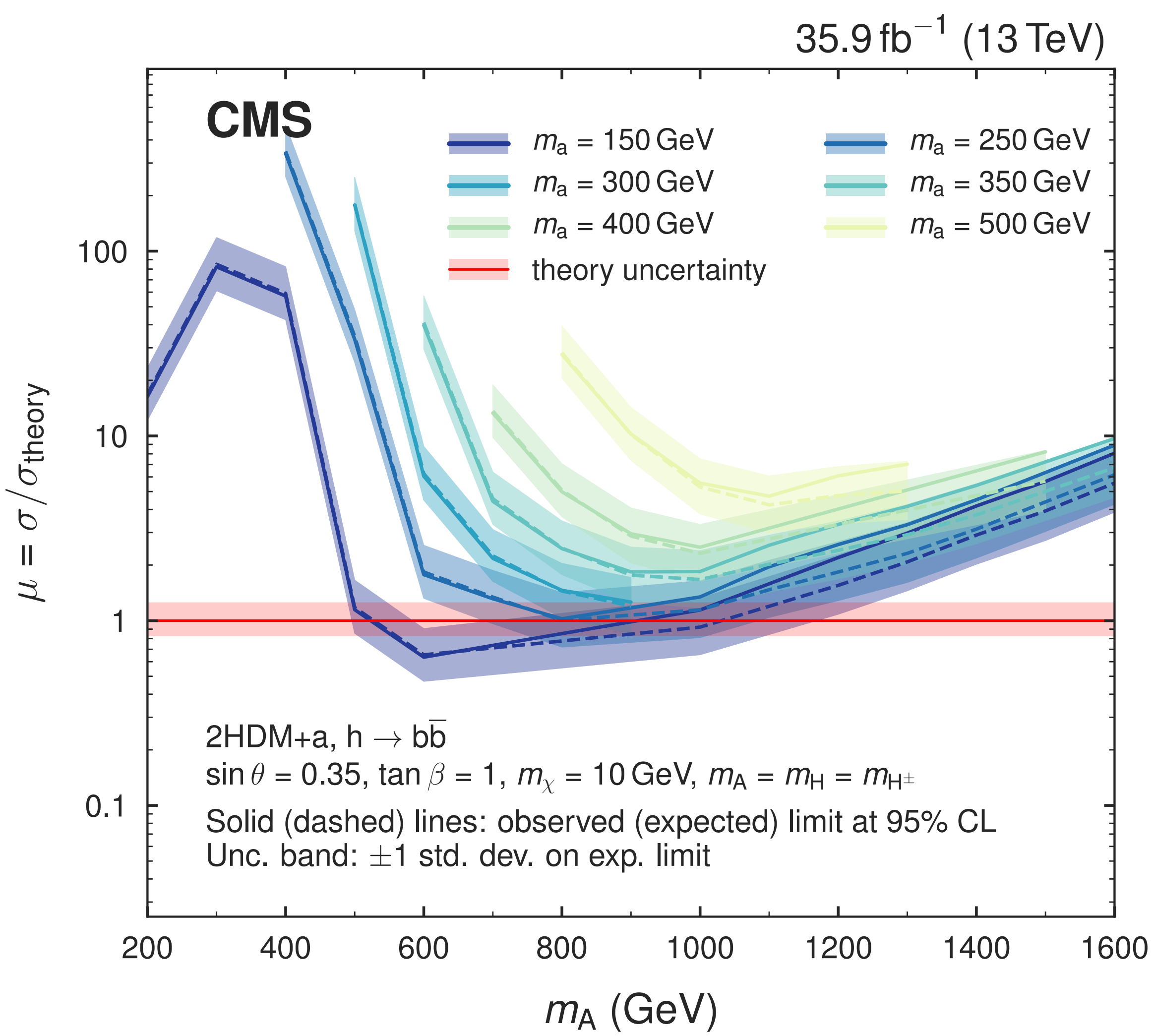

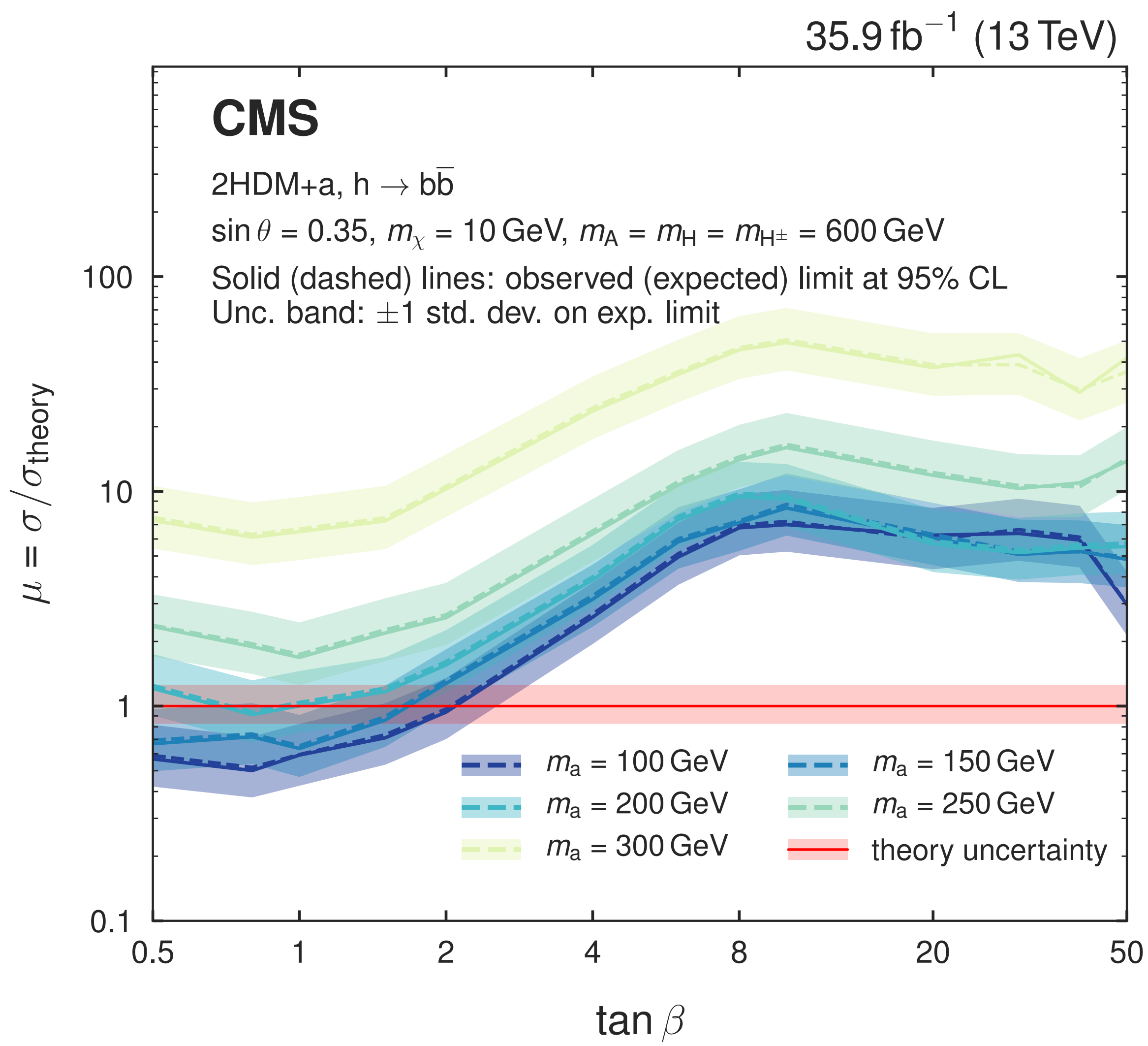

[CMS, 1811.06562]

2HDM+a: single top+E$_{T, miss}$

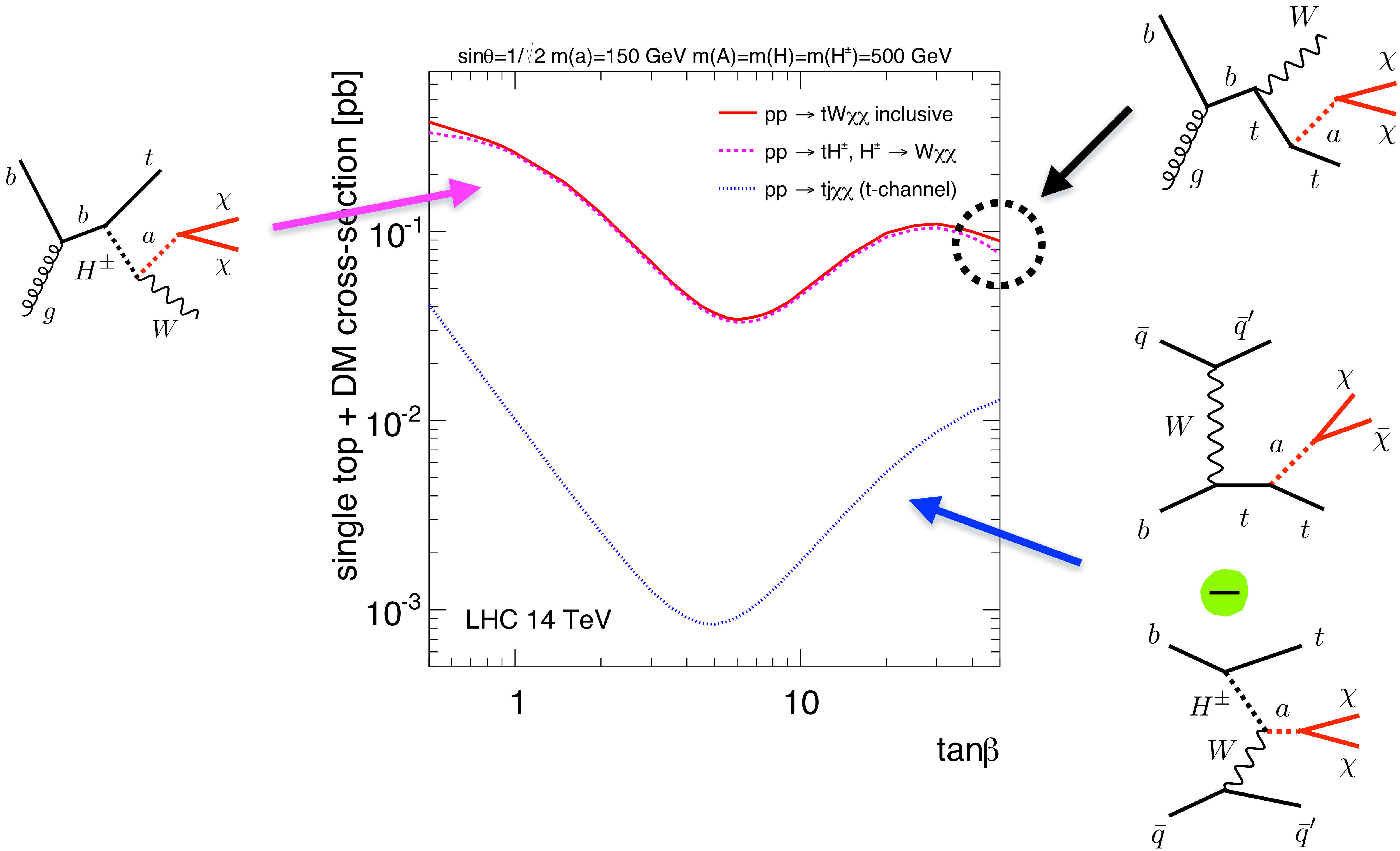

[Pani & Polesello, 1712.03874]

Single top+$E_{T,\,miss}$: signal vs. backgrounds

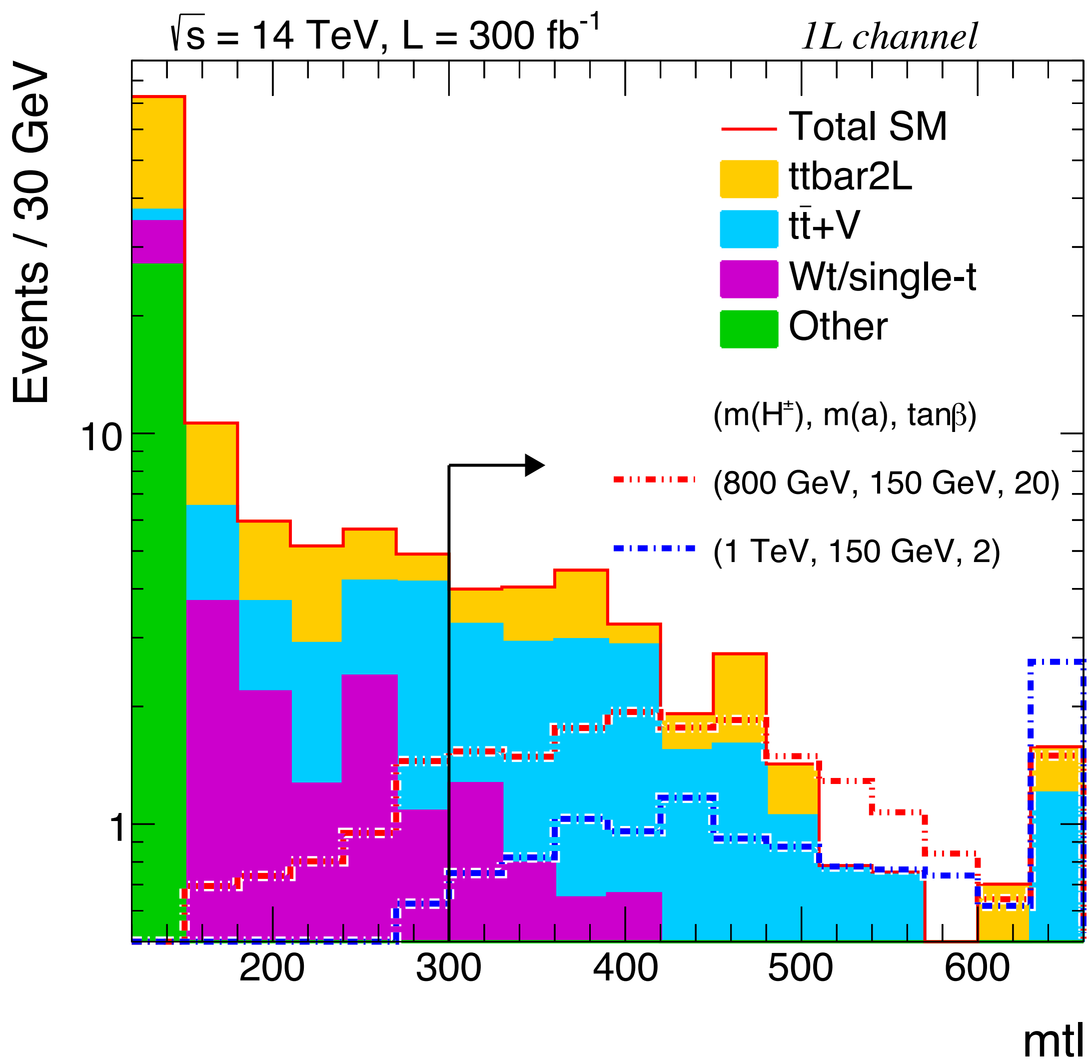

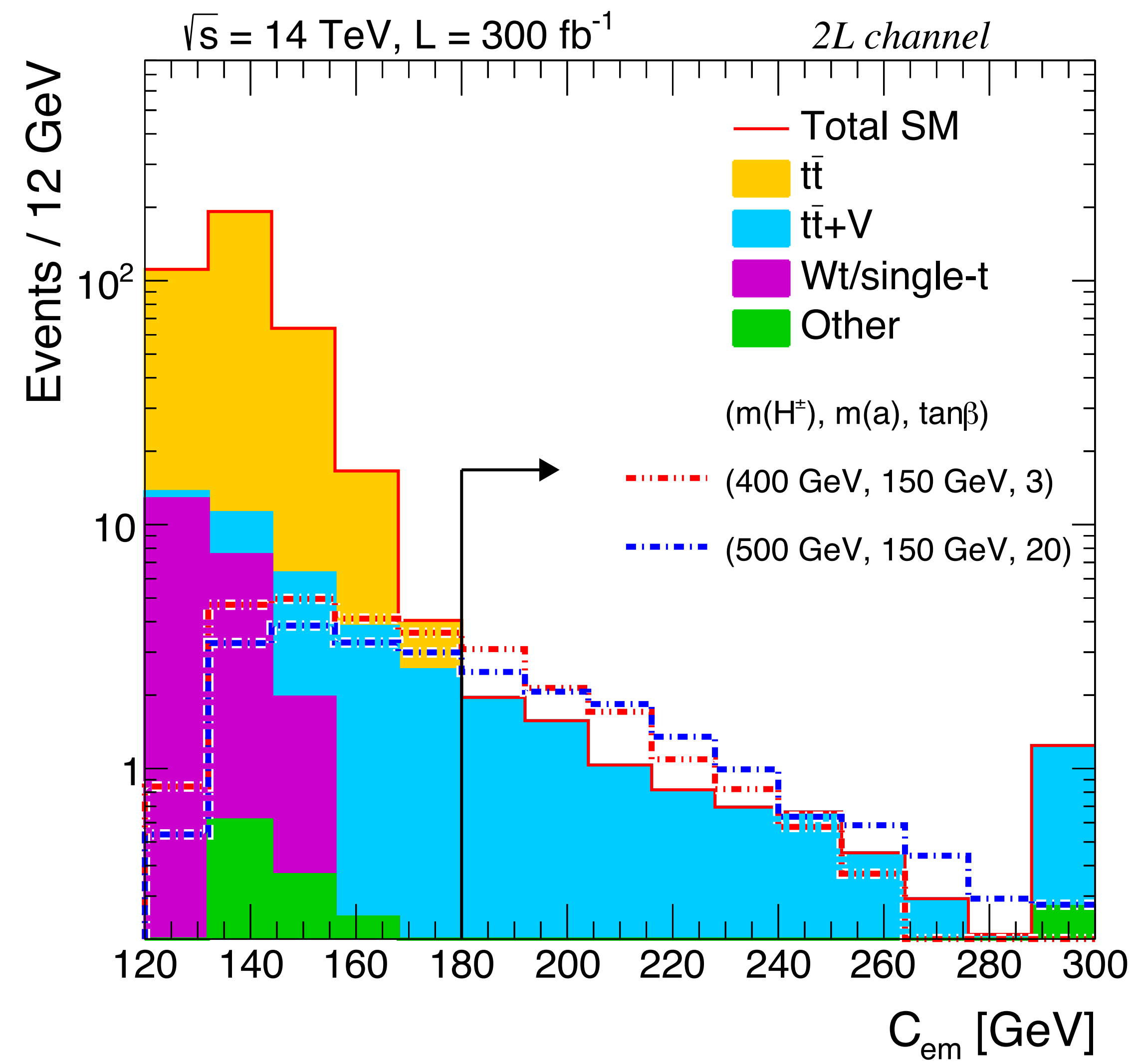

[Pani & Polesello, 1712.03874]

Single top+$E_{T, miss}$: 1-lepton analysis

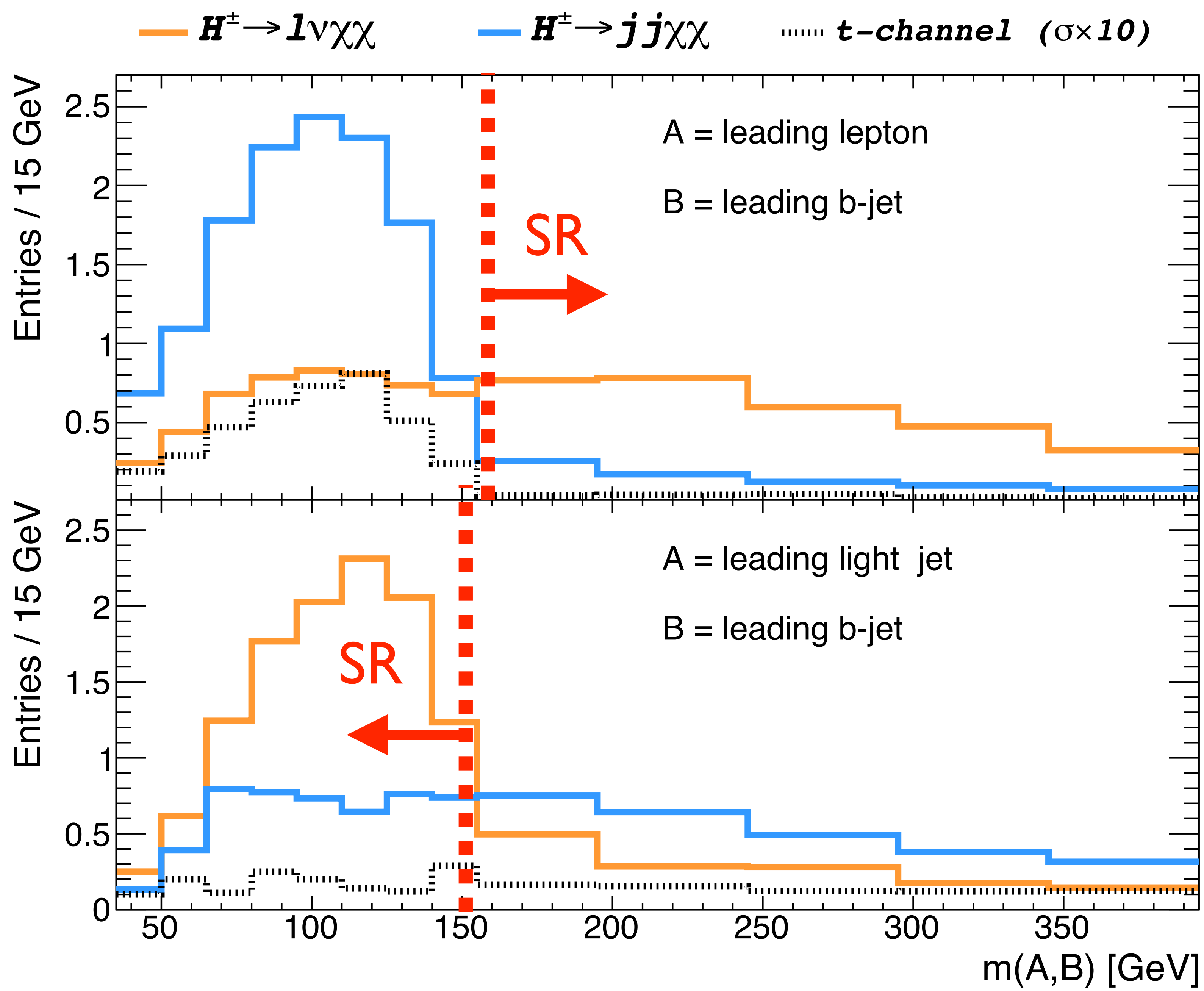

[Pani & Polesello, 1712.03874]

2HDM+a: 4-top prospects

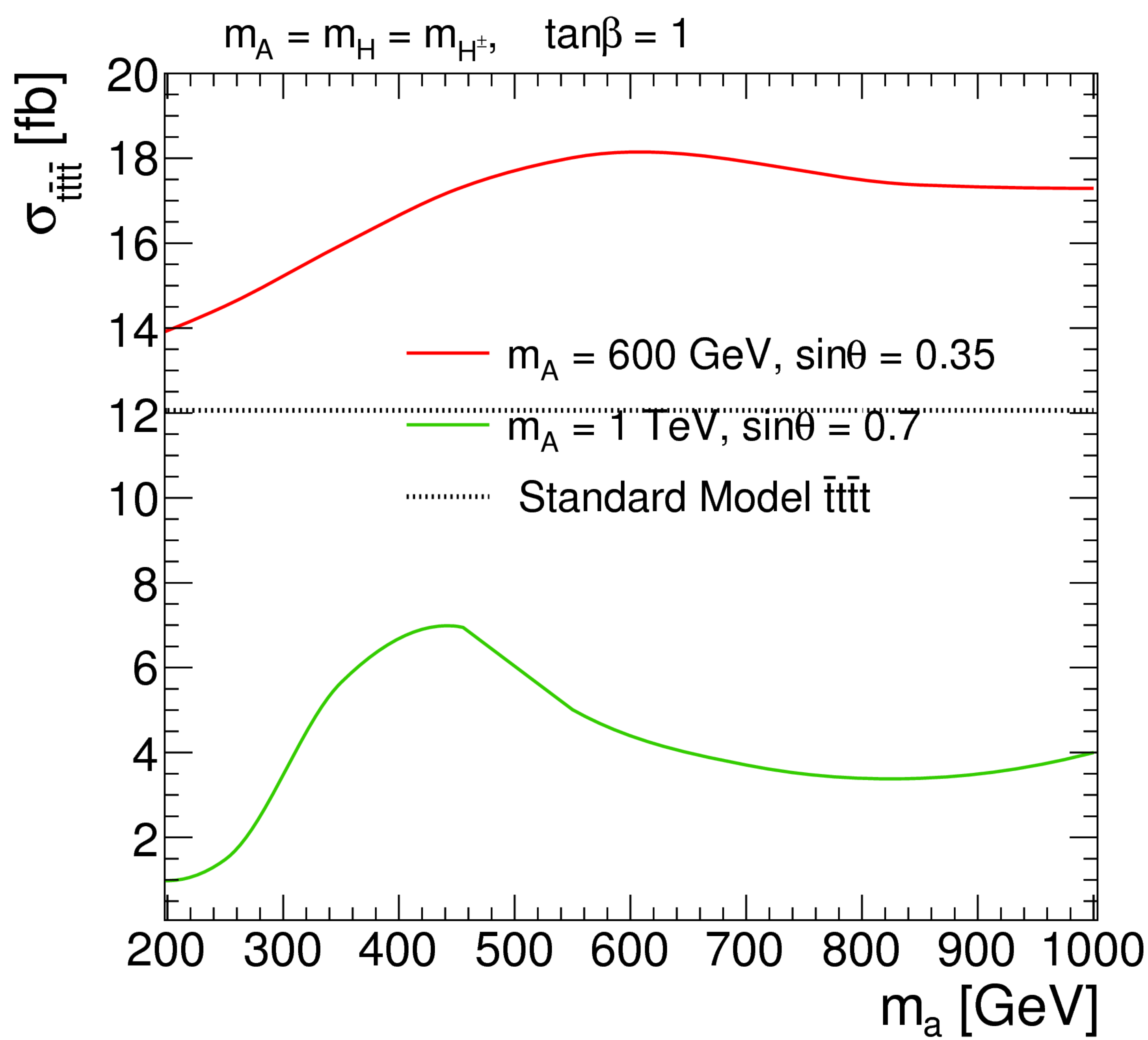

[ATL-PHYS-PUB-2018-027]

2HDM+a: 4-top prospects

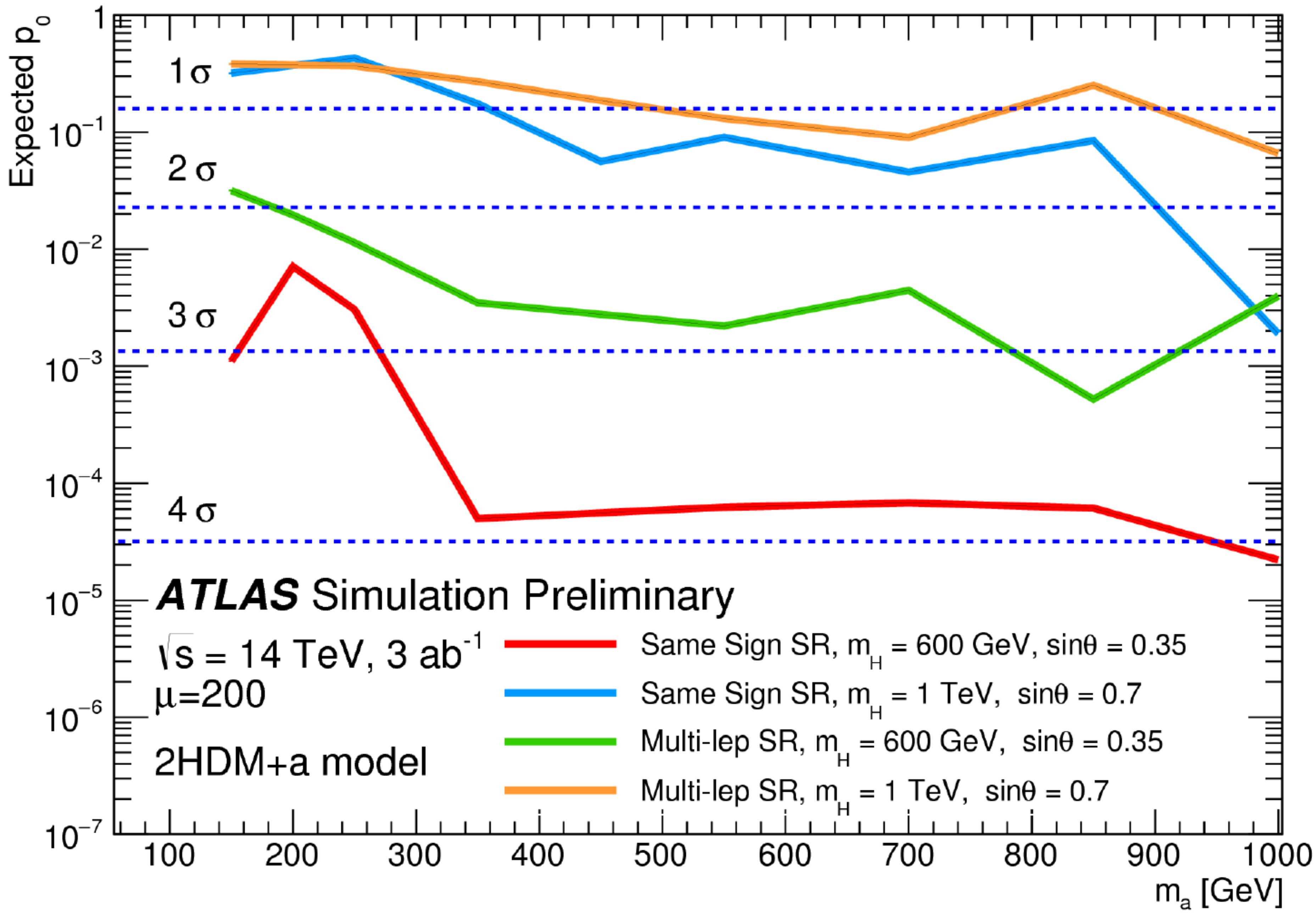

[ATL-PHYS-PUB-2018-027]

2HDM+a: 4-top prospects

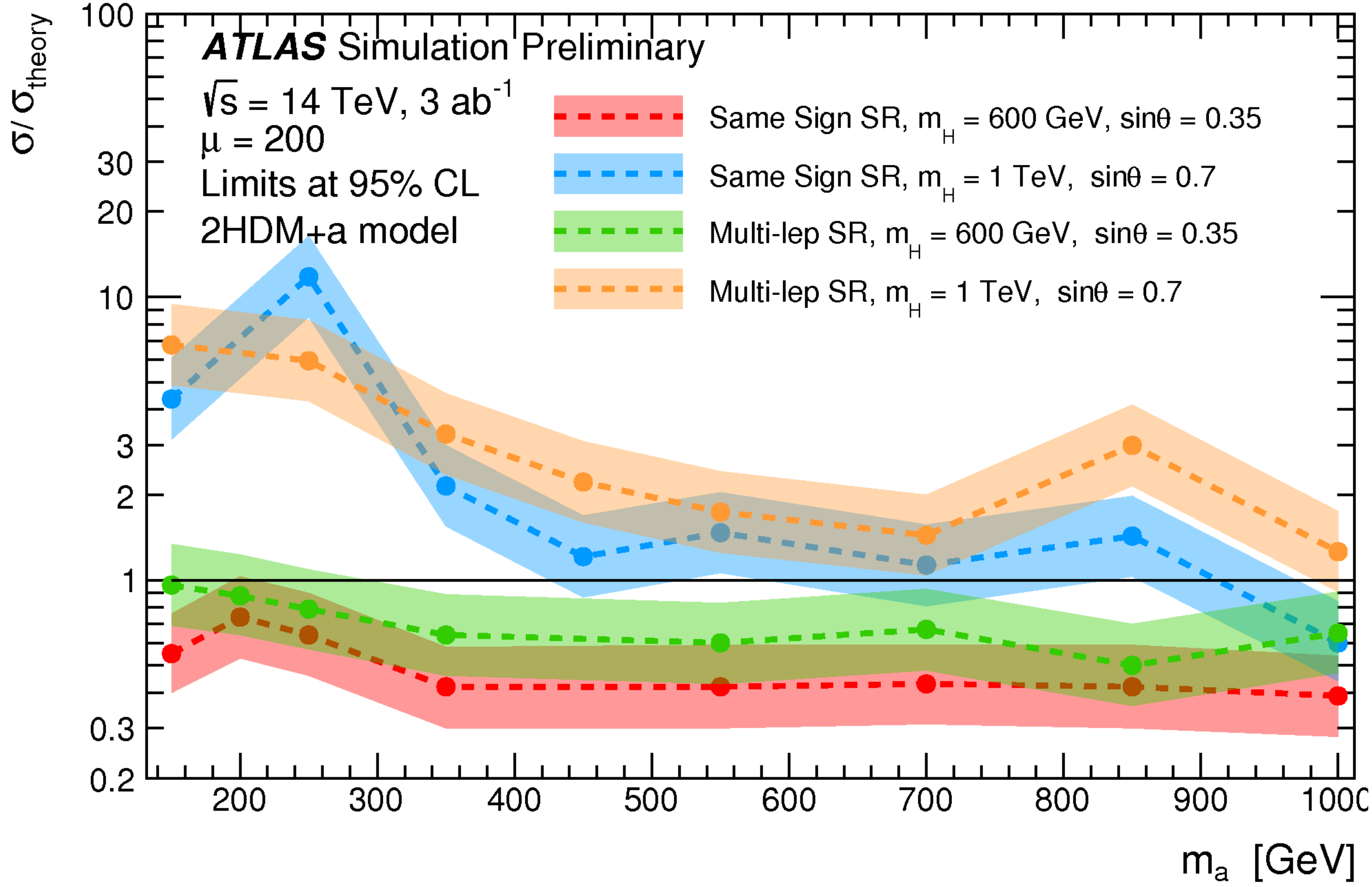

[ATL-PHYS-PUB-2018-027]

Z′-2HDM in a nutshell

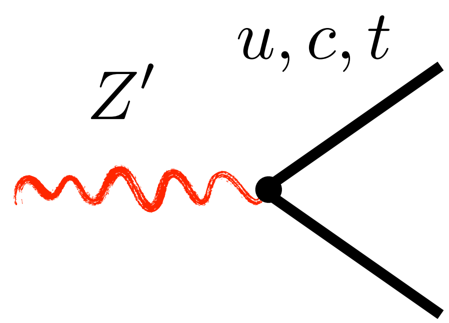

$$\propto \; g_Z \, z_u = g_Z/2$$

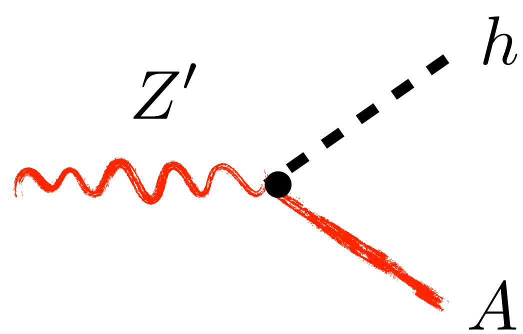

$$\propto \; g_Z \, \frac{\tan\beta}{1+\tan^2\beta}$$

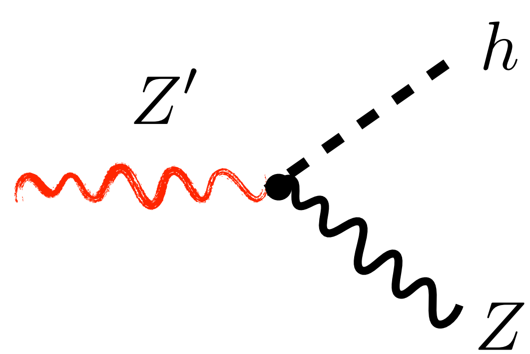

$$\propto \; g_Z \, \frac{\tan^2\beta}{1+\tan^2\beta}$$

[see e.g. Berlin, Lin & Wang, 1402.7074]

LHC constraints on spin-1 mediators

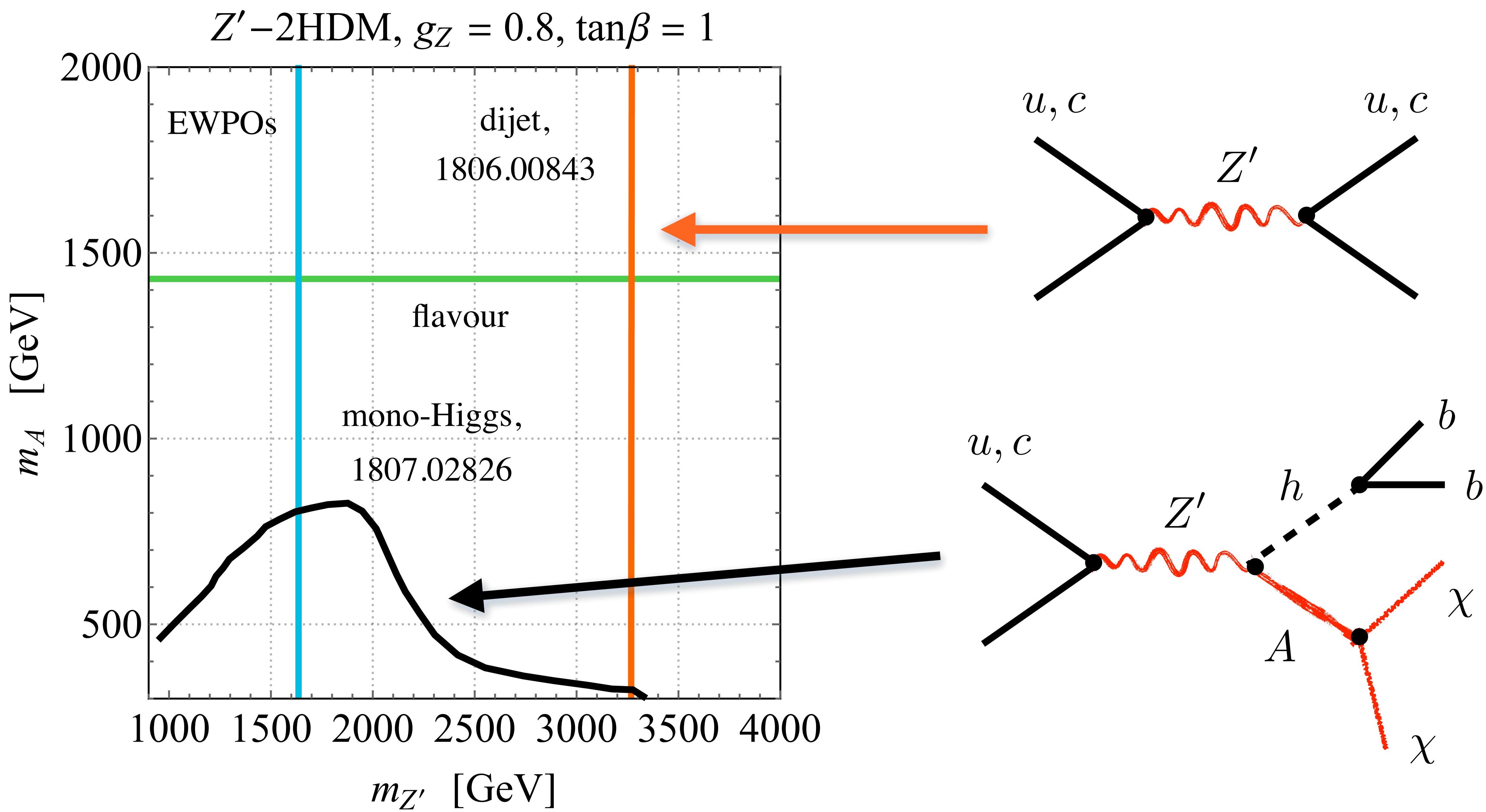

Dijet constraints on mediator mass in Z′-2HDM also stronger than mono-Higgs bounds. Other constraints more model-dependent

Dijet searches in Z′-2HDM

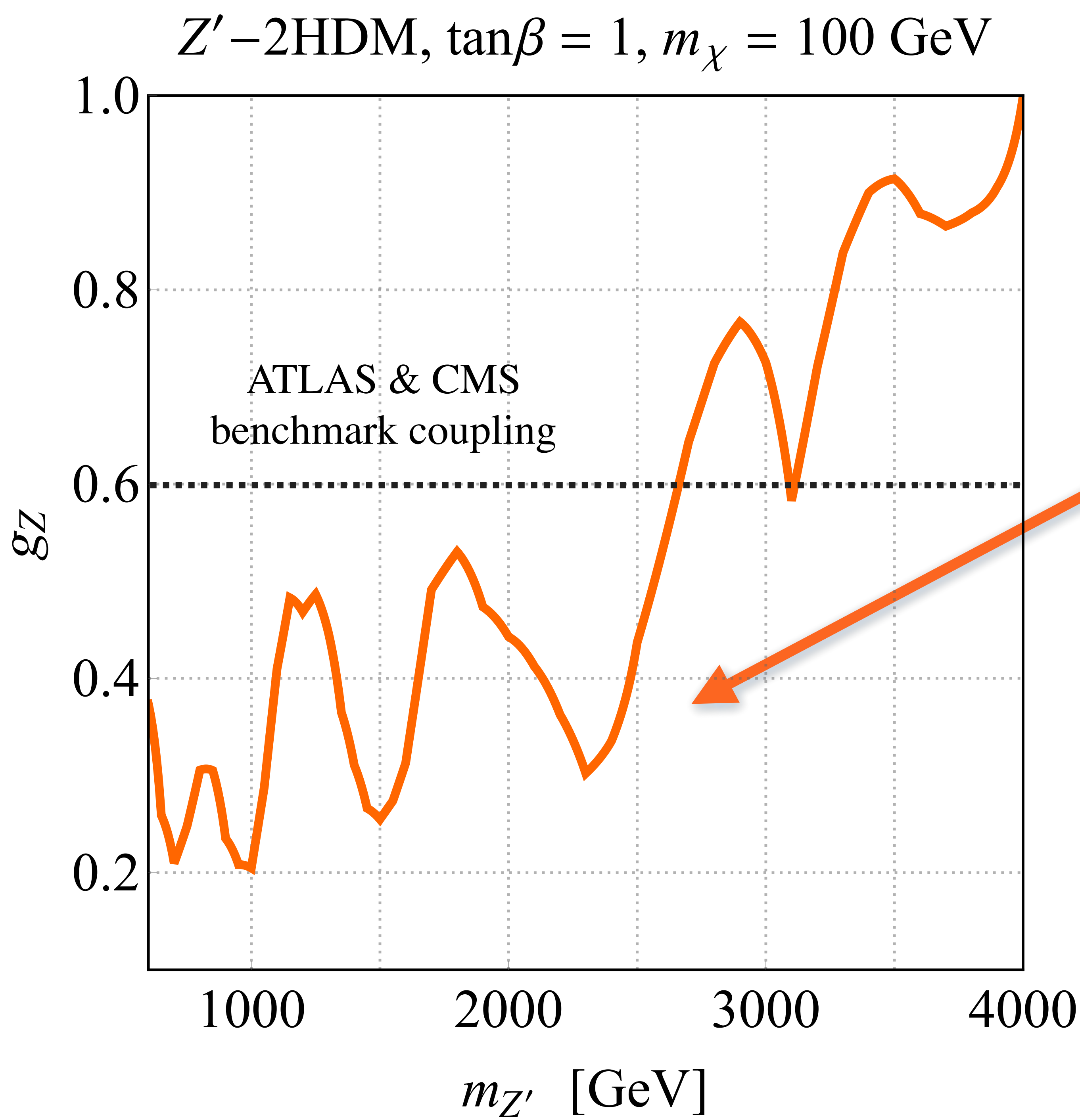

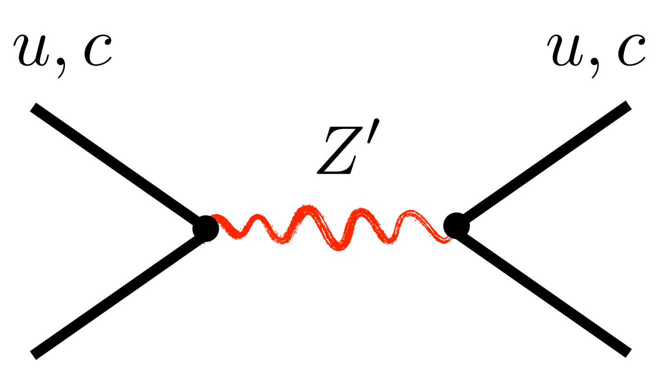

pp → Z′ → hZ → 2b2l in Z′-2HDM

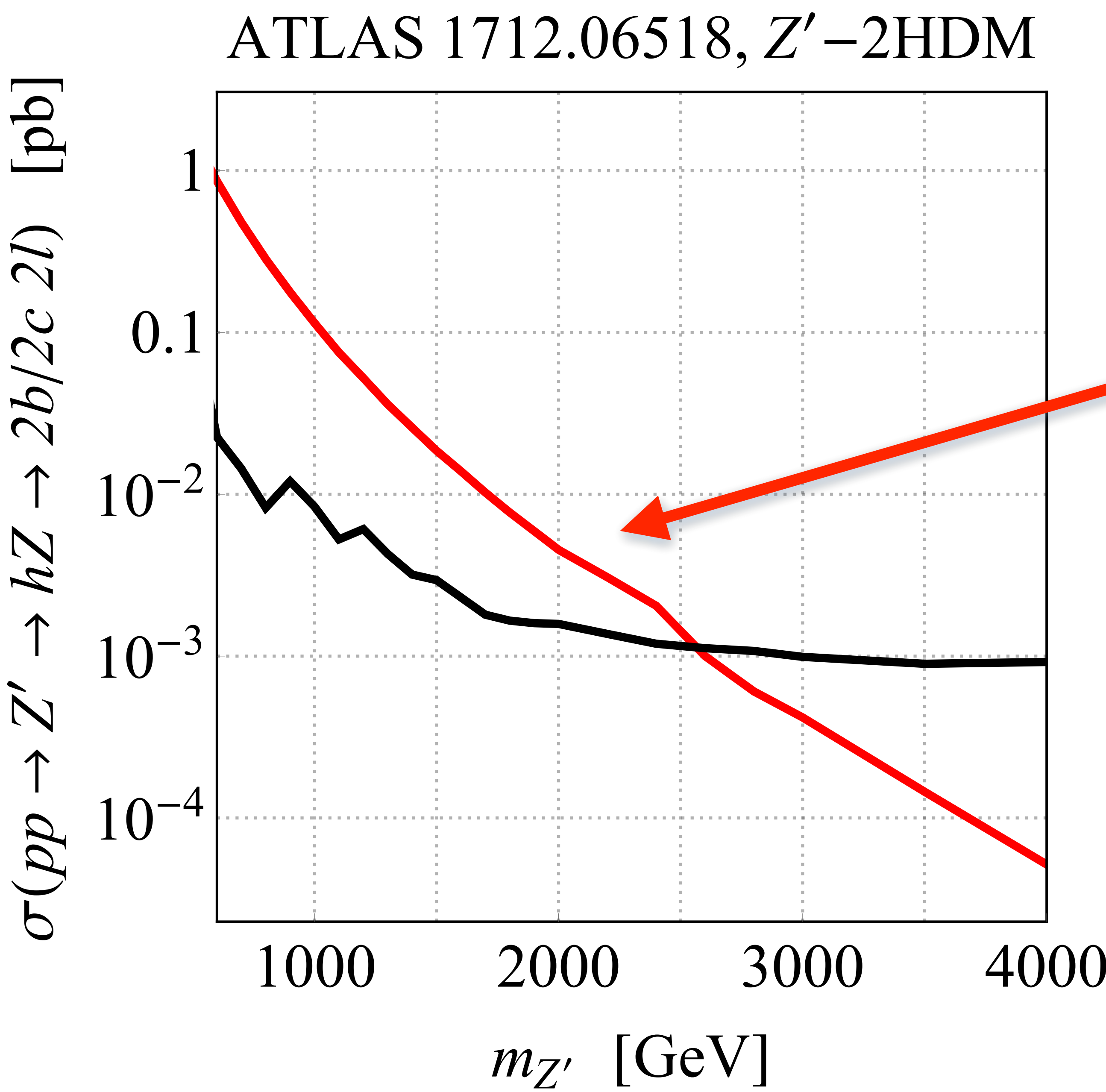

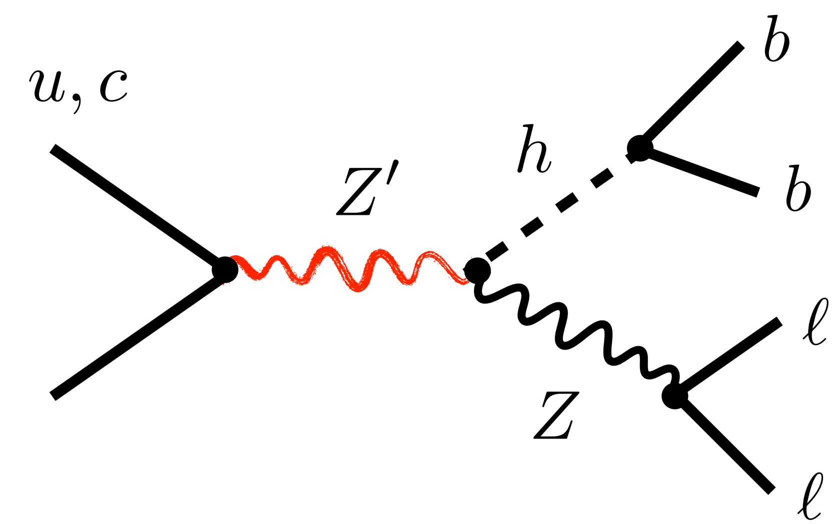

Searches for 2b2l final state exclude masses $m_{Z'}$ < 2.5 TeV in Z′-2HDM

Mono-Higgs: Z′-2HDM vs. 2HDM+a

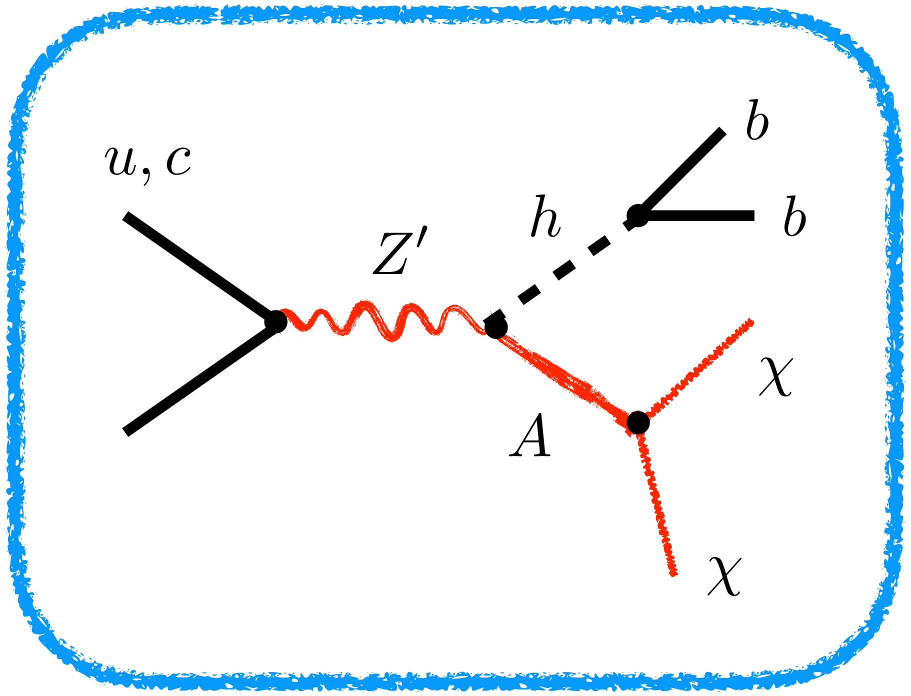

Z′-2HDM

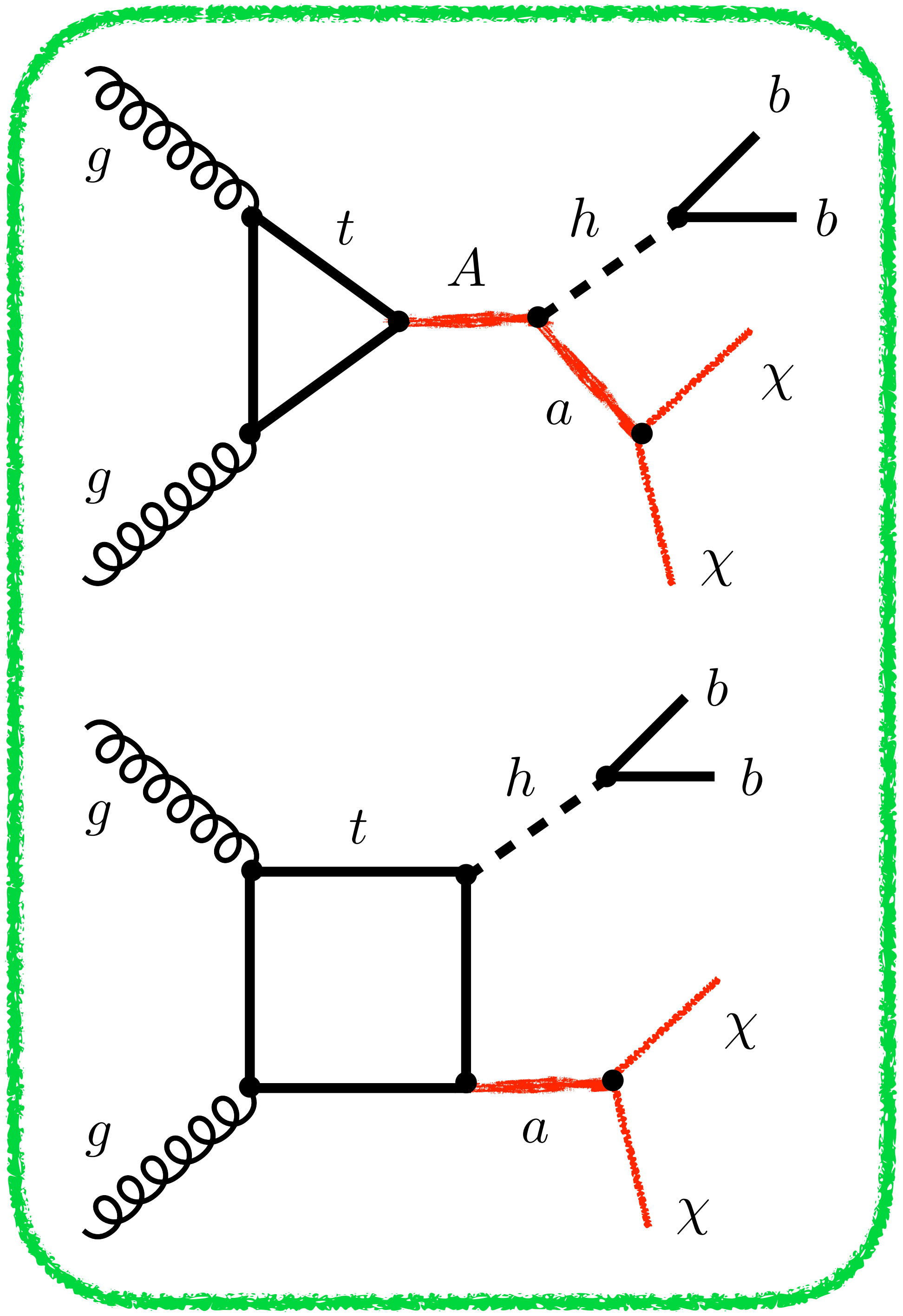

2HDM+a

Jacobian peaks

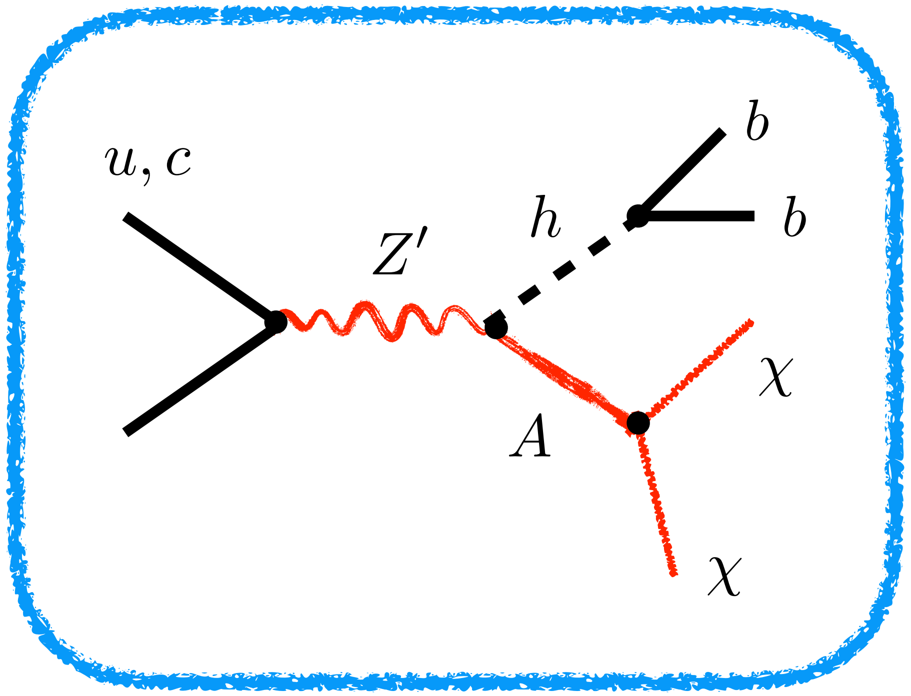

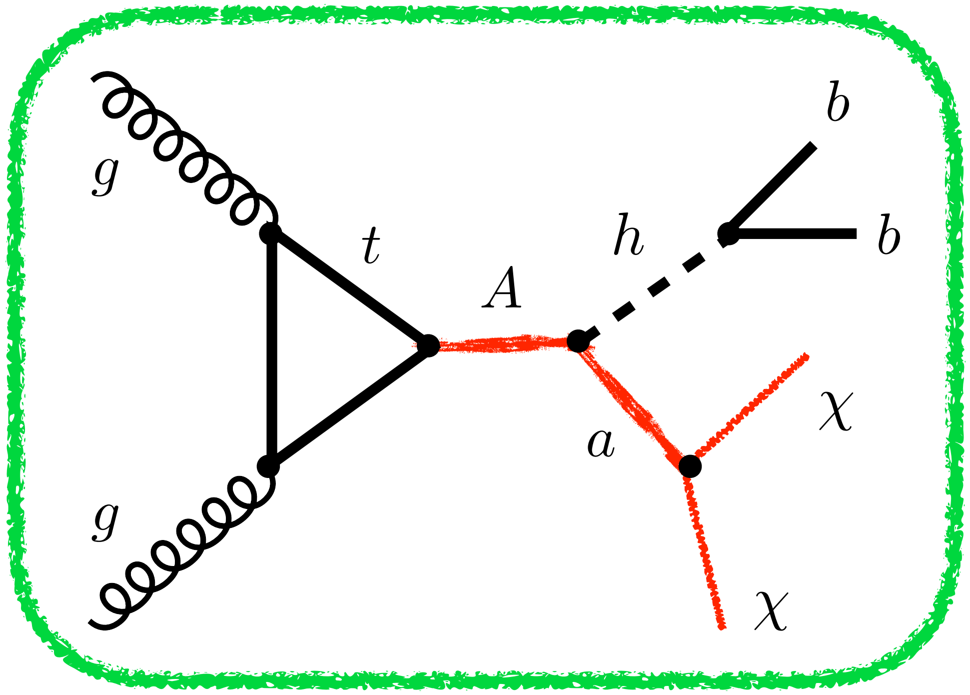

$$E_{T,\max}^{\text{miss}} \simeq \frac{\lambda^{1/2}(M_{Z'}, M_h, M_A)}{2M_{Z'}}$$

$$E_{T,\max}^{\text{miss}} \simeq \frac{\lambda^{1/2}(M_A, M_h, M_a)}{2M_A}$$

$$\lambda(m_A, m_B, m_C) = (m_A^2 - m_B^2 - m_C^2)^2 - 4m_B^2 m_C^2$$

Mono-Higgs spectra: Z′-2HDM

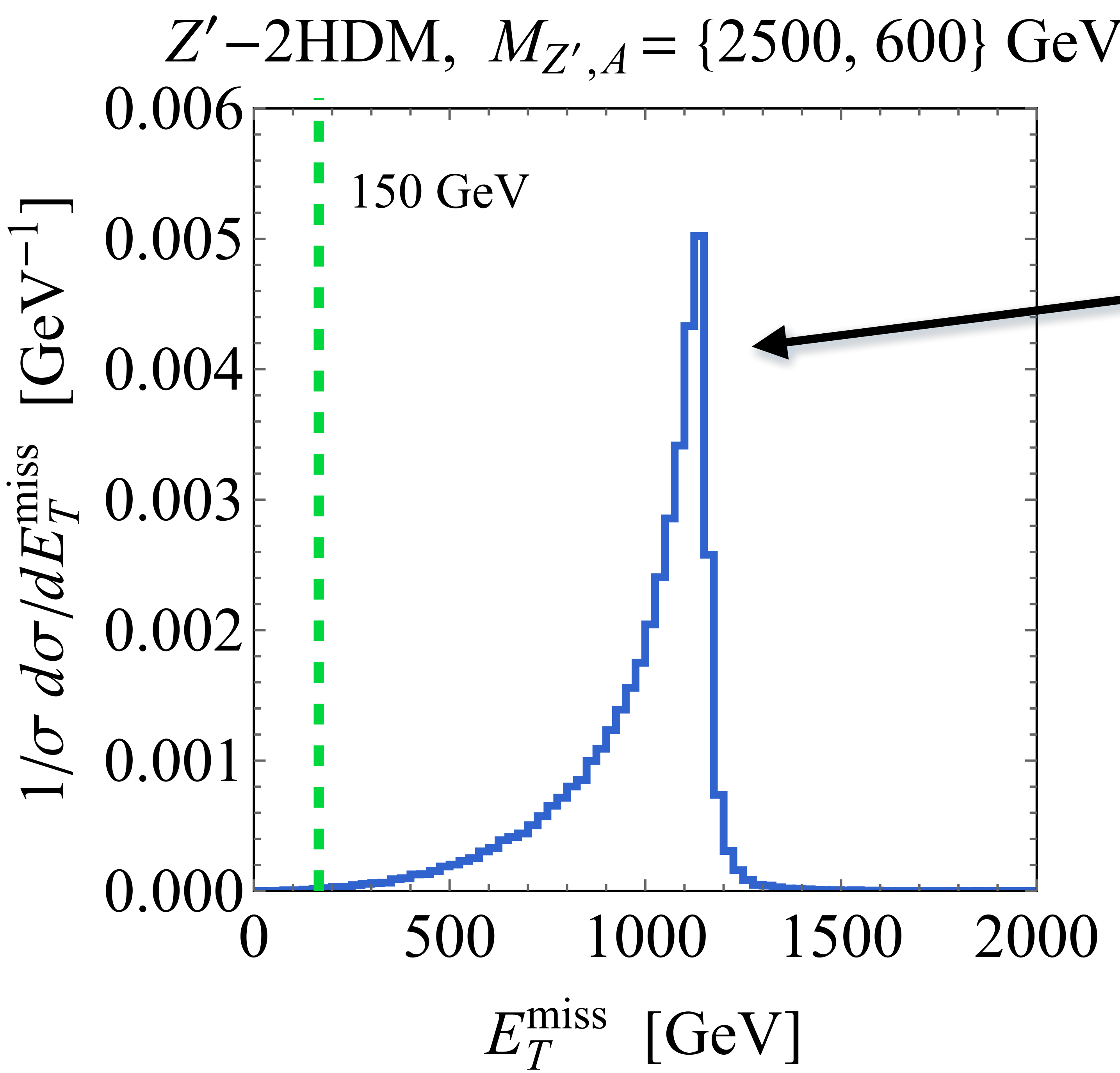

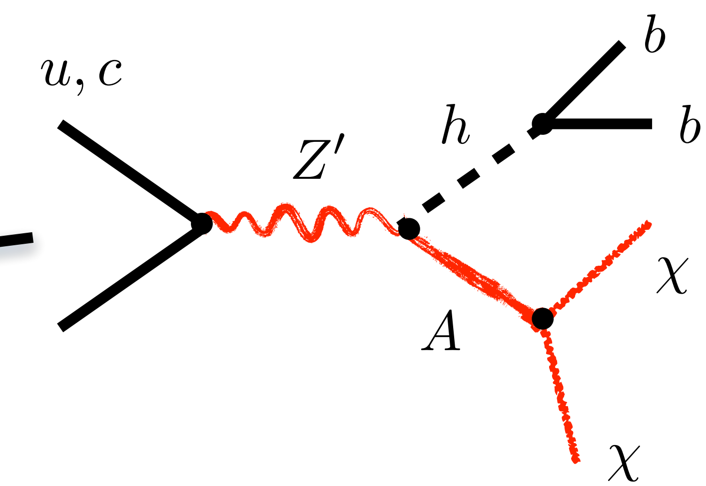

Mono-Higgs spectra: 2HDM+a

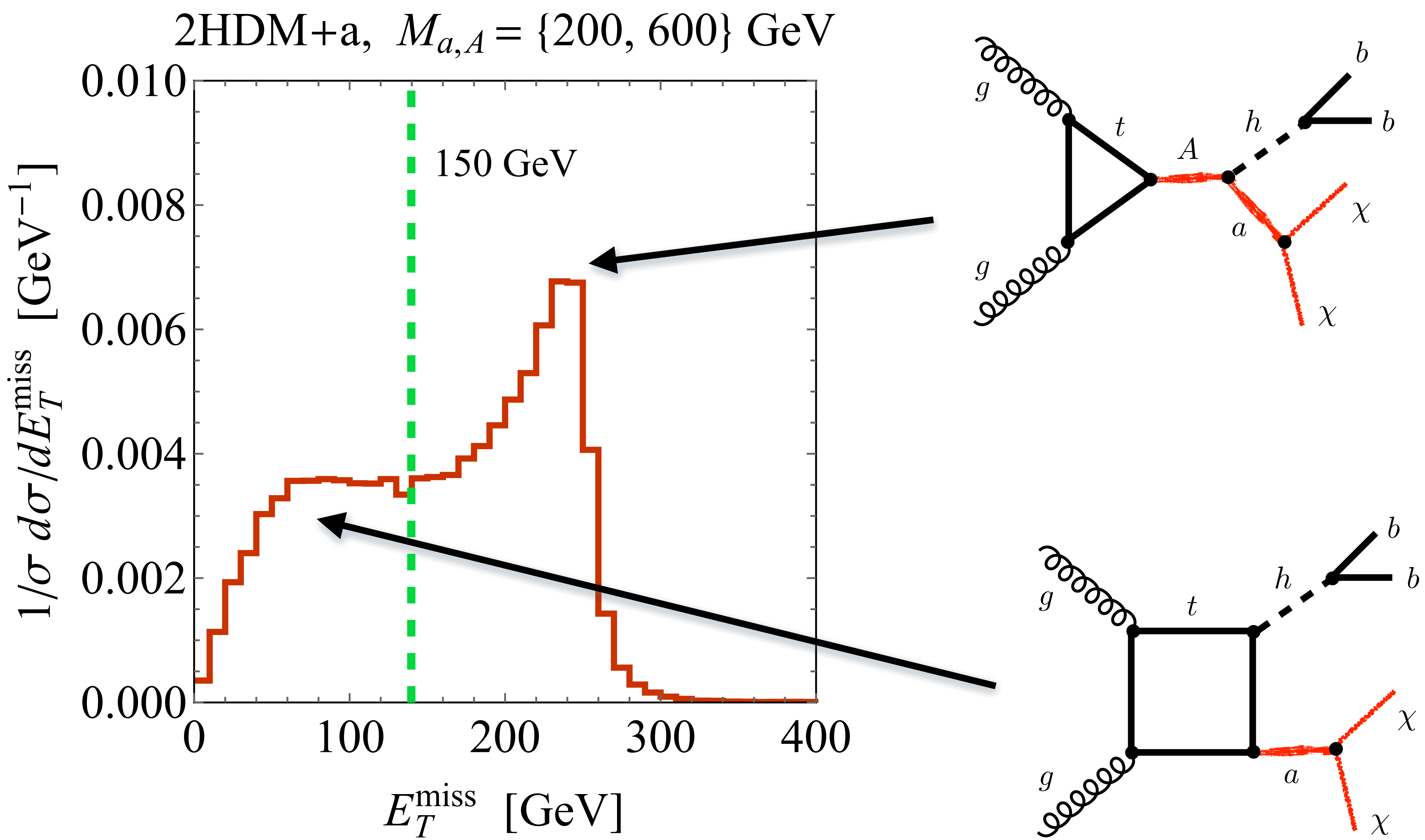

Simplified t-channel models

DM fermion singlet

scalar flavour triplet

$$\mathcal{L}_{\text{fermion},\tilde{u}} \supset \sum_{i=1,2,3} g\phi_i^* \bar{\chi} P_R u_i + \text{h.c.} \qquad \phi_i = \{\tilde{u}, \tilde{c}, \tilde{t}\}$$

universal couplings to have minimal flavour violation (MFV), which is needed to avoid flavour constraints

$$\{m_\chi,\ M_{1,2},\ M_3,\ g_{1,2},\ g_3\}$$

universality broken by $Y_u^\dagger Y_u$ flavour spurion (fine with MFV)

[Bell et al., 1209.0231; Chang et al., 1307.8120; An et al., 1308.0592; Bai & Berger 1308.0612; DiFranzo et al., 1308.2679; Papucci et al., 1402.2285; …]

Simplified t-channel models

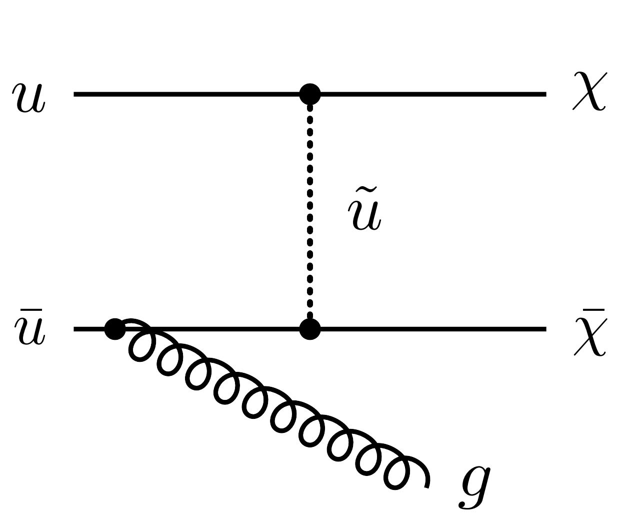

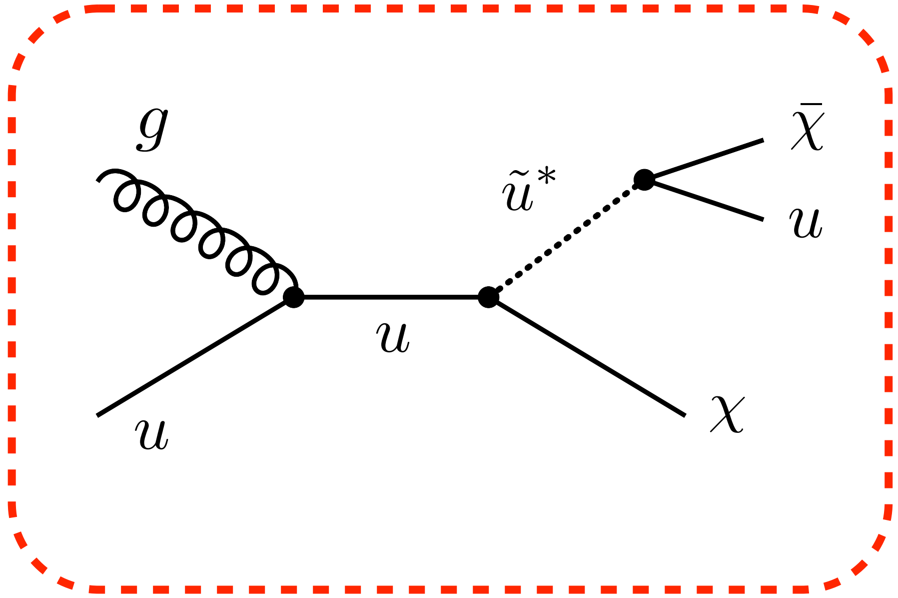

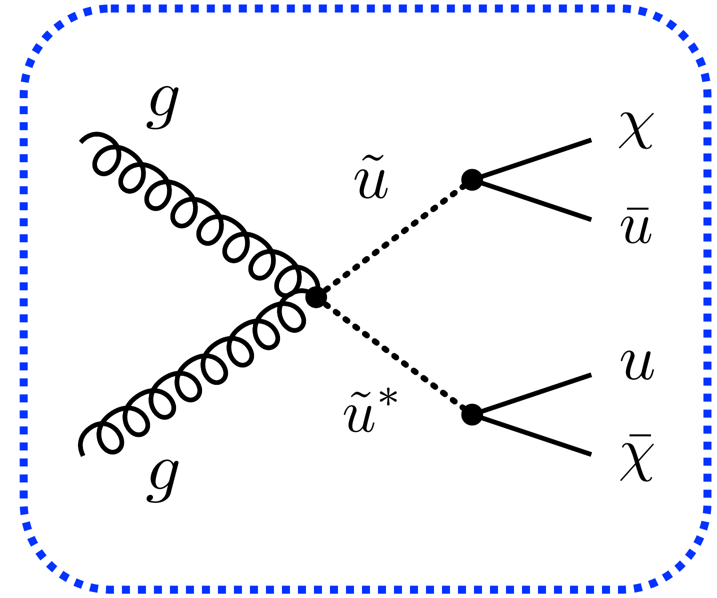

gives largest contribution to $E_{T,\,miss}$+j signal, because compared to initial state radiation (ISR) diagram phase-space enhanced, profits from gluon luminosity & jet typically harder than in ISR; dominance of associated production channel is a distinct feature of t-channel models

$E_{T,\,miss}$+2j channel can dominate over $E_{T,\,miss}$+j signal if $g_l \gg g_s$

Simplified t-channel models

[Papucci et al., 1402.2285]

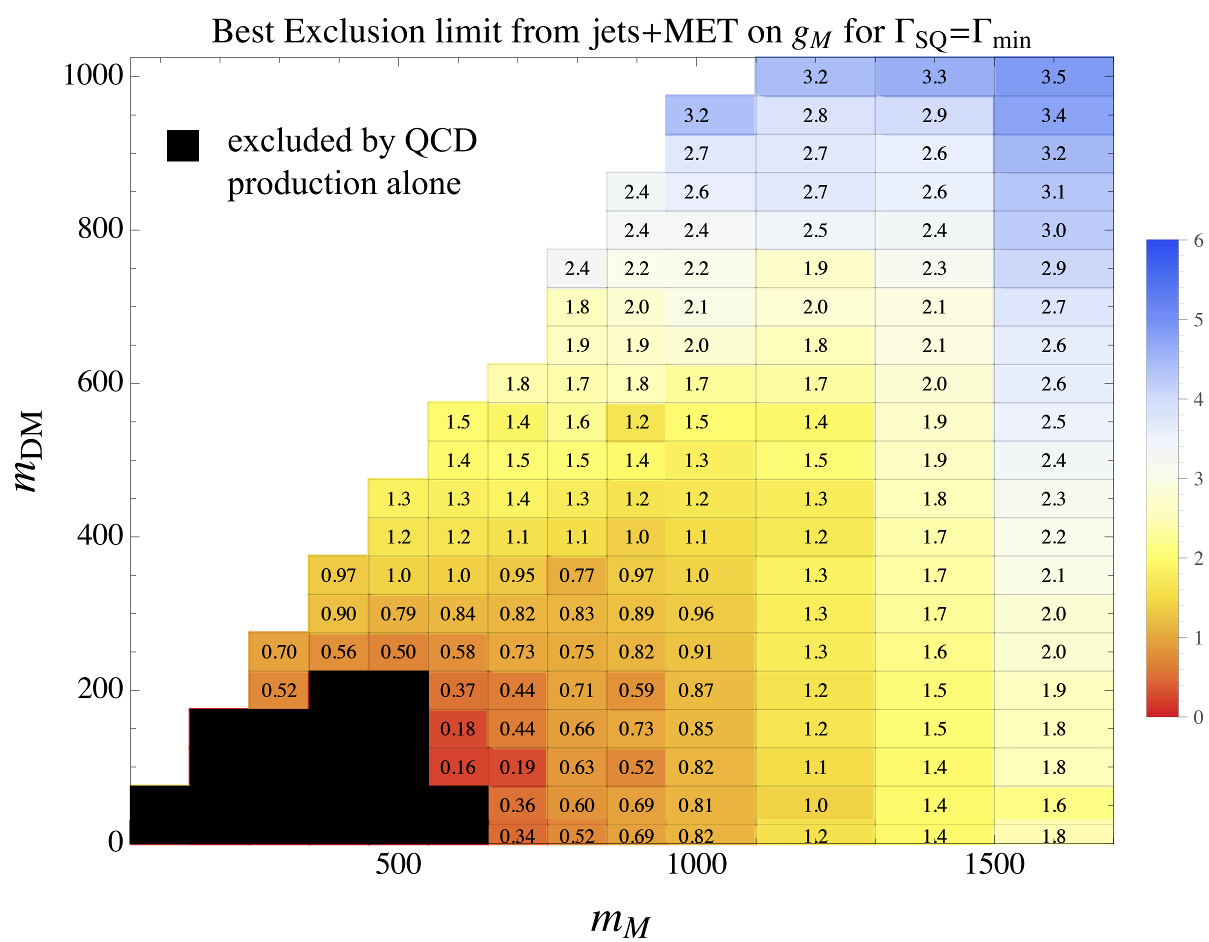

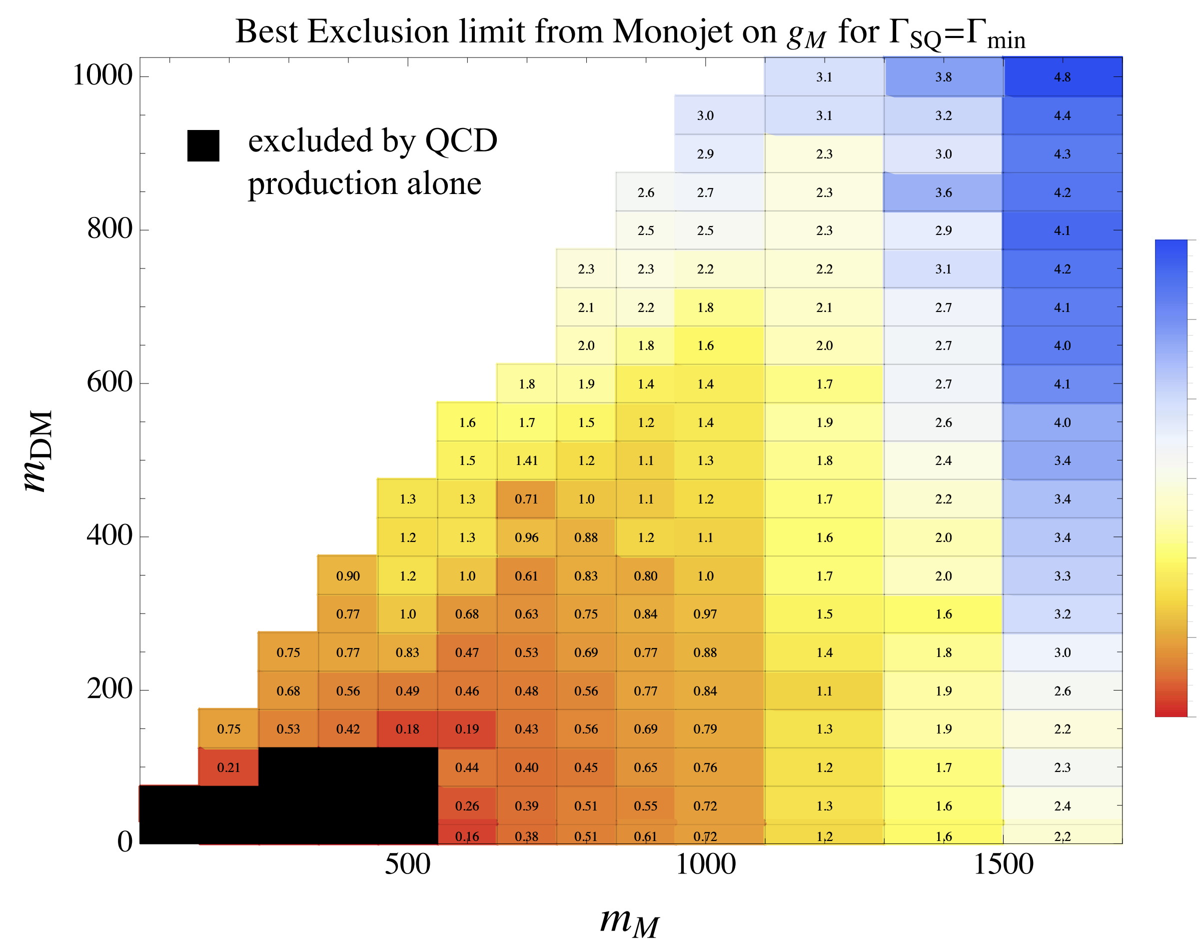

Mono-jet & supersymmetric (SUSY) searches provide comparable bounds in most of parameter space. SUSY searches often slightly better, except if mass of DM particle & mediator is degenerate

Stop searches

parameter region
constrained by
mono-jet searches

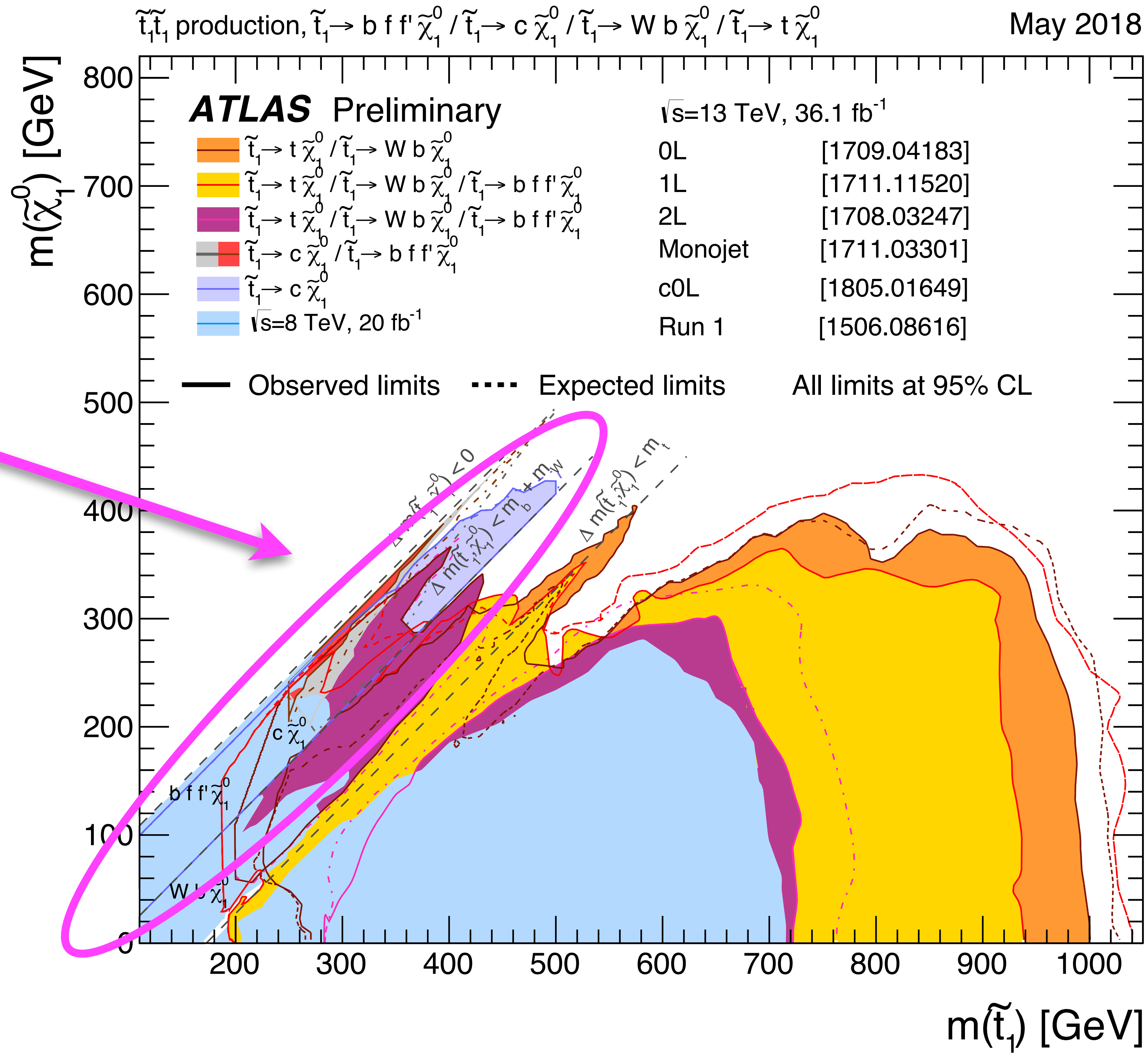

[https://twiki.cern.ch/twiki/bin/view/AtlasPublic/SupersymmetryPublicResults]